Vol. 50 · No. 4 · November 2025

RDE
Restorative Dentistry & Endodontics

## Research Articles





RDE Restorative Dentistry & Endodontics
Vol. 50 · No. 4 · November 2025
The Korean Academy of Conservative Dentistry

eISSN 2234-7666

Vol. 50 · No. 4 · November 2025

RDE
Restorative Dentistry & Endodontics

The Korean Academy of Conservative Dentistry

www.rde.ac

RDE Restorative Dentistry & Endodontics

Vol. 50 · No. 4 · November 2025

eISSN 2234-7666

## Aims and Scope

The *Restorative Dentistry and Endodontics* (officially abbreviated as Restor Dent Endod; RDE) is a peer-reviewed and open access journal providing up-to-date information regarding the research and developments on new knowledge and innovations pertinent to the field of contemporary clinical operative dentistry, restorative dentistry, and endodontics. In the field of operative and restorative dentistry, the journal deals with diagnosis, treatment planning, treatment concepts and techniques, adhesive dentistry, esthetic dentistry, tooth whitening, dental materials and implant restoration. In the field of endodontics, the journal deals with a variety of topics such as etiology of periapical lesions, outcome of endodontic treatment, surgical endodontics including replantation, transplantation and implantation, dental trauma, intracanal microbiology, endodontic materials (MTA, nickel-titanium instruments, etc), molecular biology techniques, and stem cell biology. RDE publishes original articles, review articles and case reports dealing with aforementioned topics from all over the world.

RDE is indexed/tracked/covered by Web of Science-Emerging Sources Citation Index (ESCI), Scoups, PubMed, PubMed Central, EBSCO, KoreaMed, Synapse, KCI, Crossref, DOAJ, and Google Scholar.

This Journal was supported by the Korean Federation of Science and Technology Societies Grant funded by the Korean Government (MEST).

## History

RDE (eISSN 2234-7666) is the official journal of the Korean Academy of Conservative Dentistry and was renamed from the *Journal of Korean Academy of Conservative Dentistry* (pISSN 1225-0864; eISSN 2093-8179), which was first published in 1975. It was initially published once a year but became a biannual journal in 1986, a quarterly journal in 1999, and then a bimonthly journal in 2001. From 2012, the journal name was renamed, the official language of the journal was changed to English, and it is currently published quarterly. This journal is supported in part by a Grant from the Korean Federation of Science and Technology Societies funded by the Korean Government (MEST).

## Distribution

Restor Dent Endod is not for sale, but is distributed to members of Korean Academy of Conservative Dentistry and relevant researchers and institutions world-widely on the last day of February, May, August, and November of each year. Full text PDF files are also available at the official website (https://www.rde.ac; http://www.kacd.or.kr), KoreaMed Synapse (https://synapse.koreamed.org), and PubMed Central. To report a change of mailing address or for further information contact the academy office through the editorial office listed below.

## Open Access



**Official Publication of Korean Academy of Conservative Dentistry**

Published on November 30, 2025

**Publisher**

**The Korean Academy of Conservative Dentistry**

B163, Seoul National University Dental Hospital, 101 Daehak-ro, Jongno-gu, Seoul, Korea

Tel: +82-2-763-3818

Fax: +82-2-763-3819

Email: kacd@kacd.or.kr

**Editorial Office**

**The Korean Academy of Conservative Dentistry**

B163 Seoul National University Dental Hospital, 101 Daehak-ro, Jongno-gu, Seoul 03080, Korea

Tel: +82-2-763-3818

Fax: +82-2-763-3819

Email: editor@rde.ac

**Publishing Office**

**M2PI**

#805, 26 Sangwon 1-gil, Seongdong-gu, Seoul 04779, Korea

Tel: +82-2-6966-4930

Fax: +82-2-6966-4945

Email: support@m2-pi.com

RDE Restorative Dentistry & Endodontics

# Editorial Board

RDE Restorative Dentistry & Endodontics

# Contents

Vol. 50 · No. 4 · November 2025

## Research Articles

RDE Restorative Dentistry & Endodontics

Research Article

eISSN 2234-7666
Restor Dent Endod. 2025 November;50(4):e32
https://doi.org/10.5395/rde.2025.50.e32

# Marginal adaptation of three root-end filling materials in cavities prepared with laser and ultrasonic tips: an *in vitro* comparative study

**Busra Zengin**[1], **Seda Aydemir**[2,*], **Nicholas Paul Chandler**[3]

[1]Uskudar Oral and Dental Health Center, Istanbul, Türkiye
[2]Department of Endodontics, Faculty of Dentistry, Istanbul Atlas University, Istanbul, Türkiye
[3]Sir John Walsh Research Institute, Faculty of Dentistry, University of Otago, Dunedin, New Zealand

## ABSTRACT

**Objectives:** This study evaluated the marginal adaptation of ProRoot MTA (Dentsply Tulsa Dental), Biodentine (Septodont), and TotalFill BC RRM (FKG) placed in root-end cavities prepared with ultrasonic or Er,Cr:YSGG laser tips, using scanning electron microscopy.

**Methods:** The canals of 90 extracted maxillary central incisors were prepared and obturated and their roots resected. Six groups of 15 specimens were allocated as follows: ultrasonic + ProRoot MTA, ultrasonic + Biodentine, ultrasonic + TotalFill, laser + ProRoot MTA, laser + Biodentine, and laser + TotalFill. Roots were sectioned longitudinally to expose the filling material. Apical and coronal micrographs were taken, and the greatest distance between dentin and filling material was measured. The total gap area was also calculated using further micrographs.

**Results:** Cavities prepared with the ultrasonic tips and filled with Biodentine showed significantly greater gap dimensions compared with TotalFill ($p < 0.001$) and ProRoot MTA ($p = 0.007$) in the apical region. The ultrasonic group showed significantly higher void values compared to the laser group for ProRoot MTA ($p = 0.026$), when comparing the total values of void. The Biodentine group was significantly higher than the TotalFill group in root-end cavities prepared with ultrasonic tips ($p < 0.001$). The Biodentine group was significantly higher than the ProRoot MTA group in root-end cavities prepared with the laser tip ($p = 0.002$).

**Conclusions:** Under the conditions of this study, it was determined that the root-end cavity preparation technique had an effect on the amount of gaps formed between the dentin and the three filling materials.

**Keywords:** Dental marginal adaptation; Root-end cavity; Root-end filling; Ultrasonics

**Received:** December 17, 2024 **Revised:** March 15, 2025 **Accepted:** March 31, 2025

**Citation**
Zengin B, Aydemir S, Chandler NP. Marginal adaptation of three root-end filling materials in cavities prepared with laser and ultrasonic tips: an *in vitro* comparative study. Restor Dent Endod 2025;50(4):e32.

***Correspondence to**
**Seda Aydemir, DDS**
Department of Endodontics, Faculty of Dentistry, Istanbul Atlas University, Hamidiye Anadolu Cd. No: 40. 34408, 34403 Kagithane, Istanbul, Türkiye
Email: aydemirseda@yahoo.com

## INTRODUCTION

Root canal treatment aims to eliminate bacteria from the root canal system and establish a barrier to prevent the passage of microorganisms or their products into the periapical tissues. Conventional treatment is successful in about 90% of cases [1], but if treatment fails, retreatment is indicated. If this is impossible or not successful, periapical surgery may be suggested. This involves curettage of infected or inflamed tissue, resecting the infected or damaged root apex (apicectomy), preparation of a root-end cavity, and insertion of a restorative material to prevent communication between the canal system and the surrounding tissues [2].

The resection is made perpendicular to the long axis of the root and 3 mm from its tip, as studies have shown this reduces 98% of the apical ramifications and eliminates 93% of lateral canals [2,3]. Ideally, the root-end cavity is at least 3 mm deep and anatomically parallel to the root outline. The cavity is prepared with burs, more recently, ultrasonic and laser tips [2,3]. Bur use can cause problems such as nonparallel cavity walls, palatal/lingual dentin perforation, and difficulty reaching the root tip [3]. With ultrasonic tips, smaller, central, and parallel-walled cavities can be prepared, with less risk of perforation [4]. Laser systems are also used in apical surgery. Many studies reported that the erbium laser used for apicectomy resulted in a high success rate with significant clinical benefits [5–8]. Amalgam, glass ionomer cement (GIC), zinc oxide-eugenol, composite resins, and bioceramics have all been used as root-end filling materials [2]. Mineral trioxide aggregate (MTA) (e.g., ProRoot MTA; Dentsply Tulsa Dental, Tulsa, OK, USA) is a widely used material with excellent sealing ability and biocompatibility; however, it has a long setting time and complex handling characteristics [9]. Biodentine (Septodont, Saint Maur des Fossés, France) is a tricalcium silicate-based cement that was introduced as a dentin substitute. It has good sealing properties and a short setting time [10]. TotalFill BC RRM (FKG, La Chaux-de-Fonds, Switzerland) is a bioceramic material that, in premixed putty form, is very easy to use. It has good antibacterial properties due to its high pH, but it has a long setting time [11].

Adaptation has been defined as the degree of proximity and interlocking of a filling material to the cavity wall. Good adaptation will reduce microleakage. It can be assessed by dye, radioisotope, bacterial penetration, scanning electron microscopy (SEM), and electrochemical methods, and with a fluid filtration technique [12]. SEM provides high magnification and resolution and has been preferred in research evaluating marginal adaptation [13,14].

Main contributions of this study are: (1) the comparison of the amount of gaps created by three different root-end filling materials placed in cavities prepared with two different root-end preparation techniques using SEM; (2) during the evaluation, the largest distance measurements were made at ×150 magnification in both the apical and coronal parts of the cavity; (3) the calculation of total gap measurements using the ImageJ program (National Institutes of Health, Bethesda, MD, USA) on images taken at ×34 magnification. The null hypothesis was that there would be differences in gap formation depending on the type of root-end preparation and filling materials.

## METHODS

The study was ethically approved by the ethics committee of Kocaeli University (KOU GOKAEK 2017/217). The study was performed in accordance with the ethical standards as laid down in the 1964 Declaration of Helsinki. Informed consent (including for publication) was obtained from all individual participants included in the study.

According to a power analysis (G*Power ver. 3.1.9.4; Heinrich Heine University Düsseldorf, Düsseldorf, Germany) with a 0.05 level and 80% power (effect size, 0.40), the total sample size was found to be 90 ($n$ = 15 for each group). Ninety extracted human maxillary central incisor teeth were used. The teeth had been extracted following appropriate consent procedures and were from hospital dental department collections. Teeth with similar root diameter and length, straight roots, complete root development, and no previous root canal treatment were used. Roots with resorption, fractures, open apices, or invisible canals were excluded. The teeth were cut to a root length of 15 mm. Canal patency was established by passing a size 15 K-file (Dentsply


https://doi.org/10.5395/rde.2025.50.e32

Maillefer, Ballaigues, Switzerland) through the apical foramen, from which 0.5 mm was subtracted to obtain the working length.

The root canals were prepared with ProTaper Next instruments (Dentsply Maillefer) using a VDW SILVER endomotor (VDW GmbH, Munich, Germany). The apical foramen was enlarged to an X4 (0.40/.06) instrument. The canals were irrigated with 1 mL of 2.5% NaOCl between instruments, and a final irrigation protocol (17% ethylenediamine tetraacetic acid and then 2.5% NaOCl) was used. The canals were dried with paper points (Dentsply Maillefer) and obturated with gutta-percha (Diadent, Cheongju, Korea) and AHPlus sealer (Dentsply-DeTrey, Konstanz, Germany) using lateral condensation. After obturation, the teeth were stored in an incubator at 37°C and 100% humidity for 1 week to ensure the setting of the sealer. The apical 3 mm of the roots were then resected perpendicular to the long axis with a cylindrical diamond bur (G837/010, DIA.TESSIN; Vanetti SA, Gordevio, Switzerland) at high speed under continuous air/water spray, and the roots were randomly assigned to six groups:

1. US + MTA: root-end cavity preparation with ultrasonic tip, ProRoot MTA root-end filling material
2. US + Biodentine: cavity preparation with ultrasonic tip, Biodentine filling material
3. US + TotalFill: cavity preparation with ultrasonic tip, TotalFill BC RRM filling material
4. Laser + MTA: cavity preparation with laser, ProRoot MTA filling material
5. Laser + Biodentine: cavity preparation with laser, Biodentine filling material
6. Laser + TotalFill: cavity preparation with laser, TotalFill BC RRM filling material

The 3-mm-deep and approximately 1 mm diameter root-end cavities were prepared using ultrasonic and laser tips under 2.5× loupe magnification (Carl Zeiss EyeMag Smart; Carl Zeiss Meditec AG, Jena, Germany) with illumination (SCHOTT AG, Mainz, Germany). A periodontal probe (PCPUNC15; Hu-Friedy, Chicago, IL, USA) helped ensure a standard 3-mm depth.

Ultrasonic preparations involved an electro-medical system unit (EMS miniMaster Piezon; EMS SA, Nyon, Switzerland) with diamond-coated retro tips (DT-060 Berutti; EMS SA, Le Sentier, Switzerland) at medium power, "Endo" mode [15], and maximum water coolant. Laser preparations were performed using an Er,Cr:YSGG laser (Waterlase iPlus/MD Gold; Biolase Inc., Foothill Ranch, CA, USA) with a power setting of 3.5 W, a pulse frequency of 20 Hz, 55% water, and 65% air [15]. A tool with a diameter of 600 mm and a 6-mm MGG6 sapphire tip was used in noncontact mode. Ultrasonic and laser tips were changed after every five teeth, and the preparations were irrigated with saline and dried with paper points.

Filling materials were mixed according to the manufacturer's instructions. ProRoot MTA was mixed with a powder-to-water ratio of 3:1. Biodentine was mixed with five drops of liquid added to the powder in the capsule and prepared by amalgamator for 30 seconds. TotalFill BC RRM was in ready-mixed putty form. The MTA was taken to the cavities using a 1.2-mm carrier (MTA+ Applicator; PPH Cerkamed, Stalowa Wola, Poland), and materials were placed with straight condensers and a VA10 flat plastic (G. Hartzell & Son, Concord, CA, USA). All procedures were conducted by the same operator.

After setting, the roots were prepared longitudinally with burs and with super-fine abrasive paper (400–600 grit) to expose the filling materials, which were viewed under a dental operating microscope. Then the specimens were prepared for SEM (JEOL JCM 6000 Plus; JEOL, Tokyo, Japan). The specimens were dehydrated in ethanol and dried in open air. After drying, each half was mounted on an aluminum stub and sputter-coated with gold at 2 mA and 30 seconds (Cressington 108auto sputter coater; Cressington Scientific Instruments Ltd., Watford, London, UK).

Initially, the distances between the filling materials and cavity walls were measured directly using the SEM (150×) at two points (apical and coronal) of the material/dentin interface. It was recorded as 0 in areas with no gap, and the maximum values were recorded in the apical and coronal regions (Figures 1 and 2).

Next, electron micrographs were obtained at 34× magnification for analysis (ImageJ 1.52a). Calculations were made for each sample regarding the area of the gaps between the filling material and the surrounding structures (dentin and gutta-percha). First, micrographs of the 90 roots were transferred to the computer as JPEGs and opened in ImageJ. Then, the outer surface

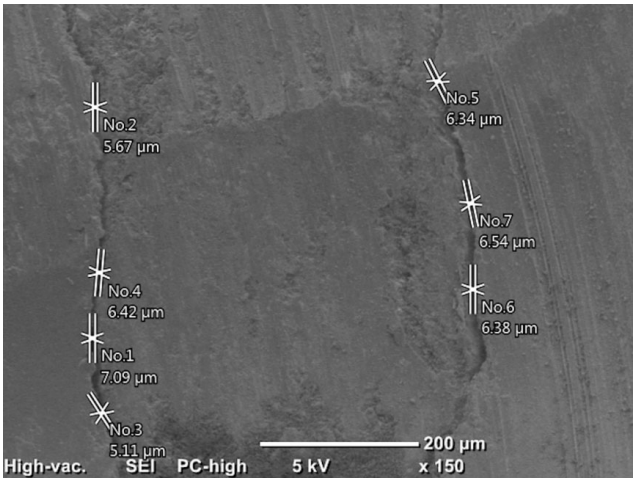


**Figure 1.** An example of measurements made at the coronal region under 150× magnification.

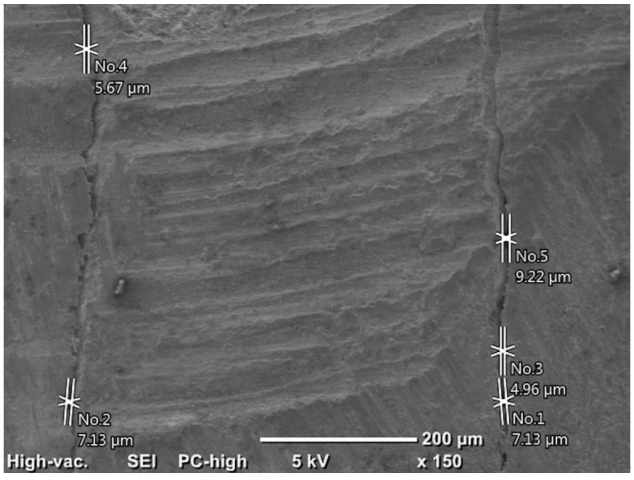


**Figure 2.** An example of measurements made at the apical region under 150× magnification.

area of the cavity was scanned with the Selection/Add to Manager tool (Figure 3). The scanning process was also carried out for the filling material surface area (Figure 4). By calculating the difference between the two areas, the void area between the material and the cavity can be determined. Figure 5 shows an example of cavities prepared with the two devices and filled with ProRootMTA.

NCSS (Number Cruncher Statistical System) 2007 (NCSS LLC, Kaysville, UT, USA) was used for statistical analysis. The suitability of quantitative data for normal distribution was tested using the Shapiro-Wilk test and graphical analysis. An independent groups *t*-test was

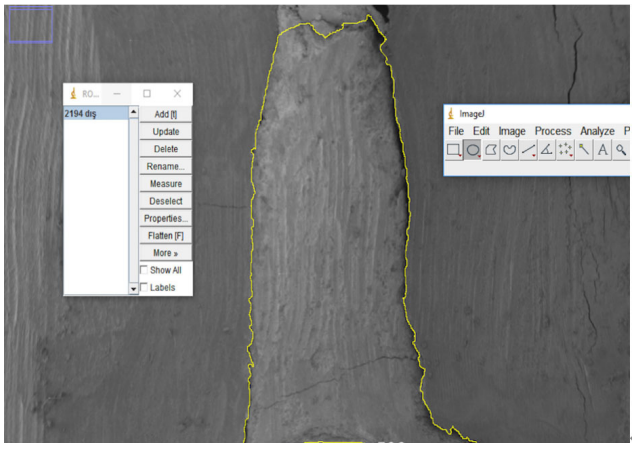


**Figure 3.** Scanning of the cavity outer surface area.

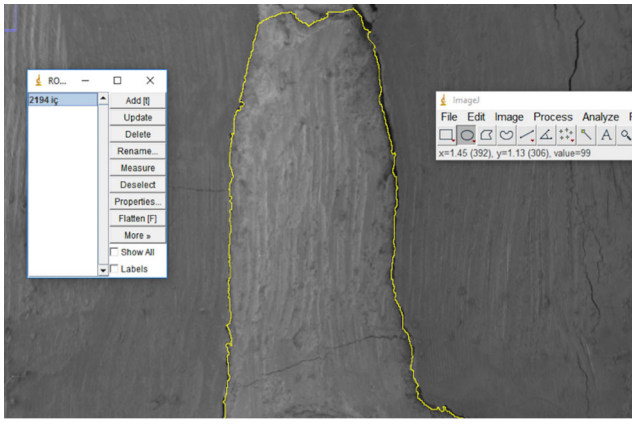


**Figure 4.** Scanning the filling material surface area.

used to compare normally distributed quantitative variables between two groups, and the Mann-Whitney *U* test was used to compare non-normally distributed quantitative variables between two groups. Kruskal-Wallis and Dunn-Bonferroni *post-hoc* tests were used to compare non-normally distributed quantitative variables between more than two groups. Statistical significance was accepted as $p < 0.05$.

## RESULTS

Table 1 shows the maximum distances between filling materials and dentin in the apical and coronal regions (µm). Table 2 shows a comparison of the maximum distance measurement values between root-end filling material and dentin at the coronal and apical regions


https://doi.org/10.5395/rde.2025.50.e32

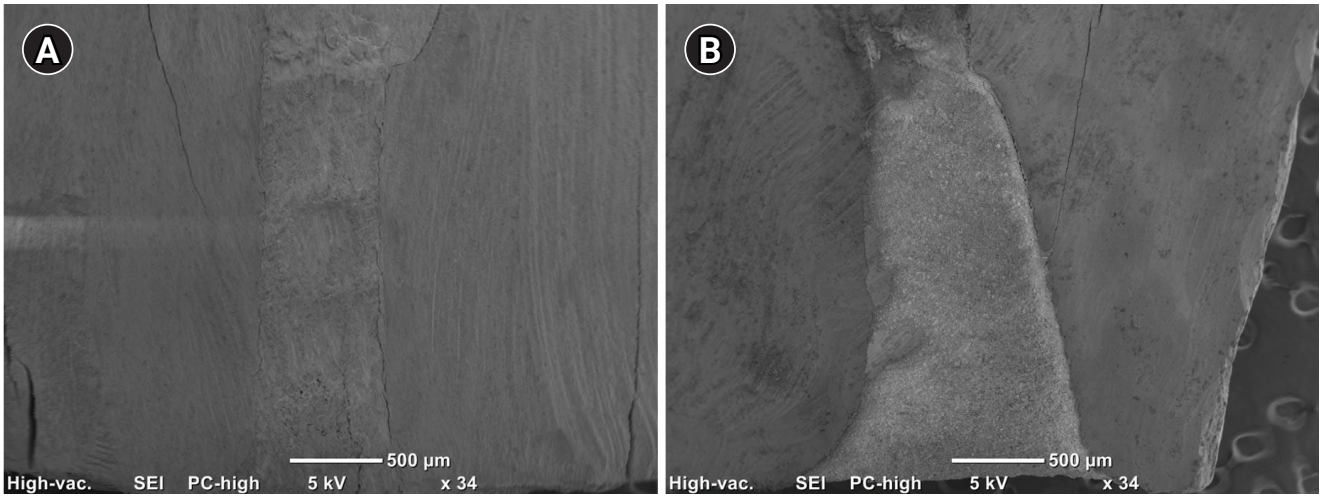


**Figure 5.** Micrographs of ProRoot MTA ultrasonic (A) and laser (B) samples under 34× magnification. ProRoot MTA: Dentsply Tulsa Dental, Tulsa, OK, USA.

**Table 1.** Maximum distance values between material and dentin at the apical and coronal regions for the six groups (µm)

| No. | US + MTA group | | US + Biodentine group | | US + TotalFill group | | Laser + MTA group | | Laser + Biodentine group | | Laser + TotalFill group | |
|---|---|---|---|---|---|---|---|---|---|---|---|---|
| | Coronal | Apical | Coronal | Apical | Coronal | Apical | Coronal | Apical | Coronal | Apical | Coronal | Apical |
| 1 | 4.26 | 5.72 | 6.73 | 10.70 | 2.92 | 3.55 | 10.10 | 13.80 | 5.16 | 5.67 | 10.30 | 8.77 |
| 2 | 4.96 | 7.45 | 7.23 | 18.30 | 0.00 | 7.09 | 0.00 | 0.00 | 4.26 | 4.93 | 7.23 | 11.90 |
| 3 | 14.90 | 21.20 | 5.01 | 9.52 | 4.76 | 7.09 | 0.00 | 8.58 | 4.09 | 7.74 | 2.13 | 0.00 |
| 4 | 5.85 | 5.67 | 7.93 | 5.16 | 3.17 | 3.55 | 7.93 | 6.78 | 7.14 | 6.47 | 4.49 | 6.42 |
| 5 | 5.01 | 7.67 | 5.85 | 8.63 | 5.05 | 8.96 | 6.02 | 5.42 | 8.76 | 11.9 | 5.16 | 12.40 |
| 6 | 9.54 | 9.22 | 21.50 | 16.50 | 4.62 | 2.92 | 7.37 | 11.00 | 3.66 | 4.91 | 5.16 | 3.62 |
| 7 | 6.69 | 7.09 | 10.70 | 20.30 | 17.80 | 3.82 | 0.00 | 0.00 | 9.23 | 9.53 | 7.09 | 11.50 |
| 8 | 3.01 | 7.80 | 10.70 | 10.70 | 2.48 | 19.30 | 7.52 | 7.23 | 5.01 | 4.26 | 8.27 | 5.16 |
| 9 | 5.01 | 5.67 | 3.82 | 8.77 | 4.90 | 5.16 | 7.93 | 8.10 | 5.18 | 5.18 | 4.54 | 5.40 |
| 10 | 4.98 | 5.18 | 4.96 | 7.91 | 5.01 | 6.26 | 3.82 | 0.00 | 5.73 | 4.41 | 3.84 | 9.25 |
| 11 | 0.00 | 0.00 | 11.50 | 31.50 | 3.19 | 2.70 | 7.14 | 2.66 | 10.8 | 11.9 | 3.55 | 4.26 |
| 12 | 6.38 | 7.23 | 12.10 | 26.30 | 4.96 | 7.09 | 6.03 | 6.63 | 9.00 | 10.4 | 0.00 | 0.00 |
| 13 | 5.67 | 7.23 | 8.09 | 8.92 | 3.55 | 3.62 | 5.21 | 8.75 | 5.49 | 5.16 | 7.98 | 6.65 |
| 14 | 17.7 | 4.49 | 22.00 | 22.20 | 2.48 | 3.27 | 4.26 | 5.73 | 0.00 | 0.00 | 4.98 | 5.18 |
| 15 | 5.72 | 7.93 | 11.20 | 11.50 | 17.09 | 7.83 | 3.55 | 7.13 | 0.00 | 0.00 | 2.92 | 4.62 |

US, ultrasonic; MTA, ProRoot MTA; TotalFill, TotalFill BC RRM.
ProRoot MTA: Dentsply Tulsa Dental, Tulsa, OK, USA; Biodentine: Septodont, Saint-Maur-des-Fossés, France; TotalFill BC RRM: FKG Dentaire, La Chaux-de-Fonds, Switzerland.

between groups (µm). The ultrasonic group was significantly higher than the laser group for Biodentine coronally ($p = 0.016$). The Biodentine group was significantly higher than the TotalFill group in root-end cavities prepared with ultrasonic tips ($p = 0.001$). There was no significant difference between groups in the laser cavities ($p > 0.05$). The ultrasonic group was significantly higher than the laser group for Biodentine apically ($p = 0.001$). Biodentine showed significantly greater gap dimensions compared with TotalFill ($p < 0.001$) and ProRoot MTA ($p = 0.007$). There was no significant difference among groups in the laser-prepared cavities ($p > 0.05$).

Table 3 shows the total void area values ($mm^2$) between root-end filling material and dentin calculated using ImageJ software. Table 4 shows a comparison of the total values ($mm^2$) of voids among groups. The ultra-

**Table 2.** Comparison of the maximum distance measurement values between root-end filling material and dentin at the coronal and apical regions among groups (μm)

| Region and method | Total | TotalFill | Biodentine | MTA | *p*-value[a] | *p*-value[b] | | |
|---|---|---|---|---|---|---|---|---|
| | | | | | | TotalFill vs Biodentine | TotalFill vs MTA | Biodentine vs MTA |
| Coronal | | | | | | | | |
| US | 5.05 (4.62–9.054) | 4.62 (2.92–5.01) | 8.09 (5.85–11.5) | 5.67 (4.96–6.69) | 0.002** | 0.001** | 0.269 | 0.205 |
| Laser | 5.16 (3.82–7.37) | 4.98 (3.55–7.23) | 5.18 (4.09–8.76) | 6.02 (3.55–7.52) | 0.836 | 0.999 | 0.999 | 0.999 |
| *p*-value[c] (US vs laser) | 0.281 | 0.367 | 0.016* | 0.87 | | | | |
| Apical | | | | | | | | |
| US | 7.45 (5.18–9.52) | 5.16 (3.55–7.09) | 10.7 (8.77–20.3) | 7.23 (5.67– 7.8) | <0.001** | <0.001** | 0.703 | 0.007** |
| Laser | 5.73 (4.41–8.75) | 5.4 (4.26–9.25) | 5.18 (4.41–9.53) | 6.78 (2.66–8.58) | 0.917 | 0.999 | 0.999 | 0.999 |
| *p*-value[c] (US vs laser) | 0.055 | 0.486 | 0.001** | 0.775 | | | | |

Values are presented as median (interquartile range).
US, ultrasonic; TotalFill, TotalFill BC RRM; MTA, ProRoot MTA.
[a]Kruskal-Wallis test, [b]Dunn-Bonferroni test, [c]Mann-Whitney *U* test.
*$p < 0.05$, **$p < 0.01$.
TotalFill BC RRM: FKG Dentaire, La Chaux-de-Fonds, Switzerland; Biodentine: Septodont, Saint-Maur-des-Fossés, France; ProRoot MTA: Dentsply Tulsa Dental, Tulsa, OK, USA.

**Table 3.** Total void area values between root-end filling material and dentin calculated using ImageJ program ($mm^2$)

| No. | US + MTA group | US + Biodentine group | US + TotalFill group | Laser + MTA group | Laser + Biodentine group | Laser + TotalFill group |
|---|---|---|---|---|---|---|
| 1 | 0.008 | 0.008 | 0.003 | 0.016 | 0.024 | 0.015 |
| 2 | 0.014 | 0.030 | 0.004 | 0.046 | 0.009 | 0.003 |
| 3 | 0.054 | 0.020 | 0.008 | 0.011 | 0.029 | 0.004 |
| 4 | 0.009 | 0.034 | 0.005 | 0.007 | 0.013 | 0.005 |
| 5 | 0.012 | 0.011 | 0.011 | 0.015 | 0.040 | 0.008 |
| 6 | 0.008 | 0.019 | 0.006 | 0.003 | 0.031 | 0.007 |
| 7 | 0.012 | 0.018 | 0.006 | 0.018 | 0.020 | 0.001 |
| 8 | 0.008 | 0.035 | 0.013 | 0.007 | 0.019 | 0.009 |
| 9 | 0.023 | 0.008 | 0.013 | 0.031 | 0.016 | 0.007 |
| 10 | 0.001 | 0.008 | 0.010 | 0.013 | 0.015 | 0.001 |
| 11 | 0.000 | 0.065 | 0.006 | 0.005 | 0.026 | 0.002 |
| 12 | 0.009 | 0.049 | 0.006 | 0.004 | 0.023 | 0.022 |
| 13 | 0.003 | 0.010 | 0.004 | 0.051 | 0.016 | 0.004 |
| 14 | 0.010 | 0.026 | 0.005 | 0.010 | 0.002 | 0.002 |
| 15 | 0.006 | 0.023 | 0.017 | 0.006 | 0.003 | 0.008 |

US, ultrasonic; MTA, ProRoot MTA; TotalFill, TotalFill BC RRM.
ProRoot MTA: Dentsply Tulsa Dental, Tulsa, OK, USA; Biodentine: Septodont, Saint-Maur-des-Fossés, France; TotalFill BC RRM: FKG Dentaire, La Chaux-de-Fonds, Switzerland.

sonic group was significantly higher than the laser group for ProRoot MTA ($p = 0.026$). The Biodentine group was significantly higher than the TotalFill group in root-end cavities prepared with an ultrasonic tip ($p < 0.001$). The Biodentine group was significantly higher than the ProRoot MTA group in root-end cavities prepared with the laser tip ($p = 0.002$). There was no significant difference between the TotalFill and Biodentine groups and the TotalFill ($p = 0.744$) and ProRoot MTA groups ($p = 0.071$) (Table 4).

## DISCUSSION

Marginal adaptation has been defined as the degree of closeness of the filling material to the cavity wall and its interdigitation [12]. Problems with the adaptation might


https://doi.org/10.5395/rde.2025.50.e32

**Table 4.** Comparison of total values ($mm^2$) of void areas between dentin and filling material among groups

| Total gap area | Ultrasonic | Laser | *p*-value[c] (ultrasonic vs laser) |
|---|---|---|---|
| Total | 0.010 (0.006–0.018) | 0.010 (0.005–0.019) | 0.671 |
| TotalFill | 0.006 (0.005–0.011) | 0.011 (0.006–0.018) | 0.081 |
| Biodentine | 0.020 (0.010–0.034) | 0.019 (0.013–0.024) | 0.486 |
| MTA | 0.009 (0.008–0.012) | 0.005 (0.002–0.008) | 0.026 |
| *p*-value[a] | 0.001** | 0.002** | |
| *p*-value[b] | | | |
| TotalFill vs Biodentine | <0.001** | 0.744 | |
| TotalFill vs MTA | 0.549 | 0.071 | |
| Biodentine vs MTA | 0.052 | 0.002** | |

Values are presented as median (interquartile range).
TotalFill, TotalFill BC RRM; MTA, ProRoot MTA.
[a]Kruskal-Wallis test, [b]Dunn-Bonferroni test, [c]Mann-Whitney *U* test.
*$p < 0.05$, **$p < 0.01$.
TotalFill BC RRM: FKG Dentaire, La Chaux-de-Fonds, Switzerland; Biodentine: Septodont, Saint-Maur-des-Fossés, France; ProRoot MTA: Dentsply Tulsa Dental, Tulsa, OK, USA.

lead to treatment failure [16]. Microcracks on the dentin surface, which adversely affect the adaptation process, might occur during ultrasonic cavity preparation [17]; however, this is not a universal finding [18]. Reduction in microcrack formation has been reported at low-to-medium ultrasonic power settings and when using diamond-coated tips [17]. Hence, a medium power setting with diamond-coated tips was preferred in this study. It has been reported that there is no difference in the frequency of microcrack formation when ultrasonic tips and Er:YAG laser are compared [19]. However, in another study, microcrack formation has been observed using ultrasonics, and none has been observed using Er,Cr:YSGG laser [20]. Er,Cr:YSGG laser was also used for root-end preparations to compare the effect of the root-end cavity preparation type on the marginal adaptation in this study.

Several techniques can be used to evaluate the adaptation provided by root-end filling materials and the quality of apical sealing [12]. SEM was used as it provides high magnification and good resolution in this study [13]. However, dehydration and exposure to high vacuum during specimen preparation may lead to cracks or shrinkage in dentin or filling material. To eliminate this, resin replicas can be used. Torabinejad *et al.* [21] found similar results in a related study using this method, but it would have been exhaustive for 90 teeth, and another study has been done without replicas [13,22]. Sections were generally obtained with diamond separators or burs, where forces and vibrations may cause the filling materials to be damaged or displaced [23]. To overcome this, guiding notches on the root surfaces were cut with a diamond separator, about 1 mm away from the root-end material. The thin dentin layer was then removed under the dental operating microscope by careful sanding.

Gondim *et al.* [14] stated that quantitative analysis based on measurement provides more objective and reliable results. The images were taken at two different magnifications: 34× and 150×. The maximum value was recorded from the distance measurements between dentin and filling material on micrographs taken at the apical 1 mm and coronal 1 mm at 150× magnification. For the micrographs at 34×, quantitative measurements were made by calculating the area with ImageJ.

For Biodentine, the gap formation in the ultrasonic group was significantly higher than in the laser group. In contrast, the other two materials did not show a significant difference between cavity techniques. In the area measurements of gaps using the ImageJ program, the ultrasonic group for ProRoot MTA was significantly higher than the laser group. This may be explained by the fact that the use of an Er,Cr:YSGG laser can increase the mechanical bonding between the dentin wall and root-end material by forming micro retentive areas and by removing the smear layer [24,25]. The difference in the results of these two measurement methods may be because when calculating the total area of the voids in

the root-end cavity with the ImageJ program, the highest single distance measurement between the filling material and dentin on the SEM images taken from the apical and coronal regions was taken into account.

Using SEM, Xavier *et al*. [22] examined the marginal adaptation of MTA Angelus (Angelus, Londrina, Brazil), Super-EBA (Bosworth, Skokie, IL, USA), and Vitremer (3M ESPE, St. Paul, MN, USA) in ultrasonically prepared cavities. Gap measurements of two different sections having 1 mm thickness, taken horizontally at 1 and 2 mm from the apex, were made at four different points under SEM. A study by Torabinejad *et al*. [21] prepared cavities using fissure burs and used MTA, amalgam, Super-EBA, and IRM (Dentsply Sirona, York, PA, USA) as fillings and examined marginal adaptation with SEM. Replicas of the vertical cuts of the samples were made with resin, and the gaps of both the teeth and the replicas were examined at four different points. However, the maximum values were recorded in the apical and coronal regions in this study in accordance with Soundappan *et al*. [26]. The cavities were prepared ultrasonically, and Biodentine, MTA, and IRM were used as filling materials. Two horizontal sections were taken, 1 and 2 mm from the apex. The horizontal sections were divided into four equal parts, and under 1,000× magnification, the most significant gaps were measured in each quarter. The greatest gap formation was seen in Biodentine, and the least in the MTA group. In contrast, in this study, more gap formation was detected in the Biodentine group compared to the MTA group. Ravi Chandra *et al*. [27] examined the marginal adaptation of a GIC, MTA, and Biodentine in ultrasonically prepared cavities using confocal laser scanning microscopy. Better marginal adaptation was detected in the Biodentine group than in GIC and MTA. The differences between the results of this study may be due to the differences in imaging technique and the section examined.

Khandelwal *et al*. [28] used dye penetration to examine microleakage of Biodentine and MTA in root-end cavities prepared using a conventional drill and ultrasonic tip. The greatest amount of microleakage was observed in MTA in cavities opened with a bur. Biodentine's high-quality sealing properties were associated with the creation of an alkaline caustic effect when the hydration products of calcium silicate cement come in contact with dentin and dissolve the collagen structure at the dentin interface. This effect results in the formation of a tag-like structure called 'mineral infiltration zone,' and with its adaptation ability due to its smaller particle size. Han and Okiji [29] showed that the uptake of calcium and silicon ions into dentin, which leads to these tag-like structures, was higher in Biodentine compared to MTA. In addition, its short hardening time, ease of manipulation, non-discolouration, and good sealing properties lead to Biodentine being a preferred material [10,26].

TotalFill RRM was introduced under the trade name EndoSequence RRM (Brasseler USA Dental, Savannah, GA, USA) as a premixed bioceramic root-end filling material. TotalFill and EndoSequence have the same properties and form [30]. Endodontic bioceramics are not sensitive to moisture and blood. They are dimensionally stable and expand slightly on setting. The initial setting time of MTA and TotalFill BC RRM putty is approximately 3 to 4 hours, while the setting time of Biodentine is approximately 10 to 12 minutes. Handling properties of TotalFill BC RRM putty are better than others [11].

Alanezi *et al*. [31] examined the bacterial microleakage of EndoSequence BC RRM and ProRoot MTA using *Enterococcus faecalis*. The materials were placed in cavities prepared using a KiS ultrasonic tip. No difference was observed between the fillings. Shokouhinejad *et al*. [32] examined the marginal adaptations of EndoSequence RRM putty, EndoSequence RRM paste, and ProRoot MTA in ultrasonically prepared cavities using SEM. After hardening, replicas of the horizontal and vertical sections of the teeth were taken. No significant difference was observed between the groups for the horizontal cross-section. In the vertical section, EndoSequence paste was reported to have significantly more voids. Lertmalapong *et al*. [33] examined the marginal adaptation of ProRoot MTA, RetroMTA, Biodentine, and TotalFill BC RRM's putty and paste forms in the treatment of teeth with open apices, placing materials at two different levels of thickness, 3 and 4 mm. Resin replicas were made and imaged with SEM, and then studied with the ImageJ program. Biodentine, TotalFill BC RRM putty, and 4 mm ProRoot MTA groups had fewer voids than the other groups. However, the external surface area of the cavity and the surface areas of the filling materials


https://doi.org/10.5395/rde.2025.50.e32

were measured separately and then calculated by taking the differences in this study, and the cavities opened ultrasonically had a greater void area in the Biodentine group than in the TotalFill group.

## CONCLUSIONS

Under the conditions of this *in vitro* study, when evaluating total void, choosing a laser instead of ultrasound for root-end preparation resulted in a smaller gap between material and dentin if MTA was used. When the root-end cavity was prepared with ultrasonics, it was observed that more gap formation occurred with Biodentine compared to TotalFill; when the cavity was prepared with laser, it was observed that more gap formation occurred with Biodentine compared to MTA. Further clinical studies are needed to evaluate the success of different root-end preparation techniques and filling materials.

### CONFLICT OF INTEREST

No potential conflict of interest relevant to this article was reported.

### FUNDING/SUPPORT

The authors have no financial relationships relevant to this article to disclose.

### AUTHOR CONTRIBUTIONS

Conceptualization: Zengin B, Aydemir S. Data curation, Investigation, Project administration: Zengin B. Formal analysis: all authors. Methodology: Aydemir S. Writing - original draft: all authors. Writing - review & editing: all authors. All authors read and approved the final manuscript.

### DATA SHARING STATEMENT

All data supporting the findings of this study are available within the article and its supplementary materials.

## REFERENCES

1. Lazarski MP, Walker WA, Flores CM, Schindler WG, Hargreaves KM. Epidemiological evaluation of the outcomes of nonsurgical root canal treatment in a large cohort of insured dental patients. J Endod 2001;27:791-796.
2. Gutmann JL. Surgical endodontics: past, present, and future. Endod Top 2014;30:29-43.
3. Kim S. Principles of endodontic microsurgery. Dent Clin North Am 1997;41:481-497.
4. Rotstein I, Ingle JI. Ingle's endodontics. 7th ed. Raleigh, NC, USA: PMPH-USA Ltd.; 2019.
5. Miserendino LJ. The laser apicoectomy: endodontic application of the CO2 laser for periapical surgery. Oral Surg Oral Med Oral Pathol 1988;66:615-619.
6. Angiero F, Benedicenti S, Signore A, Parker S, Crippa R. Apicoectomies with the erbium laser: a complementary technique for retrograde endodontic treatment. Photomed Laser Surg 2011;29:845-849.
7. Komori T, Yokoyama K, Takato T, Matsumoto K. Clinical application of the erbium:YAG laser for apicoectomy. J Endod 1997;23:748-750.
8. Gouw-Soares S, Tanji E, Haypek P, Cardoso W, Eduardo CP. The use of Er:YAG, Nd:YAG and Ga-Al-As lasers in periapical surgery: a 3-year clinical study. J Clin Laser Med Surg 2001;19:193-198.
9. Torabinejad M, Watson TF, Pitt Ford TR. Sealing ability of a mineral trioxide aggregate when used as a root end filling material. J Endod 1993;19:591-595.
10. Rajasekharan S, Martens LC, Cauwels RG, Verbeeck RM. Biodentine™ material characteristics and clinical applications: a review of the literature. Eur Arch Paediatr Dent 2014;15:147-158.
11. Trope M, Bunes A, Debelian G. Root filling materials and techniques: bioceramics a new hope? Endod Top 2015;32:86-96.
12. Torabinejad M, Lee SJ, Hong CU. Apical marginal adaptation of orthograde and retrograde root end fillings: a dye leakage and scanning electron microscopic study. J Endod 1994;20:402-407.
13. Küçükkaya Eren S, Görduysus MÖ, Şahin C. Sealing ability and adaptation of root-end filling materials in cavities prepared with different techniques. Microsc Res Tech 2017;80:756-762.
14. Gondim E, Zaia AA, Gomes BP, Ferraz CC, Teixeira FB, Souza-Filho FJ. Investigation of the marginal adaptation of root-end filling materials in root-end cavities prepared with ultrasonic tips. Int Endod J 2003;36:491-499.
15. Batista de Faria-Junior N, Tanomaru-Filho M, Guerreiro-Tanomaru JM, de Toledo Leonardo R, Camargo Villela Berbert FL. Evaluation of ultrasonic and ErCr:YSGG laser retrograde cavity preparation. J Endod 2009;35:741-744.
16. Saunders WP, Saunders EM, Gutmann JL. Ultrasonic root-

end preparation, Part 2. Microleakage of EBA root-end fillings. Int Endod J 1994;27:325-329.
17. Layton CA, Marshall JG, Morgan LA, Baumgartner JC. Evaluation of cracks associated with ultrasonic root-end preparation. J Endod 1996;22:157-160.
18. Waplington M, Lumley PJ, Walmsley AD, Blunt L. Cutting ability of an ultrasonic retrograde cavity preparation instrument. Endod Dent Traumatol 1995;11:177-180.
19. Aydemir S, Cimilli H, Mumcu G, Chandler N, Kartal N. Crack formation on resected root surfaces subjected to conventional, ultrasonic, and laser root-end cavity preparation. Photomed Laser Surg 2014;32:351-355.
20. Wallace JA. Effect of Waterlase laser retrograde root-end cavity preparation on the integrity of root apices of extracted teeth as demonstrated by light microscopy. Aust Endod J 2006;32:35-39.
21. Torabinejad M, Smith PW, Kettering JD, Pitt Ford TR. Comparative investigation of marginal adaptation of mineral trioxide aggregate and other commonly used root-end filling materials. J Endod 1995;21:295-299.
22. Xavier CB, Weismann R, de Oliveira MG, Demarco FF, Pozza DH. Root-end filling materials: apical microleakage and marginal adaptation. J Endod 2005;31:539-542.
23. Bidar M, Moradi S, Jafarzadeh H, Bidad S. Comparative SEM study of the marginal adaptation of white and grey MTA and Portland cement. Aust Endod J 2007;33:2-6.
24. Pécora JD, Cussioli AL, Guerişoli DM, Marchesan MA, Sousa-Neto MD, Brugnera Júnior A. Evaluation of Er:YAG laser and EDTAC on dentin adhesion of six endodontic sealers. Braz Dent J 2001;12:27-30.
25. Karlovic Z, Pezelj-Ribaric S, Miletic I, Jukic S, Grgurevic J, Anic I. Erbium:YAG laser versus ultrasonic in preparation of root-end cavities. J Endod 2005;31:821-823.
26. Soundappan S, Sundaramurthy JL, Raghu S, Natanasabapathy V. Biodentine versus mineral trioxide aggregate versus ıntermediate restorative material for retrograde root end filling: an ınvitro study. J Dent (Tehran) 2014;11:143-149.
27. Ravi Chandra PV, Vemisetty H, Deepti K, Reddy SJ, Ramkiran D, Krishna MJN, *et al*. Comparative evaluation of marginal adaptation of biodentine(TM) and other commonly used root end filling materials-an ınvitro study. J Clin Diagn Res 2014;8:243-245.
28. Khandelwal A, Karthik J, Nadig RR, Jain A. Sealing ability of mineral trioxide aggregate and Biodentine as root end filling material, using two different retro preparation techniques: an in vitro study. Int J Contemp Dent Med Rev 2015;2015:150115.
29. Han L, Okiji T. Uptake of calcium and silicon released from calcium silicate-based endodontic materials into root canal dentine. Int Endod J 2011;44:1081-1087.
30. Koch K, Brave D, Ali Nasseh A. A review of bioceramic technology in endodontics. Roots 2013;1:6-13.
31. Alanezi AZ, Jiang J, Safavi KE, Spangberg LS, Zhu Q. Cytotoxicity evaluation of endosequence root repair material. Oral Surg Oral Med Oral Pathol Oral Radiol Endod 2010;109:e122-e125.
32. Shokouhinejad N, Nekoofar MH, Ashoftehyazdi K, Zahraee S, Khoshkhounejad M. Marginal adaptation of new bioceramic materials and mineral trioxide aggregate: a scanning electron microscopy study. Iran Endod J 2014;9:144-148.
33. Lertmalapong P, Jantarat J, Srisatjaluk RL, Komoltri C. Bacterial leakage and marginal adaptation of various bioceramics as apical plug in open apex model. J Investig Clin Dent 2019;10:e12371.


https://doi.org/10.5395/rde.2025.50.e32

RDE Restorative Dentistry & Endodontics

Research Article

eISSN 2234-7666
Restor Dent Endod. 2025 November;50(4):e33
https://doi.org/10.5395/rde.2025.50.e33

# The influence of bioactive glass (BGS-7) on enamel remineralization: an *in vitro* study

Chaeyoung Lee[1], Eunseon Jeong[1], Kun-Hwa Sung[1,2], Su-Jung Park[1,2], Yoorina Choi[1,2,*]

[1]Department of Conservative Dentistry, School of Dentistry, Wonkwang University, Iksan, Korea
[2]Wonkwang Dental Research Institute, School of Dentistry, Wonkwang University, Iksan, Korea

## ABSTRACT

**Objectives:** The aim of this study was to compare the remineralizing capacity of bioactive glass (BGS-7, CGBIO) with other agents.

**Methods:** Twenty caries-free third molars were sectioned and demineralized. Specimens were divided into four groups: (1) control, (2) Clinpro XT varnish (Solventum), (3) 1.23% acidulated phosphate fluoride gel, and (4) a new type of $CaO$-$SiO_2$-$P_2O_5$-$B_2O_3$ system of bioactive glass ceramics (BGS-7). Agents were applied and stored in simulated body fluid at 37°C for 2 weeks. Microhardness was measured using the Vickers hardness testing method. Five specimens per group were analyzed using quantitative light-induced fluorescence (QLF) to assess mineral loss. Field-emission scanning electron microscopy (FE-SEM) and energy-dispersive X-ray spectroscopy (EDS) were used to examine the surface morphology and elemental composition. Data were analyzed using paired t-test and one-way analysis of variance ($p < 0.05$).

**Results:** BGS-7 showed the highest microhardness values and the greatest recovery in QLF analysis ($p < 0.05$). FE-SEM revealed granular precipitates on demineralized enamel in the BGS-7 group. EDS confirmed the presence of newly formed silicon and fluoride layers.

**Conclusions:** BGS-7 demonstrated superior remineralization capacity compared to other agents, suggesting its potential as an effective remineralizing material.

**Keywords:** Bioactive glass; Dental enamel; Quantitative light-induced fluorescence; Tooth demineralization; Tooth remineralization

## INTRODUCTION

When enamel is exposed for a prolonged period to an acidic environment, such as that found in caries, an imbalance between the demineralization and remineralization processes occurs, causing the cycle to shift toward demineralization. Meanwhile, remineralization is a natural repair process that primarily relies on the deposition of calcium phosphate, mainly sourced from saliva, to form a new layer on the damaged surface [1].

**Received:** March 28, 2025 **Revised:** July 15, 2025 **Accepted:** July 20, 2025

**Citation**
Lee C, Jeong E, Sung KH, Park SJ, Choi Y. The influence of bioactive glass (BGS-7) on enamel remineralization: an *in vitro* study. Restor Dent Endod 2025;50(4):e33.

***Correspondence to**
**Yoorina Choi, DDS, PhD**
Department of Conservative Dentistry, School of Dentistry, Wonkwang University, 895 Muwang-ro, Iksan 54538, Korea
Email: dbflsk@wku.ac.kr

Modern strategies for managing caries focus on halting its progression [2]. This remineralization process of enamel can be promoted by using several topical remineralizing agents [3].

Fluoride has been a cornerstone in enamel remineralization for many years, primarily working to prevent caries by inhibiting demineralization and promoting the formation of fluorapatite on the enamel surface. Fluorapatite is less soluble, therefore increasing the resistance of enamel to dissolution relative to hydroxyapatite during acid attack [4]. But its long-term viability and sustainable effects are still controversial.

Clinpro XT varnish (Solventum, St. Paul, MN, USA) is a professional fluoride varnish that is formulated to release fluoride more efficiently and maintain its release over a longer period compared to fluoride gels. While fluoride gels typically require multiple applications to provide significant fluoride absorption, Clinpro XT varnish's unique delivery system allows for more effective and sustained fluoride uptake. This ensures prolonged protection against tooth decay, especially in patients at high risk for caries [5].

Nevertheless, the maximum effectiveness of fluoride-based products in the treatment and prevention of dental caries remains limited, as their remineralizing effects are predominantly confined to the enamel surface and are insufficient to fully restore deeper or advanced carious lesions [6]. As a result, it is necessary to incorporate other agents into remineralization therapy, such as bioactive materials, which can boost remineralization when combined with fluoride and serve as a complement to it [7,8].

Bioactive glass has been developed in various forms and has been widely studied for its favorable properties as a restorative material, particularly its ability to promote enamel and dentin remineralization [6,9–11]. Numerous studies and reviews have reported that bioactive glass can enhance the remineralization of carious lesions by forming an apatite-like layer on tooth surfaces [6]. BGS-7 ($CaO$-$SiO_2$-$P_2O_5$-$B_2O_3$; CGBIO, Seoul, Korea) is a novel bioactive glass-ceramic with a composition distinct from existing bioactive glasses, but research on its application for enamel remineralization is still limited. Therefore, this study aimed to evaluate the remineralizing effect of BGS-7 on demineralized enamel. The null hypothesis was that BGS-7 would not show superior remineralization capacity compared to other remineralizing agents.

## METHODS

The products used in this study are listed in Table 1, and the overall experimental procedures are illustrated in Figure 1. The specific materials and methods are described below.

### Specimen preparation and demineralization treatment

The study protocol was approved by the Institutional Review Board of Wonkwang Dental Hospital, Iksan, Korea (WKDIRB202409-02). Twenty caries-free extracted human third molars were selected. The roots of the teeth were removed at the cementoenamel junction, and the crown was sectioned mesiodistally into two parts. The sections were embedded in acrylic resin (Ortho-Jet; Lang Dental Manufacturing Co., Wheeling, IL, USA) with the exposed enamel surface, and then the enamel surface was ground flat and polished with water-cooled 400, 600, 1,200 grit silicon carbide discs (DEERFOS Co., Seoul, Korea). Phosphoric acid (37%) was applied on the enamel surfaces for 20 minutes to form a demineralized lesion [12].

**Table 1.** Composition of the materials

| Material | Product and manufacturer | Composition |
|---|---|---|
| Clinpro-XT varnish | Solventum, St. Paul, MN, USA | Part A: silanized fluoroaluminosilicate, HEMA, water, BIS-GMA, silanized silica<br>Part B: copolymer of polyalkenoic acid, water, HEMA, calcium glycerophosphate |
| Fluoride gel | Natural-F Gel, Denbio, Gwangju, Korea | 1.23% Acidulated phosphate fluoride |
| BGS-7 | CGBIO, Seoul, Korea | 43.3% CaO, 35.2% $SiO_2$, 14.0% $P_2O_5$, 6.42% MgO, 0.52% $B_2O_3$, >99%, <6 μm |

HEMA, 2-hydroxyethyl methacrylate; BIS-GMA, bisphenol A-glycidyl methacrylate.


https://doi.org/10.5395/rde.2025.50.e33

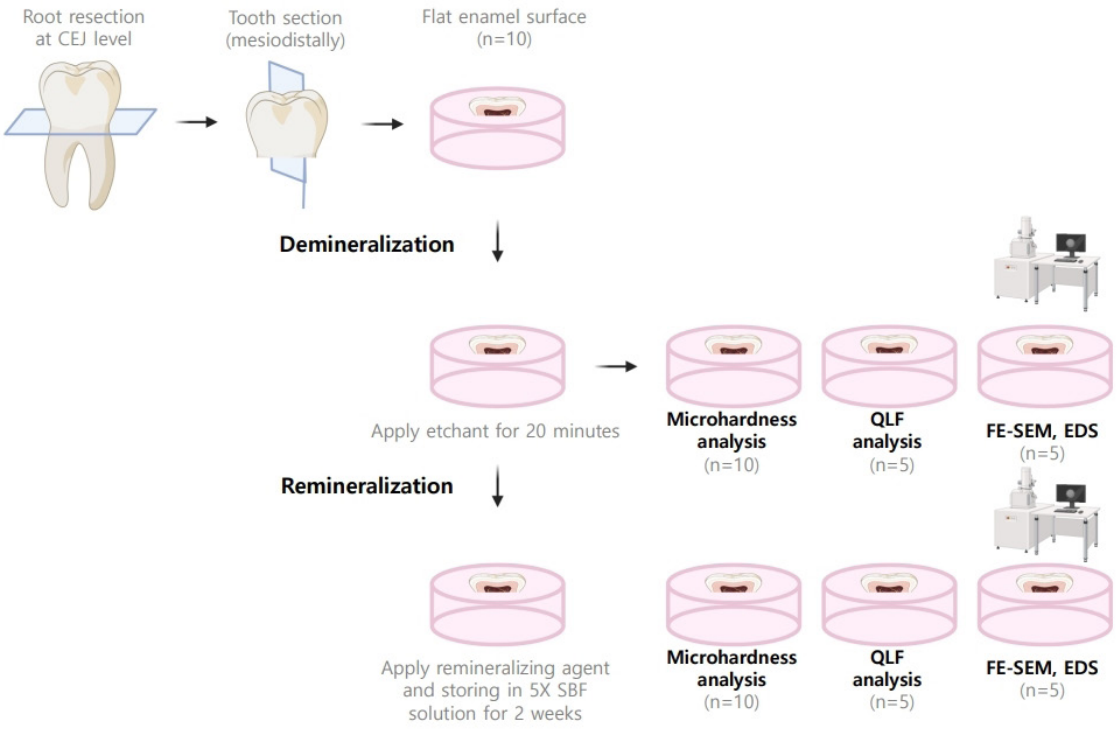


**Figure 1.** Schematic diagram of the study design and methodology. CEJ, cementoenamel junction; QLF, quantitative light-induced fluorescence; FE-SEM, field-emission scanning electron microscopy; EDS, energy-dispersive X-ray spectroscopy; SBF, simulated body fluid.

### Remineralization treatment

Four experimental groups were assigned according to treatment modalities. All specimens were divided randomly into four groups ($n$ = 10): (1) control, no application of remineralizing agent, (2) Clinpro XT varnish (group XT), (3) 1.23% APF gel (Natural-F Gel, Denbio, Gwangju, Korea; group FG), and (4) BGS-7 (group B7). After the demineralization procedure, the specimens received the following remineralizing treatments:

- Control group: No remineralizing agent was applied after demineralization.
- Group XT: Clinpro XT varnish was applied according to the manufacturer's instructions. It was applied to the enamel surface once, light-cured for 20 seconds, and then rinsed with deionized water for 30 seconds.
- Group FG: Fluoride gel was applied daily for 14 days, with each application lasting 4 minutes. Thirty minutes after each application, the specimens were carefully rinsed with deionized water for 30 seconds, according to the manufacturer's instructions.
- Group B7: A 1:1 mixture of BGS-7 and distilled water was applied to the enamel surface once for 2 hours, followed by rinsing with deionized water for 30 seconds.

Subsequently, all specimens from the four groups were stored in simulated body fluid (SBF) (Biochemazone, Edmonton, AB, Canada) at 37°C for 2 weeks.

### Surface microhardness test

All specimens were air-dried at room temperature and used for the microhardness test. The surface microhardness of the specimens was measured with a Vickers microhardness (VHN) tester (HM-122, Mitutoyo Corp, Kawasaki, Japan) at two stages: after demineralization and after remineralization. A load of 100 g was applied to the surface for 10 seconds. The average value was determined. Each group was measured at 10 different points, with each point spaced at a constant distance from the others. The difference between $VHN_{remin}$ and $VHN_{demin}$ (ΔVHN) was calculated to evaluate the remineralization effect of materials [12].

### Quantitative light-induced fluorescence measurement

Quantitative light-induced fluorescence (QLF) was performed to quantitatively assess the degree of enamel demineralization and remineralization by measuring changes in fluorescence [13]. Five specimens of each group were used for QLF. All specimens were assessed by using the Qraypen C device based on QLF technology (AIOBIO, Seoul, Korea). Before imaging, specimens were washed with distilled water and dried sufficiently with compressed air for 5 seconds, and then imaging was performed. The amount for fluorescence loss of the specimen was measured using Qray software (AIOBIO) by measuring ΔF (%), which indicates the amount of fluorescence loss, and ΔF max, which indicates the amount of the most severe fluorescence loss compared to the sound surface in the fluorescence image. Recovery amount and recovery rate were calculated as follows:

Recovery amount ($\Delta(\Delta(F))$) = $\Delta F_{remin} - \Delta F_{demin}$

Recovery rate ($\Delta F(rate)$) = $(\Delta F_{remin}-\Delta F_{demin})/\Delta F_{demin} \times 100$

### Field-emission scanning electron microscopy/energy-dispersive X-ray spectroscopy analysis

To complete the preparation process, the specimens were dehydrated using ethanol solutions (25%, 50%, 75%, 95%, and 100%) for various durations (20, 20, 20, 30, and 60 minutes). After dehydration, the specimens were examined under a field-emission scanning electron microscope (FE-SEM; S-4800, Hitachi, Tokyo, Japan) equipped with a secondary electron detector for energy-dispersive X-ray analysis (EDS) using an accelerating voltage of 6.0 kV. Images were obtained from the center of each specimen with a magnification of ×5,000 and ×25,000. The same specimens were characterized using the EDS for calcium, phosphorus, fluoride, and silicon.

### Statistical analysis

All data are expressed as the mean ± standard deviation. Paired t-test was utilized to compare the ΔVHN and ΔF of the specimens between values before and after remineralization within the group. One-way analysis of variance was used for comparison of enamel microhardness and amount of fluorescence loss of four groups ($p < 0.05$). All statistical analyses were performed using IBM SPSS version 25.0 (IBM Corp, Armonk, NY, USA). Differences were considered statistically significant at $p < 0.05$.

## RESULTS

### Surface microhardness test

Microhardness values of all groups are shown in Table 2. Among all groups, group B7 exhibited the highest ΔVHN value (58.57 ± 3.79), followed by group XT (49.22 ± 4.68), group FG (36.46 ± 2.66), and control group (0.45 ± 0.35). Statistically significant differences were observed among all groups ($p < 0.05$).

### Quantitative light-induced fluorescence measurement

The results of QLF measurement of all groups are shown in Table 3. The recovery amount and rate were calculated by comparing ΔF values, which reflect fluorescence changes due to enamel demineralization, before and after remineralizing treatment. The recovery amount and rate of group B7 were significantly higher than those of the other groups ($p < 0.05$). Group B7 exhibited the highest recovery amount and rate (1.66 ± 0.11 and 25.58

**Table 2.** Vickers microhardness values (VHN) of the experimental groups

| Group | $VHN_{demin}$ | $VHN_{remin}$ | ΔVHN |
|---|---|---|---|
| Control | $89.54 \pm 5.98^{A}$ | $89.99 \pm 6.00^{D}$ | $0.45 \pm 0.35^{D}$ |
| XT | $84.19 \pm 3.35^{B}$ | $133.41 \pm 2.56^{B}$ | $49.22 \pm 4.68^{B}$ |
| FG | $86.28 \pm 3.02^{A,B}$ | $123.04 \pm 3.83^{C}$ | $36.46 \pm 2.66^{C}$ |
| B7 | $85.97 \pm 3.26^{A,B}$ | $144.54 \pm 2.48^{A}$ | $58.57 \pm 3.79^{A}$ |

Values are presented as mean ± standard deviation.
Group definitions are provided in Table 1.
*Different uppercase letters indicate significant differences between the values in each column (between materials; $p < 0.05$).

**Table 3.** Mean amount of fluorescence loss (ΔF) of the experimental groups

| Group | $\Delta F_{demin}$ | $\Delta F_{remin}$ | Δ (ΔF) | ΔF (rate) |
|---|---|---|---|---|
| Control | $-6.46 \pm 0.11^{A}$ | $-6.32 \pm 0.13^{C}$ | $0.14 \pm 0.05^{D}$ | $2.17 \pm 0.85^{D}$ |
| XT | $-6.66 \pm 0.29^{A}$ | $-5.63 \pm 0.40^{B}$ | $1.04 \pm 0.12^{B}$ | $15.63 \pm 2.43^{B}$ |
| FG | $-6.34 \pm 0.18^{A}$ | $-5.88 \pm 0.24^{B,C}$ | $0.46 \pm 0.11^{C}$ | $7.27 \pm 1.90^{C}$ |
| B7 | $-6.5 \pm 0.16^{A}$ | $-4.84 \pm 0.26^{A}$ | $1.66 \pm 0.11^{A}$ | $25.58 \pm 2.28^{A}$ |

Values are presented as mean ± standard deviation.
Group definitions are provided in Table 1.
*Different uppercase letters indicate significant differences between the values in each column (between materials; $p < 0.05$).


https://doi.org/10.5395/rde.2025.50.e33

± 2.28, respectively), followed by group XT (1.04 ± 0.12 and 15.63 ± 2.43), group FG (0.46 ± 0.11 and 7.27 ± 1.90), and the control group (0.14 ± 0.05 and 2.17 ± 0.85). Statistically significant differences were observed among all groups ($p < 0.05$).

### Field-emission scanning electron microscopy/energy-dispersive X-ray spectroscopy analysis

#### 1. FE-SEM observation

FE-SEM images revealed distinct differences among the groups after remineralization treatment and 2 weeks of storage in SBF. In the control group, as shown in Figure 2A and B, typical features of demineralized enamel were observed, such as surface porosity with loss of enamel prism cores while retaining the periphery. In contrast, groups XT (Figure 2C, D) and FG (Figure 2E, F) showed the deposition of granular precipitates on the enamel surface. Notably, in group B7, dense granular precipitates were observed on the enamel surface (Figure 2G), and at higher magnification, characteristic needle-like crystallites were prominently observed (Figure 2H), suggesting advanced remineralization and the formation of an apatite-like layer.

#### 2. Energy-dispersive X-ray spectroscopy analysis

The results of EDS analysis of all groups of enamel specimens stored in SBF for 2 weeks are shown in Figure 3. Control group (Figure 3A) showed elemental composition consistent with demineralized enamel (Ca: 67.72%, P: 32.28%; Ca/P ratio: 2.1). Group XT (Figure 3B) showed composition primarily of calcium (66.10%) and phosphorus (33.90%) without detectable fluoride or silicon. Group FG (Figure 3C) revealed fluoride incorporation (3.75 weight percent [wt%]) along with calcium (64.35%) and phosphorus (31.89%). Group B7, in Figure 3D, showed silicon presence (5.53 wt%) from bioactive glass and fluoride content (3.01 wt%), along with calcium (65.95%) and phosphorus (25.51%).

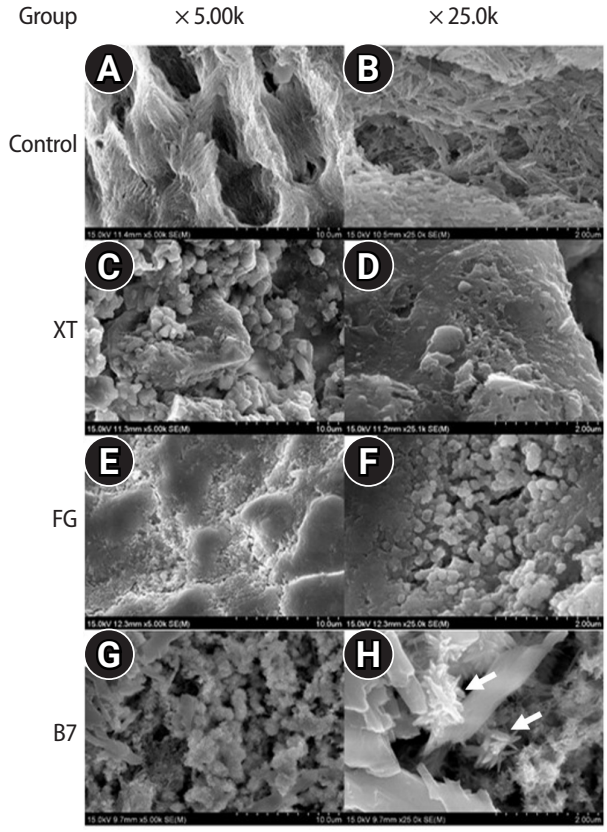


**Figure 2.** Representative field-emission scanning electron microscopy (SEM) images of all the experimental groups in this study (A, C, E, G: ×5,000; B, D, F, H: ×25,000). SEM images of enamel specimens stored in simulated body fluid for 2 weeks. (A, B) Control group: The smear layer was removed, and eroded enamel rods were observed. (C, D) Group XT and (E, F) group FG: granular precipitates were observed around the enamel rods. (G, H) Group B7: dense granular precipitate formation (G), and at higher magnification, characteristic needle-like crystallites (white arrows) were prominently observed (H). Group definitions are provided in Table 1.

## DISCUSSION

Based on the results of this study, the null hypothesis was rejected. In both surface microhardness and QLF measurements, BGS-7 demonstrated the highest values, followed by the XT, FG, and control groups, respectively, with statistically significant differences observed among all groups ($p < 0.05$) (Tables 2 and 3). These findings are consistent with previous studies, which have demonstrated that enamel surfaces treated with bioactive glass exhibit significantly greater surface microhardness recovery compared to other remineralizing agents such as fluoride or casein phosphopeptide (CPP)- amorphous calcium phosphate (ACP) [11,14]. Meanwhile, the higher microhardness recovery and fluorescence recovery rates observed for the XT varnish compared to the fluoride group are presumed to be due to the prolonged and stable fluoride release provided by its resin-modified glass ionomer (RMGI) formulation.

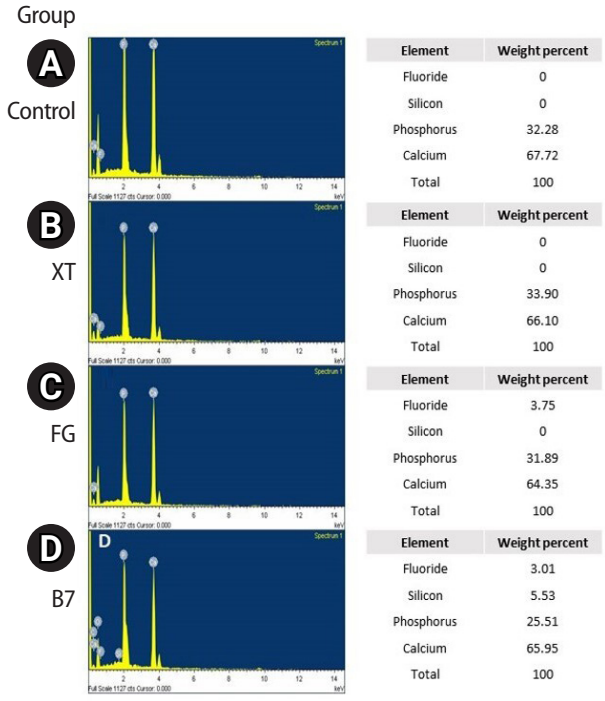


| Element | Weight percent |
|---|---|
| Fluoride | 0 |
| Silicon | 0 |
| Phosphorus | 32.28 |
| Calcium | 67.72 |
| Total | 100 |

| Element | Weight percent |
|---|---|
| Fluoride | 0 |
| Silicon | 0 |
| Phosphorus | 33.90 |
| Calcium | 66.10 |
| Total | 100 |

| Element | Weight percent |
|---|---|
| Fluoride | 3.75 |
| Silicon | 0 |
| Phosphorus | 31.89 |
| Calcium | 64.35 |
| Total | 100 |

| Element | Weight percent |
|---|---|
| Fluoride | 3.01 |
| Silicon | 5.53 |
| Phosphorus | 25.51 |
| Calcium | 65.95 |
| Total | 100 |

**Figure 3.** Energy-dispersive X-ray spectroscopy analysis of enamel specimens stored in simulated body fluid for 2 weeks. (A) Control group showed elemental composition consistent with demineralized enamel (Ca, 67.72%; P, 32.28%; Ca/P ratio, 2.1). (B) Group XT showed a composition primarily of calcium and phosphorus, without detectable fluoride or silicon. (C) Group FG revealed fluoride incorporation along with calcium and phosphorus. (D) Group B7 showed the presence of both silicon (from bioactive glass) and fluoride, along with calcium and phosphorus. Group definitions are provided in Table 1.

QLF is widely utilized as a clinical diagnostic tool for the detection and monitoring of dental caries due to its ability to detect the loss of fluorescence that occurs as a result of enamel demineralization [15]. Its capacity to objectively measure the extent of mineral loss has facilitated its application in a variety of research studies, such as pH-cycling models [13], and it has also been employed in studies monitoring the remineralization of white spot lesions *in vivo* [16]. Moreover, it offers a valuable clinical advantage by enabling objective pre- and posttreatment comparisons in clinical trials, such as those employing split-mouth designs [17]. In the present study, QLF analysis shows that BGS-7 exhibits the highest recovery amount and recovery rate, suggesting it has superior remineralization potential (Table 3).

Bioactive glass, an innovative bioactive material, has been developed and is now widely used in various clinical applications across both medicine and dentistry [9]. One of the most extensively studied forms of bioactive glass is 45S5, which has demonstrated the ability to bond with bone and has been used as a bone replacement material [10]. More recently, it has also been utilized to treat dentin hypersensitivity by blocking the dentinal tubules, as its dissolution products precipitate and adhere to the dentine surface, thereby alleviating pain [10,11]. In addition, 52S4 bioactive glass has shown greater efficacy in enamel remineralization than sodium fluoride and CPP-ACP formulations [3].

A more recently developed type of bioactive glass, BGS-7, has garnered considerable attention in biomedical research and has been actively investigated for various clinical applications [18–22]. Unlike conventional bioactive glasses (eg, 45S5 and 52S4), which are primarily composed of $SiO_2$, $Na_2O$, CaO, and $P_2O_5$, BGS-7 replaces sodium oxide ($Na_2O$) with boron trioxide ($B_2O_3$), thereby enhancing its structural and bioactive properties. The incorporation of boron is known to improve ion release kinetics through controlled dissolution, thus sustaining remineralization capacity by promoting hydroxyapatite formation [23]. Furthermore, BGS-7 contains a higher concentration of CaO than other bioactive glasses, which contributes to its superior mechanical strength, even compared to hydroxyapatite, a widely used bioactive ceramic [18].

In addition to its compositional advantages, BGS-7 has demonstrated biocompatibility, osteogenic potential, and controlled ion release properties, which are critical for bone regeneration and soft tissue integration. In orthopedics, its ability to enhance osteoblastic differentiation and osseointegration has been extensively documented [20,21], while in plastic surgery, BGS-7-polymer composites (polycaprolactone/BGS-7) have exhibited favorable bone-binding properties and clinical safety with minimal complications in clinical applications *in vivo* [22]. However, despite these promising properties, studies on the dental applications of BGS-7, particularly regarding its potential efficacy in enamel remineralization, remain limited. Thus, the present study aimed to investigate the remineralizing effect of BGS-7 on demineralized enamel.

The superior remineralization capacity of BGS-7


https://doi.org/10.5395/rde.2025.50.e33

compared to fluoride-based agents (Clinpro XT varnish and 1.23% APF gel) may be attributed to its unique apatite-like layer formation, as evidenced by FE-SEM images showing dense needle-like crystallites on demineralized enamel surfaces (Figure 2H). EDS data revealed the simultaneous presence of silicon (5.53 wt%) and fluoride (3.01 wt%) in the newly formed layers (Figure 3D), suggesting a synergistic mechanism where silica gel matrix formation facilitates sustained $Ca^{2+}/PO_4^{3+}$ deposition through silicon dissolution [24]. This prolonged ion release from BGS-7, mediated by its boron-substituted composition, contrasts with the rapid fluoride depletion observed in APF gel. Clinpro XT's intermediate performance may stem from its RMGI properties, though its efficacy remains limited by surface-level fluorapatite formation [25].

Supporting the current findings, several reviews have established that bioactive glass facilitates the formation of an apatite-like layer on enamel and dentin surfaces, enhancing remineralization of carious lesions [6]. In line with these studies, our results demonstrate that BGS-7 exhibits superior remineralization efficacy on demineralized enamel surfaces compared to the fluoride-based agents used in this study. For a more comprehensive understanding of the remineralization capacity of BGS-7, it will be necessary to conduct comparative studies with other established types of bioactive glass.

Nonetheless, this study has several limitations. VHN and QLF values for sound enamel were not obtained, which would have provided a more comprehensive baseline for comparison. Additionally, the relatively small sample size may limit the generalizability of the findings. To minimize inter-specimen variability and enhance consistency, the same specimens were used for QLF and FE-SEM analyses after microhardness measurement. However, to obtain more reliable results and to minimize interference between analyses on the specimens, it would be preferable to use separate specimens for each analysis with an increased sample size. Moreover, employing advanced analytical methods such as micro-computed tomography, X-ray diffraction, Fourier-transform infrared spectroscopy, or Raman spectroscopy would enable a more comprehensive analysis of the remineralized layer's structural and compositional characteristics [26,27]. Furthermore, future studies are needed to establish standardized clinical application protocols, including determination of the optimal concentration and duration, as well as the development of clinically convenient and effective formulations.

## CONCLUSIONS

Within the limitations of this study, we can infer that the application of BGS-7 varnish promoted the remineralization of demineralized enamel, as demonstrated by the evaluations conducted. Among the experimental groups, BGS-7 exhibited superior remineralization capacity. These results suggest the potential use of BGS-7 as a remineralizing material.

### CONFLICT OF INTEREST

No potential conflict of interest relevant to this article was reported.

### FUNDING/SUPPORT

This work was supported by the National Research Foundation of Korea (NRF) grant funded by the Korean government (MSIT) (NRF-2022R1G1A1010061).

### AUTHOR CONTRIBUTIONS

Conceptualization, Funding acquisition, Investigation, Supervision: Choi Y. Data curation, Formal analysis, Resources, Methodology: Jeong E. Project administration, Validation: Park SJ. Software: Sung KH. Visualization: Lee C. Writing - original draft: Lee C. Writing - review & editing: Choi Y.

### DATA SHARING STATEMENT

The datasets are not publicly available but are available from the corresponding author upon reasonable request.

## REFERENCES

1. Zhou J, Zhou L, Chen ZY, Sun J, Guo XW, Wang HR, *et al*. Remineralization and bacterial inhibition of early enamel caries surfaces by carboxymethyl chitosan lysozyme nanogels loaded with antibacterial drugs. J Dent 2025;152:105489.
2. Pitts NB, Zero DT, Marsh PD, Ekstrand K, Weintraub JA, Ramos-Gomez F, *et al*. Dental caries. Nat Rev Dis Primers

2017;3:17030.
3. Fallahzadeh F, Heidari S, Najafi F, Hajihasani M, Noshiri N, Nazari NF. Efficacy of a novel bioactive glass-polymer composite for enamel remineralization following erosive challenge. Int J Dent 2022;2022:6539671.
4. Nagata ME, Delbem ACB, Báez-Quintero LC, Danelon M, Sampaio C, Monteiro DR, *et al*. Effect of fluoride gels with nano-sized sodium trimetaphosphate on the in vitro remineralization of caries lesions. J Appl Oral Sci 2023;31:e20230155.
5. Anika TH, Harnirattisai C, Nakornchai S, Jirarattanasopha V. In vitro comparison of the performance of hydrophilic and conventional hydrophobic resin-based fissure sealants. Int Dent J 2025;75:100824.
6. Al Hamazani AD, Alwoseamer AT, AlWasem HO, Mlafakh HB, AlMarjan MM, Alfhaed NK, *et al*. Effect of bioactive glass on the remineralization of caries lesion: a systematic review. Int J Pharm Res Allied Sci 2022;11:120-130.
7. Innes NP, Chu CH, Fontana M, Lo EC, Thomson WM, Uribe S, *et al*. A century of change towards prevention and minimal intervention in cariology. J Dent Res 2019;98:611-617.
8. Tezvergil-Mutluay A, Seseogullari-Dirihan R, Feitosa VP, Cama G, Brauer DS, Sauro S. Effects of composites containing bioactive glasses on demineralized dentin. J Dent Res 2017;96:999-1005.
9. Körner P, Schleich JA, Wiedemeier DB, Attin T, Wegehaupt FJ. Effects of additional use of bioactive glasses or a hydroxyapatite toothpaste on remineralization of artificial lesions in vitro. Caries Res 2020;54:336-342.
10. Asadi M, Majidinia S, Bagheri H, Hoseinzadeh M. The effect of formulated dentin remineralizing gel containing hydroxyapatite, fluoride, and bioactive glass on dentin microhardness: an in vitro study. Int J Dent 2024;2024:4788668.
11. Dai LL, Mei ML, Chu CH, Lo EC. Mechanisms of bioactive glass on caries management: a review. Materials (Basel) 2019;12:4183.
12. Kim HJ, Mo SY, Kim DS. Effect of bioactive glass-containing light-curing varnish on enamel remineralization. Materials (Basel) 2021;14:3745.
13. Gomez J, Pretty IA, Santarpia RP, Cantore B, Rege A, Petrou I, *et al*. Quantitative light-induced fluorescence to measure enamel remineralization in vitro. Caries Res 2014;48:223-227.
14. Chinelatti MA, Tirapelli C, Corona SA, Jasinevicius RG, Peitl O, Zanotto ED, *et al*. Effect of a bioactive glass ceramic on the control of enamel and dentin erosion lesions. Braz Dent J 2017;28:489-497.
15. Son SA, Park SW, Jung YH, Kim JH, Park JK. Validity of quantitative values of quantitative light-induced fluorescent (QLF) device for pulp diagnosis of teeth with cracks. J Dent 2025;154:105579.
16. Güven E, Eden E, Attin R, Fırıncıoğulları EC. Remineralization of post-orthodontic white spot lesions with a fluoride varnish and a self-assembling P 11 - 4 peptides: a prospective in-vivo-study. Clin Oral Investig 2024;28:464.
17. Albashaireh ZSM, Al-Khateeb SN, Altallaq MK. Comparative evaluation of ICON resin infiltration and bioactive glass adhesive for managing initial caries lesions using quantitative light-induced fluorescence: a randomized clinical trial. J Dent 2025;159:105853.
18. Lee JH, Ryu HS, Seo JH, Chang BS, Lee CK. A 90-day intravenous administration toxicity study of CaO-SiO2-P2O5-B2O3 glass-ceramics (BGS-7) in rat. Drug Chem Toxicol 2010;33:38-47.
19. Lee JH, Jeung UO, Jeon DH, Chang BS, Lee CK. Quantitative comparison of novel CaO-SiO2-P2O5-B2O3 glass-ceramics (BGS-7) with hydroxyapatite as bone graft extender in rabbit ilium. Tissue Eng Regen Med 2010;7:540-547.
20. Lim HK, Song IS, Choi WC, Choi YJ, Kim EY, Phan TH, *et al*. Biocompatibility and dimensional stability through the use of 3D-printed scaffolds made by polycaprolactone and bioglass-7: an in vitro and in vivo study. Clin Implant Dent Relat Res 2024;26:1245-1259.
21. Lee JH, Hong KS, Baek HR, Seo JH, Lee KM, Ryu HS, *et al*. In vivo evaluation of CaO-SiO2-P2O5-B2O3 glass-ceramics coating on Steinman pins. Artif Organs 2013;37:656-662.
22. Kim YC, Yoon IA, Woo SH, Song DR, Kim KY, Kim SJ, *et al*. Complications arising from clinical application of composite polycaprolactone/bioactive glass ceramic implants for craniofacial reconstruction: a prospective study. J Craniomaxillofac Surg 2022;50:863-872.
23. Gharbi A, Oudadesse H, El Feki H, Cheikhrouhou-Koubaa W, Chatzistavrou X, V Rau J, *et al*. High boron content enhances bioactive glass biodegradation. J Funct Biomater 2023;14:364.
24. Lopez-Fontal E, Gin S. Insights into calcium phosphate formation induced by the dissolution of 45S5 bioactive glass. ACS Biomater Sci Eng 2025;11:875-890.
25. Edunoori R, Dasari AK, Chagam MR, Velpula DR, Kakuloor JS, Renuka G. Comparison of the efficacy of Icon resin infiltration and Clinpro XT varnish on remineralization of white


https://doi.org/10.5395/rde.2025.50.e33

spot lesions: an in-vitro study. J Orthod Sci 2022;11:12.
26. İlisulu SC, Gürcan AT, Şişmanoğlu S. Remineralization efficiency of three different agents on artificially produced enamel lesions: a micro-CT study. J Esthet Restor Dent 2024;36:1536-1546.
27. Dai LL, Mei ML, Chu CH, Lo ECM. Remineralizing effect of a new strontium-doped bioactive glass and fluoride on demineralized enamel and dentine. J Dent 2021;108:103633.

RDE Restorative Dentistry & Endodontics

Research Article

eISSN 2234-7666
Restor Dent Endod. 2025 November;50(4):e34
https://doi.org/10.5395/rde.2025.50.e34

# Analysis of temperature change during polymerization according to resin thickness: an *in vitro* experimental study

Kkot-Byeol Bae[1], Eun-Young Noh[1], Young-Tae Cho[2], Bin-Na Lee[1], Hoon-Sang Chang[1], Yun-Chan Hwang[1], Won-Mann Oh[1], In-Nam Hwang[1,*]

[1]Department of Conservative Dentistry, School of Dentistry, Chonnam National University, Gwangju, Korea
[2]Department of Basic Science, School of Engineering, Jeonju University, Jeonju, Korea

## ABSTRACT

**Objectives:** This study aimed to analyze the temperature changes during the light curing of conventional flowable composite resin and bulk-fill composite resin of various thicknesses using an infrared thermographic camera.

**Methods:** Flowable composite resin (G-aenial Flo, GC Co.) and bulk-fill composite resin (SDR, Dentsply Caulk) were used. Specimens with thicknesses from 0.5 mm to 5.0 mm were prepared. The infrared thermographic camera measured the temperature changes at the maximum temperature rise point during light curing. The data were analyzed for maximum temperature, time to peak temperature, and temperature rise patterns.

**Results:** For G-aenial Flo, the maximum temperature tended to decrease with increasing thickness, whereas for SDR, the maximum temperature decreased up to 2.0 mm and then remained relatively consistent from 2.0 mm to 5.0 mm. At thicknesses of 1.5 mm or less, both resins showed a rapid temperature increase within the first 5 seconds, followed by a reduced rate of increase up to 80 seconds. At thicknesses of 2.0 mm or greater, the temperature peaked and then gradually decreased. Across all thicknesses, SDR was observed to reach peak temperature more rapidly than G-aenial Flo.

**Conclusions:** Observable differences in polymerization dynamics were identified between the two resin types, particularly at greater thicknesses. Although no statistical analysis was performed, these descriptive findings suggest that infrared thermographic cameras may be useful for indirectly assessing polymerization dynamics during resin polymerization.

**Keywords:** Composite resins; Curing lights; Dental materials; Polymerization; Thermography

## INTRODUCTION

With the growing aesthetic demands of patients, composite resin usage has increased, leading to the development of various types tailored for different applications. For example, there are packable composite resins

**Received:** January 31, 2025 **Revised:** June 26, 2025 **Accepted:** July 14, 2025

**Citation**
Bae KB, Noh EY, Cho YT, Lee BN, Chang HS, Hwang YC, Oh WM, Hwang IN. Analysis of temperature change during polymerization according to resin thickness: an *in vitro* experimental study. Restor Dent Endod 2025;50(4):e34.

***Correspondence to**
**In-Nam Hwang, DDS, PhD**
Department of Conservative Dentistry, School of Dentistry, Chonnam National University, 77 Yongbong-ro, Buk-gu, Gwangju 61186, Korea
Email: hinso@jnu.ac.kr

Kkot-Byeol Bae and Eun-Young Noh contributed equally to this work as co-first authors.

for posterior teeth with excellent physical properties such as strength, composite resins for anterior teeth requiring superior surface gloss and aesthetics, indirect restorative composite resins for extensive damage, and flowable composite resins designed for ease of use [1].

Flowable composite resins, introduced in the 1990s, aimed to enhance the convenience of application processes. However, due to the reduced physical properties caused by a lower content of inorganic filler compared to conventional composite resins, their use was limited [2,3]. To increase the flowability of composite resins, the content of the main viscous monomers, such as 2,2-bis[4-(2-hydroxy-3-methacryloxy-propyloxy)-phenyl] propane (Bis-GMA) or urethane dimethacrylate (UDMA) was reduced, and the amount of low-viscosity diluent monomers such as triethylene glycol dimethacrylate (TEGDMA) was increased. Additionally, the inorganic filler content was decreased, and larger particle fillers were used instead of finer particles. Consequently, early flowable composite resins were recommended for use in applications with minimal occlusal force or abrasion, such as Class V cavities or as liners [1,4].

Subsequent generations of flowable composite resins increased the inorganic filler content, making them suitable for posterior restorations [4]. However, the higher polymerization shrinkage compared to conventional composite resins necessitated careful application [5]. Recently, flowable bulk-fill composite resins, which simplify the filling process, have been commercialized. Bulk-fill composite resins can be polymerized in thicknesses over 4 mm in a single increment, and manufacturers claim they exhibit less polymerization shrinkage compared to traditional flowable composite resins [6,7].

Light-curable composite resins undergo polymerization through addition polymerization reactions involving carbon-carbon double bonds (C=C) in the dimethacrylate monomers. The relatively unstable and high-energy C=C bonds react readily with other molecules, generating a rise in temperature during the reaction [8]. The powerful visible light within the 400-500 nm wavelength range from light-curing units activates α-diketone in the light-curable composite resin, initiating free radical formation and polymerization [9]. In the past, quartz-tungsten-halogen lamps were primarily used as light sources, but due to issues such as high heat generation and short lifespan, light-emitting diode (LED) light sources are now more commonly used. LEDs emit blue light using junctions of differing properties within a gallium-nitride-based semiconductor. Previous studies have shown that LEDs are more efficient than halogens at converting energy to light and more closely match the absorption wavelength of camphorquinone, a common photoinitiator in light-curable composite resins [10]. Additionally, recent high-output LED light-curing units with outputs exceeding 1,000 $mW/cm^2$ have been introduced, which cause significant temperature increase during polymerization due to their high power rather than the type of light source [11].

The temperature rise in composite resin during light curing is attributed to both exothermic polymerization and thermal energy from the light source [12–16]. Various studies have measured the temperature rise in composite resin and surrounding tissues using methods such as thermistors, thermocouples, differential scanning calorimetry, and differential thermal analysis [11,17–24]. However, these methods have limitations, such as measuring only a single point temperature and requiring direct contact with the surface [25]. In contrast, infrared thermography (IRT), using high-resolution infrared cameras, allows non-contact measurement of precise and sensitive temperature distributions by visualizing infrared radiation emitted from the sample. This method has been widely used in studies to visualize temperature rise during the polymerization process [16,25–28].

This study aimed to observe and compare the temperature dynamics of conventional flowable composite resins and flowable bulk-fill composite resins, which have reported differences in curing properties, using an IRT camera. Given that composite resin polymerization is an exothermic reaction, monitoring temperature changes through IRT provides indirect insight into polymerization dynamics and potentially the degree of conversion [16,29,30]. While this approach does not quantify conversion directly, it allows comparison of thermal characteristics among materials with differing composition and thickness. Because only a single specimen was tested per condition, this study did not involve statistical testing. Instead, observed trends in temperature change, time to peak temperature, and overall ther-


https://doi.org/10.5395/rde.2025.50.e34

mal dynamics were interpreted descriptively. The goal was not to test a formal hypothesis, but rather to identify material- and thickness-dependent trends that may inform future studies.

## METHODS

### Materials and equipment

In this study, the light-curing unit Dr's Light (GoodDoctors Co., Seoul, Korea) was used. The Dr's Light unit allows light output adjustments from 1% to 100% and curing time in 1-second increments up to 100 seconds. The LED curing unit utilized an 8 mm diameter guide tip, set to 80% output and an 80-second curing time. The 80% light output of the curing unit was measured using an LED-specific radiometer (GoodDoctors Co.), capable of measuring light output at 460 nm and 405 nm. To ensure consistency of light output, the irradiance from the LED unit was measured 10 times using the LED-specific radiometer, and the mean and standard deviation were calculated (Table 1). This repeated measurement was limited to verification of the light source and does not apply to the resin specimen experiments, which were conducted with a single specimen per condition. This corresponds to a high irradiance condition (approximately 1,786 mW/cm$^2$), thus categorized as a high-intensity LED light source in this study. The composite resins used in this study were SDR (Dentsply Caulk, Milford, DE, USA), a flowable bulk-fill composite resin, and G-aenial Flo (GF; GC, Tokyo, Japan), a flowable composite resin in A2 shade (Table 2).

**Table 1.** Light intensity of the LED light curing unit at 80% output

| Measurement time (sec) | Light intensity (mW/cm$^2$) |
|---|---|
| 5 | 1,787.0 ± 2.58 |
| 10 | 1,786.5 ± 2.42 |
| 20 | 1,787.0 ± 2.58 |
| 40 | 1,785.5 ± 1.58 |
| 80 | 1,786.0 ± 2.11 |

Values are presented as mean ± standard deviation.
LED, light-emitting diode.

### Infrared thermographic measurement equipment

The IRT camera used to measure surface temperature changes during polymerization in this study was the FLIR SC620 (FLIR Systems AB, Stockholm, Sweden) (Figure 1). IRT is a science that acquires and analyzes thermal information obtained from a non-contact thermal imaging device (camera). IRT measures the total emitted radiation energy, which includes energy absorbed by the object from external heat sources and radiated by the object itself, as well as energy reflected and transmitted by the object from external heat sources. This total emitted radiation energy is converted into thermal images based on infrared radiation wavelengths.

Using the Stefan-Boltzmann Law, which relates temperature to wavelength, the infrared wavelengths detected by the infrared detector are expressed as a function of temperature, thereby visually representing temperature variations in the image. The total incident energy $W_{\text{total}}$ received by the camera can be expressed as follows:

$$W_{total} = \tau\epsilon W_{obj} + \tau(1-\epsilon) W_{amb} + (1-\tau) W_{atm}$$

The first term, $\tau\epsilon W_{obj}$, represents the ambient radiative energy and the object's reflected energy. The second term, $\tau(1-\epsilon) W_{amb}$, represents the radiative energy of the object. The third term, $(1-\tau) W_{atm}$, represents the atmospheric radiative energy. Here, $\tau$ denotes the transmittance, and $\epsilon$ denotes the emissivity (absorptivity). IRT inspection is not only used for detecting defects in equipment, devices, and components across all industrial sectors but also has a wide range of applications in

**Table 2.** Materials, manufactures, and chemical composition of the matrix and filler

| Product (code) | Type | Manufacturer | Batch no. | Matrix system | Filler system Filler load, Filler load, | Shade |
|---|---|---|---|---|---|---|
| SDR (SDR) | Bulk-fill flowable | Dentsply Caulk, Milford, DE, USA | 608 | Modified UDMA, EBPDMA, TEGDMA | Ba-Al-F-B-silicate glass (68/44) | U |
| G-aenial Flo (GF) | Low-viscosity flowable | GC Co., Tokyo, Japan | 1310081 | UDMA, Bis-MEPP, TEGDMA | $SiO_2$, Sr glass (69/50) | A2 |

UDMA, urethane dimethacrylate; TEGDMA, triethylene glycol dimethacrylate; EBPDMA, ethoxylated bisphenol-A dimethacrylate; Bis-MEPP, 2,2-Bis (4-methacryloxypolyethoxyphenyl) propane.

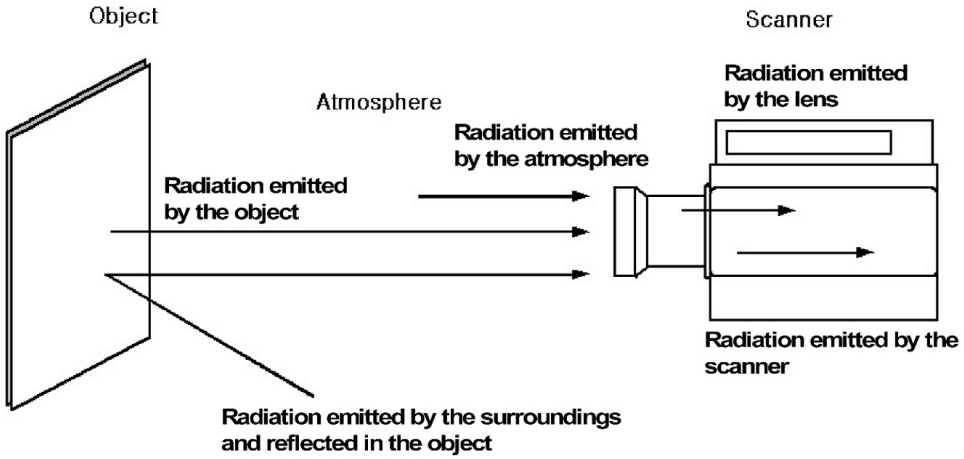


**Figure 1.** Measurement situation of infrared thermography.

**Table 3.** Specification of the infrared camera

| Specification | Value |
|---|---|
| Camera model | FLIR SC620, FLIR Systems AB, Stockholm, Sweden |
| Pixel resolution | 640 × 480 |
| Thermal sensitivity | 40 mK at 30°C |
| Detector type | Focal plane array, uncooled microbolometer |
| Spectral range (μm) | 7.5–13 |
| Frame rate (Hz) | 30–120 |
| Measure range (°C) | –40 to 1,500 |
| Accuracy (%) | ± 2 (± 2°C) |

the medical field and beyond [31]. The specifications of the infrared thermographic camera used in this study are provided in Table 3.

### Specimen preparation

Acrylic plates with thicknesses of 0.5, 1.0, 1.5, 2.0, 2.5, 3.0, 3.5, 4.0, 4.5, and 5.0 mm were cut into 40 × 40 mm squares. A 5.5 mm diameter hole was drilled in the center of each plate using a benchtop drill. To create a cavity structure with one closed side, one face of each acrylic plate was attached to a 40 × 40 mm acrylic plate with a thickness of 0.5 mm using adhesive. The cavities were then filled with flowable composite resin and high-flow bulk-fill resin. To achieve a uniform resin layer, the cavity was covered with a thin, transparent vinyl plate, and excess resin was removed by applying pressure with a glass plate. The acrylic cavity structure was used as a physical reference to control specimen thickness, and the combination of a transparent vinyl sheet and glass plate ensured a flat and uniform upper surface. Although the thickness was not directly measured after curing, the cavity design was intended to maintain consistent thickness across specimens. To improve the emissivity of the surface for accurate IRT measurements, the vinyl plate was coated with Krylon 4290 Ultra Flat Black paint (Krylon Industrial, Cleveland, OH, USA), which has an emissivity of 0.97, and allowed to dry thoroughly.

For temperature measurements, the prepared specimen was placed on a thermal insulation plate, which was made of 150 × 150 mm compressed styrofoam with a thickness of 5 mm. A 9.0 mm diameter hole in the center of the insulation plate allowed the resin-filled cavity to be exposed to the curing light source. To ensure proper alignment and reproducibility during the curing process, an "L"-shaped acrylic guide plate was attached to the edges of the specimen to secure its position. The LED light-curing unit was fixed to a rod stand and positioned perpendicular to the surface of the resin at a distance of 10 mm. To minimize external light interference and reflections, the thermal insulation plate and surrounding setup were coated with the same emissive paint. Although multiple specimens were fabricated for each resin and thickness, only one specimen per condition was used for measurement ($n = 1$).

### Measurement of polymerization heat

The prepared specimen was placed at the designated


https://doi.org/10.5395/rde.2025.50.e34

position on the thermal insulation plate, and the device was fixed such that the tip of the curing unit was positioned 10 mm away from the bottom of the specimen. The IRT camera was mounted 100 mm above the specimen, and the measurement area was adjusted and verified using the camera's imaging mode (Figure 2). The light-curing unit was set to 80% output and 80 seconds of curing time. Polymerization was initiated by turning on the light-curing unit, and simultaneously, the IRT camera began recording. The camera was set to capture 30 frames per second to collect data. All experiments were conducted in a light-blocked darkroom at room temperature. The temperatures measured by the IRT camera for each frame were converted using FLIR Tools (FLIR Systems AB). The time each frame was captured was converted to temperature per second for analysis.

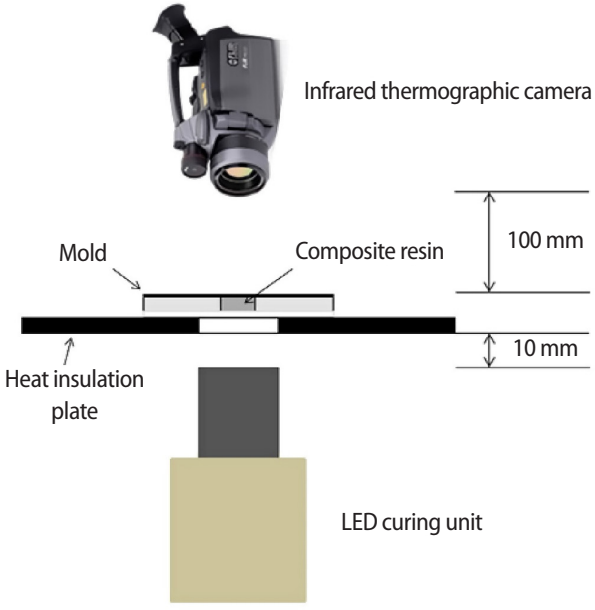


**Figure 2.** Schematic diagram set-up for the infrared thermography camera measurement of the composite surface temperature. The infrared thermographic camera is located above the composite in a mold.

### Data analysis

All temperatures within a 5.0 mm diameter circle centered at the highest temperature rise point in the center were measured. The maximum temperature at the highest temperature rise point over time was extracted using FLIR Tools. Subsequently, the maximum temperature, the time to reach maximum temperature, and the temperature rise pattern for each thickness of the two resins were analyzed. Since each condition was tested with only a single specimen ($n$ = 1), statistical analysis was not performed. Observed differences were interpreted descriptively based on thermal trends.

## RESULTS

The temperature data within the 5 mm diameter circle at the highest temperature rise point were recorded from the start to the end of polymerization (Table 4, Figure 3). The maximum temperature rise for GF decreased as the

**Table 4.** Descriptive comparison of time to peak temperature, peak temperature, and temperature at 80 seconds for SDR and G-aenial Flo at each thickness

| Thickness (mm) | Time to peak temperature (sec) | | Peak temperature (°C) | | Temperature at 80 sec (°C) | |
|---|---|---|---|---|---|---|
| | SDR | G-aenial Flo | SDR | G-aenial Flo | SDR | G-aenial Flo |
| 0.5 | - | - | - | - | 63.9[a)] | 60.0[a)] |
| 1.0 | - | - | - | - | 56.0[a)] | 54.0[a)] |
| 1.5 | - | - | - | - | 49.2[a)] | 50.6[a)] |
| 2.0 | 8.93 | 16.58 | 43.4 | 46.0 | 45.5[a)] | 48.0[a)] |
| 2.5 | 8.60 | 18.23 | 43.4[a)] | 45.3[a)] | 42.6 | 43.8 |
| 3.0 | 9.86 | 18.70 | 43.0[a)] | 43.3[a)] | 41.3 | 41.7 |
| 3.5 | 10.70 | 22.20 | 42.6[a)] | 42.8[a)] | 37.9 | 39.9 |
| 4.0 | 12.37 | 25.6 | 42.9[a)] | 41.2[a)] | 36.2 | 38.3 |
| 4.5 | 12.40 | 29.03 | 42.8[a)] | 40.1[a)] | 36.2 | 37.5 |
| 5.0 | 12.93 | 29.67 | 43.4[a)] | 41.8[a)] | 36.4 | 39.0 |

Each condition represents a single measurement ($n$ = 1). No statistical comparisons were performed.
SDR: Dentsply Caulk, Milford, DE, USA; G-aenial Flo: GC Co., Tokyo, Japan.
[a)]Highest temperature.

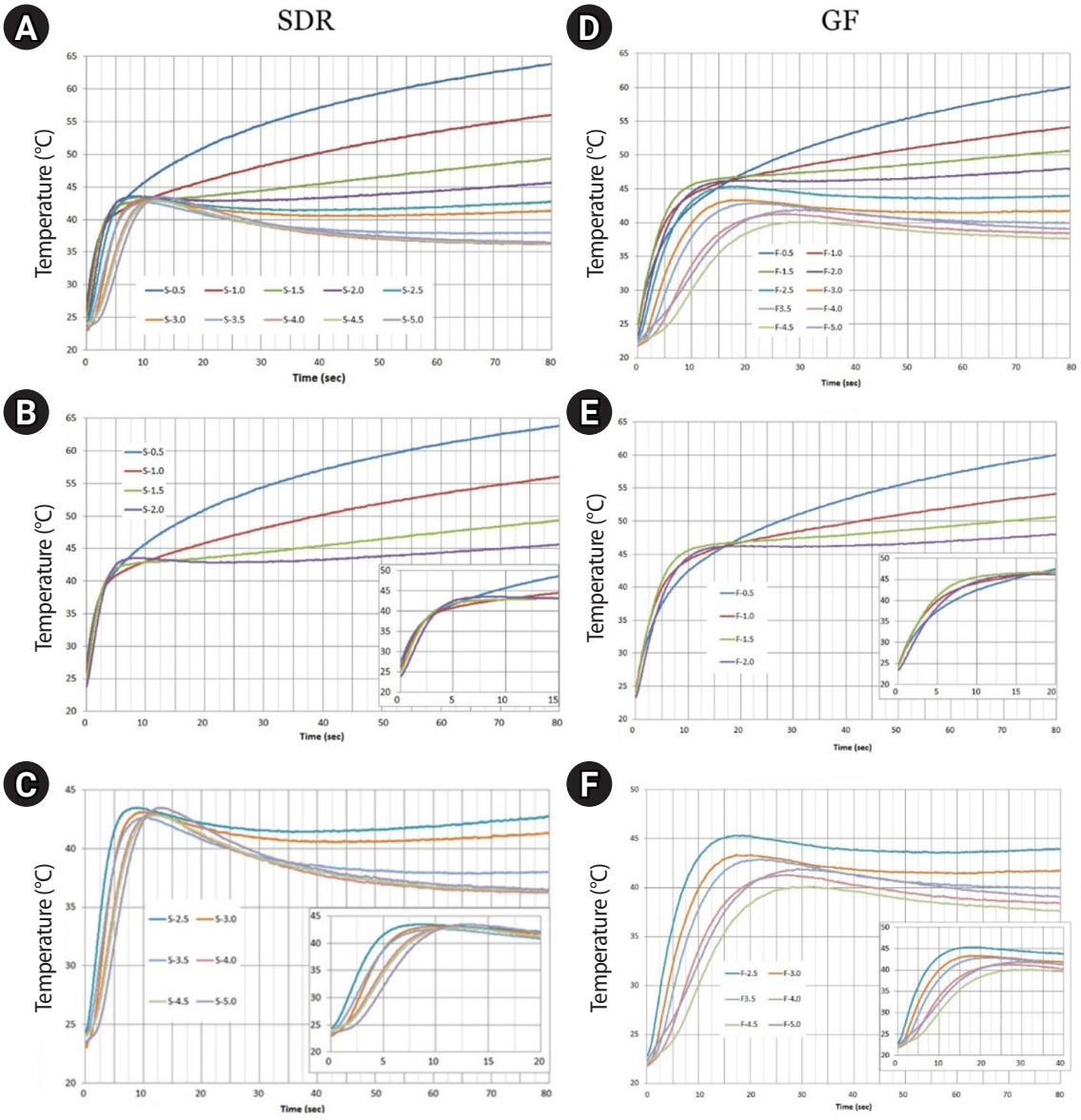


**Figure 3.** Temperature rise during light cure with a high intensity LED curing unit (Dr's Light, 1,786 mW/cm$^2$ at 80% output) for different resin thickness. (A) SDR (bulk-fill composite resin), 0.5–5.0 mm. (B) SDR, 0.5–2.0 mm. (C) SDR, 2.5–5.0 mm. (D) G-aenial Flo (GF; flowable composite resi), 0.5–5.0 mm. (E) GF, 0.5–2.0 mm. (F) GF, 2.5–5.0 mm. Each plot represents a single recorded measurement for each condition ($n$ = 1). LED, light-emitting diode. Dr's Light: GoodDoctors Co., Seoul, Korea; SDR: Dentsply Caulk, Milford, DE, USA; G-aenial Flo: GC Co., Tokyo, Japan.

thickness increased, whereas for SDR, the temperature decreased up to 2.0 mm but remained relatively constant between 2.0 mm and 5.0 mm. For thicknesses of 1.5 mm or less, neither resin showed a peak temperature. At these thicknesses, both resins exhibited a rapid temperature increase within the first 5 seconds of polymerization, followed by a reduced rate of increase, and continued to rise steadily up to 80 seconds. For thicknesses of 2.0 mm or greater, the temperature rose rapidly after the start of polymerization, reaching a maximum peak, and then gradually decreased. At a thickness of 2.0 mm, the temperature initially increased, then decreased slightly after reaching an early peak, and increased again to reach the maximum temperature at 80 seconds. For thicknesses of 2.5 mm or greater, the peak temperature coincided with the maximum temperature. In GF,


https://doi.org/10.5395/rde.2025.50.e34

the peak temperature tended to decrease as the resin thickness increased, while SDR showed relatively stable peak temperature values across thicknesses. The time required to reach peak temperature increased as the resin thickness increased, in both materials, especially beyond 2.0 mm. The time to reach the peak temperature was 8.93 seconds for SDR and 16.58 seconds for GF at 2.0 mm thickness, and 12.93 seconds for SDR and 29.67 seconds for GF at 5.0 mm thickness. Across all tested thicknesses, SDR was observed to reach peak temperature more rapidly than GF.

## DISCUSSION

The introduction of flowable composite resins has improved direct restorative techniques by enabling better adaptation to cavity walls, especially in deep or irregular areas, compared to conventional packable resins [2,3]. The GF resin used in this study contains 68 wt% (44 vol%) of inorganic filler, making it suitable for larger posterior restorations, though its higher polymerization shrinkage warrants caution [4,5]. Bulk-fill composite resins are commercially available in both high-flow and conventional packable forms. Their primary characteristic is a deeper polymerization depth compared to conventional composite resins, allowing for depths of 4 mm or more in a single increment. However, the method of filling large quantities of resin at once must overcome issues that can arise from polymerization shrinkage. According to the manufacturer, the SDR used in this study includes a high molecular weight polymerization modulator in its matrix to reduce polymerization stress. This structure delays gelation, allowing stress relief during bulk application [6]. Although SDR reached peak temperature faster than GF, this does not contradict its delayed gel point, as the two reflect distinct aspects of polymerization governed by different formulation factors [5,6]. Jang *et al.* [5] further reported that SDR exhibits less polymerization shrinkage and lower polymerization shrinkage stress compared to conventional flowable composite resins, along with a deeper polymerization depth.

Both GF and SDR used in this study employ UDMA, which is less viscous than Bis-GMA, as their primary matrix. TEGDMA is also used. Therefore, it was expected that the temperature rise between the two materials using similar matrices would be similar, and the actual measured results showed similar maximum temperature values between the two materials (Table 4). In this study, the peak temperature rise was about 20°C. However, other experiments measuring the temperature rise of flowable composite resin using IRT cameras observed a temperature rise of about 40°C [14,28]. Notably, Chang *et al.* [28] used the same materials as this study. This discrepancy is likely due to uncontrolled environmental factors, especially surrounding light sources. In this study, surrounding light sources were completely blocked using blackout curtains, and emissive paint with an emissivity of 0.97 was applied, considering reflections from the material surface. Preliminary tests showed that emissive paint improved measurement accuracy, suggesting that the lower peak temperatures were due to the experimental setup, not the paint itself.

Based on these observations, the goal of this study was to determine whether IRT cameras could be used to understand the curing characteristics, such as the degree of conversion and polymerization depth of composite resins. The findings suggest that IRT has meaningful potential for evaluating resin polymerization behavior. Previous studies have demonstrated that differential thermal analysis can estimate the degree of conversion, with trends comparable to Fourier transform infrared spectroscopy (FTIR), especially in matrices with higher TEGDMA content [22,24,29]. Both resins have high TEGDMA content for flowability, and although their exact UDMA/TEGDMA ratios are unknown, intra-material comparisons by thickness using thermal data are still feasible. It should be noted that the thermal parameters observed in this study are not direct measures of the degree of conversion. However, the temperature rise patterns, particularly maximum temperature and time to peak, may serve as indirect indicators of polymerization kinetics and material behavior. These findings align with previous studies that have demonstrated the feasibility of using thermal analysis for estimating conversion trends [29].

In addition to compositional differences, the optical properties of the materials may also have contributed to the observed temperature dynamics. The higher translucency of SDR (universal shade) enhances light

transmission and polymerization depth, making it advantageous for bulk-fill applications compared to more opaque materials like GF (A2 shade). The difference in translucency may have influenced the time to peak temperature and the rate of temperature change observed between the two materials in this study. These findings are consistent with previous studies indicating that the optimized translucency of SDR enhances light penetration and depth of cure [6]. Therefore, shade and translucency should be considered important variables in future investigations evaluating polymerization dynamics using thermal analysis.

Based on the temperature rise patterns observed in this study, it can be inferred that GF may exhibit more limited polymerization dynamics beyond 2.5 mm thickness, whereas SDR maintained more stable thermal characteristics up to 5.0 mm. These trends, including differences in time to peak temperature and thermal response, suggest that polymerization dynamics differ between the two materials, even without direct measurement of conversion. A common method for measuring polymerization depth involves comparing the microhardness at the surface and at a certain depth. Jang *et al.* [5] reported that SDR has a deeper polymerization depth than GF using this method. Analyzing the temperature rise patterns from this study shows similar trends. Although further studies are needed, temperature measurements may serve as a useful indirect tool for evaluating polymerization dynamics, particularly when comparing materials with different thickness-dependent thermal dynamics.

In interpreting the thermal data obtained in this study, it is important to acknowledge that temperature-based parameters such as peak temperature, time to peak, and post-peak slope serve as indirect indicators of polymerization dynamics rather than direct measures of the degree of conversion. The peak temperature primarily reflects the total exothermic heat released during the polymerization process. Under certain conditions, this may correlate with the extent of polymerization; however, it does not provide quantitative information about the actual monomer-to-polymer conversion ratio. The time to peak temperature is influenced by the rate of radical generation and propagation, and was used in this study to infer relative differences in polymerization kinetics between materials. In contrast, the slope of the temperature curve after the peak reflects the rate of heat dissipation and is influenced by thermal conductivity and environmental conditions rather than chemical reactivity. Furthermore, while a rapid rise in temperature and a short time to peak temperature may suggest a faster onset of polymerization, this does not necessarily imply that the overall conversion process has been completed. In bulk-fill composites like SDR, polymerization may continue beyond the temperature peak due to factors like light attenuation and delayed gelation. This concept is consistent with previous studies that demonstrated ongoing polymer network formation after the cessation of significant heat release [30]. Therefore, in the context of IRT evaluation, thermal parameters should be interpreted as supporting data for understanding polymerization trends, rather than definitive indicators of the degree of conversion. For a more accurate assessment of conversion, direct analytical methods such as FTIR or Raman spectroscopy should be employed in conjunction with thermal analysis [29].

The high-output LED curing unit (1,700 mW/cm$^2$) likely contributed to temperature increases, especially in thinner specimens [11]. For specimens with a thickness of 1.5 mm or less, no distinct peak temperature was observed; instead, the temperature continued to increase steadily throughout the 80-second curing period. In thin specimens, the continuous temperature increase and early thermal spike observed during curing likely reflect superficial heating from the light source, rather than exothermic heat from polymerization. In contrast, specimens with a thickness of 2.0 mm or greater exhibited a typical polymerization thermal profile, characterized by a rapid temperature increase, a clear peak, and a subsequent gradual decline. Moreover, in both materials, a sharp temperature rise was observed within the first 5 seconds of light exposure, especially in thinner specimens. Therefore, when interpreting thermal curves, particularly in thin samples (≤1.5 mm) and during the early phase of irradiation (first 5 seconds), it is important to consider that the measured temperature may reflect light-induced heating rather than polymerization dynamics. From a clinical standpoint, temperature rise during light curing is a concern because of its potential to affect pulpal health. While our study


https://doi.org/10.5395/rde.2025.50.e34

did not directly measure intrapulpal temperatures, previous studies have indicated that increases above 5.5°C may lead to irreversible pulp damage [32]. In light of this, the temperature rises we observed, particularly at lower resin thicknesses, highlight the importance of using curing protocols that minimize heat exposure to the pulp. Therefore, further research on light output and temperature rise by thickness is needed, which could establish application standards for IRT cameras as useful research tools for understanding the curing characteristics of light-curing composite resins.

One limitation of this study is that the specimen thickness was not remeasured after polymerization. Although the acrylic cavity structure served to standardize the thickness during preparation, minor dimensional changes due to polymerization shrinkage may have occurred and were not quantified. To improve the accuracy of polymerization-related thermal analysis in future studies, experimental designs should account for potential dimensional changes caused by polymerization shrinkage.

Many previous studies on temperature rise measurements reported results from specific points. However, the studies by Chang *et al.* [28] and this study indicate that the same temperature is not measured across all illuminated areas. Thus, traditional temperature measurement methods might have yielded different results depending on the measurement point. IRT cameras can provide more accurate results by identifying the highest temperature in a specific area and confirming the overall temperature distribution. Additionally, advancements in technology allow for temperature comparisons at very short intervals.

SDR consistently showed a shorter time to reach peak temperature compared to GF, indicating a faster thermal response during polymerization. However, this rapid temperature increase did not necessarily correspond to higher overall exothermic output or greater polymerization shrinkage stress [5,30]. These findings suggest that polymerization kinetics and stress development depend on distinct material-specific properties [5,6,30].

## CONCLUSIONS

This study demonstrated that conventional flowable and bulk-fill composite resins exhibit distinct thermal behaviors during light curing, particularly as resin thickness increases. Bulk-fill resins maintained a more consistent temperature profile and showed a faster thermal response at greater depths, supporting their use in posterior restorations that require deeper curing.

These results also suggest that IRT is a promising non-contact tool for indirectly evaluating polymerization dynamics. While the degree of conversion was not directly measured, the observed thermal patterns offer meaningful insight into material behavior. Further research involving repeated measurements and statistical validation is warranted to confirm these findings and to define clinically relevant thresholds.

## CONFLICT OF INTEREST

No potential conflict of interest relevant to this article was reported.

## FUNDING/SUPPORT

This study was not supported by any specific grant from funding agencies in the public, commercial, or not-for-profit sectors. The authors declare no financial interest in the companies whose materials are included in this article.

## AUTHOR CONTRIBUTIONS

Conceptualization: Hwang IN, Cho YT; Formal analysis: Bae KB, Noh EY, Cho YT; Investigation: Noh EY, Cho YT; Methodology: Hwang IN, Oh WM, Hwang YC; Visualization: Bae KB, Noh EY; Supervision: Lee BN, Chang HS, Hwang IN; Writing - original draft: Bae KB, Noh EY, Cho YT, Hwang IN; Writing - review & editing: Bae KB, Lee BN, Chang HS, Oh WM, Hwang YC, Hwang IN.

## DATA SHARING STATEMENT

The datasets generated and analyzed during the current study are available from the corresponding author on reasonable request. Requests for access to the data should include a clear description of the intended use and the conditions under which reuse is permitted.

## REFERENCES

1. Noort RN. Introduction of dental materials. 3rd ed. Philadelphia: MOSBY Elsevier; 2007.
2. Labella R, Lambrechts P, Van Meerbeek B, Vanherle G. Polymerization shrinkage and elasticity of flowable composites and filled adhesives. Dent Mater 1999;15:128-137.
3. Bayne SC, Thompson JY, Swift EJ, Stamatiades P, Wilkerson

M. A characterization of first-generation flowable composites. J Am Dent Assoc 1998;129:567-577.
4. Ikeda I, Otsuki M, Sadr A, Nomura T, Kishikawa R, Tagami J. Effect of filler content of flowable composites on resin-cavity interface. Dent Mater J 2009;28:679-685.
5. Jang JH, Park SH, Hwang IN. Polymerization shrinkage and depth of cure of bulk-fill resin composites and highly filled flowable resin. Oper Dent 2015;40:172-180.
6. Ilie N, Hickel R. Investigations on a methacrylate-based flowable composite based on the SDR™ technology. Dent Mater 2011;27:348-355.
7. Czasch P, Ilie N. In vitro comparison of mechanical properties and degree of cure of bulk fill composites. Clin Oral Investig 2013;17:227-235.
8. Ferracane JL. Materials in dentistry: principles and applications. 2nd ed. Philadelphia: Lippincott Williams & Wilkins; 2001.
9. Pilo R, Oelgiesser D, Cardash HS. A survey of output intensity and potential for depth of cure among light-curing units in clinical use. J Dent 1999;27:235-241.
10. Bennett AW, Watts DC. Performance of two blue light-emitting-diode dental light curing units with distance and irradiation-time. Dent Mater 2004;20:72-79.
11. Asmussen E, Peutzfeldt A. Temperature rise induced by some light emitting diode and quartz-tungsten-halogen curing units. Eur J Oral Sci 2005;113:96-98.
12. Hansen EK, Asmussen E. Correlation between depth of cure and temperature rise of a light-activated resin. Scand J Dent Res 1993;101:176-179.
13. Porko C, Hietala EL. Pulpal temperature change with visible light-curing. Oper Dent 2001;26:181-185.
14. Al-Qudah AA, Mitchell CA, Biagioni PA, Hussey DL. Thermographic investigation of contemporary resin-containing dental materials. J Dent 2005;33:593-602.
15. Shortall AC, Harrington E. Temperature rise during polymerization of light-activated resin composites. J Oral Rehabil 1998;25:908-913.
16. Uhl A, Mills RW, Jandt KD. Polymerization and light-induced heat of dental composites cured with LED and halogen technology. Biomaterials 2003;24:1809-1820.
17. Stewardson DA, Shortall AC, Harrington E, Lumley PJ. Thermal changes and cure depths associated with a high intensity light activation unit. J Dent 2004;32:643-651.
18. Cobb DS, Dederich DN, Gardner TV. In vitro temperature change at the dentin/pulpal interface by using conventional visible light versus argon laser. Lasers Surg Med 2000;26:386-397.
19. Hannig M, Bott B. In-vitro pulp chamber temperature rise during composite resin polymerization with various light-curing sources. Dent Mater 1999;15:275-281.
20. Kleverlaan CJ, de Gee AJ. Curing efficiency and heat generation of various resin composites cured with high-intensity halogen lights. Eur J Oral Sci 2004;112:84-88.
21. Vaidyanathan J, Vaidyanathan TK. Computer-controlled differential scanning calorimetry of dental composites. IEEE Trans Biomed Eng 1991;38:319-325.
22. McCabe JF. Cure performance of light-activated composites by differential thermal analysis (DTA). Dent Mater 1985;1:231-234.
23. Vaidyanathan J, Vaidyanathan TK, Wang Y, Viswanadhan T. Thermoanalytical characterization of visible light cure dental composites. J Oral Rehabil 1992;19:49-64.
24. Lloyd CH. A differential thermal analysis (DTA) for the heats of reaction and temperature rises produced during the setting of tooth coloured restorative materials. J Oral Rehabil 1984;11:111-121.
25. Al-Qudah AA, Mitchell CA, Biagioni PA, Hussey DL. Effect of composite shade, increment thickness and curing light on temperature rise during photocuring. J Dent 2007;35:238-245.
26. Hussey DL, Biagioni PA, Lamey PJ. Thermographic measurement of temperature change during resin composite polymerization in vivo. J Dent 1995;23:267-271.
27. Anić I, Pavelić B, Perić B, Matsumoto K. In vitro pulp chamber temperature rises associated with the argon laser polymerization of composite resin. Lasers Surg Med 1996;19:438-444.
28. Chang HS, Cho KJ, Park SJ, Lee BN, Hwang YC, Oh WM, *et al.* Thermal analysis of bulk filled composite resin polymerization using various light curing modes according to the curing depth and approximation to the cavity wall. J Appl Oral Sci 2013;21:293-299.
29. Imazato S, McCabe JF, Tarumi H, Ehara A, Ebisu S. Degree of conversion of composites measured by DTA and FTIR. Dent Mater 2001;17:178-183.
30. Davidson CL, Feilzer AJ. Polymerization shrinkage and polymerization shrinkage stress in polymer-based restoratives. J Dent 1997;25:435-440.
31. Usamentiaga R, Venegas P, Guerediaga J, Vega L, Molleda J, Bulnes FG. Infrared thermography for temperature


https://doi.org/10.5395/rde.2025.50.e34

measurement and non-destructive testing. Sensors (Basel) 2014;14:12305-12348.

32. Zach L, Cohen G. Pulp response to externally applied heat. Oral Surg Oral Med Oral Pathol 1965;19:515-530.

RDE Restorative Dentistry & Endodontics

Research Article

eISSN 2234-7666
Restor Dent Endod. 2025 November;50(4):e35
https://doi.org/10.5395/rde.2025.50.e35

# Phase transformation temperatures influence the reduction ratio of fatigue resistance of nickel-titanium reciprocating files at body temperature: an *in vitro* experimental study

**Walid Nehme**[1], **Alfred Naaman**[2], **Lola Pedèches**[3], **Sylvie Lê**[3,4], **Marie Georgelin-Gurgel**[3,4], **Sang Won Kwak**[5], **Hyeon-Cheol Kim**[5,6,*], **Franck Diemer**[3,4,*]

[1]Department of Endodontics, Arthur Dugoni School of Dentistry, University of the Pacific, San Francisco, CA, USA
[2]Department of Endodontics, Faculty of Dental Medicine, Saint Joseph University, Beirut, Lebanon
[3]UFR d'Odontologie et Centre Hospitalier Universitaire de Toulouse, Toulouse, France
[4]INCOMM, Metabolic and Cardiovascular Research Institute, UMR 1297 INSERM, Toulouse, France
[5]Department of Conservative Dentistry, Dental and Life Science Institute, School of Dentistry, Pusan National University, Yangsan, Korea
[6]Dental Research Institute, Pusan National University Dental Hospital, Yangsan, Korea

## ABSTRACT

**Objectives:** The objective of this study was to evaluate the effects of transformational temperatures on the cyclic fatigue resistance at body temperature of reciprocating file systems: R motion (RM), Procodile Q (PQ), and Reciproc Blue.

**Methods:** Resistance test was done in a custom-made device at room (20°C ± 1°C) and body (37°C ± 1°C) temperatures within a 60° angle of curvature and 5 mm radius of the artificial canal. The time to fracture (TTF) was recorded. The scanning electron microscope observation and differential scanning calorimetry analyses were performed. Two-way analysis of variance and Tukey *post-hoc* comparison were applied at a significance level of 0.05.

**Results:** The results showed a significant influence of temperature on instrumental breakage, regardless of the file systems ($p < 0.05$). The TTF is significantly decreased at body temperature ($p < 0.05$). PQ showed the longest TTF in both temperature conditions ($p < 0.05$). RM demonstrated a significantly higher TTF reduction ratio compared to the other files ($p < 0.05$).

**Conclusions:** Within the limitations of this study, the heat-treated files with reciprocating kinetics may have different reduction ratios of the fatigue resistance of the file systems under different temperature conditions. This characteristic is an important point of consideration when clinicians select the file system to reduce potential file fracture.

**Keywords:** Body temperature; Cyclic fatigue; Fracture resistance; Nickel-titanium file; Transformation

**Received:** April 30, 2025 **Revised:** June 3, 2025 **Accepted:** June 4, 2025

**Citation**
Nehme W, Naaman A, Pedèches L, Lê S, Georgelin-Gurgel M, Kwak SW, Kim HC, Diemer F. Phase transformation temperatures influence the reduction ratio of fatigue resistance of nickel-titanium reciprocating files at body temperature: an *in vitro* experimental study. Restor Dent Endod 2025;50(4):e35.

***Correspondence to**
**Hyeon-Cheol Kim, DDS, MS, PhD**
Department of Conservative Dentistry, School of Dentistry, Pusan National University, 20 Geumo-ro, Mulgeum-eup, Yangsan 50612, Korea
Email: golddent@pusan.ac.kr
**Franck Diemer, DDS, MSc, PhD**
Department of Conservative Dentistry and Endodontics, CHU de Toulouse, Clement Ader Institute, 31400 Toulouse, France
Email: franck.diemer@univ-tlse3.fr

Hyeon-Cheol Kim and Franck Diemer contributed equally to this work as co-corresponding authors.

## INTRODUCTION

Clinical endodontic procedures have undergone tremendous changes after the introduction of the nickel-titanium (NiTi) instrument. These instruments have undoubtfully eliminated procedural errors related to stainless-steel files, improving the mechanical preparation of the root canal system and promoting the speed and efficiency of mechanical instrumentation due to their flexibility and cutting efficiency [1,2]. Nonetheless, unpredictable file failure remains one of the most important drawbacks of NiTi files [3]. Over the past three decades, various changes have been implemented to reduce instrument separation, focusing on factors such as cross-sectional design, pitch length, groove depth, tip and taper dimensions, kinematics, and heat treatment of the alloy [4–6].

Despite the advancements in instruments, separation may occur through cyclic or torsional fatigue [3–5,7]. The cyclic fatigue failure takes place when the metal tolerance is exceeded, due to repeated compression and tension of the free-rotating instrument in a curved root canal [8]. Cyclic fatigue is the main reason for fracture of rotary files clinically [3,9]. The manufacturing process has an impact on the cyclic fatigue resistance. Grinding the instruments may leave some flaws near the surface of the wire, such as machining grooves or defects [10]. These irregularities and micro-voids related to the manufacturing of the NiTi create points for stress concentration and crack initiation, leading to instrument fractures as a result of a crack propagation process [11,12].

The stress generated on a file is influenced by various factors, including root canal anatomy and the operator's technique [13]. Moreover, the instrument's geometry, alloy composition, manufacturing process, and kinematics can significantly affect stress behavior [14]. The new generation of instruments undergoes some proprietary heat treatment aimed at optimizing the crystallographic phase of the file and increasing transformational temperatures, bringing them closer to body temperature [15,16].

Differential scanning calorimetry (DSC) is the most appropriate test to determine the transitional temperatures, such as austenite starting (A*s*), austenite peak (A*p*), austenite finishing (A*f*), martensite starting (M*s*), martensite finishing (M*f*), and to provide an idea regarding the crystallographic phase of endodontic files at a well-defined temperature [17]. A NiTi alloy with a higher A*s* transformation temperature has more martensite, resulting in enhanced flexibility and increased cyclic fatigue resistance, which is beneficial for root canal instrumentation [18]. Heat-treated files may undergo phase transformation from martensite to austenite below body temperature [19]. Working at body temperature and intermittently using heated sodium hypochlorite may alter the file's microstructure, shifting it toward a predominantly austenitic state, which is more susceptible to crack propagation than a martensitic file [19].

A recently introduced reciprocating file system, Procodile Q (PQ; Komet Medical, Lemgo, Germany), utilizes a variably tapered core combined with controlled memory alloy. There is little data about the fatigue resistance of the PQ file at room and body temperatures, compared to different reciprocating files. Therefore, the objective of this study was to evaluate the transformational temperatures and cyclic fatigue resistance of PQ at both room and body temperatures, and compare it with Reciproc Blue (RB; VDW, Munich, Germany) and R motion (RM; FKG Dentaire, La Chaux de Fonds, Switzerland). The null hypothesis is that there would be no difference in cyclic fatigue resistance among the files at both room and body temperatures.

## METHODS

The sample size was determined using XLstat (Microsoft, Redmond, WA, USA) based on a previous study [13]. A power calculation for analysis of variance (ANOVA) or analysis of covariance, for three groups (instruments) and one degree of freedom (temperature), with an effect size fixed at 1 (second), and 0.05 alpha type error and 0.95 power indicated that the number of observations should be 16 per group. Thus, 20 instruments were assigned to each group.

A total of 120 NiTi files were used in this study, with forty files assigned to each of the three experimental groups: RM, PQ, and RB groups. All files presented a #25 ISO tip, a length of 25 mm, and a regressive 0.08 taper for RB, while PQ and RM had a fixed 0.06 taper.

Before the experiments, the instruments were in-


https://doi.org/10.5395/rde.2025.50.e35

spected with a stereomicroscope (Leica M205C; Leica Microsystems, Wetzlar, Germany) to identify any defects. None of the instruments was discarded during this pre-experimental evaluation.

The cyclic fatigue resistance test was conducted using a custom-made device designed to replicate temperature conditions corresponding to room (20°C ± 1°C) and body (37°C ± 1°C) temperatures. A distilled water bath was set up with a rectangular tank measuring 40 cm in length, 25 cm in width, and 15 cm in height, accompanied by a heating device (Polystat 16000; Bioblock Scientific, Illkirch, France). A thermometer was placed at the bottom of the tank to check the temperature during the study.

The cyclic fatigue test was carried out using a hollow stainless-steel tube, mimicking the shape of a canal with a 60° angle of curvature and a 5-mm radius of curvature. The center of the curvature was positioned 5 mm from the tip of the tested file. This tube was attached to the side of the tank. An EndoPilot endo motor and handpiece (Komet USA, Rock Hill, SC, USA) were connected to the side of the tank and connected to the test device. The Reflex Dynamic program (Komet USA) is a left-reciprocating motion with the ability to vary angular velocity when it detects too much stress. It was chosen to operate all the instruments attached to the handpiece until the file fractured. Each NiTi file ($n$ = 20) from three groups, in both temperature conditions, was operated within the 16-mm length of the simulated canal. The time to fracture (TTF) was recorded using a stopwatch.

### Scanning electron microscopy observation

All fragments of each group were chosen for fractographic examination. The fractured instruments were shortened with cutting pliers (removal of the mandrel), rinsed with deionized water, cleaned in an ultrasonic bath with absolute alcohol, and then placed vertically with the fractured surface facing upward on a metal support. The specimens were fixed in place with carbon tape. The metal holder was inserted into the scanning electron microscope (JSM-6400; JEOL Ltd, Tokyo, Japan) and observed in secondary vacuum. The photomicrographs were taken between ×100 and ×300 magnifications and recorded in JPEG format.

### Differential scanning calorimetry observation

DSC analyses were performed using a DSC-8500 (PerkinElmer, Shelton, CT, USA). Before each measurement, temperature and energy calibration were performed. The samples underwent cooling to –70°C and then experienced a heating/cooling cycle within the temperature range of –70°C to 110°C, with a heating/cooling rate of 5°C/min. Three samples from each file system were used. These cycles were repeated three times for each instrument. The heating and cooling curves were recorded. Data processing was performed with Pyris software (PerkinElmer).

### Statistical analysis

A descriptive analysis was carried and the data were compared with the temperature conditions and file groups. Statview version 5.0 (SAS Institute, Cary, NC, USA) was used for statistical analysis with an alpha risk of 5%. Data were tested for normality using the Shapiro-Wilk test. Under the conditions of normal distribution, two-way ANOVA and Tukey *post-hoc* comparison were applied to compare the file groups. In all experiments, a $p$-value of less than 0.05 was considered significant.

## RESULTS

The results were collected in order to visualize and compare the different instrumental TTFs of the different instruments at room and body temperatures (Table 1) and the TTF ratio (%, body/room temperatures). The "Reflex Dynamic" program used on the EndoPilot motor never switched to its specific movement and kept its regular reciprocating movement.

The data normality was confirmed. The results showed a significant influence of temperature on instrumental breakage, regardless of the file systems ($p$ < 0.05). The breakthrough time is significantly decreased at body temperature ($p$ < 0.05), although the extent of reduction varies among the different instruments (Table 1). The PQ file showed the longest TTF in both temperature conditions ($p$ < 0.05). The RM file demonstrated a significantly bigger substantial reduction in TTF (lower ratio) compared to the other files ($p$ < 0.05).

The DSC plots, depicting both the heating and cooling

**Table 1.** Time to fracture (TTF) at each temperature and TTF reduction ratio

| Temperature (°C) | File | | |
|---|---|---|---|
| | R Motion | Procodile Q | Reciproc Blue |
| Room (20 ± 1) | 977 ± 149[a] | 993 ± 107[a] | 496 ± 72[b] |
| Body (37 ± 1) | 231 ± 23[c] | 629 ± 61[a] | 319 ± 43[b] |
| Reduction ratio (%) | 76.4* | 36.7 | 35.7 |

Values are presented as mean ± standard deviation unless otherwise specified.
R Motion: FKG Dentaire, La Chaux de Fonds, Switzerland; Procodile Q: Komet Medical, Lemgo, Germany; and Reciproc Blue: VDW, Munich, Germany.
There was significant interaction between files and temperatures ($p < 0.05$).
All file systems have longer TTF at room temperature than at body temperature ($p < 0.05$).
[a,b,c]Different superscript alphabets mean significant difference among file groups ($p < 0.05$).
*R Motion had a significantly higher TTF reduction ratio than other files ($p < 0.05$).

cycles for different types of files, are presented in Figure 1. All tested instruments showed a homogeneous thermal transition with repeatable DSC scans. The mean values of the transformational temperatures for PQ are: M*s* = 39.2, M*f* = 24.4, A*s* = 31.2, A*f* = 44.35; for RM: M*s* = 28.2, M*f* = 19.3, A*s* = 29.6, A*f* = 38.6; and for RB: M*s* = 43, M*f* = 18.6, A*s* = 25, A*f* = 48.2 (Figure 1). Both PQ and RB showed the A*p* temperature at around 40°C and 37°C, respectively, while RM had the A*p* at around 33°C (Figure 1).

The scanning electron microscopy images of the cross-sectional surface revealed typical features of fatigue fracture, such as crack initiation area (white arrow) and the fatigue zone positioned opposite to the crack initiation (Figure 2). No specific differences were observed in the test conditions of temperature. The cross-sectional shapes of the instruments varied for each file system, with an S shape for PQ and RB, and a triangular helix for RM. All the cross-sectional aspects show typical features of fatigue fracture, such as crack initiation area and fatigue zone, which is located at the opposite area to the crack initiation.

## DISCUSSION

This study aimed to assess the influence of temperature on the fracture of NiTi endodontic instruments, both at room and body temperatures, and to correlate these findings with the transformational temperatures of the NiTi alloy. While previous studies have compared the influence of body temperature on the cyclic fatigue resistance of heat-treated rotary files, research on reciprocating files remains limited, particularly regarding the PQ file and the effect of different reciprocating motion kinetics [20,21]. This study focused on ISO #25 tip size files, chosen for their widespread clinical use.

Experimental results may vary depending on their origin from different production batches. Here, the instruments used come from the same production batch at all three factories, assuming the homogeneity of the selected samples.

In choosing between a static and a dynamic model, where vertical movement back and forth could potentially extend the time to failure, we opted for a static model because a static model concentrates fatigue in a specific instrumental area [22]. Thus, the static model would be better to reduce the deviation of the data, which might result from the dynamic movement, even if such a dynamic model would make it easier to extrapolate results to more clinical conditions.

To assess heat-treated instruments accurately, body temperature was applied in this study, considering their distinct phase transformation temperatures and fracture resistance at different temperatures. To simulate clinical conditions with body temperature, a water chamber was employed. While El Abed *et al.* [23] used heat-generating pads to transfer the temperature to the files, Cheung *et al.* [13] showed that aqueous media more closely simulate irrigating solutions and avoid temperature increases.

The transitional temperatures obtained for RM are similar to those reported by Basturk *et al.* [24], with 24.4°C and 32.5°C for A*s* and A*f*, respectively. For PQ, our values were different from those reported by Generali *et al.* [25], as they were using the Procodile file, which is different from PQ. To our knowledge, there is no data on the TTF of PQ. Regarding RB, the values differ from those obtained by Plotino *et al.* [20] and Seracchini *et al.* [26]. The values of transformational temperatures may vary due to several factors, such as the method used, specimen preparation, different temperature ranges for heating/cooling, and the cooling rate.


https://doi.org/10.5395/rde.2025.50.e35

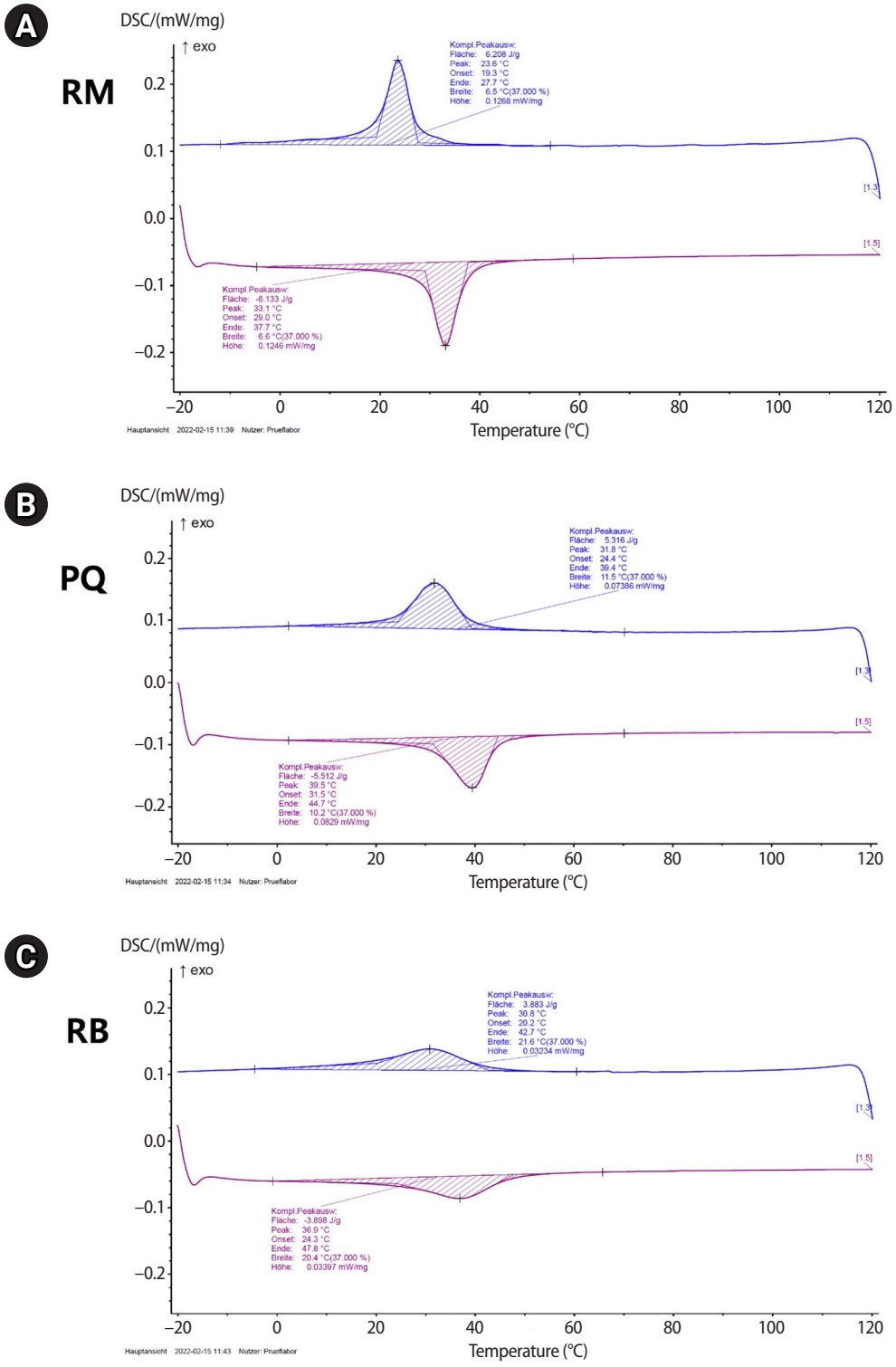


**Figure 1.** The representative plots of differential scanning calorimetry (DSC) for the three tested files. (A) R motion (RM; FKG Dentaire, La Chaux de Fonds, Switzerland), (B) Procodile Q (PQ; Komet Medical, Lemgo, Germany), and (C) Reciproc Blue (RB; VDW, Munich, Germany). Endothermic events are represented by peaks on the upper graph, indicating the absorption of heat by the sample during phase transitions, whereas exothermic events are depicted by peaks on the lower graph, signifying the release of heat by the sample during phase transitions. Note that PQ and RB showed the austenite peak (A*p*) temperature at around 40°C and 37°C, respectively. In contrast, RM had the austenite finishing (A*f*) temperature at around 33°C, which is lower than body temperature.

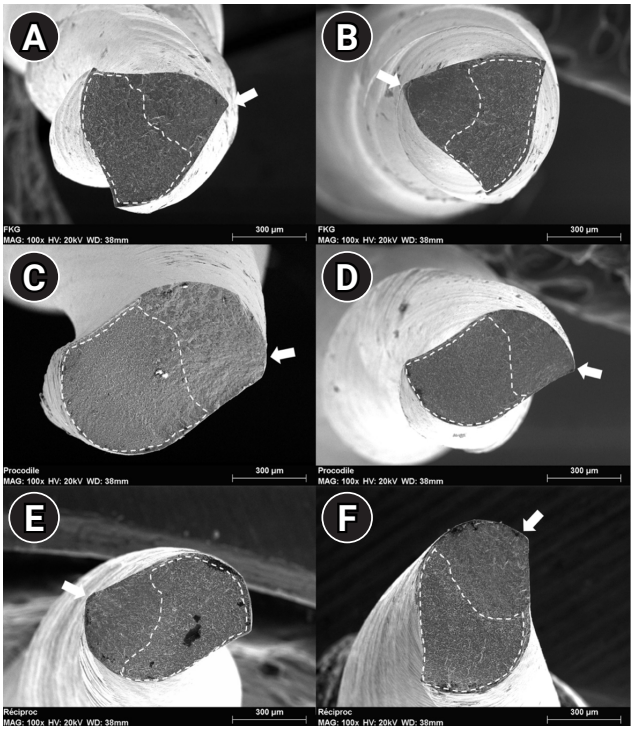


**Figure 2.** Scanning electron microscopy images captured at a magnification of ×100 depict the cross-sections of fractured fragments. (A, B) R Motion (FKG Dentaire, La Chaux de Fonds, Switzerland), (C, D) Procodile Q (Komet Medical, Lemgo, Germany), and (E, F) Reciproc Blue (VDW, Munich, Germany). The left column shows the specimens from the tests at room temperature, while the right column shows the specimens from the body temperature specimens. All the cross-sectional aspects show typical features of fatigue fracture such as crack initiation area (white arrows) and fatigue zone which is located at the opposite area to the crack initiation.

The reciprocating movement of files does not allow calculation of real instrument rotation [27]. Thus, the TTF was used to measure fracture resistance rather than the rotation number of cycles to fracture because of the motion used. For RB, the TTF in our study was higher than that obtained by Keleş *et al.* [22] and Plotino *et al.* [28], but lower than the time reported by Klymus *et al.* [21] at room temperature. Regarding RM, the results were lower at room temperature compared to those obtained by Basturk *et al.* [24], who used a dynamic model. Dynamic models tend to extend cyclic fatigue life [22]. Our study used the "Reflex Dynamic" program (that is, a reciprocating movement able to change angles of reciprocation and angular speed when torque reaches the level set) with the EndoPilot motor, but this special movement did not occur due to the low torque applied by the stainless-steel tube. That was not the case in the study of Zubizarreta-Macho *et al.* [27], which used an artificial root canal and simulated a pecking movement. They found that Reflex smart reciprocation improved the cyclic fatigue resistance of reciprocating files compared to traditional reciprocating movement.

The TTF of PQ was the highest, followed by RB and RM at both room and body temperatures. According to Plotino *et al.* [28], the cross-sectional design influences the cyclic fatigue strength, with an inverse correlation between cyclic fatigue strength and the amount of metal mass in the cross-section of NiTi files. Therefore, the higher cyclic fatigue strength of PQ compared to RM could be attributed to its cross-sectional area associated with the S-shaped and the contact with a smaller number of dentin walls. The higher cyclic fatigue resistance of PQ compared to RB might be attributed to the effect of reduced metal mass resulting from the smaller taper. Furthermore, it is proposed that the heat treatment characteristics exert a more substantial influence on the fatigue cyclic resistance of the NiTi file than other factors such as cross-sectional area and taper [29]. It is conjectured that the elevated A*s* and A*f* temperatures of PQ may have contributed to its superior cyclic fatigue resistance.

In the present study, all tested instruments had significantly faster separation at body temperature. This result is consistent with a previous report indicating that increasing temperature can negatively affect the cyclic fatigue resistance of heat-treated files [30].

The reduction in TTF at body temperature is associated with the crystallographic state of the alloy. The reduction ratio in our study was over 30% for PQ and RB, and over 70% for RM (Table 1). This could be explained by the fact that PQ and RB are in the martensite phase at room temperature and partially austenite at oral temperature. However, RM is the most impacted, as it is clearly used in both phases (fully martensite at room temperature and fully austenite at body temperature). At body temperature, its microstructure has completely switched to the austenite phase, and the file adopts a super-elastic behavior.

The DSC analysis provides a partial understanding of the impact of the operating temperature on each instrument. The A*s* temperature values (24° for RB, 29°


https://doi.org/10.5395/rde.2025.50.e35

for RM, and 31.5° for PQ) are decisive in their behavior. PQ has the longest bending fatigue life under the conditions of this study. It is influenced by oral temperature by partially reverting to the austenite phase, which does not allow it to resist as long as at room temperature. The heat treatment effect diminishes to some extent during clinical use of these instruments. All instruments had a decreased breakage time (ranging from 23 to 64%, depending on the instrument).

This study tested the fatigue resistance under the 37°C to simulate body temperature. However, the phase transformation occurs inside of root canal, which is usually filled with an irrigation solution. Thus, future research may need to measure the actual root canal temperature and apply this condition for testing of martensite-dominant instruments.

## CONCLUSIONS

Within the limitations of this study, the instruments used had variable fracture resistance depending on their geometrical profile, heat treatment, and the temperature at which they were used. The heat-treated files with reciprocating kinetics may have different reduction ratios of the fatigue resistance of the file systems under different temperature conditions. This characteristic is an important point of consideration when clinicians select the file system to reduce potential file fracture.

### CONFLICT OF INTEREST

Hyeon-Cheol Kim is an Scientific Advisory Board member of *Restorative Dentistry and Endodontics* and was not involved in the peer-review or editorial process of this article. The authors declare no other conflicts of interest.

### FUNDING/SUPPORT

The authors have no financial relationships relevant to this article to disclose.

### AUTHOR CONTRIBUTIONS

Conceptualization, Formal analysis, Software, Supervision: Nehme W, Kim HC. Data curation: Naaman A, Pedèches L. Investigation: Naaman A, Pedèches L, Lê S. Methodology: Lê S, Georgelin-Gurgel M. Project administration, Resources: Diemer F. Validation: Kwak SW, Diemer F. Visualization: Kwak SW, Kim HC. Writing - original draft: Nehme W. Writing - review & editing: Kwak SW, Kim HC, Diemer F. All authors read and approved the final manuscript.

### DATA SHARING STATEMENT

The datasets used and/or analyzed during the current study are available from the corresponding author on reasonable request.

## REFERENCES

1. Pereira ÉS, Viana AC, Buono VT, Peters OA, Bahia MG. Behavior of nickel-titanium instruments manufactured with different thermal treatments. J Endod 2015;41:67-71.
2. Peters OA, Morgental RD, Schulze KA, Paqué F, Kopper PM, Vier-Pelisser FV. Determining cutting efficiency of nickel-titanium coronal flaring instruments used in lateral action. Int Endod J 2014;47:505-513.
3. Parashos P, Messer HH. Rotary NiTi instrument fracture and its consequences. J Endod 2006;32:1031-1043.
4. Kim HC, Kim HJ, Lee CJ, Kim BM, Park JK, Versluis A. Mechanical response of nickel-titanium instruments with different cross-sectional designs during shaping of simulated curved canals. Int Endod J 2009;42:593-602.
5. Shen Y, Hieawy A, Huang X, Wang ZJ, Maezono H, Haapasalo M. Fatigue resistance of a 3-dimensional conforming nickel-titanium rotary instrument in double curvatures. J Endod 2016;42:961-964.
6. Kishore A, Gurtu A, Bansal R, Singhal A, Mohan S, Mehrotra A. Comparison of canal transportation and centering ability of twisted files, HyFlex controlled memory, and wave one using computed tomography scan: an in vitro study. J Conserv Dent 2017;20:161-165.
7. Pedulla E, Corsentino G, Ambu E, Rovai F, Campedelli F, Rapisarda S, *et al*. Influence of continuous or reciprocating optimum torque reverse motion on cyclic fatigue resistance of two single-file nickel-titanium rotary instruments. Eur Endod J 2017;2:1-6.
8. Pruett JP, Clement DJ, Carnes DL. Cyclic fatigue testing of nickel-titanium endodontic instruments. J Endod 1997;23:77-85.
9. Shen Y, Cheung GS, Bian Z, Peng B. Comparison of defects in ProFile and ProTaper systems after clinical use. J Endod 2006;32:61-65.
10. Shen Y, Haapasalo M, Cheung GS, Peng B. Defects in nickel-titanium instruments after clinical use: part 1: relationship between observed imperfections and factors leading to such defects in a cohort study. J Endod 2009;35:129-132.
11. Alapati SB, Brantley WA, Svec TA, Powers JM, Nusstein JM, Daehn GS. SEM observations of nickel-titanium rotary

endodontic instruments that fractured during clinical Use. J Endod 2005;31:40-43.
12. Kuhn G, Tavernier B, Jordan L. Influence of structure on nickel-titanium endodontic instruments failure. J Endod 2001;27:516-520.
13. Cheung GS, Shen Y, Darvell BW. Effect of environment on low-cycle fatigue of a nickel-titanium instrument. J Endod 2007;33:1433-1437.
14. Nguyen HH, Fong H, Paranjpe A, Flake NM, Johnson JD, Peters OA. Evaluation of the resistance to cyclic fatigue among ProTaper next, ProTaper universal, and vortex blue rotary instruments. J Endod 2014;40:1190-1193.
15. Grande NM, Plotino G, Silla E, Pedullà E, DeDeus G, Gambarini G, *et al*. Environmental temperature drastically affects flexural fatigue resistance of nickel-titanium rotary files. J Endod 2017;43:1157-1160.
16. Hieawy A, Haapasalo M, Zhou H, Wang ZJ, Shen Y. Phase transformation behavior and resistance to bending and cyclic fatigue of ProTaper gold and ProTaper universal instruments. J Endod 2015;41:1134-1138.
17. Zanza A, Seracchiani M, Reda R, Miccoli G, Testarelli L, Di Nardo D. Metallurgical tests in endodontics: a narrative review. Bioengineering (Basel) 2022;9:30.
18. Zupanc J, Vahdat-Pajouh N, Schäfer E. New thermomechanically treated NiTi alloys: a review. Int Endod J 2018;51:1088-1103.
19. Shen Y, Zhou HM, Zheng YF, Peng B, Haapasalo M. Current challenges and concepts of the thermomechanical treatment of nickel-titanium instruments. J Endod 2013;39:163-172.
20. Plotino G, Grande NM, Testarelli L, Gambarini G, Castagnola R, Rossetti A, *et al*. Cyclic fatigue of reciproc and reciproc blue nickel-titanium reciprocating files at different environmental temperatures. J Endod 2018;44:1549-1552.
21. Klymus ME, Alcalde MP, Vivan RR, Só MV, de Vasconselos BC, Duarte MA. Effect of temperature on the cyclic fatigue resistance of thermally treated reciprocating instruments. Clin Oral Investig 2019;23:3047-3052.
22. Keleş A, Eymirli A, Uyanık O, Nagas E. Influence of static and dynamic cyclic fatigue tests on the lifespan of four reciprocating systems at different temperatures. Int Endod J 2019;52:880-886.
23. El Abed R, Alshehhi A, Kang YJ, Al Raeesi D, Khamis AH, Jamal M, *et al*. Fracture resistance of heat-treated nickel-titanium rotary files after usage and autoclave sterilization: an in vitro study. J Endod 2022;48:1428-1433.
24. Basturk FB, Özyürek T, Uslu G, Gündoğar M. Mechanical properties of the new generation RACE EVO and R-motion nickel-titanium instruments. Materials (Basel) 2022;15:3330.
25. Generali L, Malovo A, Bolelli G, Borghi A, La Rosa GR, Puddu P, *et al*. Mechanical properties and metallurgical features of new green NiTi reciprocating instruments. Materials (Basel) 2020;13:3736.
26. Seracchiani M, Reda R, Zanza A, D'Angelo M, Russo P, Luca T. Mechanical performance and metallurgical characteristics of 5 different single-file reciprocating instruments: a comparative in vitro and laboratory study. J Endod 2022;48:1073-1080.
27. Zubizarreta-Macho Á, Albaladejo Martínez A, Falcão Costa C, Quispe-López N, Agustín-Panadero R, Mena-Álvarez J. Influence of the type of reciprocating motion on the cyclic fatigue resistance of reciprocating files in a dynamic model. BMC Oral Health 2021;21:179.
28. Plotino G, Grande NM, Testarelli L, Gambarini G. Cyclic fatigue of Reciproc and WaveOne reciprocating instruments. Int Endod J 2012;45:614-618.
29. Kim E, Ha JH, Dorn SO, Shen Y, Kim HC, Kwak SW. Effect of heat treatment on mechanical properties of nickel-titanium instruments. J Endod 2024;50:213-219.
30. Shen Y, Huang X, Wang Z, Wei X, Haapasalo M. Low environmental temperature influences the fatigue resistance of nickel-titanium files. J Endod 2018;44:626-629.


https://doi.org/10.5395/rde.2025.50.e35

RDE Restorative Dentistry & Endodontics

Research Article

eISSN 2234-7666
Restor Dent Endod. 2025 November;50(4):e36
https://doi.org/10.5395/rde.2025.50.e36

# *In vitro* experimental study comparing continuous and intermittent irrigation protocols: influence of sodium hypochlorite volume and contact time on tissue dissolution

**Alfredo Iandolo[1,2], Dina Abdellatif[1,2], Davide Mancino[3], Gwenael Rolin[1,4], Camille Coussens[5], Aurelian Louvrier[2,5,6], Felipe G Belladonna[7], Edouard Euvrard[1,2], Emmanuel João Nogueira Leal da Silva[7,8,*]**

[1]Faculty of Dental Surgery, University of Franche-Comte, CHU Besançon, Besançon, France
[2]Laboratoire Sinergies EA 4662, University of Franche-Comté, Besançon, France
[3]Faculty of Dental Surgery, Federation of Medicine Translational of Strasbourg and Federation of Materials and Nanoscience of Alsace, University of Strasbourg, Strasbourg, France
[4]INSERM CIC-1431, CHU Besançon, Besançon, France
[5]Plateforme I3DM (Impression 3D Médicale), CHU Besançon, Besançon, France
[6]Chirurgie maxillo-faciale et stomatologie, CHU Besançon, Besançon, France
[7]Department of Endodontics, School of Dentistry, Fluminense Federal University, Rio de Janeiro, Brazil
[8]Department of Endodontics, School of Dentistry, Grande Rio University, Rio de Janeiro, Brazil

## ABSTRACT

**Objectives:** This study aimed to evaluate whether continuous irrigation with larger volumes or allowing sodium hypochlorite (NaOCl) resting time is more critical for pulp tissue dissolution using a controlled artificial root canal system.

**Methods:** A three-dimensional printed artificial root canal with a lateral canal in the apical third was fabricated. Standardized bovine pulp tissue specimens were inserted, and three irrigation protocols were tested: group A (continuous NaOCl irrigation at 1 mL/min via syringe pump), group B (intermittent NaOCl irrigation with 0.1 mL and a 3-minute resting period), and group C (control, saline irrigation). The time for complete dissolution and the total NaOCl volume were recorded.

**Results:** Complete dissolution occurred in groups A and B, with significant differences in NaOCl volume and time ($p < 0.05$). In group A, complete dissolution was consistently observed after the 6th irrigation cycle, corresponding to a total NaOCl volume of 6.0 ± 0.66 mL per test. The average time required for complete dissolution in this group was 6 ± 0.66 minutes. In group B, complete dissolution occurred after the 4th cycle, with a total NaOCl volume of 0.4 ± 0.06 mL per test and a mean dissolution time of 12.6 ± 1.8 minutes.

**Conclusions:** NaOCl volume and exposure time significantly influence pulp tissue dissolution.

**Keywords:** Endodontics; Sodium hypochlorite; Tissue dissolution

**Received:** April 17, 2025 **Revised:** July 15, 2025 **Accepted:** August 5, 2025

**Citation**
Iandolo A, Abdellatif D, Mancino D, Rolin G, Coussens C, Louvrier A, Belladonna FG, Euvrard E, Silva EJNL. *In vitro* experimental study comparing continuous and intermittent irrigation protocols: influence of NaOCl volume and contact time on tissue dissolution. Restor Dent Endod 2025;50(4):e36.

***Correspondence to**
**Emmanuel João Nogueira Leal da Silva, DDS, PhD**
Department of Endodontics, School of Dentistry, Grande Rio University, Rua Herotides de Oliveira, 61/902, Icaraí, Niterói, RJ 24230-230, Brazil
Email: nogueiraemmanuel@hotmail.com

## INTRODUCTION

Sodium hypochlorite (NaOCl) is widely recognized as an effective irrigant in endodontic treatment due to its potent tissue-dissolving and antimicrobial properties [1]. However, its efficacy depends on several interrelated factors, including concentration, temperature, flow dynamics, canal anatomy, volume, and contact time with the root canal system [2]. While higher concentrations and temperatures enhance its tissue-dissolving ability [3], they also increase cytotoxicity and the risk of extrusion beyond the apex [4]. Similarly, irrigation volume and duration play critical roles in tissue dissolution and debris removal—greater volumes improve flushing action, while contact sustains chemical efficacy [5,6]. As advancements in instrumentation have made canal preparation faster and more efficient, optimizing these variables is essential for safe and effective root canal disinfection.

The evolution of endodontic instrumentation, particularly with rotary and reciprocating systems, has significantly reduced the time required for canal shaping [7]. With fewer instruments and more efficient techniques, clinicians can now achieve effective canal preparation in a fraction of the time previously needed. This shift towards faster procedures has amplified the importance of the chemical phase of root canal treatment, emphasizing irrigation's role in cleaning areas beyond the reach of mechanical instrumentation [1]. The concept of 'shaping for cleaning' highlights the reliance on irrigating solutions, particularly NaOCl, to dissolve residual pulp tissue and biofilms [8]. As a result, optimizing the irrigation protocol—balancing time and volume—has become a key focus in recent years [1]. Understanding how these parameters influence NaOCl's efficacy is crucial to achieving thorough disinfection while maintaining efficiency and patient safety.

Despite advancements in endodontic instrumentation and irrigation techniques, the practical implications of balancing irrigation time and volume remain poorly understood. While the effects of NaOCl concentration and temperature have been extensively studied, fewer investigations have explored the interplay between these two factors [9,10]. This study addresses this gap by using an artificial root canal model designed to evaluate pulp tissue dissolution under controlled irrigation conditions. By isolating and analyzing these parameters, it aims to provide evidence-based insights into their impact on tissue dissolution. Therefore, the aim of the current study was to evaluate whether continuous irrigation with larger volumes or allowing NaOCl resting time is more critical for pulp tissue dissolution. The null hypothesis tested was that there would be no difference in the tissue dissolution effectiveness between continuous and intermittent irrigation protocols using 3% NaOCl.

## METHODS

### Sample size calculation

The sample size calculation was based on data from previous studies. Power analysis was conducted using G*Power 3.1 software for Windows (Heinrich Heine University Düsseldorf, Düsseldorf, Germany) with a significance level of 0.05, statistical power of 80%, and an effect size of 0.4, following Cohen's guidelines. The analysis determined that 30 specimens (10 per group) were required to detect significant differences among the experimental groups. The sample size was also consistent with prior *in vitro* studies evaluating tissue dissolution [9,10].

### Artificial canal design and fabrication

The artificial canal system was designed using AutoCAD software (version 2024, Autodesk Inc.) and fabricated with a professional grade three-dimensional (3D) printer (Imprinter Form 3B; Formlabs, Somerville, MA, USA) at a resolution of 0.05 mm. A biocompatible transparent resin (Biomed Clear Resin, Formlabs) was used to enhance visualization during experiments. The canal design featured an apical diameter of 0.30 mm, a 6% taper, and a total length of 16 mm. Additionally, a 1-mm lateral space was positioned 3 mm from the apex, with dimensions of 0.48 mm at the minor base, 0.54 mm at the major base, and a depth of 0.5 mm [11].

For experimental feasibility, the canal system was printed in two separate parts, allowing precise insertion of pulp tissue into the lateral space. This design also enabled direct observation of tissue dissolution throughout the experiments, providing an optimal setup for evaluating irrigation protocol efficacy (Figure 1).


https://doi.org/10.5395/rde.2025.50.e36

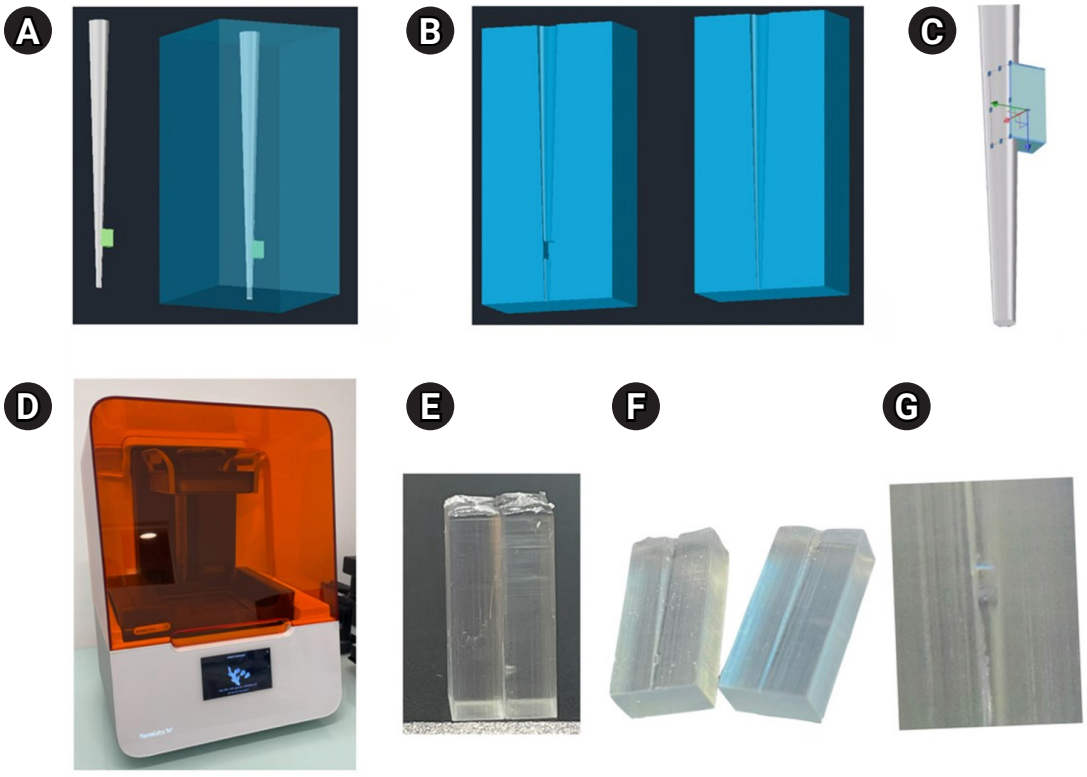


**Figure 1.** (A–C) Digital renderings of the artificial canal system, highlighting the small lateral canal positioned in the apical third. (D) The professional-grade three-dimensional (3D) printer (Imprinter Form 3B; Formlabs, Somerville, MA, USA) used to fabricate the canal system. (E) The completed 3D-printed canal model, fabricated using biocompatible transparent resin. (F) Demonstration of the model's ability to be opened and reassembled, allowing for the insertion of pulp tissue. (G) Close-up view of the small lateral canal located in the apical third of the model.

### Pulp specimen preparation

Bovine pulp tissue was collected post-slaughter from mandibular incisors of food-production animals, and the study was not classified as an animal study. Fresh, intact anterior mandibular teeth were extracted within 36 hours of slaughter and immediately stored in a 0.1% thymol solution to preserve tissue integrity. The crowns were sectioned at the cementoenamel junction using a high-speed diamond bur (Komet; Gebr. Brasseler GmbH & Co. KG, Lemgo, Germany) under continuous irrigation to prevent thermal damage. Pulp tissue was carefully extracted, rinsed with distilled water to remove any debris, and individually stored in 1.5-mL Eppendorf tubes containing 1 mL of distilled water at –20°C until experimentation.

Before the experiments, pulp samples were thawed at room temperature for 30 minutes and incubated at 37°C in a water bath for 15 minutes to simulate clinical conditions. The specimens were then standardized to 1 × 0.5 × 0.5 mm under 8× magnification (SOM 32; Karl Kaps GmbH, Asslar, Germany), using millimeter graph paper and a surgical scalpel blade (Braun, Tuttlingen, Germany) for precise cutting and measurement. Each standardized specimen was then gently inserted into the lateral canal using micro-tweezers and positioned under stereomicroscopic visualization to guarantee accurate placement without compression, folding, or deformation. This meticulous approach ensured reproducible tissue volumes and uniform conditions across all samples.

### Groups and experimental setup

All samples were weighed using a high-precision microbalance (accuracy of 0.00001 g, Explorer Semi-Micro; Ohaus Corporation, Parsippany, NJ, USA) at three stages: before the experiment, after pulp insertion, and after each irrigation cycle. The following groups were tested:

Group A: Pulp tissue was inserted into the lateral

space, and the canal was assembled. The apex was sealed with wax to simulate a closed system. NaOCl 3% (CanalPro; Coltene/Whaledent Inc., Cuyahoga Falls, OH, USA) was delivered at 1 mL/min using a syringe pump (Pilote A2; Fresenius Vial SAS, Brézins, France) with a 30-gauge side-vented needle (CanalPro Sideport Tips, Coltene/Whaledent Inc.) positioned 1 mm short of the working length. After irrigation, the canal was rinsed with 1 mL/min sterile saline, dried with sterile paper points, weighed, and opened for examination. This cycle was repeated until the pulp tissue was completely dissolved.

Group B: Pulp tissue was inserted into the lateral space, and the canal was assembled. The apex was sealed with wax to simulate a closed system. NaOCl 3% (0.1 mL) was manually delivered by an experienced operator using a syringe to fill the canal, followed by a 3-minute waiting period. The canal was then rinsed with sterile saline at 1 mL/min, dried with sterile paper points, weighed, and observed. This process was repeated until complete tissue dissolution.

Group C (control): The protocol for group B was followed, but sterile saline was used instead of NaOCl.

A total of 10 canals were prepared per group (Figures 2 and 3), and 10 irrigation cycles were performed per experiment.

### Statistical analysis

Data normality was assessed using the Shapiro-Wilk test. One-way analysis of variance was then performed to evaluate differences in pulp tissue dissolution and the time required for complete dissolution among the groups, followed by Tukey honestly significant difference *post hoc* analysis for pairwise comparisons. A significance level of 0.05 was adopted.

## RESULTS

Complete pulp tissue dissolution was achieved in all samples of groups A and B. However, the volume of NaOCl required and the time for complete dissolution differed significantly between the two groups ($p < 0.05$). In contrast, no tissue dissolution was observed in any sample from group C, where sterile saline was


**Figure 2.** (A–C) High-precision microbalance (Explorer Semi-Micro; Ohaus Corporation, Parsippany, NJ, USA) used to weigh samples at different experimental stages. (D, E) Syringe pump (Pilote A2; Fresenius Vial SAS, Brézins, France) used for controlled delivery of sodium hypochlorite during the experiments.


https://doi.org/10.5395/rde.2025.50.e36

used as the irrigant. In group A, complete dissolution was consistently observed after the 6th irrigation cycle, corresponding to a total NaOCl volume of 6.0 ± 0.66 mL per test. The average time required for complete dissolution in this group was 6.0 ± 0.66 minutes. In group B, complete dissolution occurred after the 4th cycle, with a total NaOCl volume of 0.4 ± 0.06 mL per test and a mean dissolution time of 12.6 ± 1.8 minutes (Figure 4).

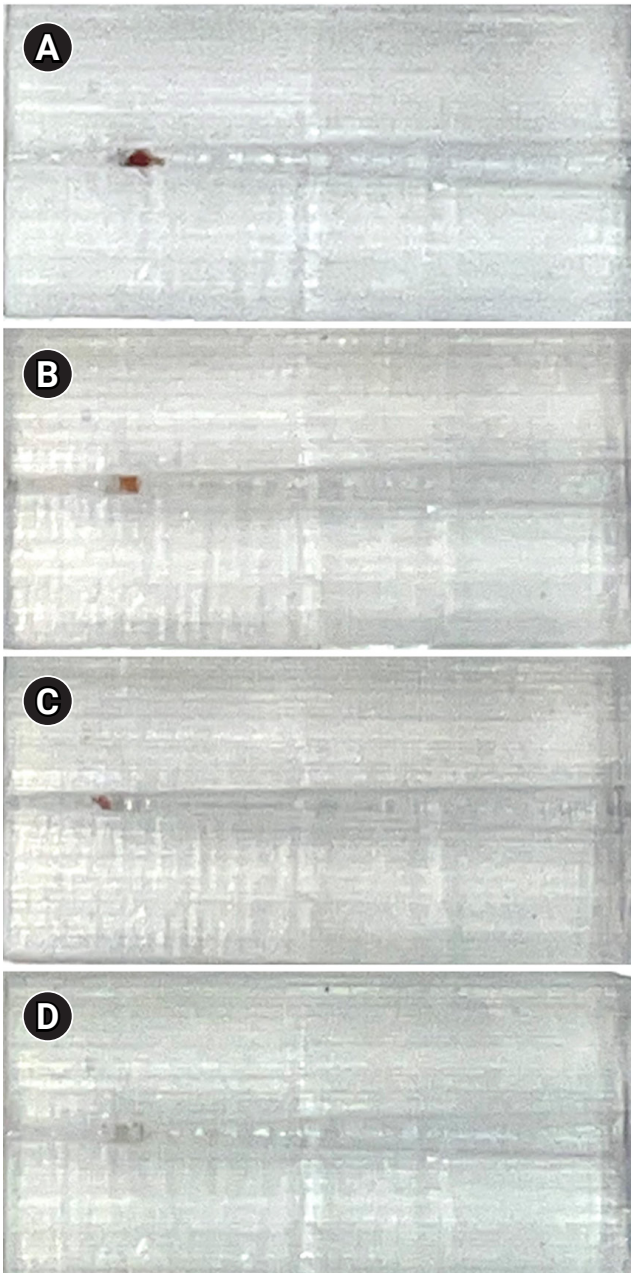


**Figure 3.** Visualization of pulp tissue within the small lateral canal located in the apical third of the artificial canal model. (A) Intact pulp tissue before irrigation. (B) Partially dissolved pulp tissue. (C) Near-complete tissue dissolution. (D) Complete dissolution of pulp tissue.

## DISCUSSION

The present study evaluated the impact of irrigation time and volume on NaOCl's tissue dissolution capacity, demonstrating that both factors significantly influence dissolution efficiency. Complete pulp dissolution was achieved in all samples exposed to NaOCl, though the required volume and time varied between groups. Group A, which received continuous irrigation at a flow rate of 1 mL/min, achieved complete dissolution in a shorter time but required a higher total volume of NaOCl. In contrast, group B, which utilized intermittent delivery with a resting phase, achieved the same outcome using significantly less NaOCl, albeit over a longer period. As a result, the null hypothesis was rejected. These findings highlight the dynamic interaction between irrigation parameters and chemical efficacy, emphasizing the need for refined irrigation protocols to enhance clinical outcomes.

Previous studies have established that NaOCl concentration, temperature, and contact time are critical factors influencing its tissue-dissolving capacity [9,10,12]. However, the relative importance of irrigation volume versus exposure time has been less explored. While the results of the present study may seem intuitive, they carry significant clinical relevance by demonstrating that

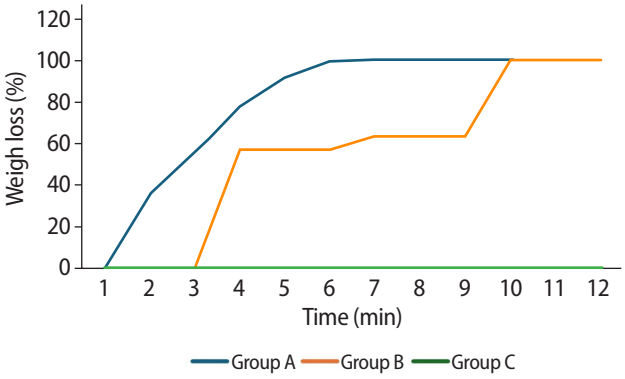


**Figure 4.** Graphic showing the percentage of pulp tissue weight loss over time in all groups. Group A, continuous 3% NaOCl at 1 mL/min; group B, intermittent 3% NaOCl, 0.1 mL with 3-min rest; and group C, saline control.

efficient tissue dissolution can be achieved through two distinct strategies: continuous irrigation with a larger volume or prolonged exposure with a minimal amount of irrigant. The findings suggest that while higher volumes accelerate tissue dissolution by continuously replenishing the active solution—and possibly through a flow and reflux effect—extended exposure to a smaller volume can achieve similar outcomes over a longer duration. These results align, to some extent, with the 'shaping for cleaning' concept, which emphasizes that mechanical instrumentation mainly facilitates irrigation rather than being solely responsible for debridement.

Advances in rotary and reciprocating instrumentation have reduced canal preparation time, increasing reliance on irrigation to remove residual pulp tissue and biofilms [7]. This study reinforces the need to optimize irrigation parameters, particularly volume and contact time, to maximize NaOCl efficacy. Although continuous irrigation ensures constant exposure to fresh irrigant, it is impractical for clinicians to maintain prolonged irrigation at high volumes during routine endodontic procedures. Therefore, this study highlights an alternative approach: even small volumes of NaOCl—sufficient to fill the root canal—can effectively dissolve tissue when given enough contact time. This strategy not only preserves chemical efficacy but also reduces operator fatigue and the excessive consumption of irrigant [9]. Optimizing irrigation protocols to balance efficiency, practicality, and clinician ergonomics is essential for improving the overall success of root canal disinfection [13–15].

A key strength of this study is the use of a controlled artificial canal system, which allowed for direct comparisons of different irrigation protocols under standardized conditions. The model included a lateral canal positioned in the apical third, with dimensions deliberately chosen to accommodate a measurable volume of pulp tissue and enable reproducible placement and dissolution assessment in this anatomically challenging area. Although these dimensions are slightly larger than typical anatomical lateral canals, they are consistent with previously validated experimental models [11] and ensured methodological reliability. Additionally, the use of bovine pulp tissue provided a consistent and reproducible substrate for dissolution analysis, ensuring methodological reliability. The precise weighing of samples before and after each irrigation cycle further strengthened the accuracy of the findings, allowing for a quantifiable assessment of NaOCl's effectiveness across different irrigation strategies. By eliminating anatomical variability and other uncontrollable clinical factors, this experimental design minimized potential biases and provided greater control over key variables, ensuring a more reliable evaluation of the specific effects of irrigation time and volume.

As with all *in vitro* studies, certain limitations must be acknowledged. The artificial canal system, while providing a controlled and reproducible environment, does not fully replicate the anatomical complexities of human root canals, such as variations in dentinal tubules, the presence of a smear layer, or biofilm interactions that could influence NaOCl penetration and efficacy [11]. Additionally, the experimental setup did not account for potential fluctuations in NaOCl concentration over time, nor the presence of organic and inorganic debris that could affect its reactivity. Another limitation is the absence of activation techniques, such as sonic or ultrasonic agitation, which are known to enhance irrigant effectiveness by improving penetration and tissue contact [13–15]. The use of a 3% NaOCl solution, although not the most concentrated option available, was deliberate, as it reflects a widely used commercial product and ensures quality control and stability throughout the experiments. Consequently, the findings primarily reflect the passive dissolution potential of NaOCl under controlled conditions. Nonetheless, the standardized methodology used in this study enabled precise isolation of the effects of irrigation time and volume, minimizing confounding variables and providing valuable insights into NaOCl dynamics that can inform future research and clinical practice.

Further research should investigate the combined effects of NaOCl volume, exposure time, and agitation methods to determine the most efficient irrigation protocol for clinical scenarios. Future studies using micro-computed tomography could provide a 3D assessment of tissue dissolution in anatomically complex canal systems. Additionally, evaluating alternative irrigants and NaOCl concentrations under similar conditions could further refine best practices for endodontic


https://doi.org/10.5395/rde.2025.50.e36

irrigation. It is important to note that this study focused exclusively on tissue dissolution and did not assess NaOCl's effectiveness against bacterial biofilms. Since biofilm removal is a critical aspect of root canal disinfection, future research should explore how different irrigation protocols influence biofilm disruption and eradication. Incorporating microbiological models would offer a more comprehensive understanding of NaOCl's role in both tissue and biofilm dissolution, ultimately improving clinical recommendations.

## CONCLUSIONS

This study demonstrated that continuous irrigation with 3% NaOCl consistently dissolved pulp tissue in 6 minutes using 6.0 mL, whereas intermittent irrigation achieved complete dissolution in 12 minutes using only 0.4 mL. These findings suggest that both volume and contact time play critical roles in tissue dissolution, and clinicians may tailor irrigation protocols based on procedural priorities such as time efficiency or chemical conservation.

### CONFLICT OF INTEREST

Emmanuel João Nogueira Leal da Silva is the Associate Editor of *Restorative Dentistry and Endodontics* and was not involved in the review process of this article. The authors declare no other conflicts of interest.

### FUNDING/SUPPORT

The authors have no financial relationships relevant to this article to disclose.

### AUTHOR CONTRIBUTIONS

Conceptualization, Methodology: Iandolo A, Abdellatif D, Belladonna F, Silva EJNL. Data curation: Mancino D, Coussens C, Louvrier A, Euvrard E. Formal analysis: Iandolo A, Abdellatif D, Mancino D, Coussens C, Louvrier A, Belladonna F, Euvrard E, Silva EJNL. Funding acquisition, Project administration: Silva EJNL. Investigation: Mancino D, Rolin G, Coussens C, Louvrier A, Euvrard E. Supervision: Belladonna F, Silva EJNL. Writing – original draft: Iandolo A, Abdellatif D, Mancino D, Belladonna F, Silva EJNL. Writing – review & editing: Iandolo A, Abdellatif D, Belladonna F, Silva EJNL. All authors read and approved the final manuscript.

### DATA SHARING STATEMENT

The datasets are not publicly available but are available from the corresponding author upon reasonable request.

## REFERENCES

1. Zehnder M, Kosicki D, Luder H, Sener B, Waltimo T. Tissue-dissolving capacity and antibacterial effect of buffered and unbuffered hypochlorite solutions. Oral Surg Oral Med Oral Pathol Oral Radiol Endod 2002;94:756-762.
2. Zehnder M. Root canal irrigants. J Endod 2006;32:389-398.
3. Naenni N, Thoma K, Zehnder M. Soft tissue dissolution capacity of currently used and potential endodontic irrigants. J Endod 2004;30:785-787.
4. Heling I, Rotstein I, Dinur T, Szwec-Levine Y, Steinberg D. Bactericidal and cytotoxic effects of sodium hypochlorite and sodium dichloroisocyanurate solutions in vitro. J Endod 2001;27:278-280.
5. McDonnell G, Russell AD. Antiseptics and disinfectants: activity, action, and resistance. Clin Microbiol Rev 1999;12:147-179.
6. Macedo RG, Wesselink PR, Zaccheo F, Fanali D, Van Der Sluis LW. Reaction rate of NaOCl in contact with bovine dentine: effect of activation, exposure time, concentration and pH. Int Endod J 2010;43:1108-1115.
7. Peters OA. Current challenges and concepts in the preparation of root canal systems: a review. J Endod 2004;30:559-567.
8. De Deus G, Silva EJNL, Souza E, Versiani MA, Zuolo M. Shaping for cleaning the root canals: a clinical-based strategy. Cham, Switzerland: Springer Nature; 2022.
9. Iandolo A, Dagna A, Poggio C, *et al*. Evaluation of the actual chlorine concentration and the required time for pulp dissolution using different sodium hypochlorite irrigating solutions. J Conserv Dent 2019;22:108-113.
10. Del Carpio-Perochena A, Monteiro Bramante C, Hungaro Duarte M, *et al*. Effect of temperature, concentration and contact time of sodium hypochlorite on the treatment and revitalization of oral biofilms. J Dent Res Dent Clin Dent Prospects 2015;9:209-215.
11. Christofzik D, Bartols A, Faheem MK, *et al*. Shaping ability of four root canal instrumentation systems in simulated three-dimensional-printed root canal models. PLoS One 2018;13:e0201129.
12. Krah-Sinan AA, Adou-Assoumou M, Xavier Djolé S, Diemer F, Gurgel M. The effects of sodium hypochlorite on organic matters: influences of concentration, renewal frequency and contact area. Iran Endod J 2020;15:18-22.
13. van der Sluis LW, Versluis M, Wu MK, Wesselink PR. Passive

ultrasonic irrigation of the root canal: a review of the literature. Int Endod J 2007;40:415-426.
14. Boutsioukis C, Arias-Moliz MT. Present status and future directions - irrigants and irrigation methods. Int Endod J 2022;55 Suppl 3:588-612.
15. Nagendrababu V, Jayaraman J, Suresh A, Kalyanasundaram S, Neelakantan P. Effectiveness of ultrasonically activated irrigation on root canal disinfection: a systematic review of in vitro studies. Clin Oral Investig 2018;22:655-670.


https://doi.org/10.5395/rde.2025.50.e36

RDE Restorative Dentistry & Endodontics

Research Article

eISSN 2234-7666
Restor Dent Endod. 2025 November;50(4):e37
https://doi.org/10.5395/rde.2025.50.e37

# Comparison of remineralization in caries-affected dentin using calcium silicate, glass ionomer cement, and resin-modified glass ionomer cement: an *in vitro* study

**Kwanchanok Youcharoen[1], Onwara Akkaratham[2], Papichaya Intajak[2], Pipop Saikaew[3], Sirichan Chiaraputt[4,*]**

[1]Department of Pedodontics and Preventive Dentistry, Faculty of Dentistry, Srinakharinwirot University, Bangkok, Thailand
[2]Department of Conservative Dentistry and Prosthodontics, Faculty of Dentistry, Srinakharinwirot University, Bangkok, Thailand
[3]Department of Operative Dentistry and Endodontics, Faculty of Dentistry, Mahidol University, Bangkok, Thailand
[4]School of Dentistry, King Mongkut's Institute of Technology, Ladkrabang (KMITL), Bangkok, Thailand

## ABSTRACT

**Objectives:** This study evaluated the ability of calcium silicate cement (CSC) as a remineralizing agent compared with conventional glass ionomer cement (GIC) and resin-modified GIC (RMGIC) to remineralize artificial caries-affected dentin.

**Methods:** Twenty-five class V cavities were prepared on extracted human third molars. Twenty teeth underwent artificial caries induction. The remaining five teeth with sound dentin serve as the positive control. The twenty demineralized teeth were subdivided into four groups ($n = 5$): carious dentin without restoration (negative control [NC]), carious dentin restored with CSC (Biodentine, Septodont), carious dentin restored with GI (Fuji IX, GC Corporation), and carious dentin restored with RMGIC (Fuji II LC, GC Corporation). Following restoration, the specimens were stored in artificial saliva for 7 days. The elastic modulus was evaluated by a nanoindentation test. The mineral composition was analyzed by scanning electron microscopy-energy-dispersive X-ray spectroscopy (SEM-EDX), and the mineral composition at the dentin-material interface.

**Results:** CSC had a higher modulus of elasticity compared to GI, RMGI, and NC groups ($p < 0.05$). Higher calcium and phosphorus content was observed under CSC restorations, as indicated by SEM-EDX examination, which may lead to better remineralization.

**Conclusions:** Compared to GI and RMGI, CSC showed the best remineralization and mechanical reinforcement in caries-affected dentin, indicating CSC for use in minimally invasive restorative dentistry.

**Keywords:** Calcium silicate cement; Caries-affected dentin; Glass ionomer cement; Nanoindentation; Scanning electron microscopy; Tooth remineralization; X-ray emission spectrometry

**Received:** April 29, 2025 **Revised:** July 13, 2025 **Accepted:** July 14, 2025

**Citation**
Youcharoen K, Akkaratham O, Intajak P, Saikaew P, Chiaraputt S. Comparison of remineralization in caries-affected dentin using calcium silicate, glass ionomer cement, and resin-modified glass ionomer cement: an *in vitro* study. Restor Dent Endod 2025;50(4):e37.

***Correspondence to**
**Sirichan Chiaraputt, DDS, M Med Sci, PhD**
School of Dentistry, King Mongkut's Institute of Technology, Ladkrabang (KMITL), 1 Soi Chalong Krung 1, Ladkrabang, Bangkok 10520, Thailand
Email: sirichan.ch@kmitl.ac.th

## INTRODUCTION

Minimally invasive dentistry focuses on preserving natural tooth structure. It also aims to treat dental caries effectively. A key part of this approach is using restorative materials. These materials not only fill the cavity but also help remineralize caries-affected dentin [1]. The proper adhesion of the restoration is facilitated by the function of an adhesive applied to the bonded interfaces [2]. Adhesive materials are recommended for this approach. These materials enhance the bonding between restorative materials and tooth structure. However, studies have shown that the bonding performance of adhesives to caries-affected dentin is inferior to that observed in sound dentin [3]. This reduced adhesion is attributed to the altered mineral composition and structural disorganization within caries-affected dentin, resulting in a more heterogeneous mineral distribution [4,5].

Materials with remineralizing properties offer a practical option for treating deep carious lesions. They provide an alternative to traditional restorative methods. These materials are called bioactive materials. They can trigger biological responses and help regenerate oral tissues [6]. Glass ionomer cements (GICs) and resin-modified glass ionomer cements (RMGICs) are widely used. They bond chemically to the tooth and can release fluoride. The released fluoride enhances remineralization. However, these materials have limitations in strength and long-term durability [7].

Calcium silicate-based materials (calcium silicate cement, CSC), such as Biodentine (Septodont, Saint-Maur-des-Fossés, France), have emerged as promising alternatives. The material offers bioactivity, biocompatibility, and the ability to induce dentin regeneration through the formation of hydroxyapatite [8]. While previous studies have explored the individual properties of these materials, comparative analyses focusing on their remineralization potential in caries-affected dentin are limited [9,10]. Biodentine is a CSC introduced in 2009, providing an advanced replacement material for dentin. According to the manufacturer's recommendation [8,11–13], it can be used in restorative treatment as a dentin substitute. It has a similar initial hardness to dentin, with the highest compressive strength compared to other CSCs [14].

A recent study presented comparative findings between two materials, Biodentine and Fuji II LC (GC Corporation, Tokyo, Japan). By using as a dentin replacement material at cervical margins for class II cavity, Biodentine and RMGIC showed a similar result in leakage score [15]. Biodentine offers a promising alternative for caries management due to its effective remineralization properties, which enhance restoration durability and adhesion. Understanding how these materials influence the mechanical properties and mineral content of affected dentin is essential for optimizing restorative strategies.

Therefore, this *in vitro* study aims to compare the remineralization potential of CSC (Biodentine) with that of conventional GIC (Fuji IX; GC Corporation, Tokyo, Japan) and RMGIC (Fuji II LC) in caries-affected dentin. The assessment involves nanoindentation testing to evaluate mechanical properties and scanning electron microscopy (SEM) with energy-dispersive X-ray spectroscopy (EDX) to analyze mineral composition at the dentin-material interface.

## METHODS

### Tooth selection and preparation

This research received ethical approval from the Ethics Committee for Human Study, Srinakharinwirot University (No. SWUEC/X-008/2565). The sample size was determined by using the G*Power program (ver. 3.1.2; Heinrich Heine University of Düsseldorf, Düsseldorf, Germany), based on the pilot study with an effect size of 0.8, an alpha value of 0.05, and a power of 80% which summed to 25 samples. Twenty-five non-carious human third molars with no visible dentin defects or restorations were studied. The teeth were maintained in 0.1% thymol solution at 4°C and used within 6 months of extraction. Thymol solution was renewed every 2 weeks in order to keep a constant antimicrobial action during storage. The acid-resistant nail varnish was applied to the surface of the entire crowns. Then, a cylindrical bur with a diameter of 1 mm was employed to prepare a cavity on the buccal surface for class V cavity dimensioning 4 mm in width, 2 mm in height, and 1.5 mm in depth. The gingival margin is located 1 mm below the


https://doi.org/10.5395/rde.2025.50.e37

cementoenamel junction. A new diamond bur was replaced after every five cavity preparations.

### Experimental design

All teeth were randomly divided into five experimental groups ($n$ = 5) including sound cavity in the deionized water (positive control [PC] group), artificial carious lesion without restoration in the deionized water (negative control [NC] group) and artificial carious lesion restored with CSC (Biodentine), GIC (Fuji IX GP EXTRA), and RMGIC (Fuji II LC). All materials were used according to the manufacturer's instructions.

### Artificial caries formation

Artificial caries was simulated using the pH-cycling model in the present experiment. Each specimen was demineralized in a demineralizing solution for 8 hours (10 mL of demineralizing solution containing 2.2 mM $CaCl_2$, 2.2 mM $NaH_2PO_4$, 50 mM acetasodium with pH at 4.8) and subsequently remineralized in remineralizing solution (10 mL of remineralizing solution containing 1.5 mM $CaCl_2$, 2.9 mM $NaH_2PO_4$, 50 mM KCl with pH at 7.0) for a total of 14 days [16].

### Restorative procedure

Artificial carious lesions were restored by CSC, GIC, or RMGIC ($n$ = 5). The material compositions are summarized in Table 1. All materials were used according to the manufacturer's recommendation. The set samples were then stored in artificial saliva ($C_8H_8O_3$, 13.2 mM; KCl, 8.4 mM; $MgCl_2$, 0.3 mM; $K_2HPO_4$, 4.6 mM; $KH_2PO_4$, 2.4 mM; $CaCl_2$, 1.1 mM; and sodium carboxymethyl cellulose, 41.3 mM) adjusted to 7.2 pH for 1 week at room temperature (25$^0$C) to simulate the oral environmental condition and to keep their hydration state [17].

### Modulus of elasticity analysis by the nanoindentation method

All teeth were sectioned longitudinally through the center of the cavities using a low-speed diamond saw (Isomet 1000; Buehler, Lake Bluff, IL, USA). The cut samples were embedded in a filled acrylic resin mold (PalaXpress Ultra; Heraeus Kulzer, Hanau, Germany). The embedded samples were ground with silicon carbide paper (#320, #600, and #1,200) in water and finished with diamond paste (3, 1, and 0.5 μm). The nano-hardness tester (FISCHERSCOPE HM2000; Helmut Fischer GmbH, Sindelfingen, Germany) was used to measure the elastic modulus. The nanoindentor is a diamond four-sided pyramid. The depth of the indentation is 5 μm with a loading resolution of 6 mN. The loading range is for 3 seconds. The diameter of the head of the indentor is 0.4 mm. A Vickers indenter was inserted at the intertubular dentin tubule surface. Distances made from each section were 10, 20, and 30 μm from the axial wall interface of the material and the dentin and 600, 1,200, and 1,800 μm from the cavosurface of the occlusal wall to standardize the test point for all groups and to minimize the experimental error. Thus, each sample contained altogether 18 pressure sites from two segments. The average value of each sample was calculated using the data from the 18 selected points. The average value of each material was the mean of five samples.

### Mineral composition analysis

For three samples, quantitative EDX spectroscopy analysis (EDX attached to SEM, JSM-5410LV; JEOL Ltd., Tokyo, Japan) was performed with 10 kV accelerating voltage to determine the mineral content of the dentin.

**Table 1.** Materials used in this study

| Material | Manufacturer | Composition |
|---|---|---|
| Fuji IX GP EXTRA | GC, Tokyo, Japan | Powder: alumino-silicate glass, polyacrylic acid |
| | | Liquid: polyacrylic acid, water |
| Fuji II LC | GC, Tokyo, Japan | Powder: alumino-silicate glass |
| | | Liquid: copolymer of polyacrylic acid, water, 2-hydroxyethyl methacrylate , camphoroquinone |
| Biodentine | Septodont, Saint-Maur-des-Fossés, France | Powder: tricalcium silicate, dicalcium silicate, calcium carbonate, calcium oxide, zirconium oxide, and iron oxide |
| | | Liquid: calcium chloride, hydrosoluble polymer, water |

### Statistical analysis

Statistical analysis was performed with IBM SPSS version 20.0 (IBM Corp, Armonk, NY, USA). Normal distribution of the means of modulus of elasticity of all groups was tested using the Shapiro-Wilk test. Differences in modulus of elasticity among the five groups were evaluated by one-way analysis of variance (ANOVA) with a Bonferroni *post hoc* test for multiple comparisons. A $p$-value <0.05 was considered significant. Mineral content and demineralization characteristics of dentin were assessed with descriptive analysis.

## RESULTS

### Dentin mechanical properties by nanoindentation

The comparative analysis of the mean elastic modulus among the five groups of dentin was investigated by one-way ANOVA statistics. The average and standard deviations of the modulus of elasticity are presented in Figure 2. The CSC group had significantly higher values of modulus of elasticity compared with the GIC, RMGIC, and NC groups ($p < 0.001$). In contrast, the mean elastic modulus of the GIC, RMG, and NC groups showed no statistical differences ($p > 0.05$).

### Mineral composition of dentin at the interface

In the PC group (Figure 3A), sound dentin showed a high level of calcium and phosphorus. The mineral content of dentin located within a 60 μm range beneath the material in the NC group (Figure 3B) displayed decreased levels of calcium and phosphorus relative to the PC group. The GIC group (Figure 3C) and the RMGIC group (Figure 3D) both exhibited lower levels of calcium and phosphorus in the dentin within a 60 μm range beneath the material, similar to the NC group. Interestingly, in the CSC group (Figure 3E), the levels of calcium and phosphate were higher than in the GIC group, RMGIC group, and NC group.

## DISCUSSION

Numerous studies have conclusively reported that remineralization is a significant reparative effect after GIC restorations. The remineralization by GIC restorations is noted by the augmented mineral content in the dentin [18,19]. A recent study of the restorative process with GIC and RMGIC in the dentin was reported. The effect of the restorative materials on dentin mechanical properties was evaluated. Measurements were taken at 7 and

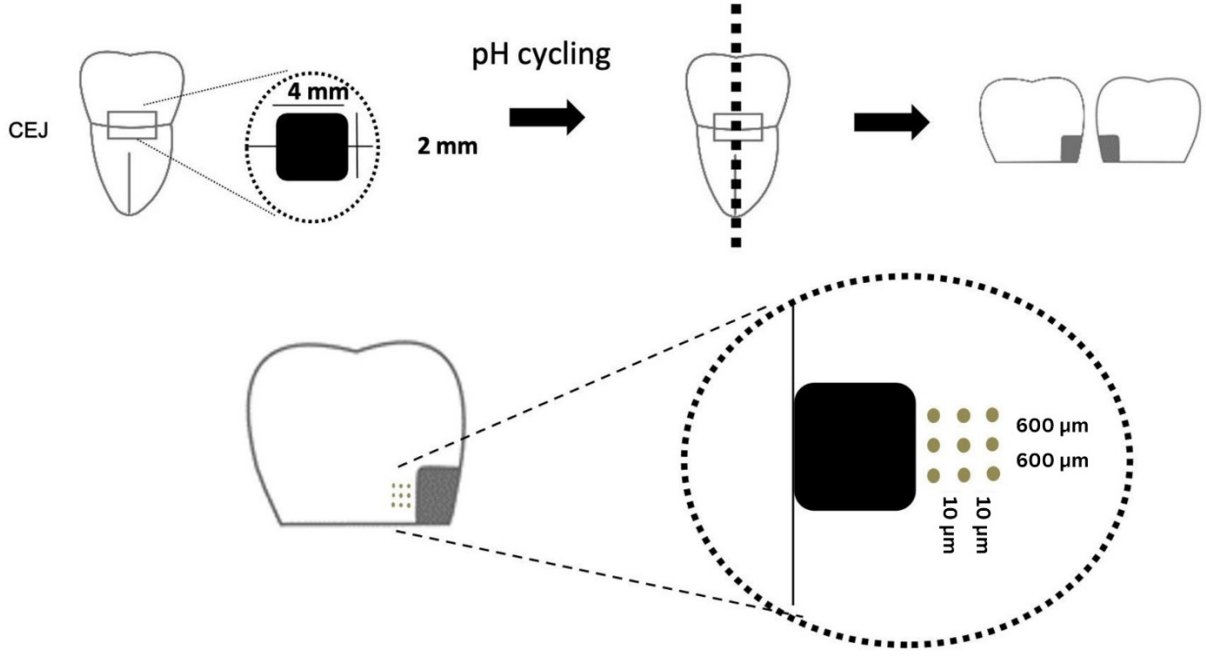


**Figure 1.** The cavity design and the exact position of the nanoindentation sites. CEJ, cementoenamel junction.


https://doi.org/10.5395/rde.2025.50.e37

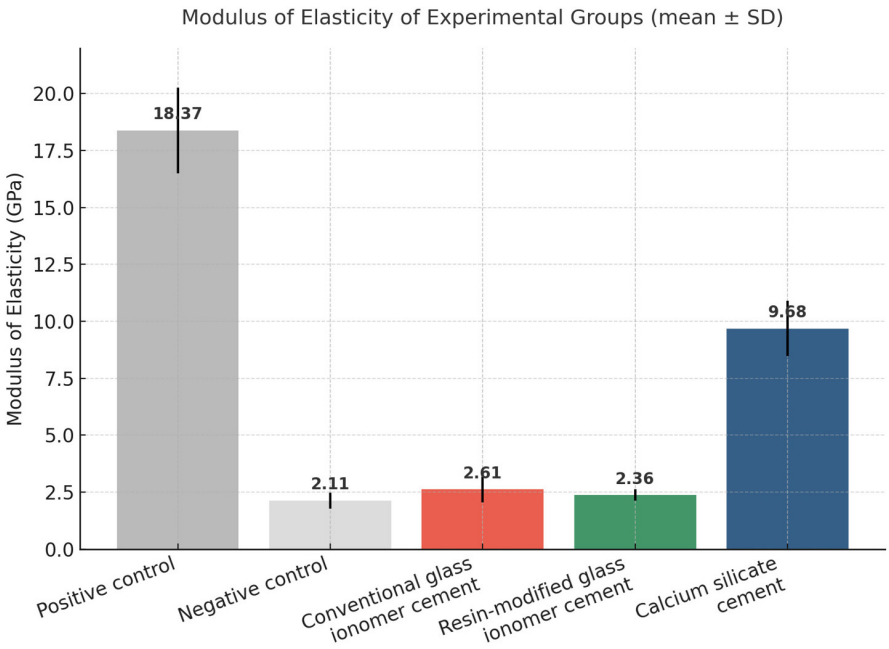


**Figure 2.** The mean values of the elastic modulus of each group. The mean values in each bar with the different letters are statistically significantly different ($p < 0.05$).

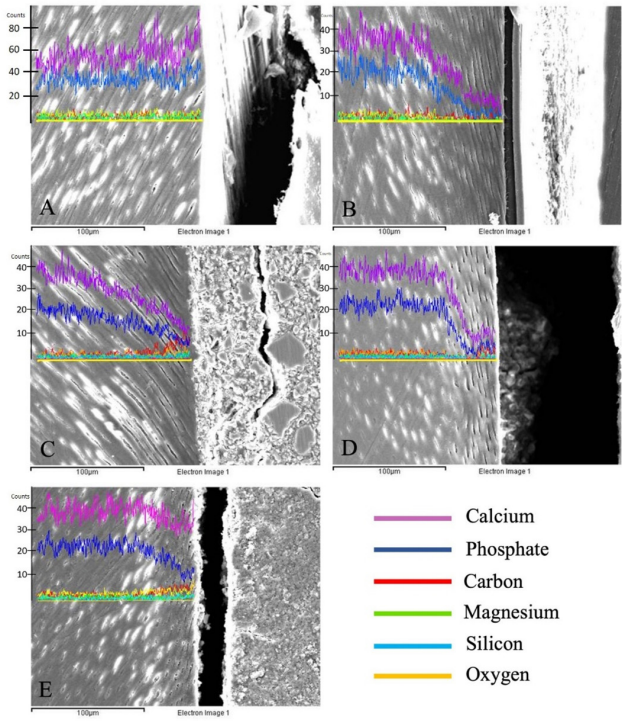


**Figure 3.** Scanning electron microscopy images with energy-dispersive X-ray analysis. (A) Positive control group. (B) Negative control group. (C) Conventional glass ionomer cement group. (D) Resin-modified glass ionomer cement group. (E) Calcium silicate cement group.

30 days after treatment. An increase in mechanical resistance was observed, especially on day 30, compared to day 1 [20]. Consistent with our study, the mechanical properties of dentin improved in both GIC and RMGIC groups at 7 days. Although there were improvements, these were not significantly different from the NC. Longer study durations may yield varying results among the GIC and RMGIC groups.

In contrast, CSC demonstrated a higher remineralizing potential than GIC and RMGIC in artificial carious lesions, as evidenced by the recovery of dentin's mechanical strength. Schwendicke *et al.* [21] stated a similar conclusion that although both cements enhanced mineral gain, it was only CSC that increased the microhardness of carious dentin. Another study using two-photon fluorescence and lifetime imaging techniques demonstrated greater and more extensive mineral deposition in samples filled with CSC compared with those filled with GIC [22]. The efficiency of a biomimetic remineralization system was tested in a previous study. It was reported that the demineralized dentin specimens treated with GIC did not remineralize effectively. It was reported that apatite did not appear in contrast to the CSC group [23].

The results of previous studies and the present study revealed the stronger remineralizing potential of CSC in comparison with GIC. The process of remineralization by GIC groups is based on an ion exchange with dentin. However, CSC induced remineralization via deposition; therefore, it could strengthen dental tissues. CSC played a role in creating mineral crystals that bridge the dentin layer, and the material so-called dentin-mineral infiltration zone [6,11,24]. The results obtained in this study revealed that CSC showed higher levels of calcium and phosphorus mineral content compared with the negative, the GIC and RMGIC groups. The differences between the results can be due to the different pH values of the two materials. The acidic nature of GIC is derived from polyalkenoic acids, in contrast to the alkaline properties of CSC. The alkalinity of CSC is due to the release of hydroxyl ions in the process of its hydration reaction. This increase in pH level may create a beneficial environment where remineralization is able to take place more efficiently inside dentin. This fact leads to the CSC group showing an increased remineralization, resulting in a better quality of the mineral, and an increase in the dentin strength [22].

Assessing the mechanical properties is widely regarded as an effective method for evaluating the quality of dentin remineralization. However, minerals regained should be evaluated by considering both the quantity and quality of the regenerated minerals [25]. Due to the small size of teeth and the natural variations in mineral distribution across different regions of dentin, this study proposed selecting test locations within the intertubular dentin region. Therefore, the nanoindentation test was used in this study [26]. This study utilized the modulus of elasticity to evaluate the mechanical integrity of the remineralized dentin, providing information on its structural strength. Nevertheless, the hardness and modulus of elasticity in dentin exhibit a linear correlation as noted in a previous study [27]. Moreover, the inclusion of EDX provided qualitative information on mineral compositions at the material dentin interface, which has been affected by Biodentine.

There are several methods available to assess the effectiveness of remineralization. In order to facilitate remineralization, specimens must be pretreated as simulated carious lesions by demineralization. This technique allows for accurate assessment of the hardness and modulus of elasticity, which are important indicators of remineralization within the tooth structure. In contrast to standard techniques, nanoindentation has good spatial resolution and can be used to assess the mechanical properties of remineralized regions with minimal preparation. As remineralization involves the re-deposition of minerals into demineralized tissue. Nanoindentation enables a detailed understanding of how these materials contribute to the mechanical strengthening of caries-affected dentin at a microstructural level [28].

In this study, dentin was prepared as caries-affected dentin, characterized by the partial dissolution of minerals. Dentin demineralization simulated through pH cycling appeared to be the most preferred method, as it closely mimics the dynamic process of caries formation in natural teeth. Consequently, the surface hardness closely resembled that of naturally carious dentin [16,29]. However, it is crucial to note that this study was conducted within laboratory settings. Therefore, the artificial carious lesion produced by the pH-cycling method may not fully simulate the appearance of natural carious lesions.

This study compared the mechanical properties of the dentin interface under the restorative materials at a specific time point. The modulus of elasticity of dentin from all groups was compared after one week of storage. The chosen storage time was based on the expectation that all tested materials had undergone remineralization. Prior research indicated that the formation of carbonate apatite reached its maximum at 7 days for Ketac Molar (3M ESPE, Seefeld, Germany) and at 14 days for Riva Light Cure (SDI, Bayswater, VIC, Australia) and Equia Forte (GC Corporation) [30]. However, Kunert *et al.* [31] demonstrated that remineralization by calcium silicate materials continued to accumulate until 28 days. Further study with different storage times is required to investigate the remineralization pattern of the tested materials.

## CONCLUSIONS

Within the limitations of the present *in vitro* study, CSC presented with better remineralizing capability and me-


https://doi.org/10.5395/rde.2025.50.e37

chanical reinforcement when used with caries-affected dentin compared with GIC and RMGIC. The higher value of elastic modulus and more calcium and phosphorus deposition in the CSC group confirmed the application of the CSC. This application could enhance the repair of dentin. These results indicate that CSC can be the restorative material of choice in minimally invasive strategies, especially in deep carious lesions. A long-term study is required to prove its clinical application and longevity.

## CONFLICT OF INTEREST

No potential conflict of interest relevant to this article was reported.

## FUNDING/SUPPORT

This study was supported by the Faculty of Dentistry, Srinakharinwirot University, Bangkok, Thailand (research grant number 348/2565).

## AUTHOR CONTRIBUTIONS

Conceptualization: Chiaraputt S, Youcharoen K. Data curation, Funding acquisition, Project administration: Chiaraputt S. Formal analysis, Supervision, Validation: Saikaew P, Chiaraputt S. Investigation, Resources: Youcharoen K, Akkaratam O. Methodology: Saikaew P, Chiaraputt S, Youcharoen K. Software, Visualization: Intajak P. Writing - original draft: Youcharoen K, Chiaraputt S. Writing - review & editing: Youcharoen K, Akkaratam O, Intajak P, Saikaew P. All authors read and approved the final manuscript.

## DATA SHARING STATEMENT

The datasets are not publicly available but are available from the corresponding author upon reasonable request.

## REFERENCES

1. World Health Organization (WHO). Prevention and treatment of dental caries with mercury-free products and minimal intervention. Geneva, Switzerland: WHO; 2022.
2. Schwendicke F, Frencken JE, Bjørndal L, Maltz M, Manton DJ, Ricketts D, *et al.* Managing carious lesions: consensus recommendations on carious tissue removal. Adv Dent Res 2016;28:58-67.
3. Isolan CP, Sarkis-Onofre R, Lima GS, Moraes RR. Bonding to sound and caries-affected dentin: a systematic review and meta-analysis. J Adhes Dent 2018;20:7-18.
4. Ağaccıoğlu M, Sirin Karaarslan E, Aytac Bal F, Benli İ. Bond strength comparison of a fiber-reinforced composite resin: different dentin conditions and preparation techniques. Microsc Res Tech 2024;87:1250-1261.
5. Karadas M, Bedir F, Demirbuga S. The role of etching protocols on bond strength of universal adhesives applied to caries-affected dentin: a systematic review and meta-analysis. Clin Oral Investig 2024;28:683.
6. Jefferies SR. Bioactive and biomimetic restorative materials: a comprehensive review: part I. J Esthet Restor Dent 2014;26:14-26.
7. Gao W, Smales RJ, Yip HK. Demineralisation and remineralisation of dentine caries, and the role of glass-ionomer cements. Int Dent J 2000;50:51-56.
8. Malkondu Ö, Karapinar Kazandağ M, Kazazoğlu E. A review on biodentine, a contemporary dentine replacement and repair material. Biomed Res Int 2014;2014:160951.
9. Gandolfi MG, Siboni F, Botero T, Bossù M, Riccitiello F, Prati C. Calcium silicate and calcium hydroxide materials for pulp capping: biointeractivity, porosity, solubility and bioactivity of current formulations. J Appl Biomater Funct Mater 2015;13:43-60.
10. Parirokh M, Torabinejad M. Mineral trioxide aggregate: a comprehensive literature review: part III: clinical applications, drawbacks, and mechanism of action. J Endod 2010;36:400-413.
11. Koubi G, Colon P, Franquin JC, Hartmann A, Richard G, Faure MO, *et al.* Clinical evaluation of the performance and safety of a new dentine substitute, Biodentine, in the restoration of posterior teeth: a prospective study. Clin Oral Investig 2013;17:243-249.
12. About I. Biodentine: from biochemical and bioactive properties to clinical applications. G Ital Endod 2016;30:81-88.
13. Dulger K, Kosar T. Comparison of three dentine replacement materials in terms of different characteristics. Aust Endod J 2025;51:81-89.
14. Kayahan MB, Nekoofar MH, McCann A, Sunay H, Kaptan RF, Meraji N, *et al.* Effect of acid etching procedures on the compressive strength of 4 calcium silicate-based endodontic cements. J Endod 2013;39:1646-1648.
15. Raskin A, Eschrich G, Dejou J, About I. In vitro microleakage of Biodentine as a dentin substitute compared to Fuji II LC in cervical lining restorations. J Adhes Dent 2012;14:535-542.
16. Marquezan M, Corrêa FN, Sanabe ME, Rodrigues Filho LE, Hebling J, Guedes-Pinto AC, *et al.* Artificial methods of dentine caries induction: a hardness and morphological com-

parative study. Arch Oral Biol 2009;54:1111-1117.
17. Besinis A, van Noort R, Martin N. Remineralization potential of fully demineralized dentin infiltrated with silica and hydroxyapatite nanoparticles. Dent Mater 2014;30:249-262.
18. Al-Abdi A, Paris S, Schwendicke F. Glass hybrid, but not calcium hydroxide, remineralized artificial residual caries lesions in vitro. Clin Oral Investig 2017;21:389-396.
19. Prokshi R, Gjorgievska E, Prokshi B, Sopi M, Sejdiu M. Survival rate of atraumatic restorative treatment restorations in primary posterior teeth in children with high risk of caries in the Republic of Kosovo-1-year follow-up. Eur J Dent 2023;17:902-909.
20. Maneenut C, Nikaido T, Foxton RM, Tagami J. Effect of glass ionomer cements on nanohardness of caries-affected dentin. Int Chin J Dent 2003;3:122-130.
21. Schwendicke F, Al-Abdi A, Pascual Moscardó A, Ferrando Cascales A, Sauro S. Remineralization effects of conventional and experimental ion-releasing materials in chemically or bacterially-induced dentin caries lesions. Dent Mater 2019;35:772-779.
22. Watson TF, Atmeh AR, Sajini S, Cook RJ, Festy F. Present and future of glass-ionomers and calcium-silicate cements as bioactive materials in dentistry: biophotonics-based interfacial analyses in health and disease. Dent Mater 2014;30:50-61.
23. Kim YK, Yiu CK, Kim JR, Gu L, Kim SK, Weller RN, *et al*. Failure of a glass ionomer to remineralize apatite-depleted dentin. J Dent Res 2010;89:230-235.
24. Atmeh AR, Chong EZ, Richard G, Festy F, Watson TF. Dentin-cement interfacial interaction: calcium silicates and polyalkenoates. J Dent Res 2012;91:454-459.
25. Bertassoni LE, Habelitz S, Marshall SJ, Marshall GW. Mechanical recovery of dentin following remineralization in vitro: an indentation study. J Biomech 2011;44:176-181.
26. Marshall GW, Marshall SJ, Kinney JH, Balooch M. The dentin substrate: structure and properties related to bonding. J Dent 1997;25:441-458.
27. Zhang YR, Du W, Zhou XD, Yu HY. Review of research on the mechanical properties of the human tooth. Int J Oral Sci 2014;6:61-69.
28. Wang Z, Wang K, Xu W, Gong X, Zhang F. Mapping the mechanical gradient of human dentin-enamel-junction at different intratooth locations. Dent Mater 2018;34:376-388.
29. Yu OY, Zhao IS, Mei ML, Lo EC, Chu CH. A review of the common models used in mechanistic studies on demineralization-remineralization for cariology research. Dent J (Basel) 2017;5:20.
30. Ghilotti J, Fernández I, Sanz JL, Melo M, Llena C. Remineralization potential of three restorative glass ionomer cements: an in vitro study. J Clin Med 2023;12:2434.
31. Kunert M, Piwonski I, Hardan L, Bourgi R, Sauro S, Inchingolo F, *et al*. Dentine remineralisation induced by "bioactive" materials through mineral deposition: an in vitro study. Nanomaterials (Basel) 2024;14:274.


https://doi.org/10.5395/rde.2025.50.e37

RDE Restorative Dentistry & Endodontics

Research Article

eISSN 2234-7666
Restor Dent Endod. 2025 November;50(4):e38
https://doi.org/10.5395/rde.2025.50.e38

# Evaluation of platelet concentrates in regenerative endodontics: a systematic review and meta-analysis

**Anna Tsiolaki**[1], **Dimitrios Theocharis**[1], **Nikolaos Tsitsipas**[1,*], **Anastasia Fardi**[2], **Konstantinos Kodonas**[3]

[1]School of Dentistry, Faculty of Health Sciences, Aristotle University of Thessaloniki, Thessaloniki, Greece
[2]Department of Dentoalveolar Surgery, Dental Implantology and Oral Radiology, School of Dentistry, Aristotle University of Thessaloniki, Thessaloniki, Greece
[3]Department of Endodontology, School of Dentistry, Aristotle University of Thessaloniki, Thessaloniki, Greece

## ABSTRACT

**Objectives:** The aim of this systematic review is to compare the effectiveness of advanced platelet concentrates as regenerative endodontic therapeutic alternatives to blood clot (BC) revascularization in immature permanent necrotic teeth.

**Methods:** Randomized controlled trials (RCTs) comparing regenerative endodontic therapies using platelet-rich plasma (PRP), platelet-rich fibrin (PRF), or platelet pellet (PP) with the BC revascularization approach in immature permanent necrotic teeth were systematically searched in PubMed, Scopus, Cochrane Library, and Web of Science until May 2025. Data was extracted and analyzed both qualitatively and quantitatively. Study quality was assessed using the Cochrane Risk of Bias tool. A meta-analysis was conducted using IBM SPSS software (version 29.0), with success rates expressed as risk ratios and 95% confidence intervals (CIs).

**Results:** The initial search yielded 4,917 studies. After removing duplicates and applying eligibility criteria, 15 RCTs were included. Meta-analysis indicated no significant difference in the risk ratio (RR), as the BC method has similar success rates with PRP (10 studies; RR = 1.01; 95% CI, 0.94–1.09; $p = 0.76$) and PRF (8 studies; RR = 0.98; 95% CI, 0.89–1.08; $p = 0.65$) at 12 months. The primary outcomes evaluated were based on clinical and radiographic success.

**Conclusions:** Current evidence suggests PRP, PRF, and BC are all effective in treating immature permanent necrotic teeth with similar success rates. However, further research is needed to assess long-term outcomes.

**Keywords:** Apexification; Platelet-rich fibrin; Platelet-rich plasma; Regenerative endodontics

## INTRODUCTION

In regenerative endodontics, biologically driven methods are used to restore the pulp-dentin complex, dentin, and root structures of the treated teeth [1]. These treatment modalities utilize stem cells, biomaterial scaffolds, and signaling molecules to promote healing, resolve symptoms, and support further root maturation leading

**Received:** July 17, 2025 **Revised:** August 28, 2025 **Accepted:** August 30, 2025

**Citation**
Tsiolaki A, Theocharis D, Tsitsipas N, Fardi A, Kodonas K. Evaluation of platelet concentrates in regenerative endodontics: a systematic review and meta-analysis. Restor Dent Endod 2025;50(4):e38.

***Correspondence to**
**Nikolaos Tsitsipas, DDS**
School of Dentistry, Faculty of Health Sciences, Aristotle University of Thessaloniki, Central Secretariat, 1st Basement, Thessaloniki, 54124, Greece
Email: ntsitsipas@gmail.com

to increased dentinal thickness, root length, and structural strength, reduced risk of fractures, and reduced tooth sensitivity. In clinical endodontics, regenerative endodontic procedures (REPs) are now considered the treatment of choice for immature permanent teeth with pulp necrosis [1–5].

In biological terms, REPs aim to replace inflamed or necrotic pulp tissue with newly formed, pulp-like tissue that ideally includes a peripheral layer of odontoblast-like cells, mimicking the structure of healthy pulp. Kim *et al*. [4] suggest that these procedures aim to resolve clinical signs and symptoms, promote root maturation, and restore neurogenesis. These therapeutic outcomes may be achieved through *cell homing*, a process in which endogenous stem or progenitor cells migrate to the site of injury through passive blood flow from the periapical tissues, leading to the formation of a blood clot (BC) that acts as a natural scaffold [4,6,7]. These regenerative stimuli can be further enhanced by platelet-derived biomaterials (platelet concentrates), such as platelet-rich plasma (PRP), platelet-rich fibrin (PRF), and platelet pellet (PP), which release growth factors that induce cell recruitment, proliferation, and differentiation.

In endodontics, platelet concentrates serve as scaffolds that support revascularization and tissue regeneration within the root canal system [8]. These techniques evolved from the traditional BC method, long regarded as the gold standard in regenerative endodontics. In this approach, bleeding is intentionally induced from the periapical tissues to create an intracanal BC. This clot functions as a natural scaffold, attracting and delivering growth factors and progenitor cells from the apical papilla into the canal space, thereby facilitating tissue regeneration [9]. It was not until 2016 that renowned organizations such as the American Association of Endodontists and the European Society of Endodontology recognized the significance of regenerative endodontic treatments (RETs), with the former proposing a standardized protocol for REPs, which included the use of scaffolds such as PRP or PRF, and the latter publishing a position statement on revitalization procedures [10,11].

The objective of the present study is to compare the clinical effectiveness of platelet concentrates as a therapeutic alternative to conventional BC revascularization for the treatment of immature permanent necrotic teeth with at least 12 months of follow-up time through a systematic review approach. According to the null hypothesis, there is no significant difference in the clinical success rates between platelet concentrates and conventional BC approaches for the treatment of immature permanent necrotic teeth over a minimum follow-up period of 12 months.

## METHODS

### Protocol and registration

A comprehensive protocol of the present systematic review has been created and registered with the PROSPERO (International Prospective Register of Systematic Reviews; registration number, CRD420251057926). The systematic review is being conducted following the Preferred Reporting Items for Systematic Reviews and Meta-Analyses (PRISMA) 2020 guidelines [12].

### Information sources and search strategy

An extensive literature search was conducted across multiple electronic databases, including the Web of Science by Clarivate Analytics (All Collections and Core Collection), the Cochrane Library, MEDLINE PubMed, and Elsevier Scopus. A combination of Medical Subject Headings (MeSH) terms was employed to identify randomized controlled trials (RCTs) investigating the use of PRP, PRF, or PP in REPs for immature necrotic teeth. The search encompassed all available records from inception through May 2, 2025. A manual search was also conducted by screening the reference lists of all included studies and relevant systematic reviews and meta-analyses. The search strategy for each database is presented in Table 1.

### Study selection and eligibility criteria

**1. PICO framework**

Population: Immature necrotic permanent teeth.
Intervention: REP using platelet concentrates.
Comparison: REP by inducing the formation of a BC as a scaffold.
Outcomes: Radiographic assessment and clinical examination.


https://doi.org/10.5395/rde.2025.50.e38

**Table 1.** Search strategy

| Databases | Search strategy |
|---|---|
| MEDLINE (PubMed) | ((((((((((“platelet rich plasma”[All Fields]) OR (“platelet rich fibrin”[All Fields])) OR (“platelet gel”[All Fields])) OR (“platelet concentrated”[All Fields])) OR (“platelet concentrate”[All Fields])) OR (“platelet pellet”[All Fields])) OR (“prp”[All Fields])) OR (“prf”[All Fields])) OR (“pp”[All Fields])) OR (“platelet rich plasma”[MeSH Terms])) OR (“platelet rich fibrin”[MeSH Terms])) AND ((((((“regenerative endodontics”[All Fields]) OR (“apexification”[All Fields])) OR (“pulp revascularization”[All Fields])) OR (“pulp revitalization”[All Fields])) OR (“regenerative endodontics”[MeSH Terms])) OR (“apexification”[MeSH Terms])) |
| | Separate combined searches of each of the terms from group #1 AND group #2 |
| | 1) “platelet rich plasma”[All Fields], “platelet rich fibrin”[All Fields], “platelet gel”[All Fields], “platelet concentrated”[All Fields], “platelet concentrate”[All Fields], (“platelet pellet”[All Fields], “prp”[All Fields], “prf”[All Fields], “pp”[All Fields], “platelet rich plasma”[MeSH Terms], “platelet rich fibrin”[MeSH Terms] |
| | 2) “regenerative endodontics”[All Fields], “apexification”[All Fields], “pulp revascularization”[All Fields], “pulp revitalization”[All Fields], “regenerative endodontics”[MeSH Terms], “apexification”[MeSH Terms] |
| Elsevier Scopus | ((TITLE-ABS-KEY (platelet AND rich AND plasma) OR TITLE-ABS-KEY (platelet AND rich AND fibrin) OR TITLE-ABS-KEY (platelet AND concentrated) OR TITLE-ABS-KEY (platelet AND concentrate) OR TITLE-ABS-KEY (platelet AND pellet) OR TITLE-ABS-KEY (platelet AND gel) OR TITLE-ABS-KEY (prp) OR TITLE-ABS-KEY (prf) OR TITLE-ABS-KEY (pp))) AND ((TITLE-ABS-KEY (regenerative AND endodontics) OR TITLE-ABS-KEY (apexification) OR TITLE-ABS-KEY (pulp AND revascularization) OR TITLE-ABS-KEY (pulp AND revitalization))) |
| | Separate combined searches of each of the terms from group #1 AND group #2 |
| | 1) TITLE-ABS-KEY (platelet AND rich AND plasma), TITLE-ABS-KEY (platelet AND rich AND fibrin), TITLE-ABS-KEY (platelet AND concentrated), TITLE-ABS-KEY (platelet AND concentrate), TITLE-ABS-KEY (platelet AND pellet), TITLE-ABS-KEY (platelet AND gel), TITLE-ABS-KEY (prp), TITLE-ABS-KEY (prf), TITLE-ABS-KEY (pp) |
| | 2) TITLE-ABS-KEY (regenerative AND endodontics), TITLE-ABS-KEY (apexification), TITLE-ABS-KEY (pulp AND revascularization), TITLE-ABS-KEY (pulp AND revitalization) |
| Cochrane Library | (“platelet rich plasma” or “platelet rich fibrin” or “platelet gel” or “platelet concentrated” or “platelet concentrate” or “platelet pellet” or “PRP” or “PRF” or “PP”) and (“Regenerative Endodontics” or “Apexification” or “pulp revitalization” or “pulp revascularization”) |
| Web of Science Core Collection | The following searches were combined (1 AND #2): |
| | 1) (((((((((ALL= (platelet rich plasma)) OR ALL=(platelet rich fibrin)) OR ALL= (platelet concentrate)) OR ALL= (platelet concentrated)) OR ALL=(platelet pellet)) OR ALL=(platelet gel)) OR ALL=(PRP)) OR ALL=(PRF)) OR ALL=(PP) |
| | 2) (((ALL= (regenerative endodontics)) OR ALL=(apexification)) OR ALL=(pulp revascularization)) OR ALL= (pulp revitalization) |
| | Separate combined searches of each the terms from group #1 AND #2: |
| | 1) ALL=(platelet rich plasma), ALL=(platelet rich fibrin), ALL= (platelet concentrate), ALL=(platelet concentrated), ALL= (platelet pellet), ALL= (platelet gel), ALL=(PRP), ALL=(PRF), ALL=(PP) |
| | 2) ALL= (regenerative endodontics), ALL=(apexification), ALL= (pulp revascularization), ALL= (pulp revitalization) |
| Web of Science All Databases | The following searches were combined (1 AND #2): |
| | 1) (((((((((TS= (platelet rich plasma)) OR TS= (platelet rich fibrin)) OR TS= (platelet concentrated)) OR TS= (platelet concentrate)) OR TS= (platelet pellet)) OR TS= (platelet gel)) OR TS= (PRP)) OR TS=(PRF)) OR TS=(PP) |
| | 2) (((TS= (regenerative endodontics)) OR TS= (apexification)) OR TS=(pulp revascularization) OR TS=(pulp revitalization) |
| | Separate combined searches of each of the terms from group #1 AND group #2: |
| | 1) TS= (platelet rich plasma), TS= (platelet rich fibrin), TS=(platelet concentrated), TS= (platelet concentrate), TS=(platelet pellet), TS=(platelet gel), TS=(PRP), TS= (PRF), TS= (PP) |
| | 2) TS=(regenerative endodontics), TS=(apexification), TS=(pulp revascularization), TS= (pulp revitalization) |

Study: RCTs with a minimum follow-up period of 12 months.

**2. Inclusion criteria**

The following criteria were applied for study inclusion:

- RCTs published in the English language.
- Studies comparing the clinical success rates of PRP, PRF, or PP with the conventional BC technique in REPs for immature necrotic permanent teeth.
- Studies reporting a minimum follow-up period of 12 months posttreatment.

**3. Exclusion criteria**

Studies that met any of the criteria listed below were excluded:

- Retrospective, preclinical animal studies, *in vitro* in-

vestigations, case control, non-randomized studies, case series, case reports, book chapters, meta-analyses, narrative, systematic, and scoping reviews.

• Studies for which the full-text version was unavailable after two unsuccessful attempts to contact the corresponding author via email.

• Studies with a follow-up period of less than 12 months.

• Studies involving primary or fully mature permanent teeth.

• Studies without a control group treated with the BC technique.

• Studies that did not report data in a comparative format suitable for analysis.

### Data collection

The titles and abstracts of all retrieved articles were independently screened by three reviewers (DT, NT, AT). During the selection process, any disputes were resolved through discussion and, when necessary, consultation with a fourth reviewer (KK). This process was consistently applied at each stage of screening. Subsequently, full-text articles of potentially eligible studies, including those identified through manual searching, were assessed for inclusion by the same three reviewers (DT, NT, AT), with final confirmation by the fourth reviewer (KK). The study selection process is demonstrated in the PRISMA flow diagram (Figure 1). The list of excluded full-text articles, along with the reasons for

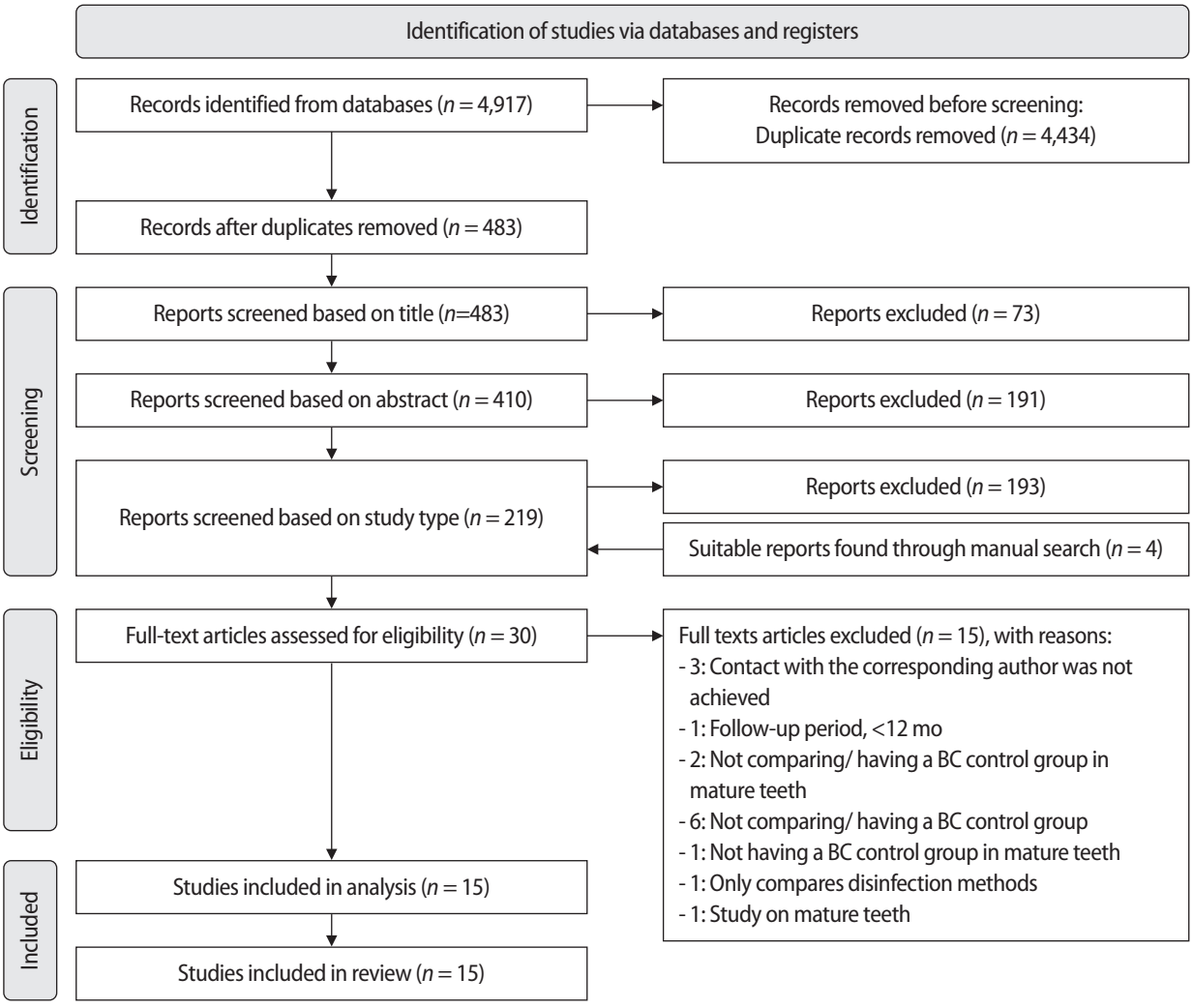


**Figure 1.** Flow diagram of the search process.


https://doi.org/10.5395/rde.2025.50.e38

their exclusion, is provided in Supplementary Table 1.

### Risk of bias assessment for individual studies

The risk of bias for each included study was independently assessed by two authors (KK, AF), using the Cochrane Risk of Bias 2.0 (RoB 2.0) tool for RCTs, which assesses five domains: the randomization process, deviations from intended interventions, handling of missing outcome data, measurement of outcomes, and selective reporting of results [13]. A study was rated as 'low risk' when all domains were judged low risk, as 'moderate risk' when at least one domain raised some concerns, and as 'high risk' when any domain was identified as high risk. Discrepancies between the two reviewers were resolved through discussion with a third reviewer (NT).

### Applied criteria and outcomes measured

The studies included were assessed using well-defined criteria to ensure that the outcomes were reliable, comparable, and reproducible. These criteria were categorized into three main domains: radiographic assessment, clinical examination, and histological evaluation. Radiographic assessments included tools such as the Periapical Index (PAI), Chen & Chen criteria, and root dimension measurements performed using cone-beam computed tomography (CBCT). These methods allowed for objective evaluation of root development and periapical healing. Clinical outcomes were evaluated based on the absence of pathological signs or symptoms (eg, pain, swelling, or sinus tract), evidence of periapical healing, tooth survival, and the results of sensibility tests. Histological evaluation of newly regenerated pulp-like tissue involves the identification of key cellular components, including odontoblasts and fibroblasts, as well as the presence of neovascularization and regenerated nerve fibers. Additionally, it assesses the status of inflammation or infection and the integrity of the periodontal ligament, along with the surrounding bone structures [14].

### Statistical analysis

Meta-analyses were conducted using SPSS software to compare the success rates between PRP or PRF and BC, with a minimum follow-up period of 12 months. Success rates were treated as dichotomous outcomes, and the effect of the interventions was expressed as risk ratios (RR) with corresponding 95% confidence intervals (CIs). The $I^2$ statistic was used to assess statistical heterogeneity among studies. In case of low heterogeneity ($I^2 \leq 50\%$), a fixed-effect model was applied, while a random-effects model was used in cases of moderate to high heterogeneity. Potential publication bias was assessed both visually through funnel plot inspection. The significance level was set at $p \leq 0.05$.

## RESULTS

### Study selection

The initial search yielded 4,917 records, from which 4,434 duplicates were removed. After screening the remaining records, 73 were excluded based on title, 191 based on abstract, and 193 based on study design. Additionally, four relevant articles were identified through a manual search. A total of 30 full-text articles were subsequently assessed for eligibility, of which 15 were excluded for various reasons (Supplementary Table 1). Ultimately, 15 studies met the inclusion criteria and were included in both qualitative and quantitative analyses. Of these, 10 studies involved the use of PRP in a total of 124 teeth [15–24], eight studies used PRF in 81 teeth [15,18,19,25–29], and one study utilized PP in 17 teeth [15]. Since PP was evaluated in a single trial, it was excluded from the meta-analysis but included in the systematic review. The total number of teeth in the BC group was 165.

With respect to treatment outcomes, the overall meta-analysis demonstrated no significant difference in the RR between PRP and BC groups (10 studies; RR = 1.01; 95% CI, 0.94–1.09; $p = 0.76$) (Figure 2), nor between PRF and BC groups (eight studies; RR = 0.98; 95% CI, 0.89–1.08; $p = 0.65$) (Figure 3). Furthermore, both comparisons exhibited no heterogeneity ($I^2 = 0.0\%$, $p > 0.99$), indicating consistency across the included studies.

### Outcomes measured

The outcomes assessed in the included studies were predominantly clinical and radiographic, with a limited number of patient-centered and research-centered outcomes also reported.

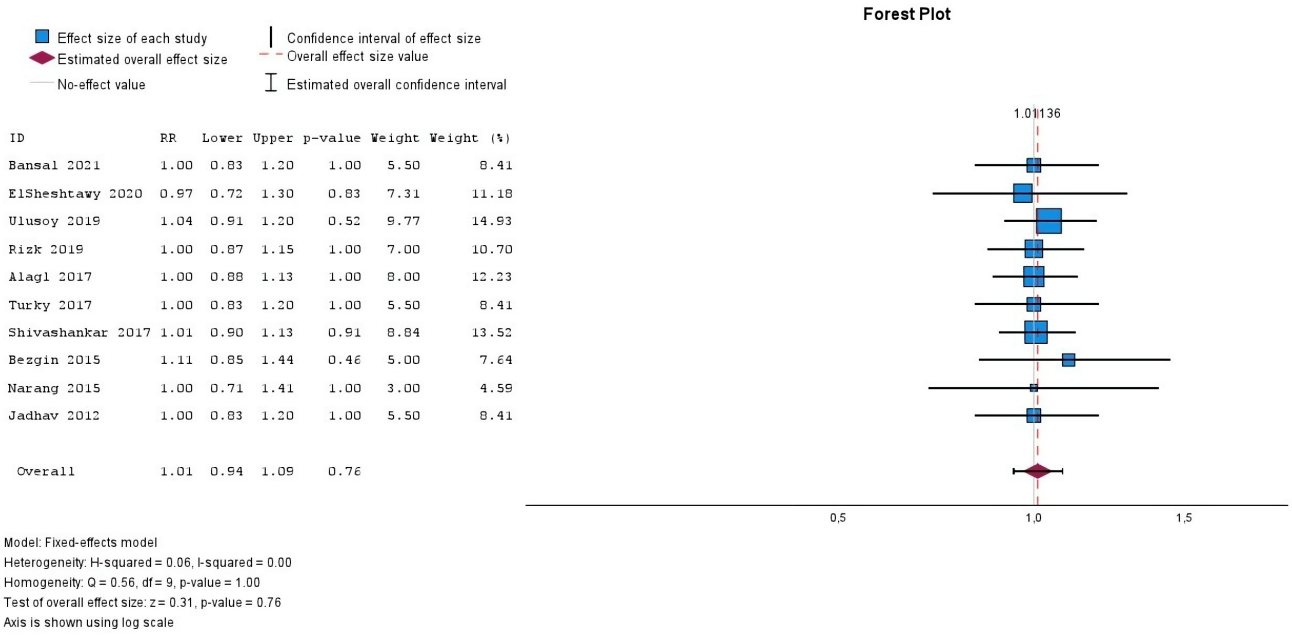


**Figure 2.** Forest plot showing the RR for treatment outcomes between platelet-rich plasma and blood clot.

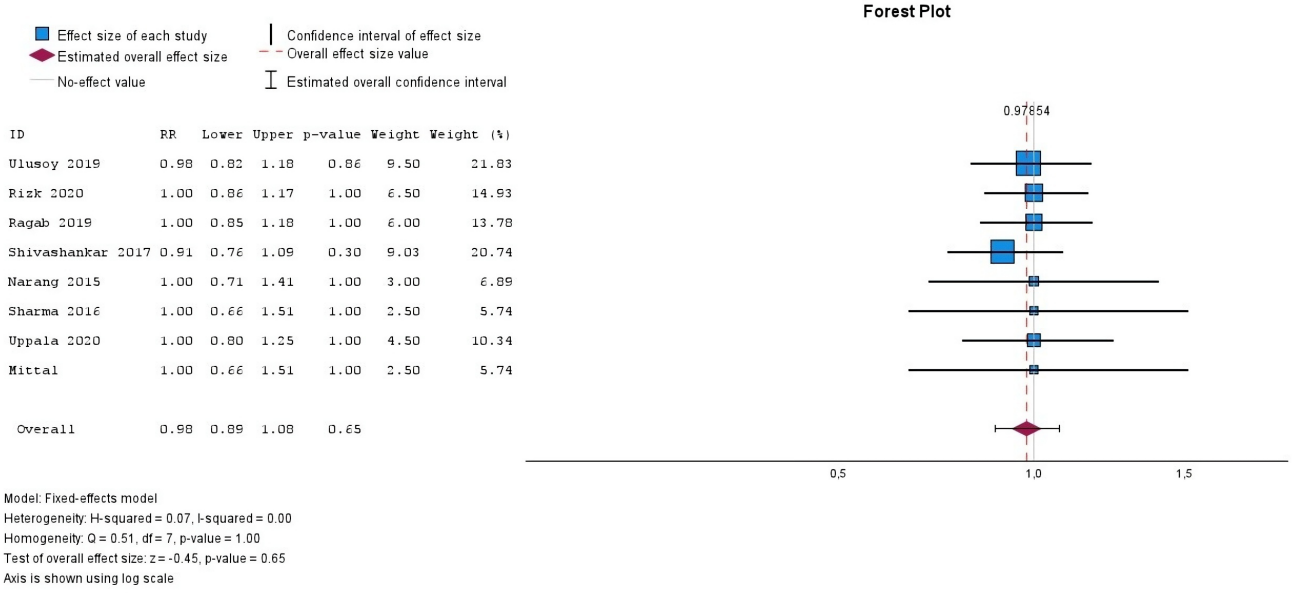


**Figure 3.** Forest plot showing the RR for treatment outcomes between platelet-rich fibrin and blood clot.

The most frequently evaluated radiographic outcomes were: root length (13 studies [15–21,24–29]), periapical healing lesion (10 studies [15,16,18–20,22,26–29]), apical closure (10 studies [15,16,19,20,22,23,26–29]), dentinal wall thickness (seven studies [16–19,27–29]), root–radiographic area (four studies [15,17,22,23]), apical diameter (four studies [17,21,24,25]), root thickness (three studies [15,24,25]), increase in bone density (three studies [20,24,25]), radiographic canal area (one study [15]), root canal diameter (one study [21]), cervical calcification barriers (one study [26]), root width (one study [15]), internal/external resorption (one study [22]), pulp chamber obliteration (one study [22]). Two studies evaluated the aforementioned measurements as well


https://doi.org/10.5395/rde.2025.50.e38

as periapical area diameter using sagittal and coronal planes of limited field of view CBCT scans [17,20].

The most commonly reported clinical outcomes included: sinus fistula formation (nine studies [15–17,19,20,22,24,25,27]), swelling (nine studies [15–17,19,20,22,24,25,]), sensibility test (eight studies of which in six cold testing [15,17,20,22,23,25], in six electric testing [15,17,20,22,23,25], in two heat testing [17,25] and in two unknown tests [18,24]), sensitivity/tenderness to percussion (six studies [15,17,19,20,22,27]), mobility (four studies [17,22,24,25]), palpation of soft tissues (three studies [19,20,27]), and other clinical symptoms like infection (two studies [17,26]).

Patient-centered outcomes were less frequently reported but included: pain (seven studies [15,16,19,20,22,24,25]), discoloration (five studies [17,22,24–26]), and tooth survival (one study [25]). Research-centered outcomes included PAI (one study [18]) and apical response (Chen & Chen criteria; one study [18]).

None of the studies presented histological evidence on regenerated tissues.

### Quality assessment of individual studies

The Cochrane Collaboration's ROB 2.0 tool for RCTs was used to conduct the risk of bias assessment. Of the included studies, 10 were rated as having a low risk of bias across most domains (Figure 4), while two had a moderate risk of bias, and three were assessed as having a high risk of bias. Overall, the body of evidence was considered to exhibit a low risk of bias. Additionally, there was no evidence of publication bias across any of the performed meta-analyses.

## DISCUSSION

Over the years, various treatment modalities have been recommended and implemented for the endodontic management of necrotic teeth with open apices. Traditionally, calcium hydroxide was broadly employed for apexification, requiring multiple treatment sessions to induce apical closure. However, this approach has been increasingly replaced by using mineral trioxide aggregate (MTA), which offers superior outcomes and enables more predictable apexogenesis [30,31]. In recent years, REPs have gained attention as a promising alternative treatment for these cases. One such technique involves the induction of a BC inside the root canal system to function as a biological scaffold for tissue regeneration. While this method has demonstrated encouraging clinical results [32], concerns have been raised regarding the presence of numerous hematopoietic cells within the BC. Upon cell death, these cells may release cytotoxic intracellular enzymes into the microenvironment, potentially compromising stem cell viability and thus impairing the regenerative process [33].

To address these limitations, platelet derivatives have emerged as a modern, biologically favorable alternative. They represent autologous bioactive preparations that can be easily obtained in clinical dental settings by centrifuging the patient's blood. These autologous biomaterials can enhance stem cell recruitment, proliferation, and differentiation, thereby promoting tissue regeneration and functional recovery. They are rich in growth factors, including platelet-derived growth factor, vascular endothelial growth factor, and transforming growth factor beta 1 (TGF-β1) [34,35]. In addition to their application in endodontics, platelet concentrates have been broadly utilized in regenerative medicine, including periodontal, oral and maxillofacial, dermatologic, and orthopedic procedures [36].

PRP is an autologous blood-derived product with a platelet concentration increased by at least 2/3 times the normal level. It serves as a biomaterial for the targeted delivery of cytokines and growth factors from platelet granules, thereby promoting tissue regeneration. PRP has been applied as a novel regeneration method in various damaged tissues, such as bone, liver, dental pulp, cartilage, and tendon [37,38].

PRF is a second-generation platelet derivative that consists of a fibrin matrix rich in platelets, leukocytes, cytokines, and growth factors, including interleukins (ILs), ie, IL-1β, IL-4, and IL-6, vascular endothelial growth factor, platelet-derived growth factor, and TGF-β1. All these components are gradually released over time, enhancing their regenerative potential. PRF has been effectively used in different therapeutic applications like sinus lift augmentation, extraction socket healing, and guided bone regeneration. In regenerative endodontics, it is utilized in cases of iatrogenic pulpal


**Figure 4.** (A) A summary of the risk of bias in the included studies and (B) a review of the authors' judgements about each risk of bias domain as percentages across the included studies.


https://doi.org/10.5395/rde.2025.50.e38

floor perforations as well as revascularization of immature necrotic permanent teeth [8,39,40].

PP is a platelet derivative with a significantly greater platelet content compared to PRP, containing approximately 12 times more platelets and TGF-β1 compared to PRP, and 17 times more than whole blood, while exhibiting a lower white blood cell content [41]. Its gel-like consistency enhances its adhesive properties, making it a promising scaffold for regenerative applications [42].

### Scaffold

In the present systematic review, a total of 15 studies were included for analysis, each investigating the application of various platelet derivatives in REPs. More than half of the studies employed PRP (10 studies), whereas PRF was used in eight studies. Despite the greater frequency of PRP use across the selected studies, PRF is often preferred over PRP as a scaffold in REPs, due to PRF's ability to provide a continuous release of growth factors for an extended time period and its superior mechanical properties [35,43]. Additionally, PRF offers practical advantages: it is completely autologous and does not require anticoagulants [40,44]. PP, which was evaluated in only one study, is characterized by an increased platelet concentration and associated growth factors, offering enhanced regenerative potential. However, the current body of evidence remains insufficient to confirm its clinical superiority over PRP or PRF [42]. In contrast, BC is a cost-effective option compared to PRF, PRP, and PP as it uses the patient's own blood without additional processing. However, BC has limitations such as instability and lower platelets and growth factor content compared to platelet derivatives [45,46].

### Tooth types and sample size

The sample sizes across the 15 included studies varied from four to 21 for the BC group, five to 19 for PRP, four to 20 for PRF, and 17 for PP. Notably, nearly half of them did not report using a sample size calculation method, nor did they provide clear details regarding randomization procedures. Furthermore, none of the studies comparing BC with PRP, PRF, or PP included more than 21 participants. These limitations highlight the need for future research with larger, well-powered samples and rigorous methodological standards to produce more definitive and generalizable findings in this field.

In nine out of the 15 studies, incisors were the most frequently treated tooth type [15,17,21,24–29]. Among these, all but one study [17] focused exclusively on maxillary incisors, with five studies specifically targeting central incisors [21,24–26,29]. Two studies included anterior teeth [16,18], while three studies treated both incisors and single-rooted premolars [20,22,23]. One study did not specify the tooth type beyond identifying them as immature permanent teeth [19]. The predominance of single-rooted teeth in these studies may be attributed to their simpler root canal anatomy, which facilitates standardization, treatment consistency, and outcome evaluation by minimizing anatomical variability and confounding factors.

### Barrier

Out of the 15 studies, MTA was primarily used as a barrier over the scaffold in six studies [15,18,20–22,26], while four studies incorporated glass ionomer cement (GIC) either between the MTA and the final restoration material or as the final restoration itself [15,20,22,26]. One study used MTA for the entire permanent restoration [23]. Two studies used collagen covered with MTA, followed by GIC [17,24], while two other studies used GIC alone [19,28]. Four studies did not use a barrier over the scaffold [16,23,27,29]. One study used a combination of biomaterials (MTA for the PRP group and collagen with MTA for the BC group), covered with a layer of GIC [25]. MTA is favored as a barrier due to its biocompatibility, ability to set in a moist environment and form a good seal, and capacity to stimulate hard tissue formation (dentin bridge formation) [47,48]. Collagen functions as an apical matrix that can prevent MTA over-extrusion and aid in periapical tissue healing [49].

When compared with GIC, MTA provides a better seal, but it sets more slowly [47,50,51]. Applying a layer of GIC over MTA may improve results, whereas using only GIC simplifies the procedure. However, immediate sealing without a barrier over the scaffold can result in issues such as polymerization shrinkage and subsequent microleakage, which can lead to scaffold contamination. Additionally, resin toxicity raises some concerns [52]. These factors must be considered when selecting a

barrier material for scaffold restoration procedures.

### Restoration

Regarding the materials used for the final restoration, composite resin was employed in nine out of the 15 studies [15,17,19–22,24,25,28], with all but one [21] placing it over a GIC base. However, two studies did not clearly specify the final restoration material used for the BC group [24,25]. GIC alone was used as the final restorative material in four studies [16,26,27,29]. Additionally, one study utilized MTA for the final restoration, although it did not provide specific data for the BC group [23].

Composite resin is commonly preferred for final restorations due to its favorable aesthetic properties, mechanical strength, and durability. However, it presents certain limitations, including polymerization shrinkage and technique sensitivity, which require a controlled, dry operating field and the application of a meticulous layering technique [53,54]. Meanwhile, GIC tolerates moisture but has lower strength and durability [55,56]. Composite resin restorations have demonstrated superior longevity and overall clinical performance in comparison to other materials [57,58]. In contrast, MTA, though utilized in one study, may be less favored due to its prolonged setting time and handling difficulties [47]. Regardless of the material chosen, the success of the final restoration depends primarily on its ability to prevent microleakage and effectively seal the access cavity, thereby protecting the underlying scaffold from exposure to oral microorganisms and potential infection.

Permanent restoration was completed during the same visit in nine studies [15,16,19,20,22,23,27–29] with one study specifying a 45-minute time frame before restoration [26]. In one study, restoration was completed after 24 hours [17], or after 1 week [21], and in two studies after 3 days, with no data for the BC group in these cases [24,25]. Finally, one study failed to provide data on the type or timing of permanent restoration [18].

Overall, composite resin is a popular choice for final restorations due to its aesthetic and functional benefits, while GIC and MTA are also used in certain cases. Timing and material selection play crucial roles in the success of the restoration procedure.

### Comparative results

There have been rapid advancements in regenerative endodontics in recent years, with new original research articles and reviews examining the efficiency of different materials such as scaffolds. A meta-analysis by Murray [59] concluded that platelet concentrates promoted apical closure more often compared to BC scaffolds, with similar success rates, periapical healing, and dentin wall thickening. However, it is worth noting that the design of the included studies is not described. Panda *et al.* [60] reviewed RCTs and other comparative studies and found no significant differences in dentin wall thickness, root length increase, or success rate between PRP or PRF and BC. However, in terms of vitality response and apical closure, PRP showed better results compared to BC. Another study by Panda *et al.* [32] compared regenerative interventions with apexification and different scaffolds from randomized and non-randomized trials with a follow-up period of ≥6 months and concluded that PRP and PRF yielded similar results to BC regarding apical closure, root length increase, and dentin wall thickness. Nevertheless, while REPs with PRP had a comparable success rate to those with BC, REPs with advanced platelet concentrates (it is not specified whether PRP or PRF was used) had a significantly better vitality response than those with BC.

In contrast to some of the outcomes presented in the aforementioned studies, the present systematic review found no statistical difference in the success rate of RETs using PRP or PRF compared to BC techniques. Similarly, Rios-Osorio *et al.* [61] concluded that BC scaffolds produce comparable clinical and radiographic results to platelet concentrates, without following a meta-analysis approach.

As for meta-analyses comparing platelet derivatives with the BC technique in RETs, important methodological differences distinguish our review from earlier reports. Rahul *et al.* [62] conducted their search in 2021 and included RCTs, non-RCTs, and prospective cohort studies with ≥12 months of follow-up. Using a network meta-analysis, they reported comparable outcomes between PRP, PRF, and BC in terms of clinical success, apical closure, and pulp sensitivity. Likewise, Verma *et al.* [63] combined RCTs with multiple non-randomized designs, including case studies, case reports, and retro-


https://doi.org/10.5395/rde.2025.50.e38

spective studies, to evaluate PRP and PRF against BC. In contrast, this review is the first to restrict inclusion exclusively to RCTs with ≥12 months' follow-up, thereby ensuring the highest level of evidence. Moreover, indirect comparisons and the use of combined experimental arms with heterogeneous controls were avoided to achieve direct head-to-head comparisons of PRP, PRF, and PP versus BC, yielding results that are both robust and clinically relevant. For instance, RCTs like the one by Rizk *et al*. [64] or Santhakumar *et al*. [65] that do not include a BC group were excluded in this study (Supplementary Table 1). Further heterogeneity was also restricted by avoiding pooling experimental groups where growth factors or other tissue-inductive molecules were used in combination with PRP or PRF [66]. Overall, this meta-analysis provides the most up-to-date and comprehensive dataset, avoiding any heterogeneity issues and ensuring methodological rigor and transparency by utilizing the Cochrane RoB 2.0 tool for bias assessment.

The limited number of randomized studies has created a research gap in this scientific field, despite some original research on this topic. Additionally, there is a lack of standardized evaluation criteria for the success of RETs. Various metrics, including clinical success, radiographic success, dentin wall thickness, increased root length, pulp sensitivity, and apical closure/periapical healing have been used in different studies and reviews, making it challenging to draw clear conclusions. Histological evaluation should play the most critical role in evaluating success by determining the type, organization, and cellular composition of newly regenerated pulp-like tissue. This includes the identification of key cellular components such as odontoblasts, fibroblasts, or mineralized tissue, the presence of newly formed blood vessels, regenerated nerve fibers, as well as the status of inflammation or infection, periodontal ligament integrity, and the condition of surrounding bone structures [14]. However, obtaining such histological data in a clinical setting is often challenging and may raise ethical concerns. Overall, more randomized studies, with standardized criteria, are needed to generate original clinical data and metrics for analysis, facilitating more accurate clinical decision-making.

### Limitations

This systematic review has several limitations. Publication bias may exist as only published studies from five main databases were included, potentially missing studies in other databases, grey literature, or unpublished sources. Language restrictions limited inclusion to English studies, possibly excluding relevant research in other languages. Finally, only studies with immature teeth, recall times over 12 months, and a BC control group were included, potentially missing other important outcomes.

## CONCLUSIONS

This systematic review suggests that PRP, PRF, and BC present viable and clinically successful approaches for the RET of immature permanent teeth with pulp necrosis. While platelet derivatives may offer potential biological advantages, current evidence does not demonstrate significant statistical superiority in terms of clinical and radiographic success. Moreover, the lack of long-term follow-up data limits the strength of any definitive clinical recommendations. Future research should prioritize carefully planned RCTs with longer recall periods, larger sample sizes, standardized outcome measures, and, where possible, histological evaluation of human teeth to provide more robust evidence and clearer clinical guidance.

## CONFLICT OF INTEREST

No potential conflict of interest relevant to this article was reported.

## FUNDING/SUPPORT

The authors have no financial relationships relevant to this article to disclose.

## AUTHOR CONTRIBUTIONS

Conceptualization, Project administration: Kodonas K. Data curation: Tsiolaki A, Theocharis D. Formal analysis: Fardi A, Kodonas K. Investigation: Tsiolaki A, Theocharis D, Tsitsipas N. Methodology: Tsitsipas N, Fardi A, Kodonas K. Supervision: Kodonas K, Fardi A. Visualization: all authors. Writing - original draft: Tsiolaki A, Theocharis D, Tsitsipas N. Writing - review & editing: Fardi A, Kodonas K. All authors read and approved the final manuscript.

## DATA SHARING STATEMENT

The datasets are not publicly available but are available from the corresponding author upon reasonable request.

## SUPPLEMENTARY MATERIALS

**Supplementary Table 1.** Excluded randomized controlled trials

## REFERENCES


1. Feigin K, Shope B. Regenerative endodontics. J Vet Dent 2017;34:161-178.
2. Rojas-Gutiérrez WJ; Pineda-Vélez E; Agudelo-Suárez AA. Regenerative endodontics success factors and their overall effectiveness: an umbrella review. Iran Endod J 2022;17:90-105.
3. Pulyodan MK, Paramel Mohan S, Valsan D, Divakar N, Moyin S, Thayyil S. Regenerative endodontics: a paradigm shift in clinical endodontics. J Pharm Bioallied Sci 2020;12:S20-S26.
4. Kim SG, Malek M, Sigurdsson A, Lin LM, Kahler B. Regenerative endodontics: a comprehensive review. Int Endod J 2018;51:1367-1388.
5. Murray PE, Garcia-Godoy F, Hargreaves KM. Regenerative endodontics: a review of current status and a call for action. J Endod 2007;33:377-390.
6. Yan H, De Deus G, Kristoffersen IM, Wiig E, Reseland JE, Johnsen GF, *et al.* Regenerative endodontics by cell homing: a review of recent clinical trials. J Endod 2023;49:4-17.
7. Yang J, Yuan G, Chen Z. Pulp regeneration: current approaches and future challenges. Front Physiol 2016;7:58.
8. Arshad S, Tehreem F, Rehab Khan M, Ahmed F, Marya A, Karobari MI. Platelet-rich fibrin used in regenerative endodontics and dentistry: current uses, limitations, and future recommendations for application. Int J Dent 2021;2021:4514598.
9. Juárez DM, Chargoy NI. Blood clot in regenerative endodontic therapy of immature permanent teeth: a review of the literature. Mex J Med Res ICSA 2024;12:58-66.
10. Lin J, Zeng Q, Wei X, Zhao W, Cui M, Gu J, *et al.* Regenerative endodontics versus apexification in immature permanent teeth with apical periodontitis: a prospective randomized controlled study. J Endod 2017;43:1821-1827.
11. Galler KM, Krastl G, Simon S, Van Gorp G, Meschi N, Vahedi B, *et al.* European Society of Endodontology position statement: revitalization procedures. Int Endod J 2016;49:717-723.
12. Page MJ, McKenzie JE, Bossuyt PM, Boutron I, Hoffmann TC, Mulrow CD, *et al.* The PRISMA 2020 statement: an updated guideline for reporting systematic reviews. Rev Esp Cardiol (Engl Ed) 2021;74:790-799.
13. Sterne JA, Savovic J, Page MJ, Elbers RG, Blencowe NS, Boutron I, *et al.* RoB 2: a revised tool for assessing risk of bias in randomised trials. BMJ 2019;366:l4898.
14. Digka A, Sakka D, Lyroudia K. Histological assessment of human regenerative endodontic procedures (REP) of immature permanent teeth with necrotic pulp/apical periodontitis: a systematic review. Aust Endod J 2020;46:140-153.
15. Ulusoy AT, Turedi I, Cimen M, Cehreli ZC. Evaluation of blood clot, platelet-rich plasma, platelet-rich fibrin, and platelet pellet as scaffolds in regenerative endodontic treatment: a prospective randomized trial. J Endod 2019;45:560-566.
16. Jadhav G, Shah N, Logani A. Revascularization with and without platelet-rich plasma in nonvital, immature, anterior teeth: a pilot clinical study. J Endod 2012;38:1581-1587.
17. ElSheshtawy AS, Nazzal H, El Shahawy OI, El Baz AA, Ismail SM, Kang J, *et al.* The effect of platelet-rich plasma as a scaffold in regeneration/revitalization endodontics of immature permanent teeth assessed using 2-dimensional radiographs and cone beam computed tomography: a randomized controlled trial. Int Endod J 2020;53:905-921.
18. Shivashankar VY, Johns DA, Maroli RK, Sekar M, Chandrasekaran R, Karthikeyan S, *et al.* Comparison of the effect of PRP, PRF and induced bleeding in the revascularization of teeth with necrotic pulp and open apex: a triple blind randomized clinical trial. J Clin Diagn Res 2017;11:ZC34-ZC39.
19. Narang I, Mittal N, Mishra N. A comparative evaluation of the blood clot, platelet-rich plasma, and platelet-rich fibrin in regeneration of necrotic immature permanent teeth: a clinical study. Contemp Clin Dent 2015;6:63-68.
20. Alagl A, Bedi S, Hassan K, AlHumaid J. Use of platelet-rich plasma for regeneration in non-vital immature permanent teeth: clinical and cone-beam computed tomography evaluation. J Int Med Res 2017;45:583-593.
21. Turky M, Kataia MA, Ali MM, Hassan RE. Revascularization induced maturogenesis of human non-vital immature teeth via platelets-rich plasma (PRP): radiographic study. J Dent Oral Heal 2017;3:97.
22. Bezgin T, Yilmaz AD, Celik BN, Kolsuz ME, Sonmez H. Efficacy of platelet-rich plasma as a scaffold in regenerative



https://doi.org/10.5395/rde.2025.50.e38

endodontic treatment. J Endod 2015;41:36-44.
23. Bansal M, Sawhny A, Singh R, Sharma S, Priyadarshi PK, Paul S. Evaluation of efficacy of platelet rich plasma as a scaffold in regenerative endodontic treatment: an in-vivo study. J Cardiovasc Dis Res 2021;12:2750-2758.
24. Rizk HM, Salah Al-Deen MS, Emam AA. Pulp revascularization/revitalization of bilateral upper necrotic immature permanent central incisors with blood clot vs platelet-rich fibrin scaffolds-a split-mouth double-blind randomized controlled trial. Int J Clin Pediatr Dent 2020;13:337-343.
25. Rizk HM, Al-Deen MS, Emam AA. Regenerative endodontic treatment of bilateral necrotic immature permanent maxillary central incisors with platelet-rich plasma versus blood clot: a split mouth double-blinded randomized controlled trial. Int J Clin Pediatr Dent 2019;12:332-339.
26. Ragab RA, Lattif AE, Dokky NA. Comparative study between revitalization of necrotic immature permanent anterior teeth with and without platelet rich fibrin: a randomized controlled trial. J Clin Pediatr Dent 2019;43:78-85.
27. Sharma S, Mittal N. A comparative evaluation of natural and artificial scaffolds in regenerative endodontics: a clinical study. Saudi Endod J 2016;6:9-15.
28. Mittal N, Parashar V. Regenerative evaluation of immature roots using PRF and artificial scaffolds in necrotic permanent teeth: a clinical study. J Contemp Dent Pract 2019;20:720-726.
29. Uppala S. A comparative evaluation of PRF, blood clot and collagen scaffold in regenerative endodontics. Eur J Mol Clin Med 2020;7:3401-3410.
30. Purra AR, Ahangar FA, Chadgal S, Farooq R. Mineral trioxide aggregate apexification: a novel approach. J Conserv Dent 2016;19:377-380.
31. Guerrero F, Mendoza A, Ribas D, Aspiazu K. Apexification: a systematic review. J Conserv Dent 2018;21:462-465.
32. Panda P, Mishra L, Govind S, Panda S, Lapinska B. Clinical outcome and comparison of regenerative and apexification intervention in young immature necrotic teeth: a systematic review and meta-analysis. J Clin Med 2022;11:3909.
33. Wei X, Yang M, Yue L, Huang D, Zhou X, Wang X, *et al.* Expert consensus on regenerative endodontic procedures. Int J Oral Sci 2022;14:55.
34. Mehta S, Watson JT. Platelet rich concentrate: basic science and current clinical applications. J Orthop Trauma 2008;22:432-438.
35. Kobayashi E, Flückiger L, Fujioka-Kobayashi M, Sawada K, Sculean A, Schaller B, *et al.* Comparative release of growth factors from PRP, PRF, and advanced-PRF. Clin Oral Investig 2016;20:2353-2360.
36. De Pascale MR, Sommese L, Casamassimi A, Napoli C. Platelet derivatives in regenerative medicine: an update. Transfus Med Rev 2015;29:52-61.
37. Xu J, Gou L, Zhang P, Li H, Qiu S. Platelet-rich plasma and regenerative dentistry. Aust Dent J 2020;65:131-142.
38. Gupta S, Paliczak A, Delgado D. Evidence-based indications of platelet-rich plasma therapy. Expert Rev Hematol 2021;14:97-108.
39. Naik B, Karunakar P, Jayadev M, Marshal VR. Role of Platelet rich fibrin in wound healing: a critical review. J Conserv Dent 2013;16:284-293.
40. Dohan DM, Choukroun J, Diss A, Dohan SL, Dohan AJ, Mouhyi J, *et al.* Platelet-rich fibrin (PRF): a second-generation platelet concentrate. Part II: platelet-related biologic features. Oral Surg Oral Med Oral Pathol Oral Radiol Endod 2006;101:e45-e50.
41. Dugrillon A, Eichler H, Kern S, Klüter H. Autologous concentrated platelet-rich plasma (cPRP) for local application in bone regeneration. Int J Oral Maxillofac Surg 2002;31:615-619.
42. Keles GC, Cetinkaya BO, Albayrak D, Koprulu H, Acikgoz G. Comparison of platelet pellet and bioactive glass in periodontal regenerative therapy. Acta Odontol Scand 2006;64:327-333.
43. Khiste SV, Naik Tari R. Platelet-rich fibrin as a biofuel for tissue regeneration. Int Sch Res Not 2013;2013:627367.
44. Oneto P, Zubiry PR, Schattner M, Etulain J. Anticoagulants interfere with the angiogenic and regenerative responses mediated by platelets. Front Bioeng Biotechnol 2020;8:223.
45. Dissanayaka WL, Zhang C. Scaffold-based and scaffold-free strategies in dental pulp regeneration. J Endod 2020;46:S81-S89.
46. Liu H, Lu J, Jiang Q, Haapasalo M, Qian J, Tay FR, *et al.* Biomaterial scaffolds for clinical procedures in endodontic regeneration. Bioact Mater 2022;12:257-277.
47. Tawil PZ, Duggan DJ, Galicia JC. Mineral trioxide aggregate (MTA): its history, composition, and clinical applications. Compend Contin Educ Dent 2015;36:247-252.
48. Parirokh M, Torabinejad M. Mineral trioxide aggregate: a comprehensive literature review: part III: clinical applications, drawbacks, and mechanism of action. J Endod 2010;36:400-413.

49. Tek GB, Keskin G. Use of mineral trioxide aggregate with or without a collagen sponge as an apical plug in teeth with immature apices. J Clin Pediatr Dent 2021;45:165-170.
50. Nicholson JW. Maturation processes in glass-ionomer dental cements. Acta Biomater Odontol Scand 2018;4:63-71.
51. Tavakoli M, Araghi S, Fathi A, Jalalian S. Comparison of coronal sealing of flowable composite, resin-modified glass ionomer, and mineral trioxide aggregate in endodontically treated teeth: an in-vitro study. Dent Res J (Isfahan) 2024;21:13.
52. Moharamzadeh K, Brook IM, Van Noort R. Biocompatibility of resin-based dental materials. Materials 2009;2:514-548.
53. Soares CJ, Faria-E-Silva AL, Rodrigues MP, Vilela ABF, Pfeifer CS, Tantbirojn D, *et al.* Polymerization shrinkage stress of composite resins and resin cements: what do we need to know? Braz Oral Res 2017;31:e62.
54. Chandrasekhar V, Rudrapati L, Badami V, Tummala M. Incremental techniques in direct composite restoration. J Conserv Dent 2017;20:386-391.
55. Sidhu SK. Glass-ionomer cement restorative materials: a sticky subject? Aust Dent J 2011;56 Suppl 1:23-30.
56. Bowen RL, Marjenhoff WA. Dental composites/glass ionomers: the materials. Adv Dent Res 1992;6:44-49.
57. Heintze SD, Loguercio AD, Hanzen TA, Reis A, Rousson V. Clinical efficacy of resin-based direct posterior restorations and glass-ionomer restorations: an updated meta-analysis of clinical outcome parameters. Dent Mater 2022;38:e109-e135.
58. Balkaya H, Arslan S, Pala K. A randomized, prospective clinical study evaluating effectiveness of a bulk-fill composite resin, a conventional composite resin and a reinforced glass ionomer in Class II cavities: one-year results. J Appl Oral Sci 2019;27:e20180678.
59. Murray PE. Platelet-rich plasma and platelet-rich fibrin can induce apical closure more frequently than blood-clot revascularization for the regeneration of immature permanent teeth: a meta-analysis of clinical efficacy. Front Bioeng Biotechnol 2018;6:139.
60. Panda S, Mishra L, Arbildo-Vega HI, Lapinska B; Lukomska-Szymanska M, Khijmatgar S, *et al.* Effectiveness of autologous platelet concentrates in management of young immature necrotic permanent teeth: a systematic review and meta-analysis. Cells 2020;9:2241.
61. Ríos-Osorio N, Caviedes-Bucheli J; Jimenez-Peña O, Orozco-Agudelo M, Mosquera-Guevara L; Jiménez-Castellanos FA, *et al.* Comparative outcomes of platelet concentrates and blood clot scaffolds for regenerative endodontic procedures: a systematic review of randomized controlled clinical trials. J Clin Exp Dent 2023;15:e239-e249.
62. Rahul M, Lokade A, Tewari N, Mathur V, Agarwal D, Goel S, *et al.* Effect of intracanal scaffolds on the success outcomes of regenerative endodontic therapy: a systematic review and network meta-analysis. J Endod 2023;49:110-128.
63. Verma S, Gupta A, Mrinalini M, Abraham D, Soma U. Comparative evaluation of autologous platelet aggregates versus blood clot on the outcome of regenerative endodontic therapy: a systematic review and meta-analysis. J Clin Exp Dent 20 25;17:e447-e460.
64. Rizk HM, Salah Al-Deen MSM, Emam AA. Comparative evaluation of Platelet Rich Plasma (PRP) versus Platelet Rich Fibrin (PRF) scaffolds in regenerative endodontic treatment of immature necrotic permanent maxillary central incisors: a double blinded randomized controlled trial. Saudi Dent J 202 0;32:224-231.
65. Santhakumar M, Yayathi S, Retnakumari N. A clinicoradiographic comparison of the effects of platelet-rich fibrin gel and platelet-rich fibrin membrane as scaffolds in the apexification treatment of young permanent teeth. J Indian Soc Pedod Prev Dent 2018;36:65-70.
66. Yang F, Yu L, Li J, Cheng J, Zhang Y, Zhao X, *et al.* Evaluation of concentrated growth factor and blood clot as scaffolds in regenerative endodontic procedures: a retrospective study. Aust Endod J 2023;49:332-343.



https://doi.org/10.5395/rde.2025.50.e38

RDE Restorative Dentistry & Endodontics

Research Article

eISSN 2234-7666
Restor Dent Endod. 2025 November;50(4):e39
https://doi.org/10.5395/rde.2025.50.e39

# Difference in light transmittance and depth of cure of flowable composite depending on tooth thickness: an *in vitro* experimental study

Seong-Pyo Bae[1], Myung-Jin Lee[1,2,3], Kyung-San Min[1,2,3], Mi-Kyung Yu[1,2,3], Kwang-Won Lee[1,2,3,*]

[1]Department of Conservative Dentistry, School of Dentistry, Jeonbuk National University, Jeonju, Korea
[2]Research Institute of Clinical Medicine, Jeonbuk National University, Jeonju, Korea
[3]Biomedical Research Institute, Jeonbuk National University Hospital, Jeonju, Korea

## ABSTRACT

**Objectives:** This study aimed to quantify light attenuation through varying tooth thicknesses and its impact on the depth of cure of composite resin.

**Methods:** Twenty extracted premolars were used to create enamel-dentin discs that were sanded progressively in 0.5 mm increments from 2.5 mm to 0.5 mm. Light irradiance was measured with and without tooth specimens to evaluate light transmittance. Resin was cured beneath different thicknesses, and the depth of cure was assessed using the Vickers hardness test.

**Results:** The results demonstrated that light transmittance significantly decreased as tooth thickness increased ($p < 0.01$), leading to reduced resin polymerization. In the 2.0-mm and 2.5-mm tooth thickness groups, the depth of cure was significantly lower than in the control group without tooth specimens ($p < 0.05$).

**Conclusions:** Ultimately, for tooth structures exceeding 2 mm, self-cure or dual-cure resin polymerization is thought to be more efficient than light polymerization.

**Keywords:** Depth of cure; Flowable composite; Light attenuation; Microhardness; Tooth structure

## INTRODUCTION

When using light-cured composite resins as restorative materials in clinical practice, it is impossible for the light from the curing unit to be directed perpendicularly to all areas of the resin. It is very difficult for light to reach the deepest parts of the cavity, the axio-pulpal line angle in the proximal box, and deep undercut areas [1,2]. To achieve optimal polymerization, manufacturers recommend light curing not only from the occlusal surface but

**Received:** August 28, 2025 **Revised:** June 17, 2025 **Accepted:** July 10, 2025

**Citation**
Bae SP, Lee MJ, Min KS, Yu MK, Lee KW. Difference in light transmittance and depth of cure of flowable composite depending on tooth thickness: an *in vitro* experimental study. Restor Dent Endod 2025;50(4):e39.

***Correspondence to**
**Kwang-Won Lee, DDS, PhD**
Department of Conservative Dentistry, School of Dentistry, Jeonbuk National University, 567 Baekje-daero, Jeonju 54896, Korea
Email: lkw@jbnu.ac.kr
Seong-Pyo Bae and Myung-Jin Lee contributed equally to this work as co-first authors.

also from the buccal and lingual sides [2]. Additionally, in cases where tooth fragments are reattached due to crown fractures, the light-cured composite resin injected into the tooth cannot be directly exposed to light; instead, the light must pass through the tooth structure to reach the composite. In such circumstances, the general light-curing process without increased curing time or light irradiance may result in insufficient polymerization of the resin [3].

Although some previous studies [4,5] have measured light attenuation regarding the distance from the light-curing unit (LCU) and the intensity of light transmitted through resin or ceramic restorations, few studies have examined light transmittance through an actual tooth structure and the properties of that polymerized composite resin. Additionally, no experiments have controlled for light leakage while the LCU is in operation. Results from previous studies have indicated that, compared to light curing in the air, there is a significant decrease in light irradiance and depth of cure of resin when light is transmitted through a tooth structure. One study [2] reported about a 98% decrease in light transmission at a tooth thickness of 5.0 mm, while other studies [6,7] using enamel and dentin filters have reported a high light attenuation of about 80% or more, depending on thickness, which led to inferior resin properties. Therefore, in this study, actual teeth were used, and a specially designed mold was used to gather the light from a specific spot on the LCU, creating a more precise light transmission circumstance. Unpolymerized residual resin monomers are known to dissolve in the oral cavity and possess tissue toxicity [8–10]. Additionally, they reduce the structural stability of the composite, consequently decreasing its mechanical properties and durability, leading to a poor long-term prognosis for the restoration [11–13]. The depth of cure of resin can be defined as the thickness at the point where the microhardness of the polymerized resin reaches 80% of the top surface hardness [14–16]. The depth of cure calculated with microhardness values can be used as an indirect indicator of conversion degree and the mechanical properties of the resin.

The purpose of this study is to quantify the intensity of the curing light attenuated by the thickness of the tooth structure, compare the differences in light transmittance, and measure the microhardness of the resin polymerized beneath the tooth structure to determine the depth of cure of the resin. The null hypothesis of this study is that "there will be no difference in light transmittance and depth of cure depending on the thickness of the tooth structure."

## METHODS

### Materials

For the study, commercially available composite resin (Filtek Supreme Flowable Restorative; 3M Oral Care, St. Paul, MN, USA) and an LCU (B&Lite S; B&L Biotech Co., Daejeon, Korea) were used. Only the A3 shade of the composite resin was used. Tooth specimens were recently extracted from maxillary and mandibular premolars of patients aged 18 to 30 years undergoing orthodontic treatment. Teeth with caries, fractures, or resorption defects were excluded, and only teeth with intact pulp chambers and no calcification or abnormal change were used. To quantitatively analyze the reduction in light transmittance through the tooth structure, a radiometer (LM-300 Curing Light Meter; TPC Dental, Walnut, CA, USA) was used. The microhardness of the resin polymerized beneath the tooth structure was measured using a Vickers hardness tester (HM-124; Mitutoyo, Kawasaki, Japan).

### Methods

#### 1. Preparation of tooth specimens

This study received approval from the Institutional Review Board of Jeonbuk National University Hospital (CUH 2024-03-036-003) to use human teeth. Twenty extracted maxillary and mandibular premolars without caries or restorations were used for the experiment. All teeth were sectioned at the cementoenamel junction using a microsaw (Isomet, low speed; Buehler, Lake Bluff, IL, USA). Next, the cusps of the occlusal surfaces were flattened using a diamond bur, and then 10 circular specimens with a diameter of 6 mm and a height of 2.5 mm were prepared. For each test group, the specimens were polished sequentially from the bottom using 600-grit wet sandpaper to create specimens with thicknesses of 2.0, 1.5, 1.0, and 0.5 mm (Figure 1). Another 10 specimens with a diameter of 4 mm were prepared using the same process.


https://doi.org/10.5395/rde.2025.50.e39

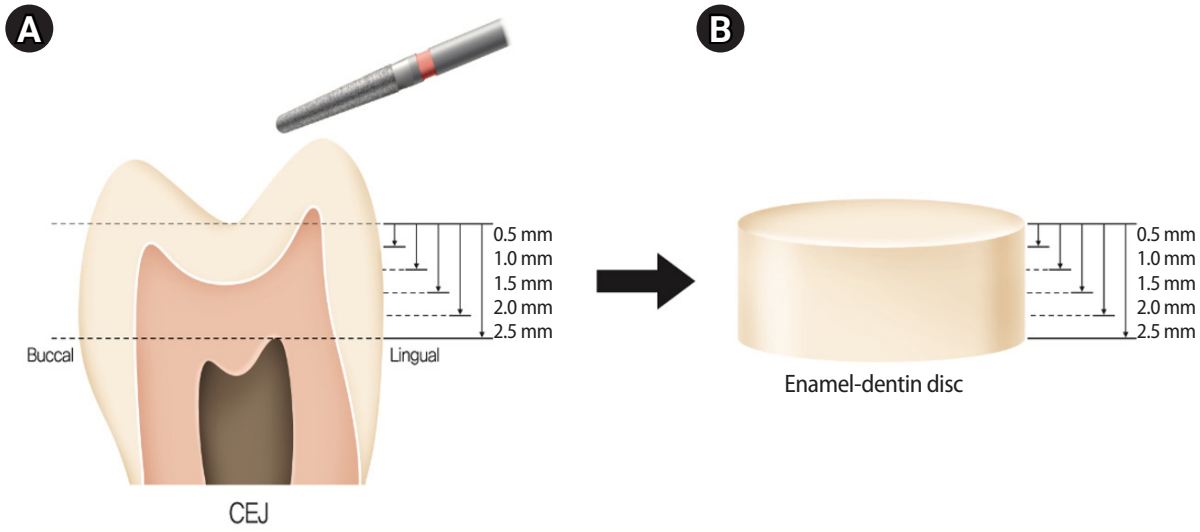


**Figure 1.** (A) Tooth sample preparation. (B) An enamel-dentin disc with different thicknesses. CEJ, cementoenamel junction.

### 2. Resin specimen preparation

Following the standard suggested by the International Organization for Standardization (ISO), a metal split mold with a diameter of 4 mm and a height of 6 mm was used. After applying a mold release agent, composite resin was injected into the mold. A mylar strip was then placed on top to flatten the surface, followed by a custom mold that placed the tooth specimen above the resin. This was followed by 20 seconds of light curing (Figure 2). The manufacturer of the composite resin used in this experiment recommends light exposure at 550–1,000 mW/cm² for 20 seconds for a 2-mm thickness. This process was uniformly conducted across all five groups (0.5/1.0/1.5/2.0/2.5 mm) by adjusting the mold according to the thickness of the tooth specimen, and 10 resin specimens were prepared for each group. After curing, the composite resin was removed from the split mold, and the uncured resin at the bottom surface was scraped off with a metal instrument. The specimens were stored in distilled water at 37°C in a dark environment for 24 hours and kept in a light-proof container at room temperature to prevent additional polymerization by ambient light until further measurements. For the control group, 10 resin specimens were prepared following the same procedure but without a tooth specimen during the curing process.

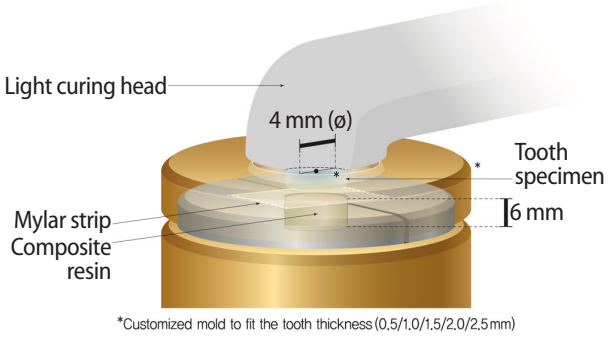


**Figure 2.** Light curing of composite resin through the tooth structure.

### 3. Measurement of light irradiance

Ten teeth with a diameter of 6 mm and specially designed molds of varying heights were used. For the control group corresponding to each tooth thickness, the mold and LCU were positioned on a radiometer without a tooth, and the irradiance was measured at a fixed distance (0.5/1.0/1.5/2.0/2.5 mm) corresponding to the thickness of the tooth used. The control was irradiated at 0.5 mm. Next, after placing the prepared tooth, the measurement was repeated in the same manner for each group (Figure 3). The average value and standard deviation were calculated, and the reduction in irradiance according to tooth thickness was compared and analyzed against the initial values. Ten tooth specimens were used for the measurements in each group, and the light irradiance of the curing unit was periodically

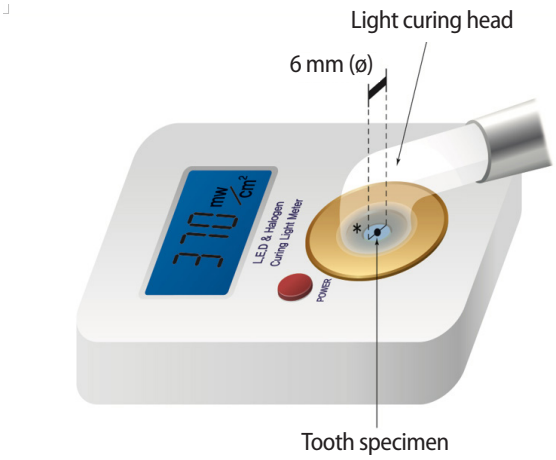


**Figure 3.** Measurement of the light irradiance of the light-curing unit through a tooth structure.

checked to ensure consistent output throughout the experiment. Prior to each measurement, the light-curing unit's irradiance was verified using a radiometer to ensure consistent output across all specimens.

#### 4. Measurement of resin microhardness and depth of cure

The microhardness (Vickers hardness number, VHN) of resin specimens prepared for each group ($n$ = 10) was measured using a Vickers hardness tester (HM-124) (Figure 4). The hardness value of the surface closest to the LCU (ie, "upper surface") was measured first. The lower, less-cured resin (ie, "lower surface") was sequentially polished in 0.1-mm increments. After each polishing step, the hardness values were recorded and compared to those of the upper surface. To minimize measurement error, the indenter was applied to the center of the specimen. A load of 200 g was applied for 20 seconds during the hardness measurement, corresponding to a force of 1.961 N. The VHN value was automatically calculated by the tester using the following formula:

$$VHN = 0.102\frac{2F\sin\left(\frac{\alpha}{2}\right)}{d^2} = 0.1891 \times \frac{F}{d^2},$$

where $F$ is the applied load (N), $\alpha$ is the angle of the indenter tip (136°), and $d$ is the mean diagonal length of the indentation (mm).

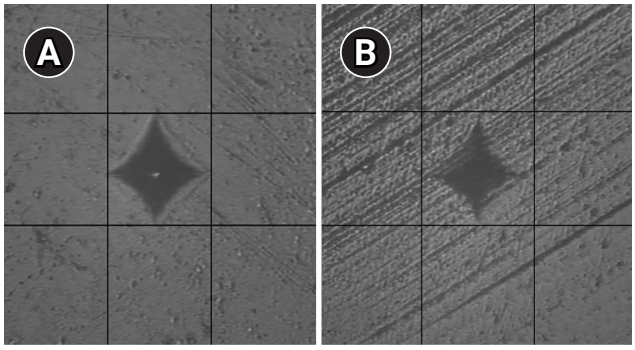


**Figure 4.** Vickers hardness indentation of upper (A) and lower surfaces (B).

The point at which the hardness value reached 80% or more of the upper surface hardness was defined as the depth of cure of the resin. For the control group, resin specimens were cured at a 0.5 mm distance in the absence of a tooth. A total of 60 specimens (10 per group) were used to calculate the average value and standard deviation of surface hardness.

#### 5. Measurement of dentin area ratio

Randomly selected tooth specimens used in the experiment were bisected vertically, and the surface was observed using scanning electron microscopy (SEM; SU8230, Hitachi, Tokyo, Japan). SEM image analysis was conducted on teeth with the same diameter as in the light transmittance experiment, measuring the area ratio of dentin at different heights. The acquired image was processed using ImageJ (ver. 1.53s, National Institutes of Health, Bethesda, MD, USA) to identify the enamel and dentin areas, and the ratio was calculated through pixel analysis. After converting the image, the enamel portion was selectively isolated, and the dentin area ratio was calculated (Figure 5).

#### 6. Data analysis

Measured data were analyzed using a statistical analysis program (IBM SPSS version 19.0; IBM Corp, Armonk, NY, USA). One-way analyses of variance and Tukey *post hoc* tests were conducted to examine the effect of tooth thickness on light transmittance. The Kruskal-Wallis test was employed to determine the statistical significance of the depth of cure of the resin, based on tooth thickness, between the control and experimental groups.


https://doi.org/10.5395/rde.2025.50.e39

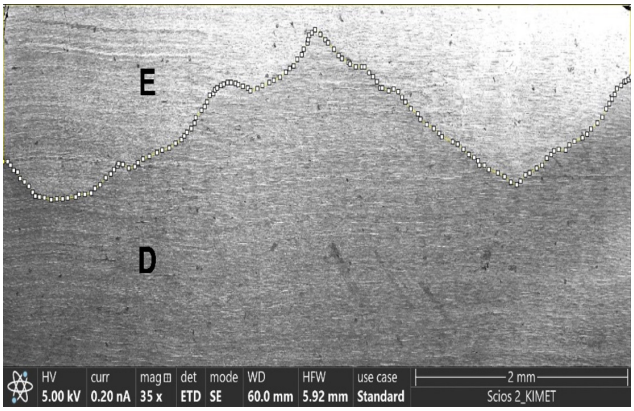


**Figure 5.** Scanning electron microscopic image of a bisected tooth specimen with a marked boundary to measure the dentin ratio. E, enamel; D, dentin.

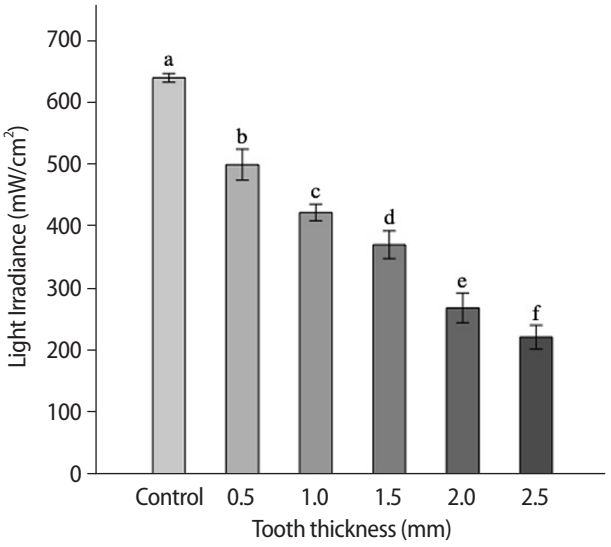


**Figure 6.** Light transmittance by tooth thickness. The control group indicates light irradiance at 0.5 mm from the light-curing unit without a tooth specimen. Values with different lowercase letters are significantly different ($p < 0.01$).

Statistical significance was defined as $p < 0.01$ for light transmittance and $p < 0.05$ for depth of cure.

## RESULTS

Figure 6 shows the mean and standard deviation of irradiance values measured in the absence of a tooth for the control group and through tooth structures of various thicknesses for the other experimental groups. Transmitted light irradiance significantly decreased as tooth thickness increased ($p < 0.01$). Among the experimental groups, the highest mean irradiance was observed in the 0.5-mm tooth group (530 mW/cm$^2$), while the lowest was in the 2.5-mm group (220 mW/cm$^2$). The reduction rates in irradiance were 21.8% for the 0.5-mm group, 32.8% for the 1.0-mm group, 40.1% for the 1.5-mm group, 54.4% for the 2.0-mm group, and 61.7% for the 2.5-mm group.

Figure 7 presents the VHN values of the upper surface of the cured resin for each group, as well as the hardness values at the point where the value reached 80% or more of the upper surface hardness. The hardness values of both the upper and lower surfaces were highest in the control group. The VHN values for the upper surface of the resin were relatively low in the 2.0-mm group (37.8) and the 2.5-mm group (34.1) compared to other groups. Except for these two groups, the hardness values in all other groups were greater than 40. Both the upper and lower hardness values were lower than those of the control when the light passed through the tooth, and hardness decreased as the thickness of the tooth increased.

Table 1 shows the depth of cure of the resin based on the measured hardness values. The depth of cure was significantly higher in the control group ($p < 0.05$) and decreased with increasing tooth thickness. The 2.0-mm and 2.5-mm tooth groups showed a significant difference in depth of cure compared to the control group, but the difference between these two groups was not significant ($p = 0.241$).

Figure 8 presents a graph of the ratio of resin depth of cure and irradiance in the experimental groups compared to the control group. As the thickness of the tooth increased, the depth of cure and light irradiance consistently decreased, and the two values showed similar patterns of reduction. In the 2.0-mm and 2.5-mm tooth groups, both values were less than 50%.

The dentin area ratio varied by the thickness of the tooth and showed a significant decrease to the occlusal surface (Table 2). It can be inferred that the greater the proportion of dentin in the tooth specimen, the greater is the reduction in light transmittance (Figure 5).

## DISCUSSION

Composite resin has become an indispensable material

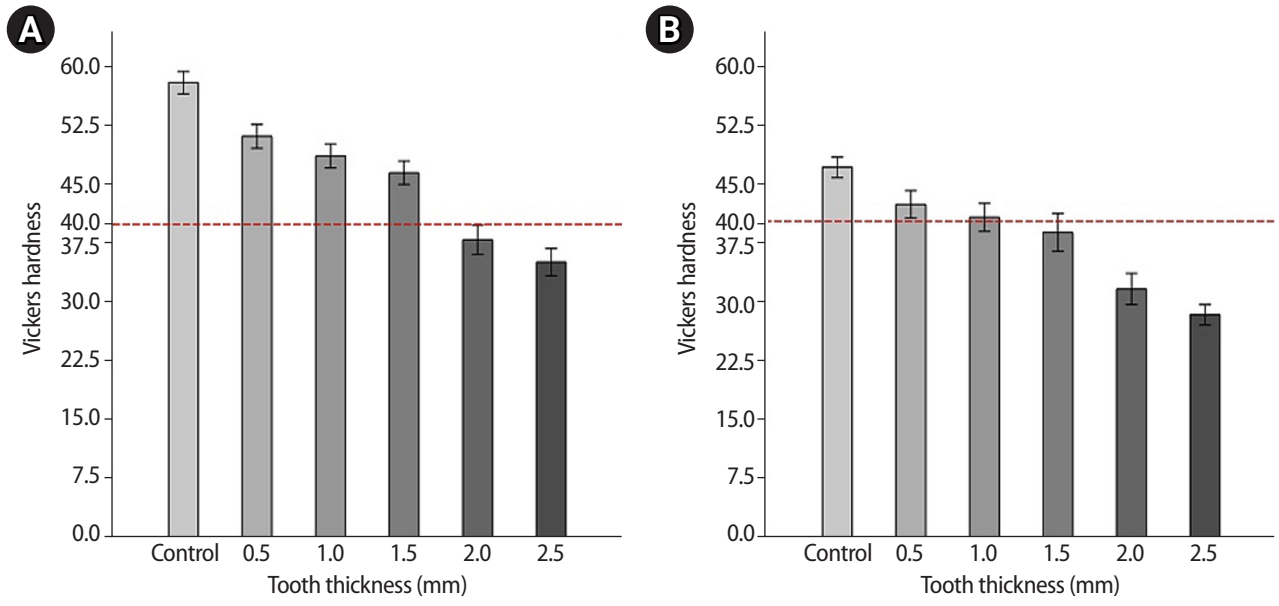


**Figure 7.** Mean microhardness values (Vickers hardness number) of the upper surface (A) and lower surface (B) of the composite resin samples. The control group indicates microhardness at 0.5 mm from the light-curing unit without a tooth specimen.

**Table 1.** Depth of cure of flowable composite based on microhardness under various tooth thicknesses

| Tooth thickness (mm) | Depth of cure (mm) | Decrease rate (%) |
|---|---|---|
| Control | $3.33 \pm 0.10^{A}$ | |
| 0.5 | $2.62 \pm 0.07^{AB}$ | 21.3 |
| 1.0 | $2.22 \pm 0.06^{BC}$ | 34.2 |
| 1.5 | $2.08 \pm 0.06^{C}$ | 41.1 |
| 2.0 | $1.26 \pm 0.08^{D}$ | 62.1 |
| 2.5 | $1.09 \pm 0.03^{D}$ | 67.2 |

Values are presented as mean ± standard deviation unless otherwise specified.
Values with different uppercase superscript letters indicate statistically significant difference ($p < 0.05$).

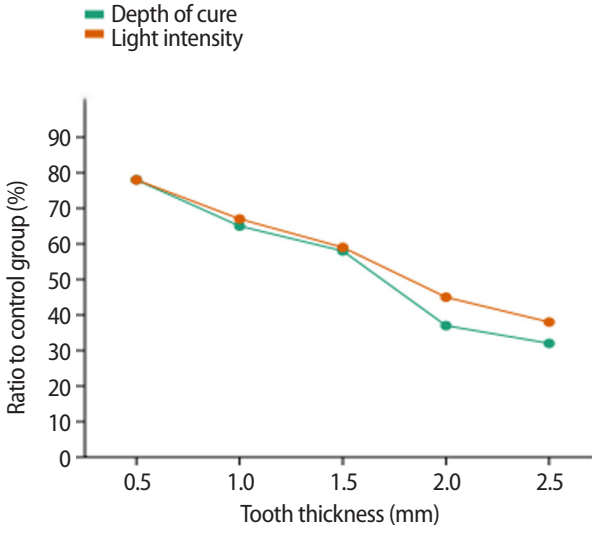


**Figure 8.** Ratio of depth of cure and light irradiance to those of the control group. Control group indicates the depth of cure and light irradiance measured at 0.5 mm from the light curing unit without a tooth specimen.

in modern restorative dentistry. Based on the polymerization mechanism, composite resins are categorized into self-cured, light-cured, or dual-cured types, with light-cured resins being used for most direct restorations. This resin is typically polymerized using blue light in the 450 to 500 nm wavelength range. When exposed to such light, the primary photoinitiator, camphorquinone, breaks down and generates free radicals, which initiate the opening of the double bonds in resin monomers. This process rapidly triggers chain growth, leading to the formation of polymer molecules. However, if the resin is not exposed to sufficient light energy, incomplete conversion of monomers occurs, resulting in inadequate polymerization. This insufficient polymerization compromises the material's physical properties and can lead to increased fracture rates, wear, secondary caries, and ultimately early failure of the res-


https://doi.org/10.5395/rde.2025.50.e39

**Table 2.** Ratio of dentin according to tooth thickness when light is transmitted

| Tooth thickness (mm) | Dentin ratio of tooth specimen (%) |
|---|---|
| 0.5 | 3.5 |
| 1.0 | 22.5 |
| 1.5 | 43.4 |
| 2.0 | 56.8 |
| 2.5 | 64.5 |

toration. Appropriate polymerization is crucial for the longevity and success of restoration.

In this study, we observed a significant reduction in light irradiance when transmitted through the tooth structure, which consequently led to a reduction in the depth of cure of resin. The reduction rate increased as the thickness of the tooth structure increased, and the null hypothesis was rejected. There has been very little research on light transmittance and the properties of resin polymerized under varying tooth thicknesses. To the best of our knowledge, this is the first study to control light leakage from a curing unit. Also, to minimize variability, all extracted teeth were premolars with intact crowns, free of caries or restorations. The enamel-dentin discs were prepared using standardized procedures to maintain consistent thickness.

In Figure 6, as the thickness of the tooth increases, there is a significant reduction in light irradiance. Specifically, in the 0.5-mm tooth thickness group, irradiance decreased by about 21.8% and 59.9% at 1.5 mm and by 61.7% at 2.5 mm. In a previous study [2] using tooth structures with thicknesses ranging from 1.5 mm to 5.0 mm, the irradiance was reduced by about 71% at 1.5 mm and by about 98% at 5.0 mm. The reduction in light irradiance based on the thickness of the tooth structure was greater in previous studies compared to this study. This difference might be attributed to the lack of control of light leakage in previous studies during curing and measurement of irradiance at 0 mm as a fixed reference point. Generally, at least 300–400 mW/cm$^2$ of irradiance is required for adequate light curing [17]. In the tooth groups with a thickness of 2.0 mm and 2.5 mm, the transmitted irradiance did not reach 300 mW/cm$^2$, suggesting that standard light-curing time may not be sufficient to achieve adequate resin polymerization.

Flowable composite resin was selected for this experiment due to its higher translucency and ease of handling in thin layers, making it suitable for evaluating light transmittance and depth of cure in constrained geometries. Depending on the type and translucency of composite resin, the recommended curing conditions vary. However, manufacturers generally suggest 20 seconds of exposure to 500–800 mW/cm$^2$ of light when polymerizing a light-cured composite at 2 mm. The curing light used in this experiment was an LED type, with an 800 mW/cm$^2$ minimum output suggested by the manufacturer.

The depth of cure of the resin also showed considerable differences depending on the thickness of the tooth structure, except for the 2.0-mm and 2.5-mm tooth groups. The average depth of cure in the control group was 3.33 ± 0.1 mm, which significantly decreased to 1.09 ± 0.03 mm as the thickness increased to 2.5 mm (Table 1). Previous studies [2,4,5] reported that the reduction in depth of cure was not as significant as the decrease in light transmittance. However, in the present study, the reductions in light transmittance and depth of cure based on tooth thickness were similar (Figure 8). This may be because the cure depth was determined by measuring the microhardness of the resin surface without using the conventional ISO scraping method. ISO introduced a method for measuring the depth of cure of resin by scraping off the uncured resin beneath, but several studies have noted that the ISO 4049 method overestimates the actual depth of cure [18]. Therefore, some authors suggest that the depth of cure be defined by comparing the hardness values of the top and bottom rather than simply scraping off the uncured resin [19,20]. Indeed, in the present experiment, the depth of cure measured after scraping off the uncured resin from all groups was higher than that based on hardness.

There are numerous studies [14,21,22] regarding the quality and properties of the polymerization of light-cured resin. The degree of conversion, which refers to the ratio of monomer conversion to composite material, is important in determining the mechanical, physical, and biological properties of a restoration. The microhardness of the resin surface is generally used as an indicator of the material's resistance to plastic deformation, wear, and attrition [23,24]. Furthermore, microhardness increases with the degree of cross-linking in

the polymerization reaction, which indirectly represents the degree of conversion [25,26]. The depth of cure of resin is closely related to the quality and physical properties of the polymerization, and many methods have been introduced to assess this variable, including measuring the thickness of the portion remaining after removing the uncured lower part, measuring the hardness of the upper and lower sections and calculating the ratio, and using an optical microscope to visually identify the uncured boundary [20,27]. Regarding hardness, the point at which the ratio between the upper and lower sections reaches 0.8 to 0.85 is generally considered the point of cure [14,16,28].

Though there is no consensus on the optimal hardness, the values of commercially available light-cured composite resins range from 30 to 100 [29,30]. Some authors suggest that the hardness of a clinical composite resin should be at least 40 [29,31]. In the present study, the average hardness value of the resin's upper surface in the 2.0-mm and 2.5-mm tooth groups did not reach 40 (Table 1, Figure 7A). This indicates that a significant reduction in light transmittance at a tooth thickness exceeding 2.0 mm might prevent sufficient resin polymerization in clinical settings. For instance, when reattaching a fractured tooth fragment through resin injection, polymerization must occur using light transmitted through the tooth structure, and additional curing time may be required to overcome the thickness of the outer tooth structure. In such cases, extending the curing time beyond the standard duration could help increase the mechanical properties.

Previous studies [7,32] have shown that applying an additional curing time 1.5 to 4 times longer than the standard can reduce residual monomer levels and elution. As the depth of cure of resin varies depending on the shade, translucency, and type of resin, there may be limitations in the results of this study, which used a single shade of light-cured resin [5,33]. Further research incorporating different composite resin shades and material properties would be beneficial in providing a more comprehensive understanding of the clinical implications.

## CONCLUSIONS

This study showed that the transmitted light intensity and the curing depth decreased as the thickness of the tooth structure increased. This was especially noticeable when the tooth thickness exceeded 2.0 mm, at which point the cured resin did not achieve clinically sufficient hardness, indicating that the resin polymerization was insufficient. Ultimately, for tooth structures exceeding 2 mm, self-cure or dual-cure resin polymerization is thought to be more efficient than light polymerization. In conclusion, clinicians may need to consider that for tooth structures greater than 2 mm in thickness, self-cure or dual-cure resin polymerization may be more effective than light curing.

### CONFLICT OF INTEREST

Kyung-San Min is the Editor-in-Chief of *Restorative Dentistry and Endodontics* and was not involved in the review process of this article. The authors declare no other conflicts of interest.

### FUNDING/SUPPORT

The authors have no financial relationships relevant to this article to disclose.

### AUTHOR CONTRIBUTIONS

Conceptualization: Min KS, Lee KW. Data curation, Investigation, Visualization: Bae SP, Lee MJ. Formal analysis: All authors. Methodology, Resources: Yu MK. Software: Bae SP. Supervision: Lee KW. Validation: Min KS. Writing - original draft: Bae SP, Lee MJ. Writing - review & editing: All authors. All authors read and approved the final manuscript.

### DATA SHARING STATEMENT

The datasets are not publicly available but are available from the corresponding author upon reasonable request.

## REFERENCES

1. Sartori N, Knezevic A, Peruchi LD, Phark JH, Duarte S. Effects of light attenuation through dental tissues on cure depth of composite resins. Acta Stomatol Croat 2019;53:95-105.
2. Hamlin NJ, Bailey C, Motyka NC, Vandewalle KS. Effect of tooth-structure thickness on light attenuation and depth of cure. Oper Dent 2016;41:200-207.
3. Ozturk N, Usumez A, Usumez S, Ozturk B. Degree of conversion and surface hardness of resin cement cured with different curing units. Quintessence Int 2005;36:771-777.


https://doi.org/10.5395/rde.2025.50.e39

4. Price RB, Murphy DG, Dérand T. Light energy transmission through cured resin composite and human dentin. Quintessence Int 2000;31:659-667.
5. Hyun HK, Christoferson CK, Pfeifer CS, Felix C, Ferracane JL. Effect of shade, opacity and layer thickness on light transmission through a nano-hybrid dental composite during curing. J Esthet Restor Dent 2017;29:362-367.
6. Arikawa H, Kanie T, Fujii K, Fukui K, Homma T. Mechanical properties of light-cured composite resins cured through filters that simulate enamel. Dent Mater J 2002;21:147-155.
7. Arikawa H, Kanie T, Fujii K, Ban S, Takahashi H. Light-attenuating effect of dentin on the polymerization of light-activated restorative resins. Dent Mater J 2004;23:467-473.
8. dos Santos RL, de Sampaio GA, de Carvalho FG, Pithon MM, Guênes GM, Alves PM. Influence of degree of conversion on the biocompatibility of different composites in vivo. J Adhes Dent 2014;16:15-20.
9. Cebe MA, Cebe F, Cengiz MF, Cetin AR, Arpag OF, Ozturk B. Elution of monomer from different bulk fill dental composite resins. Dent Mater 2015;31:e141-e149.
10. Durner J, Obermaier J, Draenert M, Ilie N. Correlation of the degree of conversion with the amount of elutable substances in nano-hybrid dental composites. Dent Mater 2012;28:1146-1153.
11. Sideridou ID, Achilias DS. Elution study of unreacted Bis-GMA, TEGDMA, UDMA, and Bis-EMA from light-cured dental resins and resin composites using HPLC. J Biomed Mater Res B Appl Biomater 2005;74:617-626.
12. Moldovan M, Balazsi R, Soanca A, Roman A, Sarosi C, Prodan D, *et al*. Evaluation of the degree of conversion, residual monomers and mechanical properties of some light-cured dental resin composites. Materials (Basel) 2019;12:2109.
13. Price RB, Shortall AC, Palin WM. Contemporary issues in light curing. Oper Dent 2014;39:4-14.
14. Galvão MR, Caldas SG, Bagnato VS, de Souza Rastelli AN, de Andrade MF. Evaluation of degree of conversion and hardness of dental composites photo-activated with different light guide tips. Eur J Dent 2013;7:86-93.
15. Polydorou O, Manolakis A, Hellwig E, Hahn P. Evaluation of the curing depth of two translucent composite materials using a halogen and two LED curing units. Clin Oral Investig 2008;12:45-51.
16. Alrahlah A, Silikas N, Watts DC. Post-cure depth of cure of bulk fill dental resin-composites. Dent Mater 2014;30:149-154.
17. Quance SC, Shortall AC, Harrington E, Lumley PJ. Effect of exposure intensity and post-cure temperature storage on hardness of contemporary photo-activated composites. J Dent 2001;29:553-560.
18. Flury S, Hayoz S, Peutzfeldt A, Hüsler J, Lussi A. Depth of cure of resin composites: is the ISO 4049 method suitable for bulk fill materials? Dent Mater 2012;28:521-528.
19. Moore BK, Platt JA, Borges G, Chu TM, Katsilieri I. Depth of cure of dental resin composites: ISO 4049 depth and microhardness of types of materials and shades. Oper Dent 2008;33:408-412.
20. DeWald JP, Ferracane JL. A comparison of four modes of evaluating depth of cure of light-activated composites. J Dent Res 1987;66:727-730.
21. Wang WJ, Grymak A, Waddell JN, Choi JJ. The effect of light curing intensity on bulk-fill composite resins: heat generation and chemomechanical properties. Biomater Investig Dent 2021;8:137-151.
22. Calheiros FC, Daronch M, Rueggeberg FA, Braga RR. Degree of conversion and mechanical properties of a Bis-GMA:TEGDMA composite as a function of the applied radiant exposure. J Biomed Mater Res B Appl Biomater 2008;84:503-509.
23. Mayworm CD, Camargo SS, Bastian FL. Influence of artificial saliva on abrasive wear and microhardness of dental composites filled with nanoparticles. J Dent 2008;36:703-710.
24. Say EC, Civelek A, Nobecourt A, Ersoy M, Guleryuz C. Wear and microhardness of different resin composite materials. Oper Dent 2003;28:628-634.
25. Watts DC, Amer OM, Combe EC. Surface hardness development in light-cured composites. Dent Mater 1987;3:265-269.
26. Rueggeberg FA, Ergle JW, Mettenburg DJ. Polymerization depths of contemporary light-curing units using microhardness. J Esthet Dent 2000;12:340-349.
27. Ferracane JL. Correlation between hardness and degree of conversion during the setting reaction of unfilled dental restorative resins. Dent Mater 1985;1:11-14.
28. Bouschlicher MR, Rueggeberg FA, Wilson BM. Correlation of bottom-to-top surface microhardness and conversion ratios for a variety of resin composite compositions. Oper Dent 2004;29:698-704.
29. Aravamudhan K, Rakowski D, Fan PL. Variation of depth of cure and intensity with distance using LED curing lights. Dent Mater 2006;22:988-994.

30. Yılmaz Atalı P, Doğu Kaya B, Manav Özen A, Tarçın B, Şenol AA, Tüter Bayraktar E, *et al*. Assessment of micro-hardness, degree of conversion, and flexural strength for single-shade universal resin composites. Polymers (Basel) 2022;14:4987.
31. Poggio C, Lombardini M, Gaviati S, Chiesa M. Evaluation of Vickers hardness and depth of cure of six composite resins photo-activated with different polymerization modes. J Conserv Dent 2012;15:237-241.
32. de Mendonça BC, Soto-Montero JR, de Castro EF, Kury M, Cavalli V, Rueggeberg FA, *et al*. Effect of extended light activation and increment thickness on physical properties of conventional and bulk-filled resin-based composites. Clin Oral Investig 2022;26:3141-3150.
33. Rodriguez A, Yaman P, Dennison J, Garcia D. Effect of light-curing exposure time, shade, and thickness on the depth of cure of bulk fill composites. Oper Dent 2017;42:505-513.


https://doi.org/10.5395/rde.2025.50.e39

RDE Restorative Dentistry & Endodontics

Research Article

eISSN 2234-7666
Restor Dent Endod. 2025 November;50(4):e40
https://doi.org/10.5395/rde.2025.50.e40

# Resolvin E1 incorporated carboxymethyl chitosan scaffold accelerates repair of dental pulp stem cells under inflammatory conditions: a laboratory investigation

**Hemalatha P Balasubramanian, Nandini Suresh*, Vishnupriya Koteeswaran, Velmurugan Natanasabapathy**

Department of Conservative Dentistry and Endodontics, Meenakshi Ammal Dental College and Hospital, Faculty of Dentistry, Meenakshi Academy of Higher Education and Research (MAHER), Maduravoyal, Chennai, Tamil Nadu, India

## ABSTRACT

**Objectives:** This study fabricated and characterized a resolvin E1 (RvE1)-loaded carboxymethyl chitosan (CMC) scaffold and determined its cytotoxicity and mineralization potential on inflamed human dental pulp stem cells (hDPSCs).

**Methods:** CMC scaffold incorporated with two concentrations of RvE1 (100 and 200 nM) was fabricated and characterized. The scaffolds' porosity, drug release kinetics, and degradation were assessed. The impact of RvE1 on inflamed hDPSCs proliferation, proinflammatory gene expression (tumor necrosis factor alpha [TNF-α]), alkaline phosphatase activity, and alizarin red S staining was evaluated.

**Results:** Scanning electron microscopy analysis demonstrated a highly porous interconnected microstructure. Release kinetics showed gradual RvE1 release peaking at day 14. Cumulative degradation of the CMC scaffold at 28 days was 57.35%. Inflamed hDPSCs exposed to 200 nM RvE1-CMC scaffold exhibited significantly improved viability compared to 100 nM. Both RvE1-CMC scaffolds significantly suppressed the expression of TNF-α at 7 days. Alkaline phosphatase activity was enhanced by both RvE1 concentrations on days 7 and 14. Alizarin red staining revealed superior mineralization potential of 200 nM RvE1 on days 14 and 21.

**Conclusions:** This study concludes 200 nM RvE1-CMC scaffold is a promising therapy for inflamed pulp conditions, enhancing cell proliferation and biomineralization potential in inflamed hDPSCs.

**Keywords:** Carboxymethyl chitosan; Dental pulp stem cells; Dentine regeneration; Pulp inflammation; Resolvin E1

**Received:** April 21, 2025 **Revised:** June 26, 2025 **Accepted:** July 14, 2025

**Citation**
Balasubramanian HP, Suresh N, Koteeswaran V, Natanasabapathy V. Resolvin E1 incorporated carboxymethyl chitosan scaffold accelerates repair of dental pulp stem cells under inflammatory conditions: a laboratory investigation. Restor Dent Endod 2025;50(4):e40.

***Correspondence to**
**Nandini Suresh, MDS**
Department of Conservative Dentistry and Endodontics, Meenakshi Ammal Dental College and Hospital, Faculty of Dentistry, Meenakshi Academy of Higher Education and Research (MAHER), Maduravoyal, Chennai, Tamil Nadu, India
Email: nandini_80@hotmail.com

Vishnupriya Koteeswaran's current affiliation: Private practition, Chennai, Tamil Nadu, India

## INTRODUCTION

Dental pulp, a mesenchymal soft connective tissue, triggers an immune response when exposed to stimuli such as dental caries and trauma [1] and demonstrates the ability to regulate pulp repair and regeneration by altering the immune response [2]. Macrophages are abundant in pulp and are drawn to the area of inflammation. M1 macrophages dominate the inflammatory response and M2 phenotype predominates when inflammation reduces [3]. The cessation of granulocyte recruitment along with macrophage differentiation at the site of tissue injury plays a crucial role in resolving inflammation and restoring tissue homeostasis [4]. Temporal resolution of pulpal inflammation by altering mediators such as transforming growth factor beta-1, interleukin-1, and tumor necrosis factor-alpha expression (TNF-α) plays a pivotal role in maintaining tissue homeostasis [1]. Currently, two therapeutic options are strategized for the repair/regeneration of inflamed pulp: (a) use of bioactive molecules that aid in sequestrated biomolecule release from dentin and (b) local drug delivery using bioactive molecules for repair and regeneration [5].

Specialized pro-resolving mediators (SPM) are derived enzymatically from polyunsaturated fatty acids (arachidonic acid and omega-3 fatty acids) and aid in arresting acute inflammation with their pro-resolving, anti-inflammatory, and anti-infective properties [6]. These advantages are considered for designing novel host-derived therapeutic strategies in clinical scenarios with inflammation. SPMs offer an advantage over corticosteroids, where the latter have been shown to inhibit the production of inflammatory mediators, enhance anti-inflammatory cytokine release, promote healing, but reduce host defense responses, hindering tissue repair [7,8].

Resolvin E1 (RvE1), a type of SPM with dual functions, is derived from the eicosapentaenoic acid pathway, inhibits transepithelial and transendothelial migration of neutrophils and stimulates phagocytosis of apoptotic neutrophils by the macrophages, and shows enhanced pulpal and periodontal repair [9,10]. Topical application of RvE1 on inflamed pulp tissue in rat models limited the inflammatory cell infiltration compared to that of ethanol or corticosteroid application [11]. Among the various concentrations tested, 100 nM of RVE1 (10, 100, and 200 nM) demonstrated an effective chemotactic effect on hDPSCs [12]. Additionally, 100 nM RvE1 incorporated into collagen sponges has been shown to reduce necrosis rates and promote pulpal repair and reparative dentin formation in rat models with non-inflamed pulp [12].

Currently, in literature, no established biomolecule delivery system exists for RvE1 in vital pulp therapy (VPT). Chitosan has gained attention as a drug delivery scaffold in dentistry [13,14]. However, modified chitosan, namely carboxymethyl chitosan (CMC), exhibits properties like calcium binding, high viscosity, and hydrodynamic volume [15]. It enhances wound healing by regulating transforming growth factor beta-1, interleukin-1, and TNF-α expression [16]. CMC, being a natural polymer, is used extensively in the field of regenerative medicine as a drug delivery scaffold due to its ability to support cell proliferation, its anti-inflammatory, anti-bacterial effect, and ability to be fabricated into various scaffold designs such as films, sponges, hydrogels, etc [17]. In a mouse air pouch inflammation model, combining resolvin D1 to chitosan scaffolds demonstrated a favorable healing response by modulating the inflammatory response and enhancing M2 polarization [18]. This type of combination can aid in the sustained release of the drug. Currently, no literature exists to assess the effect of RvE1 addition to the CMC scaffold on inflamed human dental pulp cells.

Various drug delivery systems for VPT have shown promising results in tests on mineralization potential of human dental pulp stem cells (hDPSCs); however, they were tested on normal cells and did not mimic the clinical scenario of inflamed pulp. The anti-inflammatory potential of these systems remains underexplored, leaving the effectiveness of RvE1 with a scaffold in dental pulp inflammation unclear. The null hypothesis is RvE1-loaded CMC scaffold has no significant effect on the viability, anti-inflammatory marker expression, and odontogenic differentiation capacity of lipopolysaccharide (LPS)-stimulated hDPSCs, compared to a CMC scaffold without RvE1.

The aim of this study is twofold: to fabricate and assess the characteristics of a CMC scaffold incorporated with RvE1, and to evaluate the role of RvE1-loaded CMC


https://doi.org/10.5395/rde.2025.50.e40

scaffold on the viability, expression of anti-inflammatory markers, and odontogenic differentiation ability of LPS-stimulated hDPSCs.

## METHODS

### Ethics approval

This study proposal was reviewed and approved by the Institutional Ethical Committee of Meenakshi Ammal Dental College and Hospital, Chennai, India (No. MADC/IEC-I/24/2022). Each participant provided written consent prior to their involvement in the research.

RvE1 was procured from Cayman Chemicals (Ann Arbor, MI, USA), CMC from Sigma-Aldrich (St. Louis, MO, USA), LPS from Sisco Research Laboratories (Maharashtra, India), and one-step qRT-PCR kit from DSS Takara Bio (New Delhi, India). Other chemicals were procured from HiMedia (Nashik, India) and Thermo Fisher Scientific Pvt, Ltd. (Mumbai, India).

### Fabrication of carboxymethyl chitosan scaffold

A porous scaffold was prepared by dissolving CMC powder with a degree of substitution of 0.7, a degree of deacetylation of 85%, and a molecular weight of 250,000 Da in 2% acetic acid solution and freeze-dried at –20°C for 24 hours, followed by lyophilization at –80°C for 72 hours. After processing in 1N NaOH and sterilization in ethanol series (25%–70%), the scaffolds were washed, lyophilized, and sterilized with ultraviolet for 6 hours.

### Incorporation of RvE1 in carboxymethyl chitosan scaffold

RvE1 was incorporated into sterile scaffolds using an embedding technique in a flow hood chamber to maintain a sterile environment. A solution of RvE1 in ethanol (water solubility: approximately 0.05 mg/mL at 25°C or phosphate-buffered saline [PBS] with pH 7.2), with concentrations of 100 nM and 200 nM RvE1, was prepared in PBS (pH 7.2). A volume of 100-µL PBS containing 100 nM and 200 nM RvE1 was added dropwise with a micropipette into the respective scaffolds. RvE1 incorporated CMC scaffolds ($CSR_{100}$ and $CSR_{200}$) were lyophilized again (–80°C for 24 hours). The control group was prepared by adding 100 µL of PBS and lyophilized ($CS_{PBS}$). All the prepared scaffolds were stored at –20°C until further use.

### Morphological characterization

#### 1. Porosity analysis

The microstructural analysis of samples of $CSR_{100}$, $CSR_{200}$, and $CS_{PBS}$ scaffolds was done using high-resolution scanning electron microscopy (HRSEM) (FEI Quanta FEG 200), operating at 5 kV up to ×500 magnification. The mean pore dimensions of the scaffolds were established through direct geometric examination of the HRSEM images.

### Physicochemical characterization

#### 1. Release kinetics of carboxymethyl chitosan scaffolds with RvE1

The drug release kinetics of RvE1 from the lyophilized porous CMC scaffolds ($CSR_{100}$ and $CSR_{200}$) were analysed using Ultraviolet Spectrophotometry at various time intervals up to 28 days (1st, 4th, 8th, 12th, 16th, 20th, 24th hour, and days 3, 7, 14, 21, 28). Prior to the *in vitro* release of RvE1 assessment, a linear calibration curve of standard solution was constructed by measuring the absorbance at λ = 272 nm of different concentrations (10–250 nM) of RvE1. The 100 nM and 200 nM RvE1-loaded scaffolds were immersed in 2 mL Dulbecco's PBS (DPBS) (pH 7.2, at 37°C), separately. At defined time intervals, 1 mL of solution was withdrawn from each sample and replaced with an equivalent volume of fresh PBS. RvE1 was detected at 272 nm. Absorbance values of test samples were compared against the calibration curve to quantify the cumulative release.

#### 2. *In vitro* biodegradation analysis

The sterile scaffolds were immersed in 2 mL of PBS with 10 mg/L of lysozyme (pH 6.24) and placed in an incubator at 37°C. The lysozyme was replenished every 3rd day. Controls were maintained in PBS without lysozyme. Scaffolds were removed at various time intervals up to 28 days (1, 3, 5, 7, 14, 21, and 28 days). The scaffolds were lyophilized and weighed to determine dry weight. Degradation extent was calculated using the formula:

$$Degradation\ \% = (W_i - W_f)/W_i \times 100$$

where, $W_i$ = initial dry weight, $W_f$ = final dry weight after

degradation.

### Human dental pulp stem cells isolation

Human dental pulp tissue was isolated from either normal impacted third mandibular molars or normal premolars extracted for orthodontic therapy from healthy patients (age, 14–20 years) with informed consent. Isolation of hDPSCs was done based on the methodology proposed in previous literature [19]. In brief, hDPSCs were isolated by the enzymatic digestion method. They were extracted from human pulp tissues through treatment with collagenase type I (3 mg/mL) and dispase (4 mg/mL) and then seeded into 10-cm culture plates at low density ($0.04 \times 10^5$/plate). Rapidly growing individual colonies were isolated and expanded with α-MEM supplemented with 10% fetal bovine serum, 100 μM L-ascorbic acid 2-phosphate, 2 mM L-glutamine, 100 U/mL penicillin, and 100 μg/mL streptomycin. The cultures were incubated at 37°C in a 5% $CO_2$ atmosphere. The medium was periodically changed every alternate day till the cells reached 80% confluency. A subculture was prepared with the aid of 0.2% trypsin/ethylenediaminetetraacetic acid and cells from passage 3 were phenotyped by flow cytometry for the following antibodies: anti-CD105-fluorescein isothiocyanate (FITC), anti-CD90-FITC, and anti-CD31-phycoerythrin were used in this study.

### Induction of pro-inflammatory conditions in human dental pulp stem cells using lipopolysaccharides

Cells were seeded at 60% to 80% confluency and cultured in α-MEM with or without LPS (*Escherichia coli*, 1 μg/mL) for 72 hours at 37°C with 5% $CO_2$ and the medium was replenished every day.

The categories of experiment conducted to assess the effect of the fabricated RvE1-loaded scaffolds on normal and LPS-treated hDPSCs are tabulated in Table 1. All the following experiments were performed in triplicate.

### Cell viability assay

The viability of hDPSCs was quantitatively evaluated by measuring the reduction of tetrazolium salts to colored formazan products [20]. About $5 \times 10^4$ cells were seeded onto the scaffold in 1 mL of cell medium and incubated at 37°C overnight to allow the cells to attach to the scaffold. At predetermined intervals of 7, 14 and 21 days, the culture medium was removed and 1,000 μL of 3-(4,5-dimethylthiazol-2-yl)-2,5-diphenyltetrazolium (MTT) solution (5 mg/mL) was added to the wells and cultured at 37°C under 5% $CO_2$ for 4 hours and 1,000 μL of dimethyl sulfoxide was added to each well to solubilize the crystals. Medium was changed every 2 days. Cell count was determined by measuring formazan absorbance at 570 nm using a microplate reader and visualized under an inverted microscope (×10 magnification).

### Cytokine gene expression

hDPSCs treated with LPS and RvE1-loaded CMC scaffold were subjected to RNA isolation to evaluate the expression of the pro-inflammatory cytokine TNF-α. Cell lysis was performed, and total RNA was extracted using Trizol reagent. It was then subjected to DNase treatment to remove any DNA contaminants. Agarose gel electrophoresis of RNA isolated from different groups is shown in Supplementary Figure 1. RNA quantification was carried out using a Nanodrop spectrophotometer and the extracted RNA was subjected to one-step qRT-PCR analysis to study the relative gene fold expression of TNF-α. The double Delta CT method was used for the calculation of the relative fold of expression for the gene of interest. *GAPDH* was used as the housekeeping gene (reference gene) and the normalization of data was done using the same. The primer sequences are listed

**Table 1.** Different study groups and abbreviations

| Group | Description | Abbreviation |
|---|---|---|
| Non-inflamed groups | $CS_{PBS}$ seeded with $5 \times 10^4$ hDPSCs | C-CS |
| Inflamed groups | $CS_{PBS}$ seeded with $5 \times 10^4$ LPS-treated hDPSCs | C-CSL |
| | $CSR_{100}$ seeded with $5 \times 10^4$ LPS-treated hDPSCs | 100R + CSL |
| | $CSR_{200}$ seeded with $5 \times 10^4$ LPS-treated hDPSCs | 200R + CSL |

hDPSC, human dental pulp stem cell; LPS, lipopolysaccharide; $CS_{PBS}$, CMC scaffoldpre-soaked with phosphate-buffered saline; $CSR_{100}$, CMC scaffold incorporated with 100-nM RvE1; $CSR_{200}$, CMC scaffold incorporated with 200-nM RvE1.


https://doi.org/10.5395/rde.2025.50.e40

**Table 2.** Specific primer sequences for quantitative reverse transcription polymerase chain reaction

| No. | Gene | Forward primer | Reverse primer |
|---|---|---|---|
| 1 | *GAPDH* | TGTTCGTCATGGGTGTGAAC | ATGGCATGGACTGTGGTCAT |
| 2 | *TNF-α* | TAGCCATGTTGTAGCAAACCC | TTATCTCTCAGCTCCACGCCA |

in Table 2.

### Alkaline phosphatase enzyme activity

Initially, $5 \times 10^4$ hDPSCs were seeded onto each scaffold in 24-well culture plates and cultured up to 21 days. Adherent cells were lysed using 500 μL of lysis buffer containing 0.1% Triton-X100 in alkaline phosphatase (ALP) assay buffer. After sonication for 5 minutes, samples were collected on days 7 and 14 post-odontogenic differentiation. Subsequently, the homogenized samples were centrifuged at 12,000 ×g for 20 minutes to obtain the enzyme extract. Protein concentration of the enzyme extract is given in Supplementary Table 1.

At 60% to 70% confluency, hDPSCs were induced to undergo odontoblastic differentiation upon exposure to odontogenic conditioned medium. To 960 μL of assay buffer, 20 μL of substrate (167 mM p-Nitrophenyl phosphate) was added and equilibrated at 37°C for 1 minute. Later, 20 μL of enzyme extract was added and mixed. Absorbance was measured at 405 nm using a microplate reader.

### Alizarin red S staining

Following odontoblastic conversion as described previously, cells were fixed with 4% paraformaldehyde for 20 minutes at room temperature, rinsed with DPBS, stained with 1% alizarin red for 30 minutes at room temperature, rinsed with DPBS, and visualized under an inverted microscope (×20). For quantification of alizarin red staining, the stained cells were incubated with 10% acetic acid for 30 minutes, followed by centrifugation. The resulting supernatant was collected for further analysis.

### Statistical analysis

Data were entered in an Excel spreadsheet (Microsoft 365; Microsoft Corp., Redmond, WA, USA). Normality tests were conducted using the Shapiro-Wilk test, indicating normal distribution. Independent sample t-tests compared degradation analysis and release kinetics between groups, while paired t-tests assessed intragroup degradation. Tukey test *post hoc* was used for multiple internal comparisons MTT assay, ALP activity, and alizarin red staining. One-way analysis of variance was used to assess gene expression. Significance was set at 5% and performed using IBM SPSS version 24 (IBM Corp, Armonk, NY, USA).

## RESULTS

### Morphological and physicochemical properties of the scaffolds

The microstructural analysis of scaffolds exhibited a highly porous, homogeneous structure characterized by interconnected pores. The mean pore diameters of $CS_{PBS}$, $CSR_{100}$, and $CSR_{200}$ are 91.25, 99.05, and 122.75 μm, respectively (Figure 1A–C). Degradation analysis showed that 44.61% of scaffold degraded in 3 weeks when exposed to lysozyme (Figure 1D). The release profile of RvE1 demonstrated an initial gradual release of 42.95% and 50.92% from $CSR_{100}$ and $CSR_{200}$ scaffolds, respectively, by the end of the first week. This was followed by a rapid release phase, reaching 96.5% and 88.67% for $CSR_{100}$ and $CSR_{200}$, respectively, by day 14. Subsequently, the release plateaued, indicating a sustained but minimal release thereafter (Figure 1F).

### Phenotype of human dental pulp stem cells

hDPSCs presented a typical homogeneous spindle morphology. Flow cytometry analysis confirmed that the hDPSCs used in this experiment were positive for mesenchymal cell surface markers CD105 (98.4%) (Figure 2B) and CD90 (96.9%) (Figure 2C), and negative for hematopoietic marker CD31 (0.385%) (Figure 2E).

### The role of RvE1-loaded carboxymethyl chitosan on the viability and proliferation of human dental pulp stem cells

Loading of CMC with RvE1 at concentrations of 100 nM and 200 nM demonstrated biocompatibility, with no evidence of cytotoxicity and a sustained increase in cell proliferation up to 21 days. The cultured cells exhibited a homogeneous distribution and maintained a characteristic spindle-shaped morphology. Stimula-

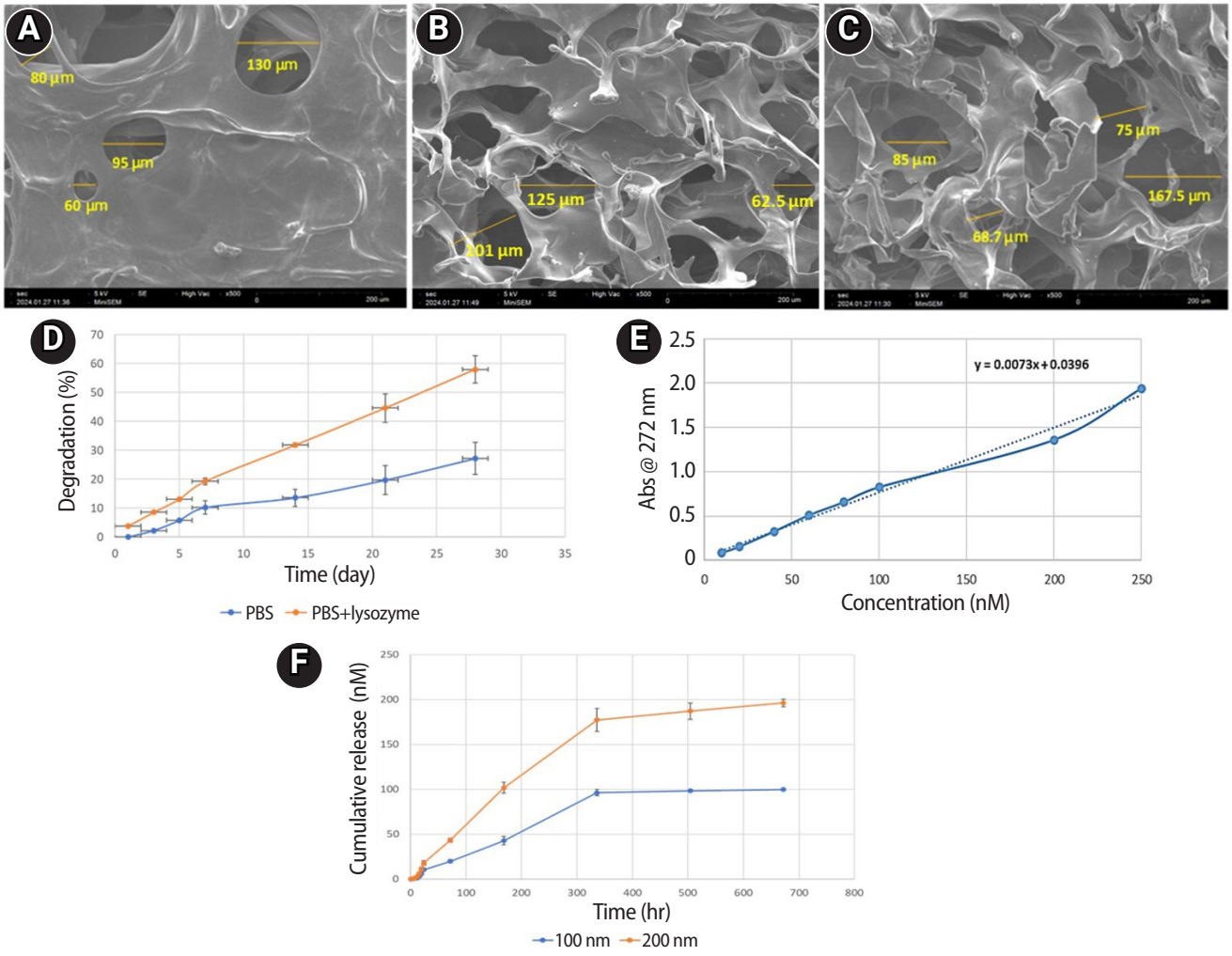


**Figure 1.** Physicochemical properties of the scaffolds. (A–C) Scaffold morphology observed under scanning electron microscopy showing a porous structure: (A) $CS_{PBS}$, (B) $CSR_{100}$, and (C) $CSR_{200}$. (D) Scaffold degradation (%) in the presence of PBS and PBS with lysozyme. (E, F) Release kinetics of resolvin E1 (RvE1): (E) standard curve showing absorbance of different RvE1 concentrations under ultraviolet spectroscopy; (F) cumulative release profile of RvE1 (nM) from $CSR_{100}$ and $CSR_{200}$ scaffolds. PBS, phosphate-buffered saline.

tion of inflammation with LPS resulted in a reduction in the viability of hDPSCs at all assessed time points. Treatment with RvE1 (100R + CSL and 200R + CSL) has shown a significant increase in cell proliferation at all time intervals compared to the inflamed C-CSL group ($p < 0.05$) and there was no significant difference ($p > 0.05$) between 100R + CSL and 200R+CSL groups in all time intervals (Figures 3 and 4A).

### The role of RvE1-loaded carboxymethyl chitosan on TNF-α expression

Treatment of hDPSCs with LPS increased the gene expression of TNF-α. Both (100 nM and 200 nM) concentrations of RvE1-loaded CMC scaffold significantly reduced the expression of TNF-α at 7 days, and 200R + CSL showed significantly lower expression of TNF-α than 100R + CSL group ($p < 0.05$) (Figure 4B).

### The role of RvE1-loaded carboxymethyl chitosan on the biomineralization potential in lipopolysaccharide-treated human dental pulp stem cells

ALP analysis and alizarin red S staining were performed to investigate the effect of RvE1-loaded CMC on the early and late biomineralization capability of LPS-stimulated hDPSCs.


https://doi.org/10.5395/rde.2025.50.e40

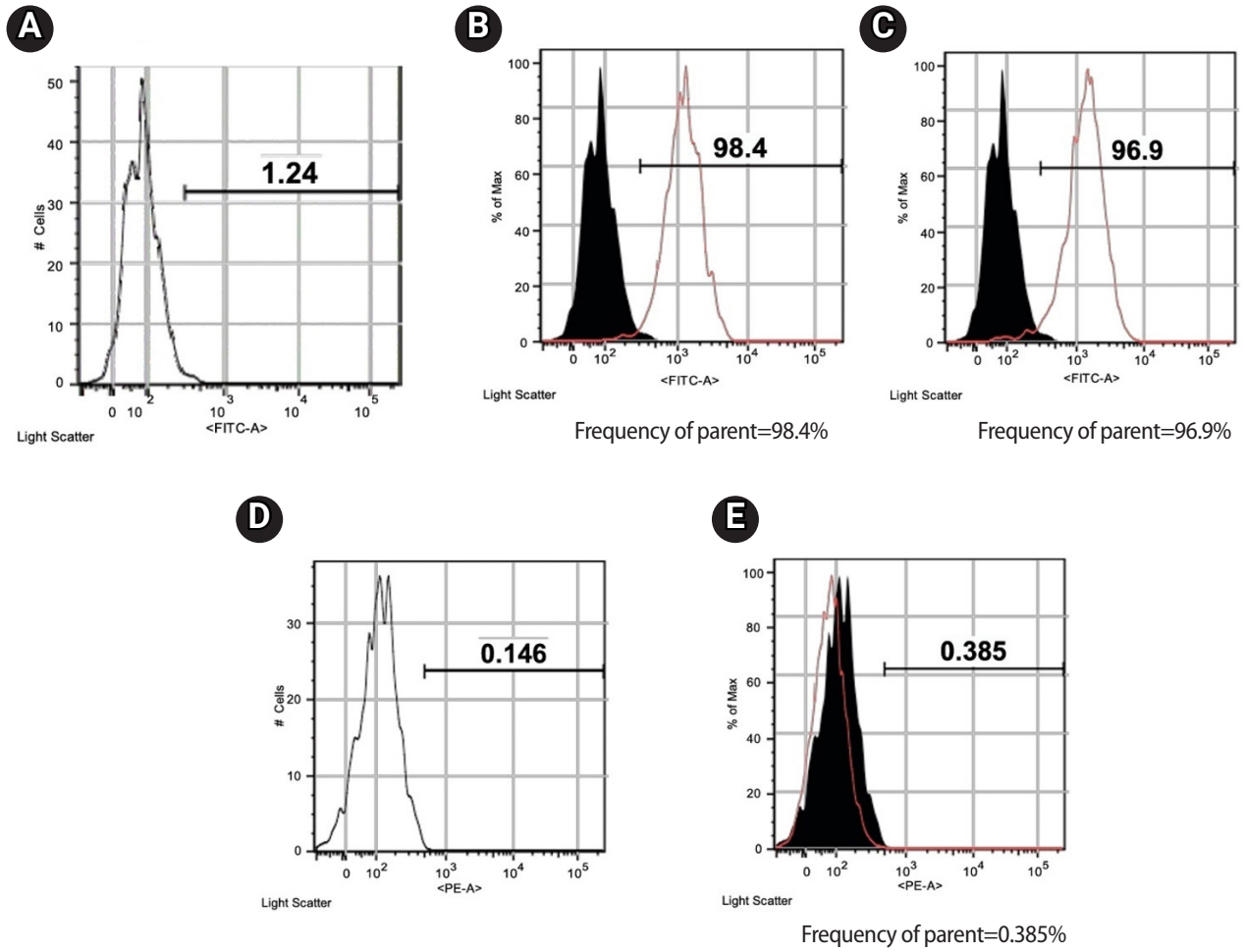


**Figure 2.** Flow cytometric analysis of mesenchymal stem antigens in human dental pulp stem cells. (A) Isotype control for FITC staining showing minimal expression; (B) CD105 expression; (C) CD90 expression; (D) Isotype control for PE staining showing minimal expression; (E) CD31 expression (negative). FITC, fluorescein isothiocyanate; PE, phycoerythrin.

**1. Alkaline phosphatase activity**

LPS-inflamed hDPSCs exhibited significantly reduced ALP activity compared to all other groups. Both 100 nM and 200 nM RvE1-loaded CMC scaffolds significantly enhanced ALP activity ($p < 0.05$). Although the 100R + CSL group showed higher ALP levels than the 200R + CSL group on days 7 and 14, the difference between the two RvE1 concentrations was not statistically significant (Figure 4C).

**2. Alizarin red S staining**

Alizarin red quantification showed that the non-inflamed group showed the highest biomineralization potential on day 21. Inducing inflammation with LPS has been shown to reduce the biomineralization ability of hDPSCs less than the non-inflamed group. RvE1-loaded CMC scaffold significantly enhanced the biomineralization potential in both concentrations on days 14 and 21 compared to the inflamed group. However, the 200 nM RvE1-loaded CMC scaffold had significantly higher biomineralization potential than the 100 nM RvE1 on days 14 and 21. Biomineralized nodules were found to be thicker and denser on treatment with 200 nM RvE1 than 100 nM on day 21 (Figure 4D–H).

## DISCUSSION

Vital pulp management aims to deliver therapeutic options for the resolution of inflammation in pulp and create a conducive environment for repair. RvE1 in-

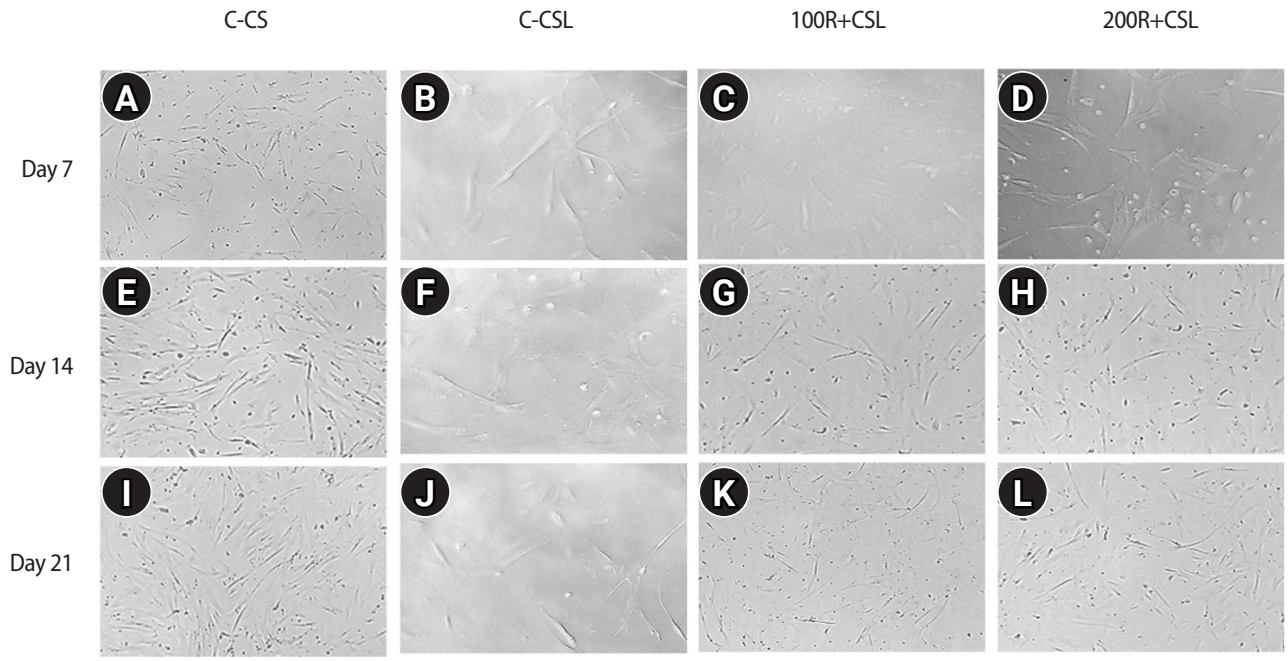


**Figure 3.** Representative inverted microscopic views (×10) of LPS- and non-LPS-treated hDPSCs cultured with CMC scaffolds loaded with or without 100 and 200 nM RvE1. (A–D) Day 7 cell morphology of LPS- and non-LPS-treated hDPSCs cultured with CMC scaffolds loaded with or without 100 and 200 nM RvE1. (E–H) Day 14 cell morphology of LPS- and non-LPS-treated hDPSCs cultured with CMC scaffolds loaded with or without 100 and 200 nM RvE1. (I–L) Day 21 cell morphology of LPS- and non-LPS-treated hDPSCs cultured with CMC scaffolds loaded with or without 100 and 200 nM RvE1. LPS, lipopolysaccharide; hDPSCs, human dental pulp stem cells; CMC, carboxymethyl chitosan; RvE1, resolvin E1. Abbreviations of experimental groups (C-CS, C-CSL, 100R + CSL, and 200R + CSL) are defined in Table 1.

teracts with ChemR23 receptors and decreases NF-κB activation in polymorphonuclear neutrophils, thereby reducing inflammation [21,22]. ChemR23 showed significant expression on hDPSCs, suggesting a potential therapeutic role [12].

A concentration of 100 nM of RvE1 was selected based on evidence from a previous study [12] and double the concentration was included for comparison in the current study. The scaffold's degradation rate and release of biomolecules over time are influenced by its degree of crosslinking and porosity [23]. In this study, SEM images illustrated a porous structure, which will provide more active sites for lysozyme to act upon, leading to adequate degradation and more efficient drug release. All three CMC scaffolds had a mean pore size in the range of 61.7–174 μm, which is comparable to that of previous studies (60–180 μm) [24,25]. Scaffolds with larger mean pore sizes of 65 and 145 μm demonstrated enhanced hDPSCs ingrowth and proliferation [25].

In this study, maximum degradation and drug release occurred at 14 days, and 43% of the scaffold degraded in 21 days. This observation is similar to previous literature, where 40% of the scaffold degraded at 21 days [26]. The initial slow drug release in this study could be attributed to the embedding technique followed by lyophilization which extends the release of RvE1 and negates its rapid degradation [27] and increases the bioavailability over a prolonged time. In a previous study, a delayed and extended release over a period of 3 days was observed in the lyophilized chitosan + RvD1 scaffold compared to the non-lyophilized counterparts [18].

LPS levels in infected root canals are observed in the range of 0.001–2 μg/mL [28,29] and inflamed pulpal conditions were simulated with 1 μg/mL LPS [30]. However, in previous studies, stimulation with LPS did not significantly affect the proliferation [30], but in contrast, this study showed a 40% survival rate for LPS-treated hDPSCs at 21 days. This can be attributed to the exposure time of up to 7 days in previous literature and up to 21 days in this study.


https://doi.org/10.5395/rde.2025.50.e40

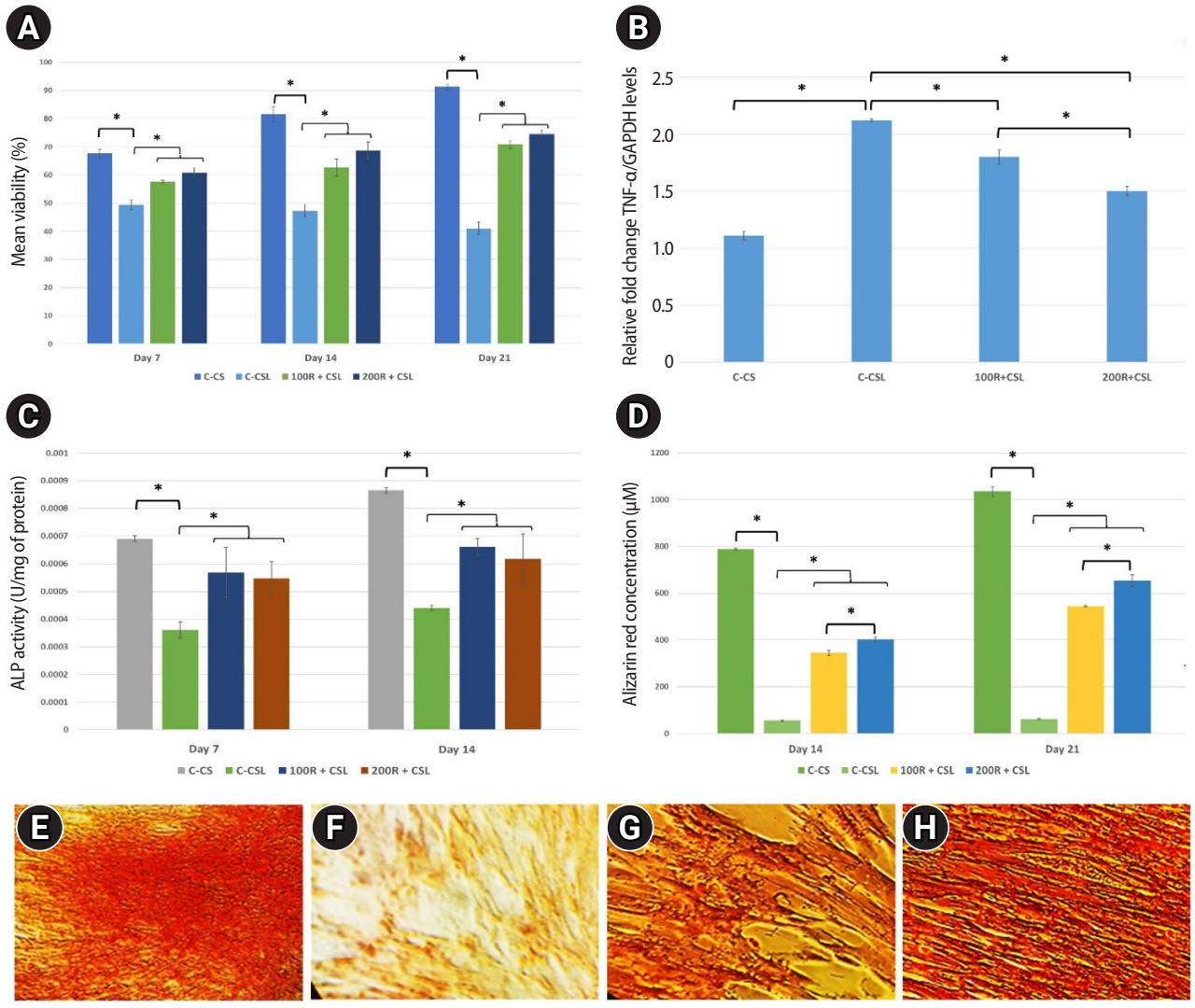


**Figure 4.** Effects of RvE1 on LPS- and non-LPS-treated hDPSCs. (A) Mean cell viability (%) of LPS- and non-LPS-treated hDPSCs cultured with CMC scaffolds loaded with or without 100 and 200 nM RvE1 at days 7, 14, and 21. (B) Expression of the pro-inflammatory cytokine TNF-α in LPS- and non-LPS-treated hDPSCs cultured with CMC scaffolds loaded with or without 100 and 200 nM RvE1 at day 7. (C) Mean ALP activity (units/mg protein) of LPS- and non-LPS-treated hDPSCs cultured with CMC scaffolds loaded with or without 100 and 200 nM RvE1 at days 7 and 14. (D) Mean alizarin red staining quantification (μM) of LPS- and non-LPS-treated hDPSCs cultured with CMC scaffolds loaded with or without 100 and 200 nM RvE1 at days 14 and 21. (E–H) Representative alizarin red staining images (×20) at day 21: (E) C-CS, (F) C-CSL, (G) 100R + CSL, and (H) 200R + CSL. RvE1, resolvin E1; LPS, lipopolysaccharide; hDPSC, human dental pulp stem cell; CMC, carboxymethyl chitosan; TNF-α, tumor necrosis factor alpha; ALP, alkaline phosphatase. hDPSC, human dental pulp stem cell; TNF-α, tumor necrosis factor alpha; ALP, alkaline phosphatase. Abbreviations of experimental groups (C-CS, C-CSL, 100R + CSL, and 200R + CSL) are defined in Table 1. *$p < 0.05$, significant difference between the groups.

The CMC scaffold with 100 nM and 200 nM RvE1 showed biocompatibility and an increase in hDPSCs viability up to 21 days. A previous study demonstrated that direct application of 100 nM RvE1 on hDPSCs exhibited greater compatibility compared to 200 nM [12]. In contrast, this study showed 200 nM to be more compatible (no significant difference from 100 nM). This could be attributed to the scaffold-based delivery of the drug to the cells in this study.

Treatment with RvE1-loaded CMC scaffolds led to a marked downregulation of TNF-α expression in a dose-dependent manner, indicating the anti-inflam-

matory efficacy of the bioactive scaffold system. TNF-α is a key pro-inflammatory cytokine that plays a pivotal role in initiating and orchestrating immune responses [31,32]. It induces the production of other cytokines, activates and upregulates adhesion molecules, and stimulates cellular proliferation [31,32]. By coordinating the early host response to tissue injury, TNF-α serves a critical regulatory role in the pathogenesis of inflammatory diseases and serves as a reliable and sensitive biomarker for assessing the severity and resolution of pulpal inflammation [31,32].

hDPSCs treatment with LPS reduced ALP activity, while co-treatment with RvE1-loaded CMC scaffold significantly improved it. On days 7 and 14, 100R + CSL and 200R + CSL showed similar ALP activity. RvE1 enhanced ALP activity by 1.5 times than inflamed hDPSCs, which was consistent with previous findings [12].

Alizarin red staining results showed that on days 14 and 21, the 200R+CSL group exhibited 7- and 10-times higher mineralization compared to the inflamed hDPSCs. Qualitative analysis revealed denser and larger mineralization nodules at 21 days, indicating enhanced mineralization. These results suggest the potential of the RvE1-CMC scaffold in promoting odontoblast-like differentiation of hDPSCs, with varying effects observed between different concentrations and time points, thus enhancing the odontogenic differentiation. This synergism between RvE1 and CMC could be attributed to the activation of the ChemR23 signalling pathway by RvE1 [21] as well as the biomimetic mineralization ability of CMC [33]. ChemR23 is expressed in ameloblasts, odontoblasts, and osteoblasts [34], and the Chemerin/ChemR23 signalling pathway is known to regulate the differentiation of ameloblasts and odontoblasts [34]. RvE1 directly affects osteoblasts, reducing RANKL (receptor activator of nuclear factor κB ligand) levels, which are elevated during inflammatory conditions, and increasing osteoprotegerin production [35]. Furthermore, CMC exhibits enhanced physicochemical properties, including strong calcium-chelating capacity and the ability to induce biomimetic mineralization [15,33], and has shown synergistic mineralization effect when combined with nanohydroxyapatite [36,37].

The healing process post-VPT comprises four stages: exudative (1–5 days), proliferative (3–7 days), osteodentin formative (5–14 days), and tubular dentin formative (>14 days) [38]. Macrophages are abundant in pulp, especially in the first 5–7 days of inflammation [39]. The increased RvE1 release at 7–14 days, accompanied by TNF-α suppression, can be advantageous by enhancing (a) macrophage polarization from M1 to M2 and (b) odontogenic differentiation during the odontogenic formative stage. This study suggests 200 nM RvE1 with a CMC scaffold as a potential clinical drug delivery system to be studied further.

The strength of this study is inducing inflammation in hDPSCs mimicking inflamed clinical conditions. The future research will be focused on assessing the other inflammatory and biomineralization markers for dentin and translating them into animal studies.

## CONCLUSIONS

Within the limitations of this study, the RvE1-loaded CMC scaffold was not toxic to the inflamed hDPSCs and 200 nM RvE1 has superior cell proliferation ability and biomineralization capacity of inflamed hDPSCs. This scaffold holds promise as a novel therapeutic strategy for alleviating pulp inflammation and promoting dentin-pulp regeneration.

### CONFLICT OF INTEREST

No potential conflict of interest relevant to this article was reported.

### FUNDING/SUPPORT

The authors have no financial relationships relevant to this article to disclose.

### ACKNOWLEDGMENTS

The authors would like to thank Mr. Prashanth K K and his team from Simbioen Labs (Chennai, India) for helping us execute this study and their meticulous assistance. We wish to inform you that this study was previously presented at the 22nd European Society of Endodontology Paris Conference, 2025. Furthermore, the conference abstract will be published in the International Endodontic Journal. This disclosure is provided to ensure transparency and proper acknowledgment of prior dissemination.

### AUTHOR CONTRIBUTIONS

Conceptualization, Investigation: Suresh N, Balasubramanian HP, Koteeswaran V. Data curation, Formal analysis, Methodol-


https://doi.org/10.5395/rde.2025.50.e40

ogy: Balasubramanian HP, Suresh N. Funding acquisition, Resources, Visualization: Balasubramanian HP. Project administration, Software: all authors. Supervision, Validation: Suresh N, Koteeswaran V, Natanasabapathy V. Writing - original draft: Balasubramanian HP. Writing - review & editing: Suresh N, Koteeswaran V, Natanasabapathy V. All authors read and approved the final manuscript.

## DATA SHARING STATEMENT

The datasets are not publicly available but are available from the corresponding author upon reasonable request.

## SUPPLEMENTARY MATERIALS

**Supplementary Figure 1.** Agarose gel electrophoresis of RNA isolated from different groups
**Supplementary Table 1.** Protein concentration of enzyme extract determined by Lowry's method

## REFERENCES


1. Galler KM, Weber M, Korkmaz Y, Widbiller M, Feuerer M. Inflammatory response mechanisms of the dentine-pulp complex and the periapical tissues. Int J Mol Sci 2021;22:1480.
2. Cooper PR, Holder MJ, Smith AJ. Inflammation and regeneration in the dentin-pulp complex: a double-edged sword. J Endod 2014;40:S46-S51.
3. Locati M, Mantovani A, Sica A. Macrophage activation and polarization as an adaptive component of innate immunity. Adv Immunol 2013;120:163-184.
4. Campbell EL, Louis NA, Tomassetti SE, Canny GO, Arita M, Serhan CN, *et al.* Resolvin E1 promotes mucosal surface clearance of neutrophils: a new paradigm for inflammatory resolution. FASEB J 2007;21:3162-3170.
5. Komabayashi T, Zhu Q, Eberhart R, Imai Y. Current status of direct pulp-capping materials for permanent teeth. Dent Mater J 2016;35:1-12.
6. Serhan CN. Pro-resolving lipid mediators are leads for resolution physiology. Nature 2014;510:92-101.
7. Tsianakas A, Varga G, Barczyk K, Bode G, Nippe N, Kran N, *et al.* Induction of an anti-inflammatory human monocyte subtype is a unique property of glucocorticoids, but can be modified by IL-6 and IL-10. Immunobiology 2012;217:329-335.
8. Koedam JA, Smink JJ, van Buul-Offers SC. Glucocorticoids inhibit vascular endothelial growth factor expression in growth plate chondrocytes. Mol Cell Endocrinol 2002;197:35-44.
9. Serhan CN, Savill J. Resolution of inflammation: the beginning programs the end. Nat Immunol 2005;6:1191-1197.
10. Balta MG, Loos BG, Nicu EA. Emerging concepts in the resolution of periodontal inflammation: a role for resolvin E1. Front Immunol 2017;8:1682.
11. Dondoni L, Scarparo RK, Kantarci A, Van Dyke TE, Figueiredo JA, Batista EL. Effect of the pro-resolution lipid mediator resolvin E1 (RvE1) on pulp tissues exposed to the oral environment. Int Endod J 2014;47:827-834.
12. Chen J, Xu H, Xia K, Cheng S, Zhang Q. Resolvin E1 accelerates pulp repair by regulating inflammation and stimulating dentin regeneration in dental pulp stem cells. Stem Cell Res Ther 2021;12:75.
13. Leonor IB, Baran ET, Kawashita M, Reis RL, Kokubo T, Nakamura T. Growth of a bonelike apatite on chitosan microparticles after a calcium silicate treatment. Acta Biomater 2008;4:1349-1359.
14. Pighinelli L, Kucharska M. Chitosan-hydroxyapatite composites. Carbohydr Polym 2013;93:256-262.
15. Chen XG, Park HJ. Chemical characteristics of O-carboxymethyl chitosans related to the preparation conditions. Carbohydr Polym 2003;53:355-359.
16. Peng S, Liu W, Han B, Chang J, Li M, Zhi X. Effects of carboxymethyl-chitosan on wound healing in vivo and in vitro. J Ocean Univ China 2011;10:369-378.
17. Fonseca-Santos B, Chorilli M. An overview of carboxymethyl derivatives of chitosan: their use as biomaterials and drug delivery systems. Mater Sci Eng C Mater Biol Appl 2017;77:1349-1362.
18. Vasconcelos DP, Costa M, Amaral IF, Barbosa MA, Águas AP, Barbosa JN. Development of an immunomodulatory biomaterial: using resolvin D1 to modulate inflammation. Biomaterials 2015;53:566-573.
19. Perry BC, Zhou D, Wu X, Yang FC, Byers MA, Chu TM, *et al.* Collection, cryopreservation, and characterization of human dental pulp-derived mesenchymal stem cells for banking and clinical use. Tissue Eng Part C Methods 2008;14:149-156.
20. Mosmann T. Rapid colorimetric assay for cellular growth and survival: application to proliferation and cytotoxicity assays. J Immunol Methods 1983;65:55-63.
21. Arita M, Ohira T, Sun YP, Elangovan S, Chiang N, Serhan CN. Resolvin E1 selectively interacts with leukotriene B4 receptor BLT1 and ChemR23 to regulate inflammation. J Immunol 2007;178:3912-3917.
22. Samson M, Edinger AL, Stordeur P, Rucker J, Verhasselt V, Sharron M, *et al.* ChemR23, a putative chemoattractant re-

ceptor, is expressed in monocyte-derived dendritic cells and macrophages and is a coreceptor for SIV and some primary HIV-1 strains. Eur J Immunol 1998;28:1689-1700.

23. Kim H, Kim HW, Suh H. Sustained release of ascorbate-2-phosphate and dexamethasone from porous PLGA scaffolds for bone tissue engineering using mesenchymal stem cells. Biomaterials 2003;24:4671-4679.
24. Baskar K, Saravana Karthikeyan B, Gurucharan I, Mahalaxmi S, Rajkumar G, Dhivya V, *et al*. Eggshell derived nano-hydroxyapatite incorporated carboxymethyl chitosan scaffold for dentine regeneration: a laboratory investigation. Int Endod J 2022;55:89-102.
25. Zhang Q, Yuan C, Liu L, Wen S, Wang X. Effect of 3-dimensional collagen fibrous scaffolds with different pore sizes on pulp regeneration. J Endod 2022;48:1493-1501.
26. Bellamy C, Shrestha S, Torneck C, Kishen A. Effects of a bioactive scaffold containing a sustained transforming growth factor-β1-releasing nanoparticle system on the migration and differentiation of stem cells from the apical papilla. J Endod 2016;42:1385-1392.
27. Mitchell S, Thomas G, Harvey K, Cottell D, Reville K, Berlasconi G, *et al*. Lipoxins, aspirin-triggered epi-lipoxins, lipoxin stable analogues, and the resolution of inflammation: stimulation of macrophage phagocytosis of apoptotic neutrophils in vivo. J Am Soc Nephrol 2002;13:2497-2507.
28. Jacinto RC, Gomes BP, Shah HN, Ferraz CC, Zaia AA, Souza-Filho FJ. Quantification of endotoxins in necrotic root canals from symptomatic and asymptomatic teeth. J Med Microbiol 2005;54:777-783.
29. Martinho FC, Chiesa WM, Zaia AA, Ferraz CC, Almeida JF, Souza-Filho FJ, *et al*. Comparison of endotoxin levels in previous studies on primary endodontic infections. J Endod 2011;37:163-167.
30. Xu F, Qiao L, Zhao Y, Chen W, Hong S, Pan J, *et al*. The potential application of concentrated growth factor in pulp regeneration: an in vitro and in vivo study. Stem Cell Res Ther 2019;10:134.
31. Elsalhy M, Azizieh F, Raghupathy R. Cytokines as diagnostic markers of pulpal inflammation. Int Endod J 2013;46:573-580.
32. Hehlgans T, Pfeffer K. The intriguing biology of the tumour necrosis factor/tumour necrosis factor receptor superfamily: players, rules and the games. Immunology 2005;115:1-20.
33. Wang R, Guo J, Lin X, Chen S, Mai S. Influence of molecular weight and concentration of carboxymethyl chitosan on biomimetic mineralization of collagen. RSC Adv 2020;10:12970-12981.
34. Ohira T, Spear D, Azimi N, Andreeva V, Yelick PC. Chemerin-ChemR23 signaling in tooth development. J Dent Res 2012;91:1147-1153.
35. El Kholy K, Freire M, Chen T, Van Dyke TE. Resolvin E1 promotes bone preservation under inflammatory conditions. Front Immunol 2018;9:1300.
36. Saravana Karthikeyan B, Madhubala MM, Rajkumar G, Dhivya V, Kishen A, Srinivasan N, *et al*. Physico-chemical and biological characterization of synthetic and eggshell derived nanohydroxyapatite/carboxymethyl chitosan composites for pulp-dentin tissue engineering. Int J Biol Macromol 2024;271:132620.
37. Gurucharan I, Saravana Karthikeyan B, Mahalaxmi S, Baskar K, Rajkumar G, Dhivya V, *et al*. Characterization of nano-hydroxyapatite incorporated carboxymethyl chitosan composite on human dental pulp stem cells. Int Endod J 2023;56:486-501.
38. Yamamura T. Differentiation of pulpal cells and inductive influences of various matrices with reference to pulpal wound healing. J Dent Res 1985;64 Spec No:530-540.
39. Mjör IA, Dahl E, Cox CF. Healing of pulp exposures: an ultrastructural study. J Oral Pathol Med 1991;20:496-501.


https://doi.org/10.5395/rde.2025.50.e40

RDE Restorative Dentistry & Endodontics

Research Article

eISSN 2234-7666
Restor Dent Endod. 2025 November;50(4):e41
https://doi.org/10.5395/rde.2025.50.e41

# Effect of moisture and pH on setting time and microhardness of three premixed calcium silicate-based root canal sealers: an *in vitro* experimental study

**Sooyoun Kim***

Department of Conservative Dentistry, KyungHee University Dental Hospital at Gangdong, Seoul, Korea

## ABSTRACT

**Objectives:** The study aimed to investigate how environmental conditions impact the setting time and microhardness of premixed calcium silicate-based sealers.

**Methods:** The setting time and microhardness of three sealers (Endoseal MTA [MARUCHI], One-Fil [MEDICLUS], and Well-Root ST [VERICOM]) were evaluated under four environmental conditions: unsoaked, distilled water-soaked, phosphate-buffered saline-soaked, and pH 5-soaked gypsum molds ($n$ = 12/group/condition). The setting time was measured with Gilmore needles, and microhardness was assessed using a Vickers tester after 3 days. Welch's analysis of variance and Games-Howell *post hoc* tests were used for statistical analysis.

**Results:** The sealer type and environmental conditions significantly influenced setting time and microhardness ($p$ < 0.001). The initial and final setting times were the shortest in the unsoaked samples. For Endoseal MTA and One-Fil, the unsoaked condition exhibited significantly shorter setting times than the soaked conditions. Well-Root ST exhibited significantly longer setting times in acidic conditions. Surface microhardness was highest in the unsoaked group ($p$ < 0.001). Among the soaked groups, the phosphate-buffered saline-soaked group had the lowest hardness for Endoseal MTA, whereas the pH 5-soaked group exhibited the lowest hardness for One-Fil and Well-Root ST. Endoseal MTA consistently demonstrated a lower microhardness than the other sealers ($p$ < 0.001).

**Conclusions:** Moisture, pH, and solution chemistry influenced the setting time and microhardness of premixed calcium silicate sealers. Although acidic conditions generally prolong the setting time and reduce hardness, the effects vary based on the sealers used and the setting environment.

**Keywords:** Calcium silicate; Dental cements; Hardness; Hydrogen-ion concentration; Humidity

**Received:** May 30, 2025 **Revised:** August 5, 2025 **Accepted:** September 3, 2025

**Citation**
Kim S. Effect of moisture and pH on setting time and microhardness of three premixed calcium silicate-based root canal sealers: an *in vitro* experimental study. Restor Dent Endod 2025;50(4):e41.

***Correspondence to**
**Sooyoun KIM, DDS, MS**
Department of Conservative Dentistry, KyungHee University Dental Hospital at Gangdong, 892 Dongnam-ro, Gangdong-gu, Seoul 05278, Korea
Email: sydent99@gmail.com

## INTRODUCTION

The microbiological objectives of endodontic treatment include eliminating bacteria from the root canal system and sealing all the entry and exit points. Antimicrobial interventions, such as chemomechanical procedures and intracanal medications, ensure bacterial elimination, whereas root canal obturation primarily accomplishes a hermetic seal [1]. Endodontic sealers encapsulate residual bacteria by sealing the dentinal tubules, thus preventing reinfection of the root canal [2]. Commonly used sealers include zinc oxide-eugenol, calcium hydroxide, glass ionomers, resin-based epoxy resins, methacrylate resin, and calcium silicate-based sealers (CSBSs) [3]. CSBSs are typically formulated using synthetic calcium silicate, Portland cement, or mineral trioxide aggregates (MTA) [4].

MTA, such as ProRoot MTA (Dentsply, Tulsa, OK, USA), a type of calcium silicate cement, is recognized for its favorable clinical outcomes. Initially developed as a root-end filling material, MTA has been applied in pulp capping, pulpotomy, apexogenesis, apical barrier formation in teeth with open apices, root perforation repairs, and root canal filling. The effectiveness of MTA has been ascribed to its superior sealing ability, antibacterial properties, and biocompatibility. It exhibits high pH, prolonged setting time, and low compressive strength [5,6]. Following the successful outcomes attributed to the use of MTA, calcium silicate-based materials are increasingly being used as sealers in root canal procedures. Unlike conventional sealers, CSBSs are hydraulic and hygroscopic, and require water to initiate a distinctive setting process [4]. Premixed and injectable sealers are considered user-friendly; they remain unset in syringes and undergo setting reactions only upon exposure to aqueous environments [7].

The physical properties of sealers, including setting time, flow, radiopacity, solubility, dimensional stability, and pH change, have been evaluated in previous studies [8,9]. Variations in the setting times were reported and were influenced by the study design. High pH and flowability have been observed, facilitating effective sealer distribution within root canal anatomical variants [4]. Calcium silicate-based materials are recognized for their exceptional biocompatibility, bioactive properties, antibacterial effects, and low solubility, with excellent sealing and setting capabilities in humid environments [10,11]. Environmental conditions can also influence these properties. A significant delay in the setting time has been noted in the absence of sufficient moisture [12,13]. Sealers rely on moisture within the dentinal tubules, which varies in quantity, to initiate and complete the setting reaction [7]. An unset or partially set sealer may permit rapid penetration of irritants, such as bacteria or bacterial byproducts, following obturation [2].

During canal obturation, sealers are exposed to fluids near the apex, where adjacent tissues may exhibit normal or acidic pH owing to infection or inflammation [14]. In other studies, exposure to an acidic environment reduced the microhardness of MTA and MTA-like materials [15]. Moreover, CSBS exhibits a lower microhardness when exposed to both acidic and phosphate-buffered saline (PBS) conditions, with acidic conditions having a more pronounced effect [16].

According to the ISO 6876/2012 standards, a dental plaster mold with a cavity of 1 mm in height and 10 mm in diameter is recommended for materials requiring moisture for the setting reaction. Some studies have used dental plaster molds; however, most of these studies focused primarily on humid environments [12,17,18] In this study, gypsum-molded specimens were exposed to PBS, which simulates the ionic composition of tissue fluids by providing phosphate ions and maintaining a stable, near-neutral pH through its buffering capacity, as well as to an acidic solution at pH 5 (hydrochloric acid), representing the chemical environments of healthy and inflamed periapical tissues, respectively. These varying conditions are expected to distinctly affect the setting behavior and properties of CSBSs.

This study aimed to evaluate the effects of environmental conditions on the initial and final setting times and the microhardness of three premixed calcium silicate-based root canal sealers. The null hypotheses were as follows: (i) No differences exist in the setting time or microhardness among the sealers. (ii) Moisture does not affect the setting time or microhardness of the sealers. (iii) pH changes do not affect the setting time or microhardness of the sealers.


https://doi.org/10.5395/rde.2025.50.e41

## METHODS

### Specimen preparation

Three commercially available premixed CSBSs, Endoseal MTA (MARUCHI, Wonju, Korea), One-Fil (MEDICLUS, Cheongju, Korea), and Well-Root ST (VERICOM, Chuncheon, Korea), were evaluated. The chemical compositions of the sealers are listed in Table 1. All samples were analyzed before the manufacturers' specified expiration dates.

According to the ISO 6876:2012 standards, dental plaster molds with an internal diameter of 10 mm and a height of 1 mm were used for evaluating sealers requiring moisture for the setting reaction. The molds in the initial group for each material were maintained at 37°C and 100% relative humidity for 24 hours, following ISO standards, and served as the control group (unsoaked mold, US). Additional molds were exposed to distilled water [DW] (DW-soaked mold, DW), PBS at pH 7.4 (PBS-soaked mold, PBS), or hydrochloric acid (HCl) at pH 5 (pH 5-soaked mold, pH 5). The sealers and the setting environment conditions are summarized in Table 2. The pH was measured using a calibrated pH meter (WTW, Inolab pH7110; Weilheim, Germany) with buffer solutions (pH 4, 7, and 10). The room temperature during measurements was maintained at 25°C. Each mold was individually immersed in a plastic flask containing 40 mL of the respective solutions and stored at 100% relative humidity and 37°C for 24 hours ($n$ = 12/group/condition).

Sealers were injected into the molds and stored at 100% relative humidity and 37°C. For the PBS-soaked and pH 5-soaked groups, a 40-μL drop of the respective solution was applied to stimulate sustained direct exposure to these fluids, which may be encountered in clinical inflammatory conditions or post-irrigation environments, followed by an overhead projector film. For the DW group, no additional drops were used, as exposure to ≥95% relative humidity in a water bath is generally accepted to provide adequate environmental moisture for setting without excess surface liquid. A glass plate was placed over the sealer to ensure a flat and uniform surface.

To assess the differences in moisture content between the US and DW-soaked molds, the weight of each mold was measured at three different time points: 1 hour after setting (prior to storage at 100% humidity), after storage, and after drying in a vacuum oven.

### Setting time

Setting time was evaluated using Gilmore needles (ASTM International, West Conshohocken, PA, USA). The initial setting time was defined as the time required for the test cement to solidify sufficiently to withstand a Gilmore needle (113.4 g, tip diameter 2.12 mm). The final setting time was defined as the time required to resist a heavier Gilmore needle (453.6 g, tip diameter 1.06 mm) without significant indentation. The initial and final setting times were monitored at 5-minute intervals, starting 20 minutes before the anticipated setting time based on a pilot study. The time at which the needle no longer indented the sealer surface was recorded. Each specimen was tested three times, and the needle tip was cleaned after each measurement.

**Table 2.** Sealers tested under four conditions (unsoaked, distilled Water, PBS, pH 5) with 12 samples per condition

| Sealer | Condition | Sample size (n) |
|---|---|---|
| Endoseal MTA | Unsoaked | 12 |
| One-Fil | Distilled water | 12 |
| Well-Root ST | PBS (pH 7.4) | 12 |
| | pH 5 (HCl) | 12 |

PBS, phosphate-buffered saline.
Endoseal MTA: MARUCHI, Wonju, Korea; One-Fil: MEDICLUS, Cheongju, Korea; Well-Root ST: VERICOM, Chuncheon, Korea.

**Table 1.** Types and compositions of sealers investigated in this study

| Sealer | Manufacturer | Lot | Composition |
|---|---|---|---|
| Endoseal MTA | MARUCHI, Wonju, Korea | CD231027 | Calcium silicates (dicalcium silicates), tricalcium aluminates, calcium aluminoferrite, calcium sulfates, zirconium oxide, bismuth trioxide, thickening agent |
| One-Fil | MEDICLUS, Cheongju, Korea | OS41T048 | Calcium aluminosilicate compound, zirconium oxide, hydrophilic polymer (thickening agent) |
| Well-Root ST | VERICOM, Chuncheon, Korea | WR3D340S | Calcium silicate compound, calcium sulfate dehydrate, calcium sodium phosphosilicate, zirconium oxide, titanium oxide, thickening agents |

### Surface microhardness measurement

During incubation, gauze saturated with PBS or HCl was placed on the samples according to their assigned groups. The samples were incubated at 37°C under 100% relative humidity for 3 days. To ensure the maintenance of appropriate pH levels, the gauze pieces were replaced every 12 hours. The DW group with no gauze was used; moisture was maintained by incubation under high relative humidity.

The samples were then ground using 1,200-grit silicon carbide paper and wet-polished with minimal hand pressure to facilitate indentation and minimize preparation effects on surface microhardness. The microhardness was measured using a Vickers microhardness tester (HM-221, Mitutoyo, Tokyo, Japan). Square-based and pyramid-shaped diamond indenters were used, applying a load of 0.1 kgf for both Endoseal MTA and One-Fil, and 1 kgf for Well-Root ST. This adjustment was made according to the pilot test, which revealed that the lower load of 0.1 kgf did not produce visible or reproducible indentations on Well-Root ST samples under our testing conditions. The indentation time was set to 10 seconds at room temperature. Vickers hardness was calculated using the following formula:

$$HV = \frac{2F\sin\frac{136^\circ}{2}}{d^2}$$

$$HV = 1.854\frac{F}{d^2}$$

where $F$ represents the load in kilograms of force, $d$ is the mean of the two diagonals in millimeters, and $HV$ is the Vickers microhardness. The microhardness values were measured three times and the average values were calculated.

### Statistical analysis

Statistical analyses were performed using the SPSS software, version 29.0 (IBM Corp., Armonk, NY, USA). Data normality was assessed using the Shapiro-Wilk test. Weight changes were compared using the Mann-Whitney *U*-test. The effects of CSBS type and environmental conditions on the setting time and microhardness were analyzed using Welch's analysis of variance, followed by the Games-Howell *post hoc* test. The significance level was set at $p < 0.05$.

## RESULTS

The differences in the moisture content between the US and DW-soaked molds are presented in Figure 1. Significantly lower moisture content was observed in US gypsum molds compared with DW-soaked molds after 24 hours at 37°C and 100% relative humidity, as determined by the Mann-Whitney *U*-test ($p < 0.001$).

### Setting time

A significant two-way interaction between the CSBS and environmental conditions was observed for both the initial and final setting times ($p < 0.001$) (Tables 3 and 4, Figure 2). The CSBS type and environmental conditions significantly influenced the initial and final setting times ($p < 0.001$). Shorter initial and final setting times were recorded in the US group than in the pH 5 group ($p < 0.001$).

For Endoseal MTA, the US group exhibited significantly shorter initial setting times than the soaked group. However, no significant differences were observed between the DW, PBS, and pH 5 conditions. A similar pattern was noted for the final setting time; however, the PBS and pH 5 groups had significantly longer setting times than the DW group.

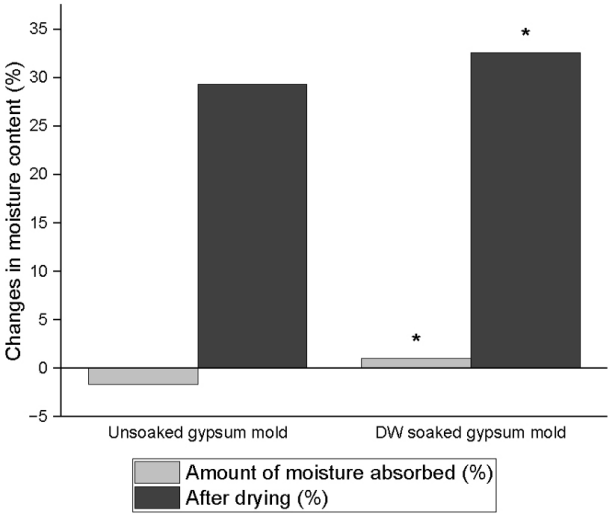


**Figure 1.** Moisture content changes of unsoaked and distilled water (DW)-soaked gypsum molds. *$p < 0.05$, statistically significant.


https://doi.org/10.5395/rde.2025.50.e41

**Table 3.** Initial setting time (min) of CSBSs under different environmental conditions

| Type of CSBS | Unsoaked | Distilled water | PBS | pH 5 |
|---|---|---|---|---|
| Endoseal MTA | $9.12 \pm 1.97^{Aa}$ | $51.20 \pm 13.1^{Ba}$ | $66.8 \pm 13.57^{CDa}$ | $62.13 \pm 6.92^{BDa}$ |
| One-Fil | $12.93 \pm 4.53^{Aa}$ | $32 \pm 7.47^{Bb}$ | $29.65 \pm 5.18^{Bb}$ | $41.57 \pm 5.32^{Bb}$ |
| Well-Root ST | $36.47 \pm 6.27^{Ab}$ | $47.82 \pm 15.75^{Aa}$ | $40.8 \pm 7.02^{Ab}$ | $74.05 \pm 8.82^{Ba}$ |

Values are presented as mean ± standard deviation.
CSBS, calcium silicate-based sealer; PBS, phosphate-buffered saline.
Different uppercase letters indicate significant differences ($p < 0.05$) within the same row; different lowercase letters indicate significant differences within the same column.
Endoseal MTA: MARUCHI, Wonju, Korea; One-Fil: MEDICLUS, Cheongju, Korea; Well-Root ST: VERICOM, Chuncheon, Korea.

**Table 4.** Final setting time (min) of CSBSs under different environmental conditions

| Type of CSBS | Unsoaked | Distilled water | PBS | pH 5 |
|---|---|---|---|---|
| Endoseal MTA | $27.43 \pm 4.68^{Aa}$ | $81.28 \pm 13.75^{Ba}$ | $116.35 \pm 12.3^{Ca}$ | $113.3 \pm 10.38^{Ca}$ |
| One-Fil | $32.93 \pm 8.9^{Aa}$ | $80.98 \pm 21.52^{Ba}$ | $79.03 \pm 13.88^{Bb}$ | $144.63 \pm 5.32^{Cb}$ |
| Well-Root ST | $72.32 \pm 5.75^{ABb}$ | $76.32 \pm 16.73^{Aa}$ | $57.23 \pm 9.75B^{Cc}$ | $100.28 \pm 4.98^{Da}$ |

Values are presented as mean ± standard deviation.
CSBS, calcium silicate-based sealer; PBS, phosphate-buffered saline.
Different uppercase letters indicate significant differences ($p < 0.05$) within the same row; different lowercase letters indicate significant differences within the same column.
Endoseal MTA: MARUCHI, Wonju, Korea; One-Fil: MEDICLUS, Cheongju, Korea; Well-Root ST: VERICOM, Chuncheon, Korea.

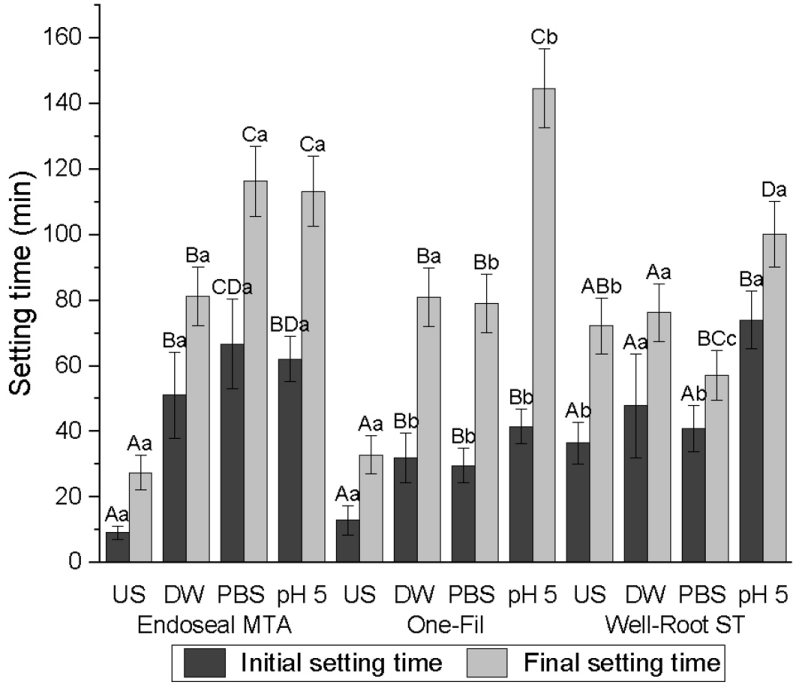


**Figure 2.** Initial and final setting times (min) of calcium silicate-based sealers (CSBSs) under different environmental conditions. Different uppercase letters indicate significant differences ($p < 0.05$) within the same sealer, and different lowercase letters denote significant differences within the same environmental condition. Endoseal MTA: MARUCHI, Wonju, Korea; One-Fil: MEDICLUS, Cheongju, Korea; Well-Root ST: VERICOM, Chuncheon, Korea. US, unsoaked; DW, distilled water; PBS, phosphate-buffered saline.

One-Fil displayed comparable trends, with significantly shorter initial and final setting times in the US group than in the soaked groups. The pH 5 group exhibited a significantly longer initial setting time than the PBS group. The final setting time was markedly prolonged in the pH 5 group, exceeding that of all the other conditions.

For the well-rooted ST, the initial and final setting times for the US, DW, and PBS groups did not differ significantly. However, exposure to the acidic pH 5 solution significantly delayed both the initial and final setting times that to all other groups.

### Surface microhardness

Both CSBS type and environmental conditions significantly affected the microhardness ($p < 0.0001$) (Table 5, Figure 3). Across all the tested sealers, the US group consistently exhibited significantly higher Vickers microhardness values than the soaked groups (DW, PBS, and pH 5) ($p < 0.0001$). Among the soaked groups, PBS

**Table 5.** Vickers microhardness values (kgf/mm$^2$) of CSBSs under different environmental conditions

| Type of CSBSs | Unsoaked | Distilled water | PBS | pH 5 |
|---|---|---|---|---|
| Endoseal MTA | $18.52 \pm 2.04^{Aa}$ | $2.2 \pm 0.23^{Ba}$ | $1.37 \pm 0.16^{Ba}$ | $3.13 \pm 0.42^{Ba}$ |
| One-Fil | $26.81 \pm 3.2^{Ab}$ | $17.37 \pm 2.99^{Bb}$ | $12.63 \pm 2.39^{Cb}$ | $9.8 \pm 2.12^{Db}$ |
| Well-Root ST | $33.07 \pm 2.09^{Ac}$ | $13.78 \pm 2.06^{Bc}$ | $15.15 \pm 2.18^{Bb}$ | $10.5 \pm 1.59^{Cb}$ |

Values are presented as mean ± standard deviation.
CSBS, calcium silicate-based sealer; PBS, phosphate-buffered saline.
Different uppercase letters indicate significant differences ($p < 0.05$) within the same row; different lowercase letters indicate significant differences within the same column.
Endoseal MTA: MARUCHI, Wonju, Korea; One-Fil: MEDICLUS, Cheongju, Korea; Well-Root ST: VERICOM, Chuncheon, Korea.

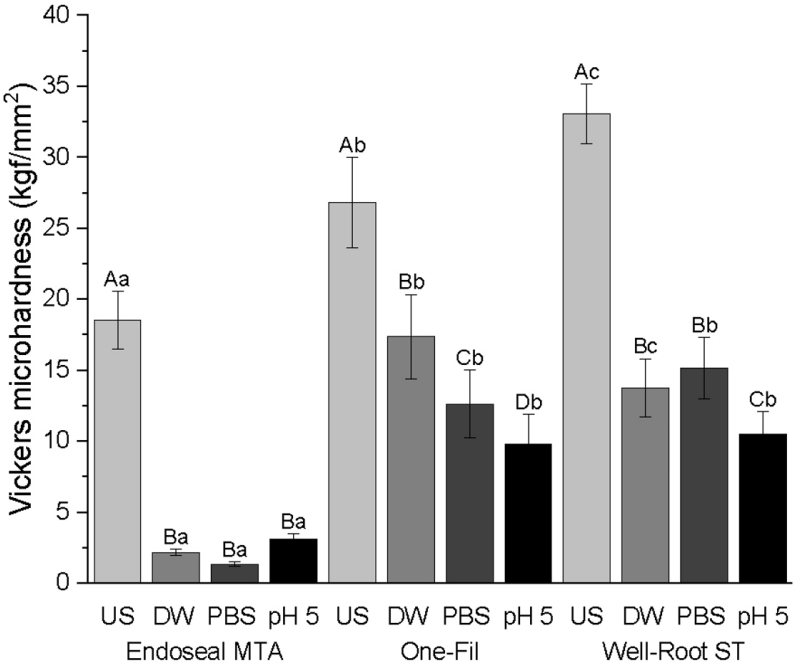


**Figure 3.** Vickers microhardness of calcium silicate-based sealers (CSBSs) under different environmental conditions. Different uppercase letters indicate significant differences ($p < 0.05$) within the same sealer, and different lowercase letters denote significant differences within the same environmental condition. Endoseal MTA: MARUCHI, Wonju, Korea; One-Fil: MEDICLUS, Cheongju, Korea; Well-Root ST: VERICOM, Chuncheon, Korea. US, unsoaked; DW, distilled water; PBS, phosphate-buffered saline.


https://doi.org/10.5395/rde.2025.50.e41

exposure resulted in the lowest microhardness in Endoseal MTA, which was significantly lower than that of the DW and pH 5 groups. For One-Fil, the pH 5 group had the lowest value ($p < 0.0001$) and that of the PBS group was significantly lower than that of the DW group. For Well-Root ST, the pH 5 group produced the lowest microhardness, whereas the DW and PBS groups exhibited similar microhardness values without significant differences. Across all tested conditions, Endoseal MTA exhibited significantly lower Vickers microhardness values than One-Fil and Well-Root ST ($p < 0.0001$).

## DISCUSSION

Advancements in bioceramic technologies have increased the use of CSBSs in endodontics. These sealers have compositions and properties similar to those of MTA, but offer additional benefits, including nonstaining characteristics, reduced impurities, and smaller particle sizes [4,19]. Excellent flowability, high pH, good dimensional stability, and adequate radiopacity have been reported for CSBSs *in vitro* [8,20,21]. As the properties of root canal sealers significantly influence the quality of root canal fillings and require an adequate setting time [20], evaluating the setting time and surface microhardness as indicators of the setting process is essential [15].

In the present study, the setting times and microhardness of three premixed CSBSs were investigated. The CSBSs are hydraulic and require water for initiating the setting process. In the presence of water, calcium silicate reacts to form calcium silicate hydrate gels, leading to the production of calcium hydroxide [4]. However, the inclusion of water in the sealer significantly increases the initial setting time and decreases the microhardness of CSBSs [7,22]. In this study, a significant increase in setting time was observed in the DW group of Endoseal MTA and One-Fil compared with that in the US group. Additionally, all CSBSs demonstrated a significant decrease in the surface microhardness in the DW group compared to that in the US group. Therefore, the second null hypothesis, which states that moisture has no influence on the setting time and microhardness of the CSBSs, was rejected.

Plaster of Paris molds were used to evaluate the setting time and microhardness. Gypsum is known for its irregular shape and porous structure, which enable it to absorb and retain water or moisture [23]. Because moisture is essential for the setting of calcium silicate-based materials, variations in the moisture content can significantly influence the setting time [12,22]. Several previous studies utilized gypsum molds following the ISO 6876 guidelines to assess the setting time and properties of CSBSs [24,25]. These studies effectively simulated the moist conditions necessary for sealer hydration, with one study incorporating both *in vivo* and *in vitro* experiments to replicate periapical tissue environments [25]. Thus, the present study further combined gypsum molds with controlled PBS and acidic solutions to mimic the chemical conditions of healthy and inflamed periapical tissues more precisely, thereby providing new insights into how these specific ionic and pH variations affect sealer behavior under clinically relevant conditions.

The environmental conditions were regulated through divergence during the storage of the plaster molds. Both the US and soaked molds immersed in different media were used. Moisture content was assessed by measuring the weight changes, which revealed a significant difference between the US and DW-soaked molds. The final setting times of the sealers in the DW group did not vary significantly, whereas those in the PBS group varied significantly among the three sealers. The Vickers microhardness values varied significantly between the US and DW groups for all the tested sealers, leading to rejection of the first null hypothesis.

Nekoofar *et al*. [14] reported that the mean pH of pus from periapical abscesses is typically acidic. Such acidic environments may influence the properties of root canal sealers, which are often exposed to inflamed or infected conditions. Moreover, acidity can affect the structure, hydroxyapatite formation, and antibacterial activity of these materials [26,27]. In contrast, healthy blood is slightly alkaline, with a typical pH of 7.4, and PBS is commonly used to simulate tissue fluids containing phosphate [28]. To mimic the clinical conditions during canal filling, gypsum molds were exposed to two distinct pH conditions to simulate both inflammatory and healthy environments. Significant differences in the initial and final setting times were observed between

the PBS and pH 5 groups for One-Fil and Well-Root ST and in microhardness for Endoseal MTA and Well-Root ST, leading to the rejection of the third null hypothesis.

An ideal root canal sealer should have a slow setting time to allow adequate working time. If incompletely set, extrusion of sealers beyond the apical foramen may trigger periapical inflammation [8,29]. However, prolonged setting times influenced by formulation and root canal moisture were noted. Setting times have also been found to increase in dry canals [4,7].

Microhardness reflects the resistance of a material to deformation under a specified load. Although not included in the ISO standards, it can serve as an indirect measure of material setting [16]. Microhardness also influences the ease of CSBS removal during non-surgical retreatment [4]. In this study, all the materials demonstrated significantly higher microhardness in the US group than in the pH 5 group. These findings are consistent with those of previous research that reported significantly lower mean microhardness in both the acidic and PBS groups than in the control [16].

PBS provides a stable ionic milieu containing phosphate ions and maintains a near-neutral pH through its buffering capacity, which significantly influences the surface reactions of CSBSs. The presence of phosphate ions in PBS promotes the formation and deposition of calcium phosphate compounds such as hydroxyapatite on the surfaces of calcium silicate materials [30]. This bioactive layer can potentially alter the microhardness values measured on sealer surfaces by creating a mineralized interface that is softer or structurally different from the fully set cement matrix [10,30,31]. Moreover, PBS's buffering action helps maintain stable pH levels, preventing extreme alkalinity that would typically accelerate the hydration reaction and the formation of calcium silicate hydrate gel, which is an important contributor to the mechanical strength of the set sealer [30,32]. Consequently, the microhardness in PBS is affected by both surface calcium phosphate deposition and the modulation of cement hydration kinetics.

Differences in sealer compositions may account for the variations in the setting time and microhardness. In MTA, tricalcium silicate is more reactive, contributing to its initial strength, whereas dicalcium silicate has a more sustained effect over time. Dicalcium silicate cement has also demonstrated strong apatite-forming activity and minimal degradation under acidic conditions [33]. Endoseal MTA is a premixed type pozzolan-based MTA sealer with dicalcium silicate as its primary component. The use of fine pozzolanic particles allows the premixed material to flow efficiently with the desired working consistency and also reduces the setting time [34,35]. However, during the pozzolanic reaction, these cements undergo a gradual reduction in free calcium hydroxide while increasing the formation of stable crystals composed of calcium silicate hydrate and calcium aluminate hydrate. These processes are believed to contribute to the reduced mechanical strength of materials [36,37]. This may explain the low microhardness observed in Endoseal MTA under all environmental conditions. Additionally, Well-Root ST contains tricalcium silicate, which is found in both PBS and pH 5 environments [16]. This could account for the significantly shorter final setting time observed in Well-Root ST than in One-Fil.

Well-Root ST exhibited significantly higher microhardness in the PBS group than in the pH 5 group. Conversely, Endoseal MTA exhibited significantly higher microhardness values in the pH 5 group than in the PBS group. These findings fairly vary from those of previous studies, which reported significantly lower microhardness values for MTA when exposed to an acidic environment compared to solutions with a pH of 7.4 [32,37]. However, one study reported no statistically significant difference in the microhardness of Endoseal MTA between PBS and pH 5.4 solutions [16]. This study further supported their findings using scanning electron microscopy (SEM), which revealed predominantly amorphous structures under both conditions, with the acidic group showing fewer planar-like crystals and clusters than the PBS group. Because SEM analysis was not conducted in this study, the underlying microstructural basis remains speculative in the absence of direct microstructural evidence, which is a major limitation of this study.

The microhardness of CSBSs is predominantly influenced by the extent of hydration and formation of calcium silicate hydrate (C-S-H) phases, which serve as the primary binders imparting strength [29]. Although a higher calcium silicate content generally correlates with an increased potential for cement hydration and


https://doi.org/10.5395/rde.2025.50.e41

setting, this relationship is complex and is based on the specific phase composition, additives, and particle size distribution. For instance, the presence of calcium aluminates or other supplementary minerals can affect the nucleation and growth of hydrates, thereby affecting microhardness [30,38]. Therefore, simple correlations between the calcium silicate content and microhardness should be approached with caution, recognizing that material formulation and environmental interactions critically determine the final mechanical properties.

Despite the valuable insights obtained, a limitation of this study is that it did not fully isolate the individual contributions of pH, moisture content, and the specific chemical nature of the immersion solutions to the observed changes in setting time and microhardness. Previous studies have demonstrated that acidic pH primarily disrupts the hydration and crystallization processes within CSBSs, resulting in delayed setting and reduced microhardness [15,16]. Moisture availability is critical for the initiation and progression of hydration reactions. However, excessive moisture can increase porosity and solubility, potentially weakening the cement matrix [7,22]. Furthermore, the chemical composition of the immersion media, such as the presence of phosphate ions in PBS, can facilitate apatite or calcium phosphate deposition on the material surface, thereby affecting the microhardness independently of the bulk setting [29]. Because these factors may interact in complex ways, future studies are warranted to disentangle and quantify their distinct effects on material performance.

Although Silva *et al*. [25] correlated *in vitro* and *in vivo* setting times using animal models, they primarily focused on biological responses rather than replicating the physicochemical environment of the root canal system. This study investigated the setting characteristics of premixed CSBSs by comparing ISO standards with simulated conditions that mimic the root canal and periapical environments. Clinically, the setting time and microhardness of CSBS may be affected by moisture in the root canal, inflammation, or periapical fluid, potentially affecting the long-term success of root canal therapy. Further studies are warranted to evaluate the clinical performance of CSBS under various environmental conditions.

## CONCLUSIONS

The setting environment significantly influenced the setting time and microhardness of the CSBSs. Longer setting times were observed for these sealers when exposed to moisture, PBS, or an acidic environment, except for Well-Root ST, which exhibited prolonged setting times only in acidic environments. Additionally, all three sealers demonstrated reduced microhardness when exposed to moisture, PBS, or acidic environments, compared to the values observed under ISO standard conditions (US group). These findings highlight the importance of environmental factors in CSBS performance, with potential implications for clinical applications.

### CONFLICT OF INTEREST

No potential conflict of interest relevant to this article was reported.

### FUNDING/SUPPORT

The authors have no financial relationships relevant to this article to disclose.

### ACKNOWLEDGEMENTS

The author acknowledges MARUCHI (Wonju, Korea), MEDICLUS (Cheongju, Korea), and VERICOM (Chuncheon, Korea) for providing the Endoseal MTA, One-Fil, and Well-Root ST calcium silicate-based root canal sealers, respectively, used in this study.

## REFERENCES

1. Vera J, Siqueira JF, Ricucci D, Loghin S, Fernández N, Flores B, *et al*. One- versus two-visit endodontic treatment of teeth with apical periodontitis: a histobacteriologic study. J Endod 2012;38:1040-1052.
2. Allan NA, Walton RC, Schaeffer MA. Setting times for endodontic sealers under clinical usage and in vitro conditions. J Endod 2001;27:421-423.
3. Sfeir G, Zogheib C, Patel S, Giraud T, Nagendrababu V, Bukiet F. Calcium silicate-based root canal sealers: a narrative review and clinical perspectives. Materials (Basel) 2021;14:3965.
4. Hargreaves KM, Berman LH. Cohen's pathways of the pulp. 11th ed. St Louis, MO: Elsevier 2016. p. 30.
5. Parirokh M, Torabinejad M. Mineral trioxide aggregate: a

comprehensive literature review: part I: chemical, physical, and antibacterial properties. J Endod 2010;36:16-27.
6. Torabinejad M, Parirokh M. Mineral trioxide aggregate: a comprehensive literature review: part II: leakage and biocompatibility investigations. J Endod 2010;36:190-202.
7. Xuereb M, Vella P, Damidot D, Sammut CV, Camilleri J. In situ assessment of the setting of tricalcium silicate-based sealers using a dentin pressure model. J Endod 2015;41:111-124.
8. Park MG, Kim IR, Kim HJ, Kwak SW, Kim HC. Physicochemical properties and cytocompatibility of newly developed calcium silicate-based sealers. Aust Endod J 2021;47:512-519.
9. Vertuan GC, Duarte MA, Moraes IG, Piazza B, Vasconcelos BC, Alcalde MP, *et al*. Evaluation of physicochemical properties of a new root canal sealer. J Endod 2018;44:501-505.
10. Prati C, Gandolfi MG. Calcium silicate bioactive cements: biological perspectives and clinical applications. Dent Mater 2015;31:351-370.
11. Ferreira CMA, Sassone LM, Gonçalves AS, de Carvalho JJ, Tomás-Catalá CJ, García-Bernal D, *et al*. Physicochemical, cytotoxicity and in vivo biocompatibility of a high-plasticity calcium-silicate based material. Sci Rep 2019;9:3933.
12. Koo J, Kwak SW, Kim HC. Differences in setting time of calcium silicate-based sealers under different test conditions. J Dent Sci 2023;18:1042-1046.
13. Wongkornchaowalit N, Lertchirakarn V. Setting time and flowability of accelerated Portland cement mixed with polycarboxylate superplasticizer. J Endod 2011;37:387-389.
14. Nekoofar MH, Namazikhah MS, Sheykhrezae MS, Mohammadi MM, Kazemi A, Aseeley Z, *et al*. PH of pus collected from periapical abscesses. Int Endod J 2009;42:534-538.
15. Bolhari B, Nekoofar MH, Sharifian M, Ghabrai S, Meraji N, Dummer PM. Acid and microhardness of mineral trioxide aggregate and mineral trioxide aggregate-like materials. J Endod 2014;40:432-435.
16. Yang DK, Kim S, Park JW, Kim E, Shin SJ. Different setting conditions affect surface characteristics and microhardness of calcium silicate-based sealers. Scanning 2018;2018:7136345.
17. Qu W, Bai W, Liang YH, Gao XJ. Influence of warm vertical compaction technique on physical properties of root canal sealers. J Endod 2016;42:1829-1833.
18. Teixeira CG, da Silva MA, Janini AC, de Moura JD, Rocha DG, Pelegrine RA, *et al*. Setting time of calcium silicate-based sealers at different acidic pHs. G Ital Endod 2023;37:10.32067/GIE.2023.37.01.21.
19. Donnermeyer D, Bürklein S, Dammaschke T, Schäfer E. Endodontic sealers based on calcium silicates: a systematic review. Odontology 2019;107:421-436.
20. Zhou HM, Shen Y, Zheng W, Li L, Zheng YF, Haapasalo M. Physical properties of 5 root canal sealers. J Endod 2013;39:1281-1286.
21. Candeiro GT, Correia FC, Duarte MA, Ribeiro-Siqueira DC, Gavini G. Evaluation of radiopacity, pH, release of calcium ions, and flow of a bioceramic root canal sealer. J Endod 2012;38:842-845.
22. Kim HJ, Lee JS, Gwak DH, Ko YS, Lim CI, Lee SY. In vitro comparison of differences in setting time of premixed calcium silicate-based mineral trioxide aggregate according to moisture content of gypsum. Materials (Basel) 2023;17:35.
23. Jorgensen KD, Kono A. Relationship between the porosity and compressive strength of dental stone. Acta Odontol Scand 1971;29:439-447.
24. Kim HI, Jang YE, Kim Y, Kim BS. Physicochemical changes in root-canal sealers under thermal challenge: a comparative analysis of calcium silicate- and epoxy-resin-based sealers. Materials (Basel) 2024;17:1932.
25. Silva EJ, Ehrhardt IC, Sampaio GC, Cardoso ML, Oliveira DD, Uzeda MJ, *et al*. Determining the setting of root canal sealers using an in vivo animal experimental model. Clin Oral Investig 2021;25:1899-1906.
26. Hochrein O, Zahn D. On the molecular mechanisms of the acid-induced dissociation of hydroxy-apatite in water. J Mol Model 2011;17:1525-1528.
27. Bosaid F, Aksel H, Azim AA. Influence of acidic pH on antimicrobial activity of different calcium silicate based-endodontic sealers. Clin Oral Investig 2022;26:5369-5376.
28. Marques MR, Loebenberg R, Almukainzi M. Simulated biological fluids with possible application in dissolution testing. Dissolution Technol 2011;18:15-28.
29. Camilleri J. Characterization and hydration kinetics of tricalcium silicate cement for use as a dental biomaterial. Dent Mater 2011;27:836-844.
30. Gandolfi MG, Ciapetti G, Taddei P, Perut F, Tinti A, Cardoso MV, *et al*. Apatite formation on bioactive calcium-silicate cements for dentistry affects surface topography and human marrow stromal cells proliferation. Dent Mater 2010;26:974-992.
31. Jeon MJ, Ahn JS, Park JK, Seo DG. Investigation of the crystal formation from calcium silicate in human dentinal tubules


https://doi.org/10.5395/rde.2025.50.e41

and the effect of phosphate buffer saline concentration. J Dent Sci 2024;19:2278-2285.
32. Giuliani V, Nieri M, Pace R, Pagavino G. Effects of pH on surface hardness and microstructure of mineral trioxide aggregate and Aureoseal: an in vitro study. J Endod 2010;36:1883-1886.
33. Han L, Kodama S, Okiji T. Evaluation of calcium-releasing and apatite-forming abilities of fast-setting calcium silicate-based endodontic materials. Int Endod J 2015;48:124-130.
34. Silva EJ, Carvalho NK, Prado MC, Zanon M, Senna PM, Souza EM, *et al*. Push-out bond strength of injectable pozzolan-based root canal sealer. J Endod 2016;42:1656-1659.
35. Turanli L, Uzal B, Bektas F. Effect of material characteristics on the properties of blended cements containing high volumes of natural pozzolans. Cem Concr Res 2004;34:2277-2282.
36. Rodrıguez-Camacho R, Uribe-Afif R. Importance of using the natural pozzolans on concrete durability. Cem Concr Res 2002;32:1851-1858.
37. Lee YL, Lee BS, Lin FH, Yun Lin A, Lan WH, Lin CP. Effects of physiological environments on the hydration behavior of mineral trioxide aggregate. Biomaterials 2004;25:787-793.
38. Camilleri J. Characterization of hydration products of mineral trioxide aggregate. Int Endod J 2008;41:408-417.

*Restorative Dentistry and Endodontics* (*Restor Dent Endod, RDE*) is a peer-reviewed and open-access electronic journal providing up-to-date information regarding the research and developments on new knowledge and innovations pertinent to the field of contemporary clinical operative dentistry, restorative dentistry, and endodontics. In the field of operative and restorative dentistry, the journal deals with diagnosis, treatment planning, treatment concepts and techniques, adhesive dentistry, esthetic dentistry, tooth whitening, dental materials, and implant restoration. In the field of endodontics, the journal deals with a variety of topics such as etiology of periapical lesions, outcome of endodontic treatment, surgical endodontics including replantation, transplantation and implantation, dental trauma, intracanal microbiology, endodontic materials (MTA, nickel-titanium instruments, etc), molecular biology techniques, and stem cell biology. *RDE* publishes research articles, review articles and case reports dealing with aforementioned topics from all over the world.

Manuscripts submitted to *RDE* should be prepared according to the instructions below. For issues not addressed in these instructions, the author should refer to the Recommendations for the Conduct, Reporting, Editing, and Publication of Scholarly Work in Medical Journals (http://www.icmje.org/recommendations/) from the International Committee of Medical Journal Editors (ICMJE).

## Research and Publication Ethics

All of the manuscripts should be prepared based on strict observation of research and publication ethics guidelines recommended by the Council of Science Editors (https://www.councilscienceeditors.org), International Committee of Medical Journal Editors (ICMJE, https://www.icmje.org), World Association of Medical Editors (WAME, https://www.wame.org), and the Korean Association of Medical Journal Editors (KAMJE, https://www.kamje.or.kr/en/main_en).

All studies involving human subjects or human data must be reviewed and approved by a responsible Institutional Review Board (IRB). Please refer to the principles embodied in the Declaration of Helsinki (https://www.wma.net/policies-post/wma-declaration-of-helsinki-ethical-principles-for-medical-research-involving-human-subjects) for all investigations involving human materials. Animal experiments also should be reviewed by an appropriate committee (IACUC) for the care and use of animals. Also, studies with pathogens requiring a high degree of biosafety should pass review of a relevant committee (Institutional Biosafety Committee). The approval should be described in the Methods section. For studies of humans including case reports, state whether informed consents were obtained from the study participants (or from a parent or legal guardian if the participant is unable to provide consent). The editor of *RDE* may request submission of copies of the documents regarding ethical issues.

The *RDE* will follow the guidelines of the Committee on Publication Ethics (COPE, https://publicationethics.org) for the settlement of any misconduct.

## Authorship

Authorship credit should be based on (1) substantial contributions to conception and design, acquisition of data, and analysis and interpretation of data; (2) drafting the article or revising it critically for important intellectual content; (3) final approval of the version to be published; and (4) agreement to be accountable for all aspects of the work in ensuring that questions related to the accuracy or integrity of any part of the work are appropriately investigated and resolved. Authors should meet these four conditions.

**Role of Corresponding Author:** The corresponding author takes primary responsibility for communication with the journal during the manuscript submission, peer review, and publication process. The corresponding author typically ensures that all of the journal's administrative requirements, such as providing the details of authorship, ethics committee approval, clinical trial registration documentation, and conflict of interest forms and statements, are properly completed, although these duties may be delegated to one or more

co-authors. The corresponding author should be available throughout the submission and peer review process to respond to editorial queries in a timely manner, and after publication, should be available to respond to critiques of the work and cooperate with any requests from the journal for data or additional information or questions about the article.

**Contributors:** Any researcher who does not meet all four ICMJE criteria for authorship discussed above but contribute substantively to the study in terms of idea development, manuscript writing, conducting research, data analysis, and financial support should have their contributions listed in the Acknowledgments section of the article.

**Changes to Authorship:** Any changes to authorship (the addition, deletion or rearrangement of author names in the authorship of accepted manuscript) needs to be approved by the Editor-in-Chief after a written confirmation by a corresponding author including the reason the name should be rearranged and all the signature of co-authors.

For more information, please refer to the Research and Publication Ethics page on the journal website.

## Copyrights, Open Access, Data Sharing, and Archiving

**Copyright:** Copyright in all published material is owned by the Korean Academy of Conservative Dentistry. Authors must agree to transfer copyright (https://rde.ac/src/author_form.pdf) during the submission process. The corresponding author is responsible for submitting the copyright transfer agreement to the publisher.

**Open Access Policy:** *RDE* is an open-access journal. Articles are distributed under the terms of the Creative Commons Attribution License (https://creativecommons.org/licenses/by-nc/4.0/), which permits unrestricted non-commercial use, distribution, and reproduction in any medium, provided the original work is properly cited. Author(s) do not need permission to use tables or figures published in *RDE* in other journals, books, or media for scholarly and educational purposes.

**Data Sharing:** *RDE* encourages data sharing wherever possible unless this is prevented by ethical, privacy, or confidentiality matters. Authors may deposit their data in a publicly accessible repository and include a link to the DOI within the text of the manuscript.

**Clinical Trials:** *RDE* accepts the ICMJE Recommendations for data sharing statement policy. Authors may refer to the editorial, "Data Sharing Statements for Clinical Trials: A Requirement of the International Committee of Medical Journal Editors," in the Journal of Korean Medical Science (https://doi.org/10.3346/jkms.2017.32.7.1051).

**Archiving Policy:** It is accessible without barrier from PubMed Central (https://www.ncbi.nlm.nih.gov/pmc/journals/2010/), Korea Citation Index (https://kci.go.kr), or National Library of Korea (https://nl.go.kr) in the event a journal is no longer published.

For more information, please refer to the Editorial Policy page on the journal website.

## Article Processing Charge

There are no author submission fees or other publication-related charges. All cost for the publication process is supported by the Publisher.

## Submission of Manuscripts

**Copyright Assignment:** Authors submitting a paper do so on the understanding that the work and its essential substance have not been published before and are not being considered for publication elsewhere. The submission of the manuscript by the authors means that the authors automatically agree to assign exclusive copyright to *RDE* if and when the manuscript is accepted for publication.

**Submission:** *RDE* requires electronic submission of all manuscripts. All manuscripts must be submitted to *RDE* through the website (https://www.editorialmanager.

com/rde/) with a cover letter to the editor. Manuscripts may be submitted at any time. Authors may send queries concerning the submission process, manuscript status, or journal procedures to the Editor. Please contact the Editor by E-mail at editor@rde.ac.

**Blinded Peer Review Process:** Manuscripts that do not conform to the general aims and scope of the journal will be returned immediately without review. All other manuscripts will be reviewed by experts in the corresponding field (at least two referees). The Editorial Board may request authors to revise the manuscripts according to the reviewer's opinion. The revised manuscript may go through a second review by referees. A final decision on approval of publication of the submitted manuscripts is made by the Editorial Board.

## Manuscript Preparation

### General Requirements

- **Publication types:** Articles falling into the following categories are invited for submission: Research Articles, Case Reports, Review Articles, Editorials, Open Lectures, and Comments for the Reader's Forum.
- **Language:** The language of publication is English. It is recommended that international authors who are not native speakers of English seek help during manuscript preparation. The authors must have the article reviewed by a professional English editorial service before submission and submit the certificate of English proofreading as a supplement. The terminology used should follow the most recent edition of Dorland's Illustrated Medical Dictionary.
- **General text style:** Use Times New Roman 10-point font. Scientific units should be followed by the International System of Units. When non-standard terms appearing 3 or more times in the manuscript are to be abbreviated, they should be written out completely in the text when first used with the abbreviation in parenthesis. For medicine, use generic names. If a brand name should be used, insert it in parentheses after the generic name.
- **Statistical analysis:** Authors are strongly encouraged to consult a statistician for statistical analysis. Manuscripts with inappropriate statistical analysis methods will be returned to the authors without being reviewed.
- **Ethical approval:** All studies using human and animal subjects or specimens obtained from such subjects (such as extracted teeth) should include an explicit statement in the Methods section identifying the review and approval by the ethics committee for each study and provide an approval number. Manuscripts must be accompanied by a statement in the cover letter that the experiments were undertaken with the understanding and written consent of each subject and according to the above-mentioned principles.
- **Permissions:** If all or parts of previously published quotations, tables, or illustrations are used, permission must be obtained from the copyright holder concerned. The authors will be held responsible for failing to acquire proper permission before submission.
- **Reporting guideline:** For specific study designs, such as randomized controlled trials, studies of diagnostic accuracy, meta-analyses, observational studies, and non-randomized studies, we strongly recommend that authors follow and adhere to the reporting guidelines relevant to their specific research design. Randomized controlled trials should be presented according to the CONSORT guidelines (http://www.consort-statement.org). For case reports, authors should follow the CARE guidelines (https://www.care-statement.org). Authors should upload a completed checklist for the appropriate reporting guidelines during initial submission. Some reliable sources of reporting guidelines are EQUATOR Network (https://www.equator-network.org/) and NLM (https://www.nlm.nih.gov/services/research_report_guide.html).
- **Data statement:** Authors should state the availability of data in submission. If you have made your research data available in a data repository, you can link your article directly to the dataset. If the data is unavailable to access or unsuitable to post, authors must indicate why during the submission process, for example by stating that the research data is confidential. The statement will appear with your published article.

## Manuscript Structure and Format

Key features and limits of articles are summarized below. However, the limits are negotiable with the editor.

| Type | Abstract | Reference (max) | Table/Fig (max) |
|---|---|---|---|
| Review Article | · Unstructured<br>· Max 200 words | 70 | NL |
| Research Article | · Structured<br>: Objectives / Methods / Results / Conclusions<br>· Max 250 words | 40 | Total 8 |
| Case Report | · Unstructured<br>· Max 200 words | 30 | Total 6 |
| Editorial | No abstract | 10 | Total 2 |
| Open Lectures | No abstract | NL | NL |
| Comments for the Reader's Forum | No abstract | NL | NL |

NL, no limit.

Units, symbols, figures, tables, and references used must conform to the current issue or the linked article on our website.

- **Title page:** The title page of the manuscript should include the title of the article, the full name of the author(s), academic degrees, institutional affiliations, a running title (of seven or fewer words), correspondence, and declarations.
  - Title: The title should be concise and precise. It should be of 20 or less words, or it should fit within two lines. Only the first letter of the first word of the title should be capitalized.
  - Authors: Listed authors should include only those individuals who have made a significant creative contribution. *RDE* allows multiple authors to be specified as having equally contributed to the article as co-first authors or co-corresponding authors. While the contact information of all the corresponding authors is published in the article, only one corresponding author (the submitting author) is solely responsible for communicating with the journal.
  - Correspondence: The affiliation, address, telephone number, and e-mail address should be given.
  - Declarations: The declarations include conflicts of interest, funding, authors' contributions, ORCID, data availability statement, and acknowledgments.

| | |
|---|---|
| Conflicts of interest | If there are any conflicts of interest, authors should disclose them in the manuscript. Disclosures allow editors, reviewers, and readers to approach the manuscript with an understanding of the situation and background of the completed research. If there are no conflicts of interest, authors should include the following sentence: "No potential conflict of interest relevant to this article was reported." |
| Funding | All sources of funding applicable to the study should be stated here explicitly. |
| Authors' contributions | The contributions of all authors must be described using the CRediT (https://casrai.org/credit/) taxonomy of author roles. |
| | **Author Contributions**<br>Conceptualization: name; Data curation: name; Formal analysis: name; Funding acquisition: name; Investigation: name; Methodology: name; Project administration: name; Resources: name; Software: name; Supervision: name; Validation: name; Visualization: name; Writing - original draft: name; Writing - review & editing: name. (name: the last name and initials; eg, Cho BH) |
| ORCID | All authors are required to provide ORCID identification numbers. Please list the names of all authors and include the corresponding ORCID iD next to each name. |
| | **ORCID**<br>Byeong-Hoon Cho https://orcid.org/0000-0001-9641-5507<br>Kyung-San Min https://orcid.org/0000-0002-1928-3384 |
| Data availability statement | **Data are available in a public, open-access repository:**<br>Please state the repository name, the persistent URL, and any conditions of reuse. All data that are publicly available and used in the writing of an article should be cited in the text and the reference list, whether they are data generated by the author(s) or by other researchers.<br><br>**Data are available upon reasonable request:**<br>Please describe the data (eg, de-identified participant data), who has access to the data, their publishable contact information, and the conditions under which reuse is permitted.<br><br>**All study-related data is included in the publication or provided as supplementary information:**<br>Please ensure this does not include patient identifiable data.<br><br>**Data sharing is not relevant because no datasets were created and/or analyzed for this study:**<br>Please state 'Not applicable' in this section.<br><br>**No data are available:**<br>Please state 'Not applicable' in this section. |

| | |
|---|---|
| Acknowledgments | All persons who have made substantial contributions, but who have not met the criteria for authorship, are acknowledged here. |

- **Abstract:** The abstract should consist of a single paragraph with no more than 250 words for research articles and 200 words for case reports or review articles and should give details of what was done. The structured abstracts of research articles are to contain the following major headings: **Objective, Methods, Results, Conclusion**; and Keywords of no more than six words in alphabetical order. The abstracts of review articles or case reports don't need a structured format, but keywords should be listed. The keywords should be from Medical Subject Headings (MeSH) when possible (https://meshb.nlm.nih.gov/search) but non-MeSH subject headings may be used if deemed appropriate by the authors. Keywords should be written in small alphabetic letters with the first letter in capital. Separate each word by a semicolon.
- **Main text**
  - Introduction: The introduction should briefly review the pertinent literature in order to identify the gap in knowledge that the study is intended to address. The purpose of the study, the tested hypothesis, and its scope should be described.
  - Methods: The explanation of the experimental methods should be concise and sufficient for repetition by other qualified investigators. Procedures that have been published previously should not be described in detail. However, new or significant modifications of previously published procedures need full descriptions. Clinical studies or experiments using laboratory animals or pathogens should mention approval of the studies by relevant committees in this section. The sources of special chemicals or preparations should be given along with their location (name of company, city and state, and country). If the study utilized a commercial product, the generic term should be used and the product name, manufacturer, city, and country should be stated in parentheses. The methods of statistical analysis and the criteria for determining significance levels should be described.

An **ethics statement** should be placed here when the studies are performed using clinical samples or data, and animals. An exemplary is shown below.

| | |
|---|---|
| Human | The study protocol was approved by the Institutional Review Board of OOO (IRB No: OO-OO-OO). Informed consent was obtained by all participants (or the participant's legal guardian) / Informed consent was waived by the IRB. |
| Animal | The procedures used and the care of animals were approved by the Institutional Animal Care and Use Committee at OOO University (approval No. ******). |
| Clinical trial | This is a randomized clinical trial on the second phase, registered at the Clinical Research Information Service (CRIS, https://cris.nih.go.kr), No. *******.<br>* Other international registration is also acceptable. |

Description of participants: Ensure correct use of the terms sex (when reporting biological factors) and gender (identity, psychosocial or cultural factors), and, unless inappropriate, report the sex or gender of study participants, the sex of animals or cells, and describe the methods used to determine sex or gender. If the study was done involving an exclusive population, for example in only one sex, authors should justify why, except in obvious cases (eg, prostate cancer). Authors should define how they determined race or ethnicity and justify their relevance.

  - Results: This section should present only the observations with minimal reference to earlier literature or possible interpretations by the authors. Data must not be duplicated in Tables and Figures. In tables and figures, magnification rates and units should be stated. SI (Le système International d'Unités) units should be used. Tables, figures, and legends of tables and figures may be included in the text or attached as separate pages at the end of the manuscript. Files containing figures and tables must also be submitted as separate files.
  - Discussion: The discussion section should describe the major findings of the study. Both the strengths and the weaknesses of the observations should be discussed. In addition, suggestions for further research topics may be included if needed.
  - Conclusions: A brief conclusion based on the findings of the study and a comment on the potential clinical relevance of the findings should be summarized. The conclusion section should be described in a narrative manner, without numbering.
- **References:** References should be obviously related

to the document. In the text, references should be cited with Arabic numerals in brackets, numbered in the order cited. The reference list should be typed double-spaced on a separate page and numbered in the order the reference citations appear in the text. For journal citations, include surnames and initials of authors, complete title of article, name of journal (abbreviated according to the NLM Catalog; https://www.ncbi.nlm.nih.gov/nlmcatalog/journals/), volume, inclusive page numbers, and year of publication. When books are cited, either inclusive page numbers or chapter numbers should be included. Please note that theses or doctoral dissertations, which have not been published in peer-reviewed journals, should not be cited as references.

If needed, single or double authors should be acknowledged in the text, eg, Ford and Roberts. If there are more than two authors, the first author followed by *et al*. is sufficient, eg, Tobias *et al*.

We recommend the use of EndNote for reference management and formatting. For reference style and format, please refer to the following examples.

| | |
|---|---|
| Journal article | 1. Oh HK, Shin DH. Effect of adhesive application method on repair bond strength of composite. Restor Dent Endod 2021;46:e32.<br>List all authors when six or fewer (ex. reference 1); when seven or more, list six and add *et al*. (ex. reference 2 and 4).<br><br>2. Bergamo ET, Yamaguchi S, Lopes AC, Coelho PG, de Araújo-Júnior EN, Benalcázar Jalkh EB, *et al*. Performance of crowns cemented on a fiber-reinforced composite framework 5-unit implant-supported prostheses: in silico and fatigue analyses. Dent Mater 2021;37:1783-1793.<br><br>3. Shah RA, Hsu JI, Patel RR, Mui UN, Tyring SK. Antibiotic resistance in dermatology: the scope of the problem and strategies to address it. J Am Acad Dermatol 2021 Sep 20 [Epub]. https://doi.org/10.1016/j.jaad.2021.09.024.<br><br>4. Van Meerbeek B, Vargas M, Inoue S, Yoshida Y, Peumans M, Lambrechts P, *et al*. Adhesives and cements to promote preservation dentistry. Oper Dent 2001;(Supplement 6):119-144.<br><br>5. Yoshida Y, Van Meerbeek B, Okazaki M, Shintani H, Suzuki K. Comparative study on adhesive performance of functional monomers. J Dent Res 2003;82(Special Issue B):Abstract 0051, pB-19. |
| Book & Book chapter | 6. Seltzer S, Bender IB. The dental pulp: biologic considerations in dental procedures. 3rd ed. Lippincott; 1984. p400.<br><br>7. Fouad AF, Levin L. Pulpal reactions to caries and dental procedures. In: Hargreaves KM, Cohen S, Berman LH, eds. Cohen's pathways of the pulp. 10th ed. Mosby Elsevier; 2010. p504-528. |
| Website | 8. International Association of Dental Traumatology (IADT). The dental trauma guide [Internet]. IADT; 2014 [cited 2021 Jun 10]. Available from: https://dentaltraumaguide.org |
| Corporate publication | 9. ISO-Standards ISO 4287 Geometrical Product Specifications Surface texture. Profile method: terms, definitions and surface texture parameters. 1st ed. Geneve: International Organization for Standardization; 1997. p1-25. |

- **Tables:** Tables should be included in the text so that they may be edited if necessary. The title of each table should be placed on the top. The first letter of the first word should be capitalized. All abbreviations should be explained in each table. Footnotes should be indicated in superscript as [a), b), c)], and so on.
- **Figures:** Illustrations must be submitted in electronic format with file sizes appropriate for publication. Figures should be submitted as .tif or .jpg files. PowerPoint files are not accepted. All images should be at least 300 dpi and 5 × 5 cm in size, with 500 dpi recommended. If the figures represent a series of related content, it is recommended to present them as panels (A, B, C...) within a single figure. Figure legends should be included as text so that they be edited if necessary. All abbreviations should be explained in each figure. Microscopic images should include the staining method and magnification (eg, hematoxylin and eosin stain, ×400). Figures may use arrows, arrowheads, asterisks, circles, or other indicators as needed for clarity, with each indicated element described in the figure legends.
- **Other types of articles**
  - Review articles: Review articles should be divided into Introduction, Review, and Conclusions. The Introduction section should focus on placing the subject matter in context and justifying the need for the review. The Review section should be divided into logical sub-sections in order to improve readability and enhance understanding. Search strategies must be described and the use of state-of-the-art evi-

dence-based systematic approaches is expected. The use of tabulated and illustrative material is encouraged. The Conclusion section should reach clear conclusions and/or recommendations on the basis of the evidence presented. If a review includes a meta-analysis as part of a systematic review, it should be submitted as a research article.

- Case reports: Case reports should be divided into Introduction, Case Report(s), Discussion, and Conclusions. They should be well illustrated with clinical images, radiographs, diagrams, and where appropriate, supporting tables and graphs. However, all illustrations must be of the highest quality.
- Comments for the Reader's forum: Reader's forum will present various questions, suggestions, and critiques on the subjects of operative dentistry, restorative dentistry, and endodontics from the readers.

## Manuscript Files Accepted

- **Final version:** After a paper has been accepted for publication, the author(s) should submit the final version of the manuscript. The names and affiliations of authors should be double-checked, and if the originally submitted image files were of poor resolution, higher-resolution image files should be submitted at this time. Illustrations must be submitted in electronic format with file sizes appropriate for publication. All images should be at least 300 dpi and 5 × 5 cm in size, with 500 dpi recommended. Symbols (eg, circles, triangles, squares), letters (eg, words, abbreviations), and numbers should be large enough to be legible on reduction to the journal's column widths. All symbols must be defined in the figure caption. When submitted as separate files, name of the author, and illustration number should be stated in the file name. If references, tables, or figures are moved, added, or deleted during the revision process, renumber them to reflect such changes so that all tables, references, and figures are cited in numeric order.
- **Errata and Corrigenda:** To correct errors in published articles, the corresponding author should contact the journal's Editorial Office with a detailed description of the proposed correction. Corrections that profoundly affect the interpretation or conclusions of the article will be reviewed by the editors. Corrections will be published as corrigenda (corrections of author's errors) or errata (corrections of publisher's errors) in a later issue of the journal.

### Contacting the Journal

Editorial assistant: Hye-Young Lee
*RDE* editorial office
The Korean Academy of Conservative Dentistry
B163, Seoul National University Dental Hospital, 101 Daehak-ro, Jongno-gu, Seoul 03080, Korea
Tel: +82-2-763-3818, Fax: +82-2-763-3819, E-mail: editor@rde.ac

### History of the Recommendations

Enacted in March 2, 2012
Modified: August 4, 2023
Last modified: November 4, 2024

RDE Restorative Dentistry & Endodontics

# Author's checklist

Authors have written the manuscript in compliance with Instructions to Authors and Recommendations for the Conduct, Reporting, Editing, and Publication of Scholarly Work in Medical Journals (https://www.icmje.org/icmje-recommendations.pdf) from the International Committee of Medical Journal Editors, and the Guideline of Committee on Publication Ethics (https://publicationethics.org).

## Cover letter

☐ Manuscript's title
☐ Statement that your paper has not been previously published and is not currently under consideration by another journal.
☐ Brief description of the research you are reporting in your paper, why it is important, and why you think the readers of the journal would be interested in it.
☐ Contact information for you and any co-authors.
☐ Confirmation that you have no competing interests to disclose.

## Title page

☐ Title page including the title of the article, the full name of the author(s), academic degrees, positions, institutional affiliations, a running title (of 7 or less words), correspondence, and declarations.

## Declaration

☐ Conflicts of interest, funding, authors' contributions, ORCID, data availability statement, and acknowledgments

## Abstract

☐ Original article: <250 words; structured abstract— Objective, Methods, Results, Conclusion
☐ Review article: <200 words; unstructured abstract
☐ Case report: <200 words; unstructured abstract

## Keyword

☐ Keywords should be from MeSH subject headings when possible.

## Main text

☐ Information regarding approval of an institutional review board and obtaining informed consent should be mentioned.
☐ Original article: Introduction/Methods/Results/Discussion/Conclusions
☐ Review article: Introduction/Review/Conclusions
☐ Case report: Introduction/Case Report(s)/Discussion/Conclusions

## Reference

☐ Refer to the reference format in the author's guideline.

### Table

☐ If tables are included, they should be included as text and not as illustrations so that they may be edited if necessary.

### Figure

☐ Figure legends should be included as text and not as illustrations so that they may be edited if necessary.

### Author's form

☐ All authors have completed the Copyright Transfer Agreement and Ethics Concerning Human Subjects.

### Conflict of interest form

☐ All authors have completed the COI Statement.

### Permission

☐ The authors are responsible for obtaining permission from the copyright holder to reprint any previously published material in RDE.

RDE Restorative Dentistry & Endodontics

# Copyright transfer agreement

Manuscript title _____

_____

Corresponding author name _____

Fax _____ E-mail _____

The authors of the article hereby agree that the Korean Academy of Conservative Dentistry holds the copyright on all submitted materials and the right to publish, transmit, sell, and distribute them in the journal or othermedia.

## Corresponding author

**Print name** _____

**Signed** _____ **Date** _____

## Co-authors

**Print name** _____ **Print name** _____

**Signature/Date** _____ **Signature/Date** _____

**Print name** _____ **Print name** _____

**Signature/Date** _____ **Signature/Date** _____

**Print name** _____ **Print name** _____

**Signature/Date** _____ **Signature/Date** _____

**Print name** _____ **Print name** _____

**Signature/Date** _____ **Signature/Date** _____